

HEIFER INTERNATIONAL CENTER

LITTLE ROCK, ARKANSAS



**THE PENNSYLVANIA STATE UNIVERSITY
SCHREYER HONORS COLLEGE**

DEPARTMENT OF ARCHITECTURAL ENGINEERING

SIKANDAR PORTER-GILL
SPRING 2014

A thesis submitted in
partial fulfillment of the requirements for a bachelor degree in Architectural Engineering
with honors in Architectural Engineering

Reviewed and approved* by the following:

Thomas Boothby
Professor
Thesis Supervisor

Richard Mistrick
Associate Professor
Honors Advisor

*Signatures are on file in the Schreyer Honors College



HEIFER INTERNATIONAL CENTER

LITTLE ROCK, ARKANSAS

GENERAL BUILDING DATA

Construction dates | February 2004 to January 2006
Construction method | Construction Management at Risk
Height | 4 stories, 65 ft.
Size | 98,000 GSF
Cost | \$18 million



LEED Platinum Building

ARCHITECTURE

The semi-circular shape is influenced by Heifer International's goal to reduce world hunger and help communities in need. The circular form stems from the "ripple effect" produced from a community helped by the charity's donation of livestock. The LEED Platinum Building occupies a previously contaminated industrial site, that reclaimed wetland areas. An open floor plan maximizes day lighting gain and minimizes energy usage through light and occupancy sensors. The unique form of the roof diverts water to a five-story 20,000 gallon rainwater retention tank.

LIGHTING/ELECTRICAL

Building provided with 480Y/277V system, with a total of 2000A.

- 1600A transferred to MDP, running at 3-phase, 4 wire

The L/E systems save approximately 57% over conventional buildings, due to:

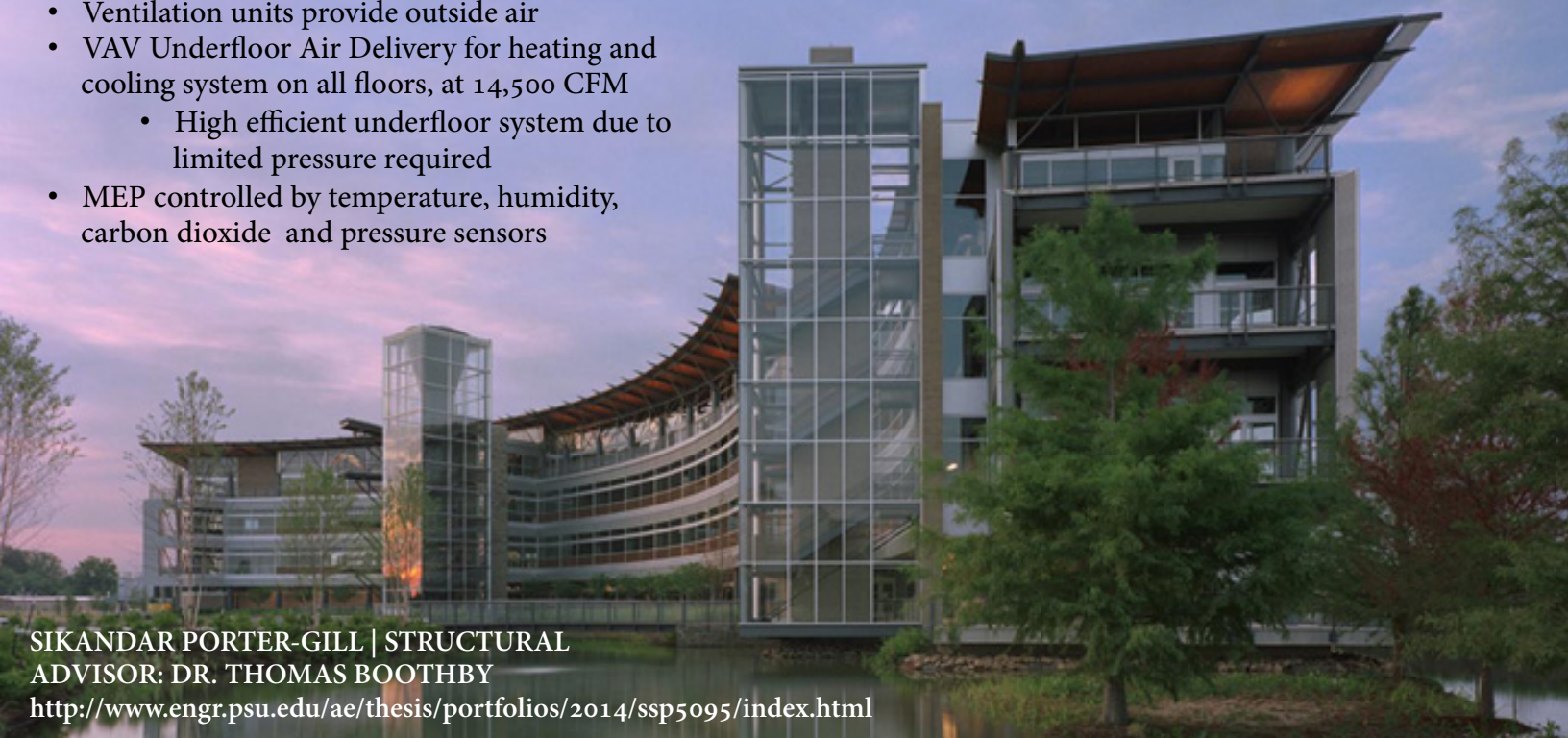
- Natural day lighting
- Space occupancy sensors
- T5 lamps

MEP SYSTEMS

- Ventilation units provide outside air
- VAV Underfloor Air Delivery for heating and cooling system on all floors, at 14,500 CFM
 - High efficient underfloor system due to limited pressure required
- MEP controlled by temperature, humidity, carbon dioxide and pressure sensors

STRUCTURE

- Geopier™ Foundation System, with traditional piers and grade beams, supporting a slab on grade
- Framing consists mostly of 2'-0" diameter HSS, supporting a 2 ½" concrete slab on 3" composite deck, supported by a beam and girder system
- Wind and seismic loading is resisted by a steel plate shear wall system acting in both directions, for both the floor and roof diaphragms



ABSTRACT

Heifer International Center is located in Little Rock, Arkansas, and is the primary headquarters for Heifer International, a non-profit whose goal is to reduce world hunger and poverty. The architect wishes to pursue a new aesthetic look through the use of a different structural material, as the system is exposed. The new hybrid system of glulam and steel causes a reclassification of the building as Type IV, per the International Building Code 2009 §602.4, and prevents the use of the current Underfloor Air Distribution System. This obstacle leads to a new overhead VAV system, with new sizing of the supply and return ductwork required. A thermal bridge on the fourth level was also extensively studied and eliminated in a redesign involving new structural and wall components.

An architectural study was performed on the new exposed structural system. A guideline was established to aide with the design of not just the architectural components of the building, but to also positively lead the design of the engineering systems of the building. The desire to enhance the architecture by changing the structural material influenced mechanical, electrical and the interior aesthetic of the building. The use of glulam in the design provided a unique opportunity to investigate a queen post truss, which lends to integration between the mechanical and structural disciplines. Mechanical and electrical equipment was also incorporated into and hung from the truss.

The non-profit's goal is to reduce world hunger and help communities in need. This astonishing, semi-circular glass clad building is four stories high and roughly 490 feet by 62 feet wide, with a 98,000 gross square footage. It overlooks downtown Little Rock and the Arkansas River. The semi-circular shape of the building stems from the "ripple effect" produced from a community helped by the charity's donation of livestock. Heifer International Center is one of the few Platinum Certified LEED Buildings in the Southern United States. The building is oriented in the east-west direction, to maximize natural lighting. An inverted roof is used to divert rainwater to a five story tower, capable of storing 20,000 gallons of water. An additional goal of the project was to infuse the non-profit's core beliefs into the redesigned engineering systems.

TABLE OF CONTENTS

Abstract	iii
Index of Figures	vii
Index of Tables	x
Index of Key Words	xi
Acknowledgements	xii
Chapter 1	1
1.1 Introduction to the Building	2
1.2 Existing Structural Information	3
Foundation System.....	4
Gravity Systems	5
Lateral System.....	8
Joint Details	10
1.3 Materials	13
Concrete	13
Steel	13
Other Material	13
1.4 Determination of Design Loads	14
National Code for Live Load and Lateral Loads.....	14
Gravity Loads.....	14
Snow Loads.....	14
Rain Loads.....	14
Lateral Loads.....	14
Load Paths.....	14
1.5 Gravity Loads	16
1.6 Lateral System and Loads – Simplified Model	17
ETABS Model.....	18
Seismic Loading	22
Wind Loading.....	27
Torsional Irregularities	32
Overturning Moment.....	33
Energy/Virtual Work Diagram	35
Lateral System Spot Checks	36
Lateral System Conclusion – Simplified Model.....	42
1.7 Problem Statement	43
1.8 Proposed Solution	44
Breadth Topics	45
MAE Coursework Requirement	46
Schreyer Honors College Requirement.....	46
1.9 Conclusion to Proposed Solution	47
Chapter 2	48
2.1 Gravity System Redesign	49
Considerations of the Typical Bay Layout	50
Composite Decking Selection.....	50
Beam Design of Typical Floor and Roof.....	51
Queen Post Girder Design.....	54
General Framing Plan.....	57
Fire Rating.....	58

Column Design	58
Foundation Consideration.....	58
Comparison of Gravity Systems	59
2.2 Lateral System Redesign.....	63
Computer Modeling Input	63
Torsional Irregularities	67
Loads Applied to Model.....	71
Building Overturning Moment.....	72
Understanding Load Paths	73
Shear Wall Design	74
Seismic Joint	74
2.3 Comparison of Existing and Redesigned Systems.....	76
2.4 MAE Requirements	80
Chapter 3	81
3.1 Mechanical and Envelope Breadth.....	82
Preliminary Duct Sizing.....	82
Thermal Bridge Elimination	83
Chapter 4	91
4.1 Architecture Breadth	92
Impacts from Structural Redesign	93
Architectural Design Guidelines	94
Chapter 5	105
5.1 Composite Wood-Concrete Floor System.....	106
Design Standards of TCC	107
Types of TCC Systems.....	108
Cyclic Loading Effects to TCC	112
Conclusion to TCC	113
Additional References	113
Chapter 6	114
6.1 Conclusion.....	115
References and Work Cited.....	116
Appendix A.....	119
Appendix A.1 - Existing Lateral System Modeling.....	120
Evolution of the ETABS Model.....	120
Elevations of Shear Walls.....	121
ETABS SPSW to Concrete Conversion	122
Controlling Case Data Output.....	125
Appendix A.2 - Existing Seismic and Wind Analysis.....	127
Seismic Loading Calculations	127
Seismic Amplification Factor.....	128
Wind Loading Calculations.....	129
Appendix B.....	133
Appendix B.1 - Typical Office Beam Design.....	134
Loading.....	135
Flexure and Reactions.....	135
Computer Analysis Data.....	136

Member Sizing.....	137
Appendix B.2 - Queen Post Design Hand Calculation	139
Appendix B.3 - Typical Office Queen Post Design	149
Loading.....	149
Flexure and Reactions.....	149
Axial Cable and Girder Forces.....	149
Computer Analysis Data.....	150
Top Chord Member Sizing.....	152
Tension Cable Sizing.....	158
Steel Square HSS Sizing	160
Deflection Check.....	161
Appendix B.4 - Roof Beam Design.....	162
Loading.....	162
Flexure and Reactions.....	162
Computer Analysis Data.....	163
Member Sizing.....	164
Appendix B.5 - Roof Queen Post Design	168
Loading.....	168
Flexure and Reactions.....	168
Axial Cable and Girder Forces.....	168
Computer Analysis Data.....	169
Top Chord Member Sizing.....	171
Member Summary, Tension Cable and Steel Square HSS Sizing	178
Deflection Check.....	180
Appendix B.6 - Summary of Beam Sizes	181
Appendix B.7 - Typical Office Perimeter Beam.....	182
Appendix B.8 - SAP2000 Queen Post Model.....	183
Original Model.....	183
Member Releases	183
Loading.....	183
Axial Loading.....	183
Appendix B.9 - Column Sizing.....	184
Appendix C	185
Appendix C.1 - HSS24x0.5 Column.....	186
Appendix C.2 - Seismic and Wind Loading.....	187
Seismic ASCE 7-10	187
Wind ASCE 7-10.....	197
Appendix C.3 - Torsional Irregularity and Seismic Amplification Factor.....	202
Appendix C.4 - Building Overturning Check.....	206
Appendix C.5 - Lateral System Hand Checks	208
Appendix C.6 - Trace Locations.....	213
Appendix D.....	214
Appendix D.1 - Thermal Bridge Study.....	215
Column Design	215
Worst Case Thermal Gradient.....	217
Middle Case Thermal Gradient.....	218

INDEX OF FIGURES

Figure 1: Exterior view of Heifer International Center	2
Figure 2: Interior view of Heifer International Center.....	2
Figure 3: Typical floor plan	3
Figure 4: Comparison of typical framing layout.....	5
Figure 5: Interior composite decking detail	6
Figure 6: Photograph during erection of HSS framing.....	6
Figure 7: Roof tree-flare connection detail	7
Figure 8: Detail connection of roof wide flange to T&G	7
Figure 9: Typical SPSW elevation, section and plan.....	8
Figure 10: Typical shear connection.....	10
Figure 11: Typical moment connection supporting	10
Figure 12: Typical balcony section.....	11
Figure 13: Seismic joint detail	12
Figure 14: Photograph of seismic joint.....	12
Figure 15: 3D view of ETABS model	18
Figure 16: ETABS shell stress distribution diagram	19
Figure 17: Inherent torsional force formed in walls	19
Figure 18: 3D view of shear transfer (seismic y-direction)	20
Figure 19: Elevation showing shear decrease on ground floor.....	20
Figure 20: Center of mass and center of rigidity from ETABS.....	20
Figure 21: Shear wall pier labeling convention for east side of the building	21
Figure 22: Seismic loading distribution.....	22
Figure 23: Wind loading distribution.....	27
Figure 24: Wind analysis, Case 1, NS and EW	27
Figure 25: Wind analysis, Case 2, NS	28
Figure 26: Wind analysis, Case 2, EW	28
Figure 27: Wind analysis, Case 3, NS and EW	29
Figure 28: Wind analysis, Case 4, NS	30
Figure 29: Wind analysis, Case 4, EW	30
Figure 30: 3D view of member utilization, x-direction loading	35
Figure 31: Member utilization of Shear Wall 13 at 12, y-direction loading.....	35
Figure 32: Basic Combinations for ASCE 7-1998	36
Figure 33: Diagram showing location of joints referenced	40
Figure 34: Heifer International Education and Visitor Center.....	43
Figure 35: Potential queen post options.....	44
Figure 36: Typical floor plan	49
Figure 37: Simplified floor plan	49
Figure 38: Beams, girders and perimeter beams of typical office	51
Figure 39: Beams, girders and perimeter beams of roof.....	52
Figure 40: Load path of queen post	54
Figure 41: Simplified hinge queen post girder	54
Figure 42: Computer model of queen post girder.....	55
Figure 43: Connection detail for cable of queen post girder	55
Figure 44: Glulam top chord is eccentrically loaded due to the cable.....	56
Figure 45: Conceptual design with holster plate and held with a clevis.....	56

Figure 46: Conceptual design with plate penetration wood glulam beam and held with a clevis	56
Figure 47: Isometric view of general framing plan	57
Figure 48: Plan view of general framing plan (East side)	57
Figure 49: Comparison of existing and redesigned gravity systems	59
Figure 50: Existing structural system isometric in view.....	60
Figure 51: Redesigned structural system isometric in view	60
Figure 52: Existing system typical bay (with dimensions).....	61
Figure 53: Redesigned system typical bay (with dimensions).....	61
Figure 54: Redesigned structural system and potential mechanical and electrical.....	62
Figure 55: LFRS of east end of building	64
Figure 56: LFRS of east end of building from RAM SS	64
Figure 57: LFRS of west end of building	65
Figure 58: LFRS of west end of building from RAM SS	65
Figure 59: ASCE-7 10 Figure 12.8-1 Torsional Amplification Factor.....	67
Figure 60: Type 5 Nonparallel System Irregularity	69
Figure 61: Load path diagram of building	73
Figure 62: SW-13 at column line 12 section	74
Figure 63: East end of the Heifer International Center.....	75
Figure 64: West end of the Heifer International Center	75
Figure 65: High capacity girder hangers for glulam	76
Figure 66: 3D isometric of floor plan highlighting walls to be redesigned	78
Figure 67: Construction photo with no evident LFRS	78
Figure 68: Exterior shot of columns	83
Figure 69: Columns exposed on exterior and interior	83
Figure 70: Worst case heat travel.....	84
Figure 71: Worst case thermal gradient	85
Figure 72: Middle condition thermal gradient.....	85
Figure 73: Phase 1 - Column Construction.....	86
Figure 74: Phase 2 - Column Construction.....	86
Figure 75: Phase 3 - Column Construction.....	86
Figure 76: Phase 4 - Column Construction.....	87
Figure 77: Phase 5 - Column Construction.....	87
Figure 78: Phase 6 - Column Construction.....	88
Figure 79: Phase 7 - Column Construction.....	88
Figure 80: Final column design to prevent thermal bridge.....	89
Figure 81: Building section of redesigned column	90
Figure 82: Interior aesthetic changes due to gravity redesign	92
Figure 83: Interior aesthetic from existing gravity system	92
Figure 84: Site circulation of the Heifer International campus.....	95
Figure 85: Primary and secondary circulation through Heifer International campus.....	96
Figure 86: Local aggregate to match color and texture	97
Figure 87: Porous pavement used in parking areas	97
Figure 88: Pedestrian and vehicular activity accommodated in parking lot.....	97
Figure 89: Integration of walkways and incorporation of drainage system.....	98
Figure 90: Indigenous plantings used on the campus	98

Figure 91: Central and secondary walkways	98
Figure 92: Circular form of campus.....	99
Figure 93: Circular form of building	99
Figure 94: Inverted sloped roof.....	100
Figure 95: Water collection system tower (far left) and local wetland (front right).....	100
Figure 96: Covered entrance to building	100
Figure 97: Natural daylighting in interior of building	101
Figure 98: Exterior shot of natural daylighting penetrating building façade.....	101
Figure 99: Interior natural lighting	102
Figure 100: Exterior view of interior artificial light	102
Figure 101: Interior spacious environment	102
Figure 102: Reference point on plan to mark circular center	103
Figure 103: Plan of tree columns	104
Figure 104: Inspiration for tree column canopy	104
Figure 105: Plan detail of tree column connection	104
Figure 106: Section detail of tree column connection	104
Figure 107: The Vihantasalmi Bridge of Finland.....	106
Figure 108: Semi-prefabricated TCC floor system in New Zealand (Yeoh et al.).....	107
Figure 109: Shear connector and wire mesh (Clouston et al.).....	108
Figure 110: Shear key connection, longitudinal view (Fragiacomo et al.).....	108
Figure 111: Shear key connection, cross section, (Fragiacomo et al.)	109
Figure 112: Hilti dowel cross section (Gutkowski et al.)	109
Figure 113: Glued composite, stress and strain distribution (Henrique et al.)	110
Figure 114: Bending test of glued composite member (Henrique et al.).....	110
Figure 115: Custom lag bolt system (Swenson et al.)	111
Figure 116: Tested beam before failure (Swenson et al.)	111
Figure 117: Shear failure of wood notch (Balogh et al.)	112
Figure 118: Midspan flexural failure (Balogh et al.)	112

INDEX OF TABLES

Table 1: Concrete properties used in original design.....	13
Table 2: Steel properties used in original design.....	13
Table 3: Other material properties used in original design.....	13
Table 4: Live loads used in original design.....	16
Table 5: Dead loads used in original design.....	16
Table 6: Breakdown of floor dead loads used in original design.....	16
Table 7: Seismic Forces for Entire Building.....	22
Table 8: NS Regular earthquake loading (positive moment).....	23
Table 9: NS Reverse earthquake loading (negative moment).....	23
Table 10: EW Regular earthquake loading (positive moment).....	23
Table 11: EW Reverse earthquake loading (negative moment).....	23
Table 12: Existing seismic story drift.....	25
Table 13: ASCE 7-1998 Table 9.8.2.8 for maximum story drift.....	26
Table 14: Wind analysis, Case 1.....	27
Table 15: Wind analysis, Case 2, NS.....	28
Table 16: Wind analysis, Case 2, EW.....	28
Table 17: Wind analysis, Case 3, NS and EW.....	29
Table 18: Wind analysis, Case 4, NS.....	30
Table 19: Wind analysis, Case 4, EW.....	30
Table 20: Existing wind building drifts.....	31
Table 21: ASCE 7-1998 Table 9.5.2.3.2 Plan Structural Irregularities.....	32
Table 22: Steel plate shear wall deflection check (seismic).....	40
Table 23: Steel plate shear wall deflection check (wind).....	41
Table 24: Floor system comparison.....	50
Table 25: IBC 2009 Construction type classification summary.....	53
Table 26: Comparison of existing and redesigned gravity systems.....	59
Table 27: Summary of west end seismic forces.....	71
Table 28: Summary of east end seismic forces.....	71
Table 29: Summary of west end wind forces.....	72
Table 30: Summary of east end wind forces.....	72
Table 31: SW-13 at column line 12 rebar design summary.....	74
Table 32: Air handling unit summary.....	82
Table 33: TRANE Ductulator sizing.....	82
Table 34: Redesigned HSS envelope.....	84
Table 35: Existing HSS envelope.....	84
Table 36: Glass façade envelope.....	84

INDEX OF KEY WORDS

A

Accidental Torsional Moment, 68

B

batt insulation, 84
Bentley RAM Structural System, 46
Building drift, 72

C

cable, 54
CMU masonry back wall, 8
composite deck, 5
composite wood-concrete, 106
construction sequence, 86
Cracked sections, 66
CSI ETABS 2013, 18
Custom lag bolt system, 111

D

Dan West, 2

E

Education and Visitor Center, 43
Equivalent Lateral Force Analysis, 68
expansive clays, 4
Extreme Torsional Irregularity (Type 1b), 67

F

fire rating, 58

G

Geopiers, 4
Glued composite members, 110
glulam, 49

H

hanger, 76
Hilti and shear key connection, 109
HSS shapes, 6

I

indeterminate structure, 54
inverted roof, 3

L

Little Rock, Arkansas, 3

N

neutral axis, 106
Nonparallel System Irregularity Type 5, 69

O

orthogonal combination procedure, 69
overhead ductwork system, 82
overhead VAV system, 43
overturning moment, 72

P

Passing on the Gift, 94
post, 54

Q

Queen Post, 54

R

RAM Concrete, 66
RAM Frame, 66
Revit, 57
Rigid diaphragm, 66

S

SAP2000, 55
Seismic Design Category, 22
Seismic drifts, 71
seismic joint, 12
Shear connector and wire mesh, 108
Shear key connection, 108
shear wall system, 63
steel plate shear wall, 8

T

thermal bridge, 82
thermal bridges, 45
thermal gradient, 85
timber-concrete composite, 106
top chord, 54
Torsional Irregularity (Type 1a), 67
TRANE Ductulator®, 82
tree-column, 6
Type IIIB, 43
Type IV Construction, 43

U

underfloor air distribution system, 82
U-value, 84

ACKNOWLEDGEMENTS

I wish to take a moment to express my gratitude towards the many people that took time out of their busy professional lives to help me with my thesis project. Of special importance, with without this project would not be possible are Heifer International, Polk Stanley Wilcox Architects and Cromwell Architects Engineers, Inc.

Additionally, the hours of dedication from the Pennsylvania State University's Architectural Engineering faculty warrants huge thanks. Especially,

- Dr. Thomas Boothby
- Prof. Heather Sustersic
- Dr. Walter G. M. Schneider III
- Prof. Kevin Parfitt
- Dr. Linda Hanagan
- Mr. Issa J. Ramaji
- Dr. Ryan Solnosky
- Dr. Richard Mistrick

Moreover, my friends whom inspired me to continue my work; as we each helped each other through the hardest parts of thesis,

Natasha Beck

Macenzie Ceglar

Chris Cioffi

Angela Mincemoyer

Kristin Sliwinski

Alyssa Stangl

John Vais

In addition, I would like to thank Chelsea Billotte, Kieran Carlisle, Jeff Martin, Matt Neal and Faye Poon for their valuable input and patience throughout the semester.

Lastly, I would like to thank Prof. Moses Ling, Dr. Andrés Lepage, Prof. Robert Holland and Mr. Corey Wilkinson who encouraged me and dealt with my many questions over the past several years.



Heifer International



Polk Stanley Wilcox Architects



Cromwell Architects Engineers, Inc.

CHAPTER 1

THE HEIFER INTERNATIONAL CENTER

1.1 INTRODUCTION TO THE BUILDING

Heifer International’s headquarters mirrors Heifer’s goal of reaching out to a community in need. Heifer International wished their headquarters to match what they were teaching to the world. The shape of the building and campus were inspired by Heifer International’s founder Dan West who expressed, “In all my travels around the world, the important decisions were made where people sat in a circle, facing each other as equals.” This was extended to show the ripple effect Heifer has on needy communities, through their donation of livestock. These communities agree to pass on the offspring of the animal to others—thus creating a ripple effect throughout the community.



Photo courtesy Timothy Hursley

Figure 1: Exterior view of Heifer International Center

Heifer International Center, shown in Figure 1, is a four-story office building, standing 65 feet tall, with 98,000 square feet. It was constructed between February 2004 and January 2006, at a cost of approximately \$18 million. The design team from Polk Stanley Wilcox Architects and Cromwell Architects Engineers, Inc. were faced with the large challenge of providing an open office plan, in a semi-circular shape, while concurrently offering educational and visual interactions, and sustainable features that would express Heifer International’s mission of ending world hunger and poverty. This was certainly a challenge for the design team—expressing the abstract meanings of the charity through the physical form of the building.

Heifer International Center continues Heifer’s mission of teaching—the public is allowed access to the facility through tours provided by Heifer personnel, showcasing the sustainable features of the office building. This form of interaction with the building not only educates the community about sustainability, but attracts volunteers and workers to Heifer International — aiding in their desire to help needy communities.

The building has an open floor plan that allows natural light to penetrate to the center of each level, provides views of the river and cityscape, and offers extensive community exchange

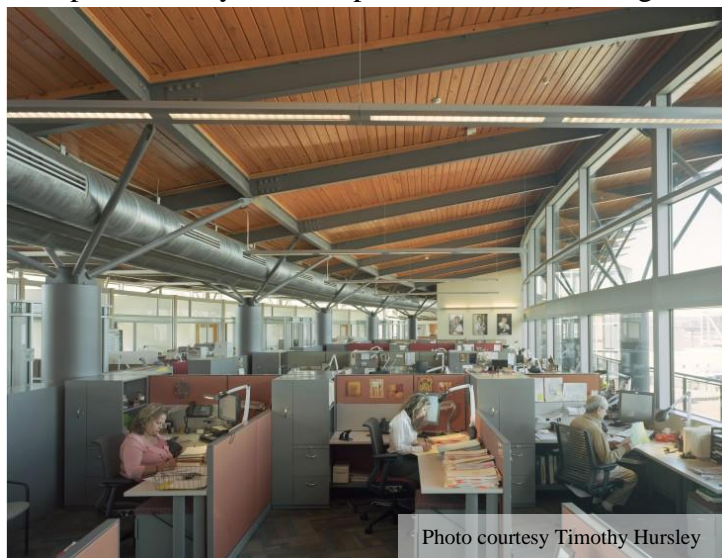


Photo courtesy Timothy Hursley

Figure 2: Interior view of Heifer International Center

points with easy access to exterior balconies on each level. This is shown in Figure 2.

A unique feature of the building includes the use of a custom tree-column design that supports the inverted roof at both exterior and interior points. The tree column allows the inverted roof to cantilever over the fourth floor office. The roof is inverted for two reasons. The first is to direct rainwater toward the large silo-tower for storage and greywater use, while the second is to provide the ideal angle for a possible future solar panel array.

Heifer International Center is placed in an industrial section of Little Rock, Arkansas, that is currently being revitalized. This led to many advantages that the design team used to the building and site’s benefit. The site that Heifer International Center occupies was contaminated with industrial waste, and through land reclamation, the soil was removed from the site and taken to a facility to be treated and used elsewhere in the Arkansas region. The site offered more than just the ability to help reclaim natural land—many bricks and other materials were found during the cleanup process. Most of these reclaimed materials were incorporated into the landscape, and a few were crushed down

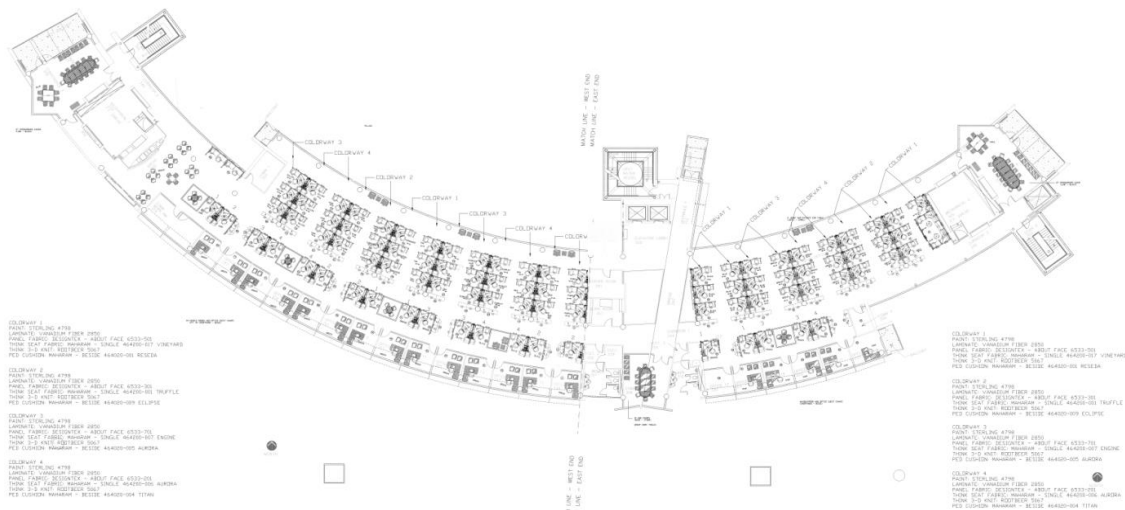


Figure 3: Typical floor plan

and used in the footings for the building. The industrial section of the city also housed the steel mill that manufactured Heifer International’s steel structure—AFCO Steel Inc. is located only a few blocks away from Heifer’s site. Additionally, the mostly glass-clad building is built using Ace Glass Co Inc. as the fabricator of the glass, located less than 100 yards from the building.

1.2 EXISTING STRUCTURAL INFORMATION

Heifer International Center is a four story steel structure that is laterally supported by steel plate shear walls. The floor system is a composite decking system, which is supported with large HSS pipes for the framing system. The framing system bears onto a system of piers and footings. Grade beams also bear onto the system of piers and footings but support the slab-on-grade instead. A section of the Ground Level is recessed into the ground 2’-0” to accommodate a larger mechanical room.

Foundation System

Geotechnical Report

Grubbs, Hoskyn, Barton & Wyatt, Inc. performed a geotechnical survey of the site in January of 2003. The survey¹ encountered expansive clays on the east side of the building and soft and compressible soils on the west side of the building. Expansive clays expand when they gain water, and contract when they lose water—potentially heaving, or raising, the site elevation four and eight inches. On the east side, the report recommended that the weak soils should be undercut during site grading—approximately 4'-0" to 6'-0". Undercutting involves removing the soil to the specified depth and replacing it with compacted engineered soil. The soil removed would be replaced with low-plasticity clayey sand, sandy clay or gravelly clay. The geotechnical engineer stated that undercutting would allow the use of a slab-on-grade system; however, the use of two potential systems to increase the bearing capacity of the soil would have to be implemented.

The geotechnical engineer recommended either Rammed Aggregate Piers or Drilled Piers, for the foundation system. A Rammed Aggregate Pier[®] (RAP) System by Geopier Foundation Company, Inc., is used to mechanically improve the soil conditions of the site. The RAP system uses “vertical ramming energy” to add layers of crushed aggregate to the site. Generally, Geopiers[™] are formed by drilling 30-inch diameter holes and ramming aggregate into the hole, until a “very stiff, high-density aggregate pier[s]” are formed. This crushed aggregate increased the soil’s capacity to between 5 to 7 ksf for the Heifer International Center. Additional Geopiers[™] were provided per structural drawings, due to larger loads or the higher potential for uplift at certain sections of the building. The geotechnical engineer stated, “Total settlement of shallow footings on Geopier[™] elements would be expected to be less than about 1.0 inch and differential settlement less than about 0.5 inch.”

Foundation Design

The design teams chose a RAP[®] System, which allowed the use of conventional slab-on-grade, footings and grade beams. The RAP[®] System had the added benefit of increasing the bearing capacity and decreasing the size of the footing.

Heifer International Center also is provided with grade beams to distribute loads to column piers and footings. These grade beams support the slab and prevent the slab from deflecting or settling. The design uses various sizes of grade beam, which are reinforced using #4 stirrups at 24" O.C. #5 and #8 longitudinal reinforcing bars are also used.

¹ Geotechnical survey provided by Polk Stanley Wilcox Architects with permission from owner.

Gravity Systems

Floor System

Heifer International Center’s floor system is composed of girders and beams supporting composite steel deck filled with a concrete slab. The greater part of the beams supporting the floor system are W16x26s and W14x22s, shown in yellow and orange in Figure 4. Each beam has a camber ranging from $\frac{3}{4}$ ” to 1”. The framing nearer the center of the building is irregular due to the large interior architectural opening, walkway bridge and lobby space, shown in blue on Figure 4. The framing at each end of the building, on the east and west, is also irregular due to the large mechanical spaces, cantilevered balconies and stairwells, shown in blue on Figure 4. The mechanical spaces are generally supported by W16 beams.

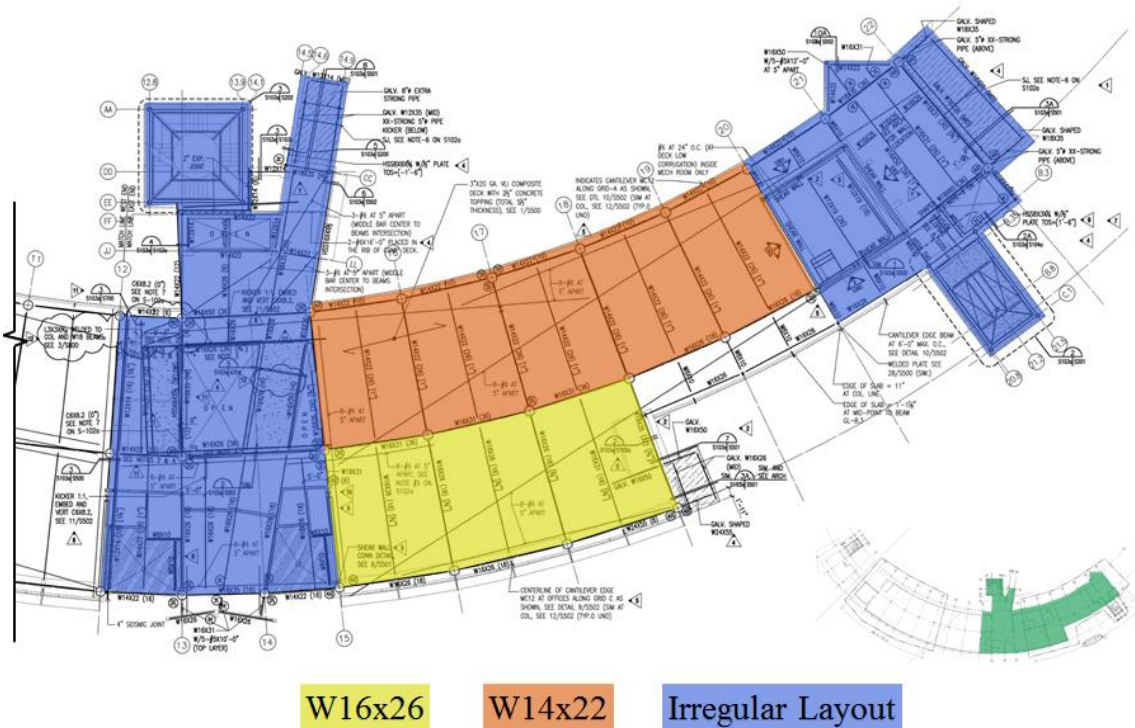


Figure 4: Comparison of typical framing layout

Each floor of the Heifer International Center has a similar layout to that shown in the half-plan in Figure 4 above.

A typical bay is 20’-0” x 30’-0”, where the floor is supported by a system of beams and girders. The beams and girders collect the loads of the 3VLI 20 gauge composite deck with 2 ½” of normal weight concrete topping for a total thickness of 5 ½”. The decking compositely acts with the framing members to take advantage of concrete in compression and steel in tension. A detail showing the composite deck configuration with a wide-flange is shown in Figure 5. In addition, at the edges of the building (or the interior sections that are open to below) the composite deck is ended with a bent edge plate.

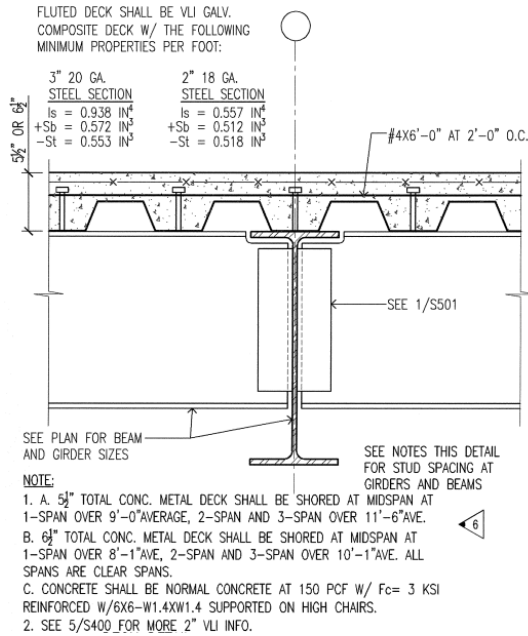


Figure 5: Interior composite decking detail

particularly concerned about tolerances maintaining tolerances on concrete columns, and the attendant difficulty of connecting to the beams. Due to these concerns, the design was changed to round steel, HSSs, which vary from 10” to 24” in diameter. A photograph of the HSS during the erection process is shown in Figure 6.

Roof System

The roof-framing plan varies from the floor framing plans—due to the tree-column designs that flare out on the fourth level and attach to the roof girders. These girders support steel beams, which in turn support a timber wood roof deck. The roof cantilevers approximately 8’-0” beyond the edge of the building, while simultaneously inverting the roof to form a valley. A Thermoplastic Membrane topped with a 4” glued laminated wood decking makes up the first two layers of the roof, Figure 8. The wood decking has a tongue-and-groove assembly and is connected to 3” of continuous wood lumber using 8d nails at 6” O.C. This system is bolted to the top flange of the roof steel members. The roof system is shown in Figure 8 and connects to the flare connection shown in Figure 7.

It should be noted that all of the floor slabs, although they are supported by the composite decking, are also reinforced with #4 at 6” O.C. in order to control cracks that occur naturally over the girders. This cracking occurs when the slab tries to take tension to make the beam continuous over the girder. A reason for the insertion of this reinforcement is to reduce the magnitude of the deflection occurring at each level due to the use of under-floor air distribution plenums for the mechanical system.

Framing System

The framing system consists of large round HSS shapes, which continue from the ground level to the fourth floor. Originally concrete

columns were considered; however, the contractor and steel fabricator were



Figure 6: Photograph during erection of HSS framing

Lateral System

Heifer International Center is a four story steel structure and is laterally supported by steel plate shear walls. The floor system is a composite decking system, which is supported with large HSS pipes for the framing system. The framing system bears onto a system of piers and footings. A section of the Ground Level is recessed into the ground 2'-0" to accommodate a larger mechanical room.

A typical steel plate shear wall (SPSW) is shown in Figure 9, which shows the continuous shear plates that are installed into the wall system. For clarity, the shear plates are shown in red, in both section and plan. These plates are reinforced with C-channels spaced at 24" O.C., welded perpendicular to the shear plates attached to the wall. The C-channels are shown in blue in Figure 9 below. Several shear walls along the ground floor use a composite steel plate shear wall and CMU masonry back wall, which is approximately 6" thick.

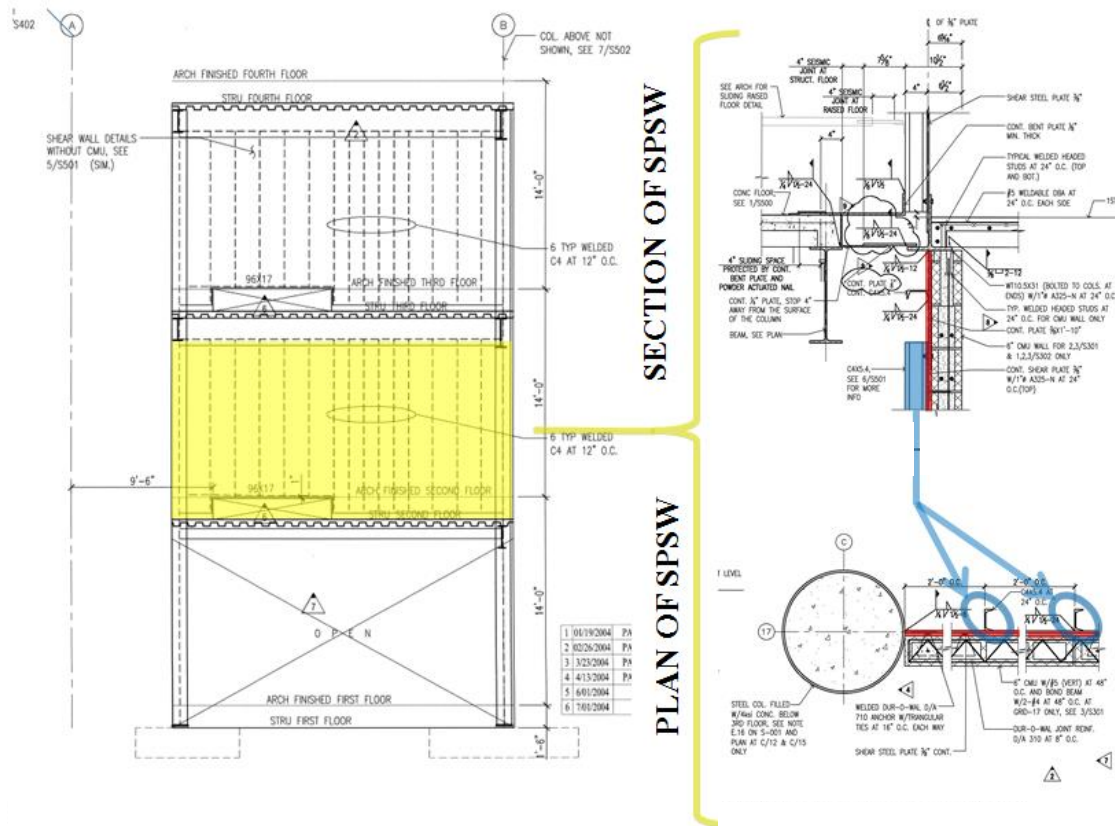


Figure 9: Typical SPSW elevation, section and plan

Lateral stability is ensured in part by the floor deck, which acts as a rigid diaphragm spanning between SPSWs. SPSWs resist horizontal shear, and effectively act as a vertical girder—the columns act as the flanges and the steel plate acts as the web. The SPSWs span from the foundation to the bottom of the fourth floor. The floor slab is also reinforced with additional #6 at 5” O.C. to assist with diaphragm action of lateral loads during a seismic event. According to the design team, this reinforcement is very important around floor openings—analogueous to reinforcing openings in the flange of a beam.

Lateral loads at the roof are collected by the roof deck diaphragm and then transferred to the round steel columns, passing through the flare out connections of the tree-columns. This lateral load from the columns is transferred to the fourth floor diaphragm, and the lateral load is collected by the SPSWs.

Due to the irregularities of the building’s shape and the 440’-0” length, the semi-circular building was divided into two approximately even sections with a seismic joint. These two halves were analyzed separately for lateral loads, using both static and dynamic methods. Essentially, two separate structures, with separate lateral systems, are joined together to act as one unit. For this technical report, only the east side of the building was analyzed.

Joint Details

Bolted Connections

Most of the connections are shear connections in Heifer International Center, and are bolted in three or four rows. This is shown in Figure 10 below.

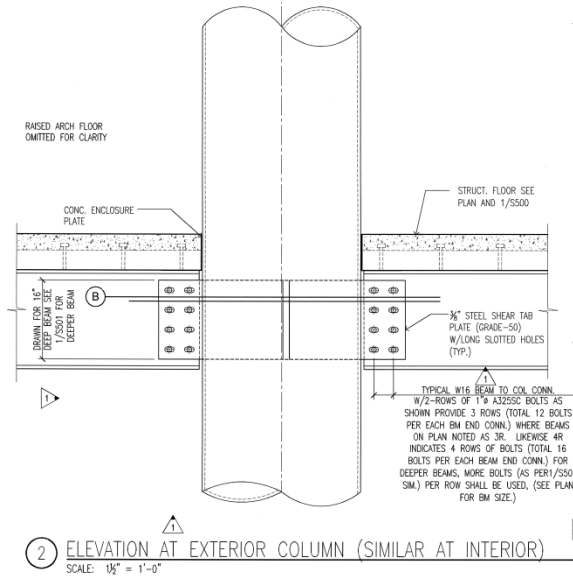


Figure 10: Typical shear connection

Moment Connections

Small, cantilevered balconies are anchored to the building using moment connections, which is shown in Figure 11.

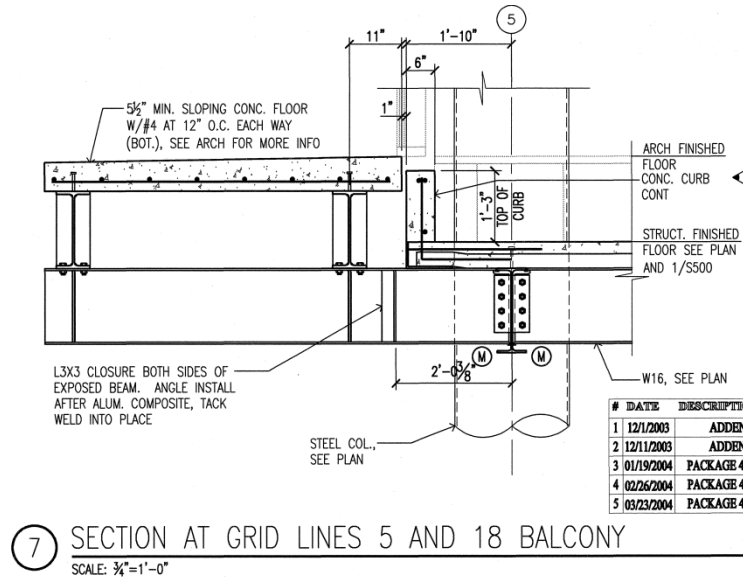


Figure 11: Typical moment connection supporting

East and West End Balconies

Heifer International Center has large balconies on the east and west that use a shear connection to attach to the building. These balconies are also supported by tension members, HSS pipes. Figure 12 shows a detail section of how the balcony is supported by the shear connection and pipes.

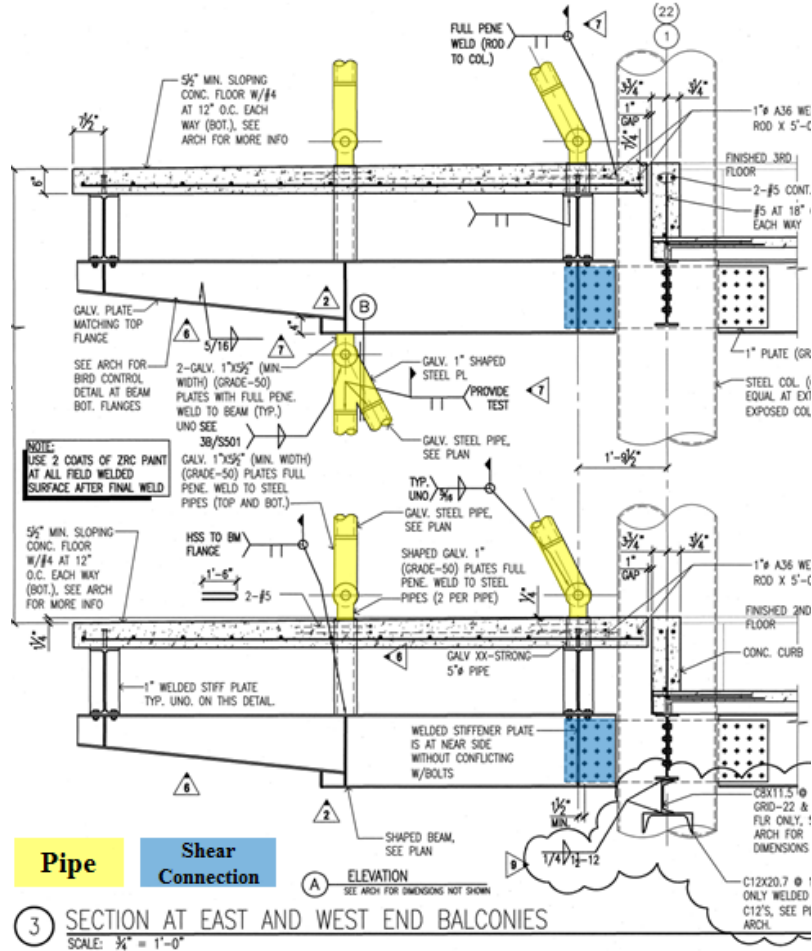


Figure 12: Typical balcony section

1.3 MATERIALS

Heifer International Center used the following materials. Their respective stress and strength properties are provided below.

Concrete

	Minimum Strength (ksi)	Air Entraining	Water Reducing Admix Required
Reinforced Footing	3	None	Yes
Reinforced Walls, Grade Beams and Columns	4	5% AIR	Yes
Interior Slab on Grade	3	None	Yes
Typical Floor Slab	3	None	Yes
Walkway	3	5% AIR	Yes
Precast Column, Plank	5	5% AIR	Yes

Table 1: Concrete properties used in original design

Steel

Shape	ASTM	Grade	Fy (ksi)
Beams and Girders	A992 or A572	50	50
Hollow Round Columns	A252	3	45
Columns	A992 or A572	50	50
Tube Members	A-500	B	46
Plates	A-36	5%	36
Misc. Steel	A-36	None	36
Connection Bolts	A325-SC	-	-

Table 2: Steel properties used in original design

Other Material

Material	ASTM	Notes
Concrete Masonry Units	C-90	Lightweight, Type I Moisture Controlled $f'_m = 1500$ psi
Mortar	C-270	Type S $f'_m = 1800$ psi
Grout		$f'_c = 2500$ psi
Reinforcing Bars	A-615	Fy = 60

Table 3: Other material properties used in original design

1.4 DETERMINATION OF DESIGN LOADS

This piece of the report reviews the loads used in the design of Heifer International Center, and other local Arkansas laws that influenced the design and construction. It should be noted that these may not be the same values used in the redesign of the building, discussed further in the report.

National Code for Live Load and Lateral Loads

Live Load	ASCE-7 1998 Chapter 4
Wind Load	ASCE-7 1998 Chapter 6

Gravity Loads

Live Loads

Live loads used in the design of Heifer International Center were referenced using ASCE-7 1998 Chapter 4.

Dead Loads

Dead load allowances were assumed for the typical floor at 95 PSF and roof at 30 PSF. The 95 PSF floor load takes into account the composite decking, potential ponding of concrete, computer technology, mechanical and sprinkler infrastructure.

Snow Loads

Ground snow loads for Pulaski County Arkansas are 10 PSF, according to ASCE-7 1998 Chapter 7; however, the timber roof loads increased the design load to 30 PSF due to the high possibility of snow drift into the valley of the roof.

Rain Loads

Rain loads were calculated for Heifer International Center using ASCE-7 1998 Chapter 8.

Lateral Loads

Wind Loads

Loads due to wind were calculated using ASCE 7 1998 Chapter 6. The design team used an Exposure Category C (§ 6.5.6.1), with a 90mph wind speed.

Seismic Loads

The geotechnical report states that the “...site is located in Seismic Zone 1,” according to the Pulaski County Arkansas State criteria—an “area of low anticipated seismic damage.” The design team referenced ASCE-7 1998 Chapter 9 and the Arkansas Act 1100, Zone 1, of 1991.

Load Paths

Gravity Load Path

The composite deck will carry a load on a floor and transfer it to the beams and girders framing each level. As the floor system collects the load, the load is shifted to the framing system composed of large HSS pipes. This is transferred down to the ground

level and is resolved onto piers, footings and grade beams. The foundation system dissipates this load into the soil that has been engineered using Geopier™ technology.

Roof loads follow a similar path, except the roof diaphragm is composed of wood timber instead of a concrete composite deck. The timber transfers the loads to steel beams and girders, which in turn distribute the loads to tree-column connections. These intricate connections dissipate the energy down to the foundation using the large HSS pipes that compose the framing system.

Lateral Load Path

The façade of the building picks up the distributed load of the wind and transfers this to the floor diaphragm. The steel plate shear wall collects this horizontal force from the diaphragm and generates a vertical force down, towards the foundation system. The foundation system is then allowed to dissipate the base shear generated by the lateral loads.

1.5 GRAVITY LOADS

The dead and live load used in the original design are tabulated below in Table 4 and Table 5, and were taken from the structural drawings. Table 5 references the total dead load used on the project. During analysis and redesign portions of this project, it was advantageous to have a breakdown of the floor dead loads. This breakdown is shown in Table 6².

Live Loads	
Occupancy or Use	Load (psf)
Floors (typical)	80
Balcony	100
Stairs	100
Mechanical	150
Sidewalk	250
Roof Minimum	20
Snow Load	10
Ground Snow Load	10

Table 4: Live loads used in original design

Dead Loads	
Occupancy or Use	Load (psf)
Floors (typical)	95
Roof	30

Table 5: Dead loads used in original design

Breakdown of Floor Dead Loads	
Occupancy or Use	Load (psf)
Concrete and steel deck	63
Concrete ponding	8
Computers	12
Lights	4
Mechanical	4
Sprinkler	3
Miscellaneous	1

Table 6: Breakdown of floor dead loads used in original design

² Breakdown of floor dead loads provided by Cromwell Architects Engineers, Inc.

1.6 LATERAL SYSTEM AND LOADS – SIMPLIFIED MODEL

The Heifer International Center is laterally supported by steel plate shear walls. Due to the irregularities of the building's shape and the roughly 440'-0" length, the semi-circular building was divided into two approximately even sections with a seismic joint. These two halves were analyzed separately for lateral loads, using both static and dynamic methods. Essentially, two separate structures, with separate lateral systems, are joined together to act as one unit. For this technical report, only the east side of the building was analyzed.

Lateral stability is ensured in part by the floor deck, which acts as a diaphragm spanning between SPSWs. SPSWs resist horizontal shear, and effectively act as a vertical girder—the columns act as the flanges and the steel plate acts as the web. The SPSWs span from the foundation to the bottom of the fourth floor. The floor slab is also reinforced with additional #6 at 5" O.C. to assist with diaphragm action of lateral loads during a seismic event. According to the design team, this reinforcement is very important around floor openings—analogueous to reinforcing openings in the flange of a beam.

Lateral loads at the roof are collected by the roof deck diaphragm and then transferred to the round steel columns, passing through the flare out connections of the tree-columns. This lateral load from the columns is transferred to the fourth floor diaphragm, and the lateral load is collected by the SPSWs.

Please see Lateral System on page 8 for further details.

ETABS Model

The lateral system for Heifer International Center was modeled in CSI ETABS 2013. This structural modeling program was introduced in AE 530, Computer Modeling of Buildings. The complex geometry of the building was modeled in ETABS, and found to incorrectly execute. The building was simplified to a rectangle 64'-0" x 225'-0" long. The full length of the building was not used because of the seismic joint that splits the building at approximately its midpoint. It should be noted that in the redesign section of this project a model was developed which accounted for the full shape of the building.

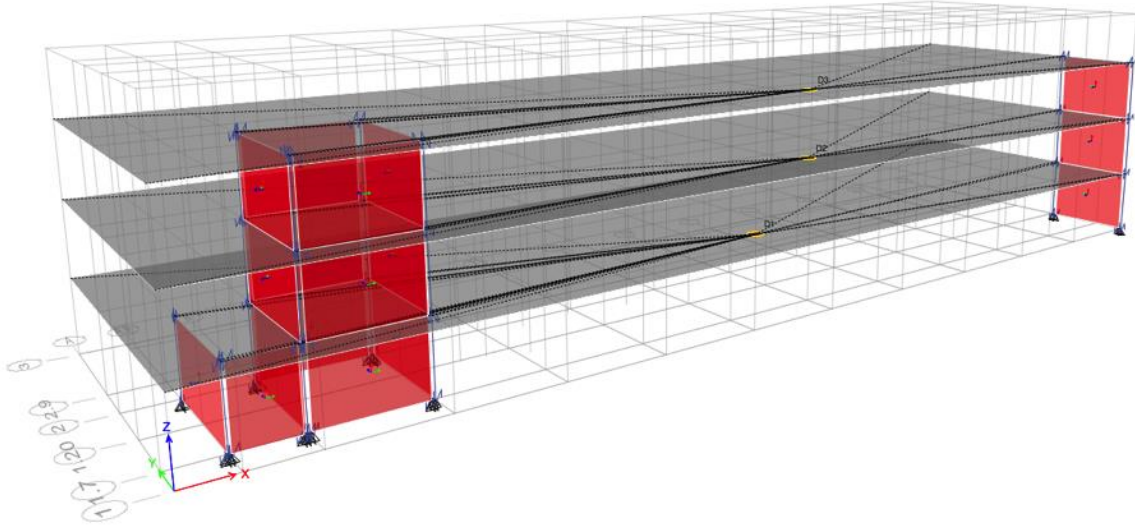


Figure 15: 3D view of ETABS model

Effective Steel Plate Shear Wall Depth

Steel plate shear walls were converted to an effective depth of concrete, due to an instability error that occurred in the model. The simplified rectangular building was modeled with concrete shear walls, which were 2.98" thick. This workaround was possible using the stiffness equation for a shear wall that is assumed fixed-fixed at the top and bottom.

$$k = \frac{1}{\frac{h^3}{12EI} + \frac{1.2h}{AG}}, \quad \text{where } I = \frac{tb^3}{12} \text{ and } A = b \cdot t$$

Equation 1: Stiffness equation for fixed-fixed shear wall

The stiffness of the SPSW was calculated for the various base dimensions, and converted into an effective depth of a concrete shear wall (assuming $f'c = 4000 \text{ psi}$). These calculations can be found in Appendix A.1 - Existing Lateral System Modeling.

Computer Modeling Assumptions

The gravity system of the building was not modeled in this technical report, only the lateral system. The floors were modeled as rigid diaphragms, to transfer the lateral load applied at each level. Heifer International Center has a composite deck and slab floor

system, making it a good approximation of a rigid diaphragm performance. The base condition of the columns and walls were pinned, based on structural documents.

Structural documents indicated that the columns supporting the steel plate shear walls assisted with lateral interactions. An ETABS link was established between the modeled walls and columns, which were able to ensure the column and wall acted as one. A link was established between each column and floor, at each story level.

ETABS Model Validity

The ETABS model proved to calculate forces that were within reasonable engineering judgment. This was based on the transfer of shear forces through the model, for a dummy load of 1000 kips at the top level, in the x-direction. The observed deflections and forces in each of the walls were realistic. This was further established using a built in ETABS shell stress distribution diagram, shown in Figure 16 below.

The dummy load is acting along the length of the building, in the x-direction. This is causing a tensile stress on the left side of the building’s shear walls, and a compressive force on the right side of the shear walls.

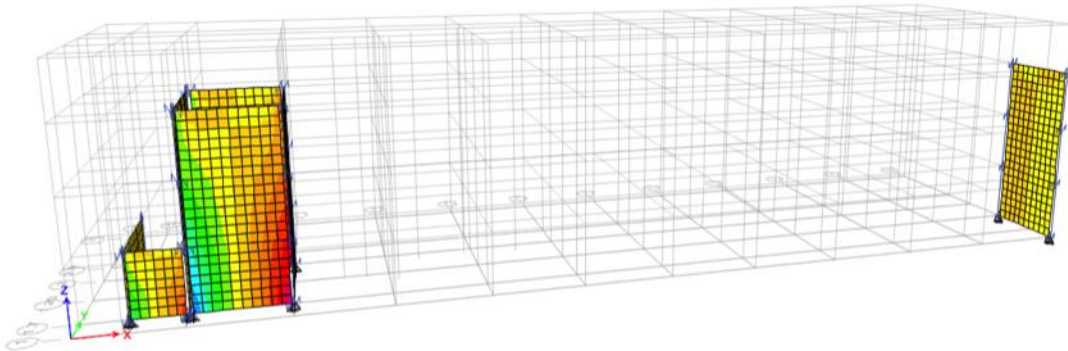


Figure 16: ETABS shell stress distribution diagram

The validity of the model was further confirmed by the inherent torsion formed in the shear walls, after a more detailed examination of the forces and the respective direction of force in each wall. Figure 17 depicts the inherent torsional force formed in the three vertical walls, with a dummy 1000 kip x-direction loading.

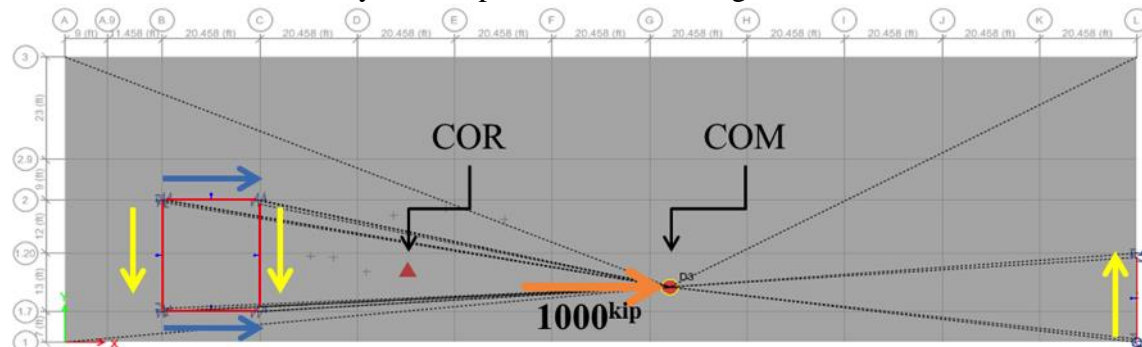


Figure 17: Inherent torsional force formed in walls

Seismic and wind loads also followed a conventional load path, further confirming the validity of the model. For a seismic load applied on the y-direction of the model, the shear forces increased as the load transferred down the building—supportive of normal shear transfer in buildings. This is shown in the 3D view of the building to the right, in Figure 18.

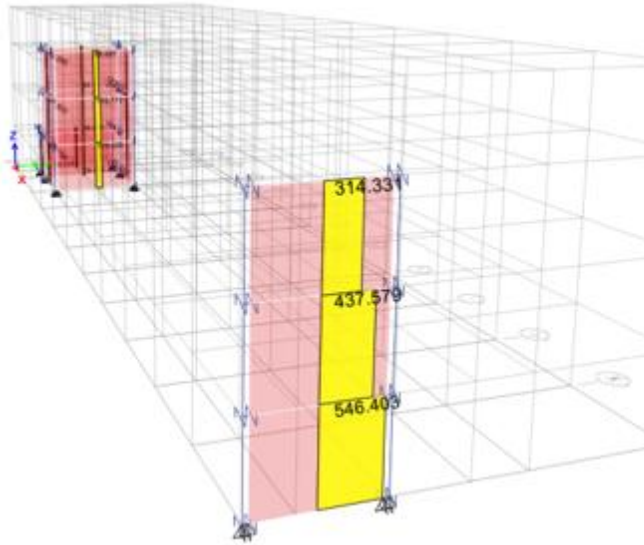


Figure 18: 3D view of shear transfer (seismic y-direction)

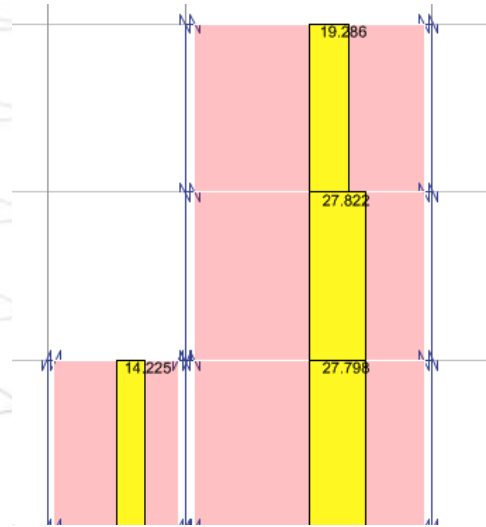


Figure 19: Elevation showing shear decrease on ground floor

A decrease in shear was found in one of the walls, that is explained by the increase in the number of shear walls on this floor. This can be seen on the ground floor of the elevation below, Figure 19, where the shear decreases in the larger shear wall, and is instead picked up by the smaller shear wall offset from the main shear wall on the ground story.

The center of mass and center of rigidity were calculated by the computer, and are shown in Figure 20 below.

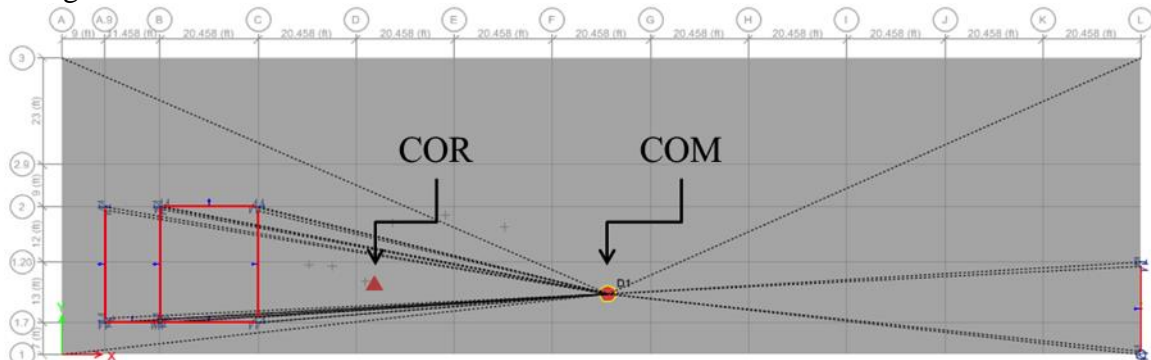


Figure 20: Center of mass and center of rigidity from ETABS

The ETABS model was programmed using pier labeling, and used the convention of Figure 21 in referencing shear walls. This pier labeling convention is used throughout this report.

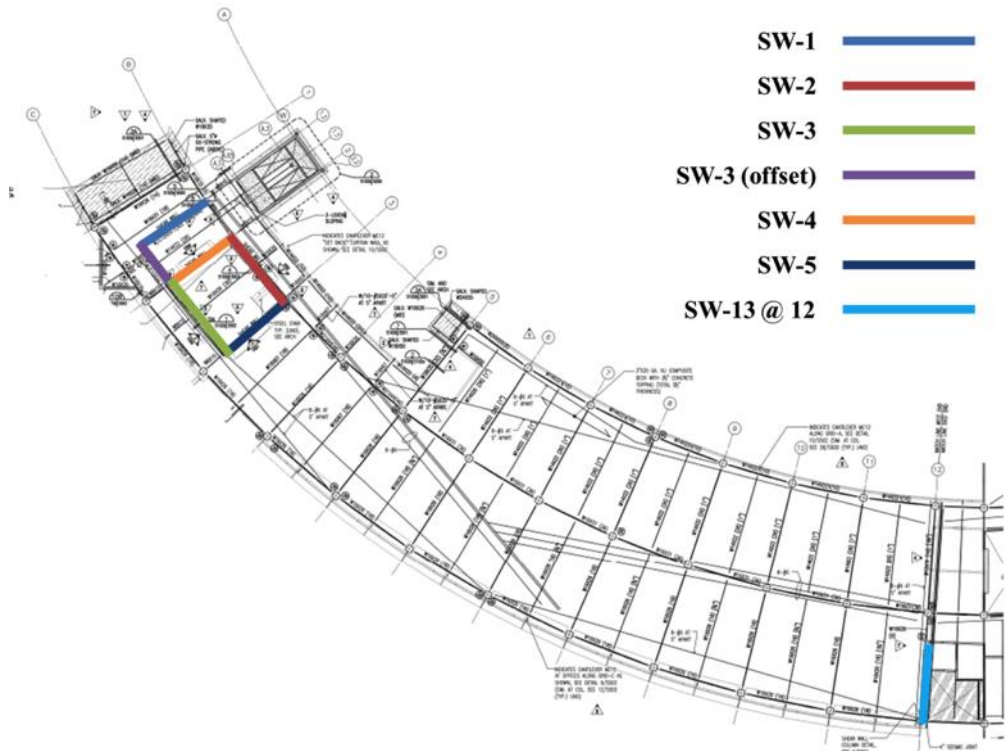


Figure 21: Shear wall pier labeling convention for east side of the building

Seismic Loading

Heifer International Center is located in Little Rock, Arkansas in Seismic Design Category C. The seismic forces experienced by the entire building are summarized below, calculated in compliance with ASCE 7-1998.

Level	w (kips)	w*h ^k	C _{vx}	Story Forces
Stair Tower Top	45	4025	0.008	12
Roof Story	2126	148691	0.307	425
Story 4	3436	161535	0.334	462
Story 3	3358	106928	0.221	306
Story 2	3358	56404	0.117	161
Story 1	3225	6529	0.013	19

Table 7: Seismic Forces for Entire Building

The entire seismic forces were divided by two, to conservatively distribute the forces to the east side of the building, due to the seismic joint. Stair Tower Top, Roof Story and Story 4 each are transferred to the top of the lateral system, which only spans to the base of the fourth floor, as previously discussed in past Technical Assignments. The loads were then analyzed in ETABS 2013 to calculate forces that would be distributed throughout the lateral system. Calculation of the North-South and East-West Seismic Loading can be found in Appendix A.2 - Existing Seismic and Wind Analysis, as well as calculation of inherent and accidental torsions, and the incorporation of amplification factors.

Seismic forces and initial torsional moments, assuming $A_x = 1.0$, were programed into the computer. Deflections at each level were determined for each of the four seismic cases and used to calculate the amplification factor for each respective case. The new amplified torsional moments were then set into the ETABS model, and used to calculate the final shear and moment in each shear wall of the building.

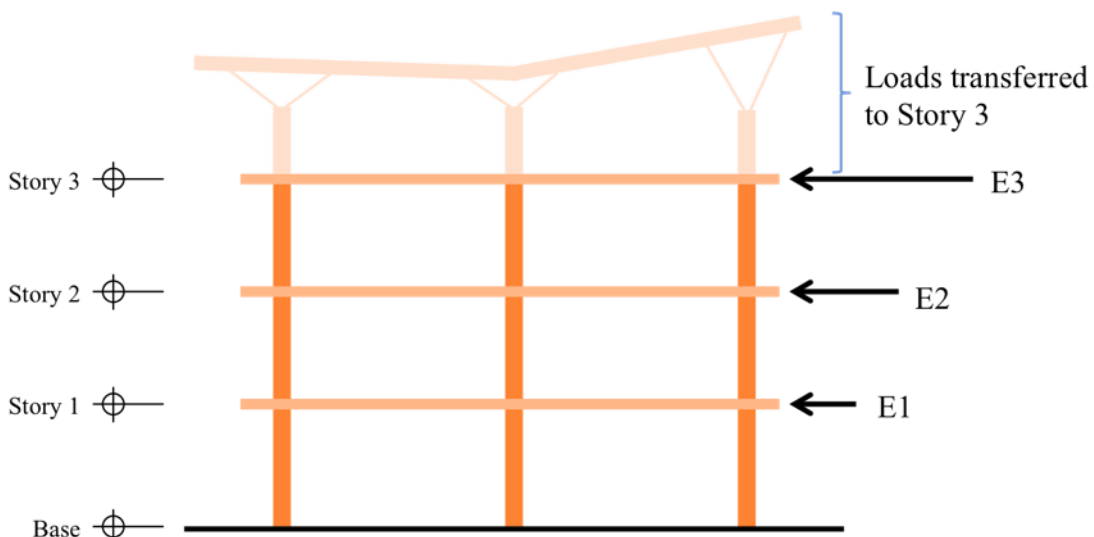


Figure 22: Seismic loading distribution

North-South Seismic Loading

Regular Earthquake Loading (Positive Moment)

	Forces	Moments	X Center of Rigidity	Y
Story 3	449	11026.7	68.0288	17.6914
Story 2	153	3752.0	69.0701	18.2824
Story 1	81	1979.2	68.933	18.5144

A 2.40 amplification factor has been applied to these loads

Table 8: NS Regular earthquake loading (positive moment)

Reverse Earthquake Loading (Negative Moment)

	Forces	Moments	X Center of Rigidity	Y
Story 3	449	17592.8	68.0288	17.6914
Story 2	153	5986.2	69.0701	18.2824
Story 1	81	3157.7	68.933	18.5144

A 1.60 amplification factor has been applied to these loads

Table 9: NS Reverse earthquake loading (negative moment)

East-West Seismic Loading

Regular Earthquake Loading (Positive Moment)

	Forces	Moments	X Center of Rigidity	Y
Story 3	449	1437.3	68.0288	17.6914
Story 2	153	489.1	69.0701	18.2824
Story 1	81	258.0	68.933	18.5144

A 1.0 amplification factor has been applied to these loads

Table 10: EW Regular earthquake loading (positive moment)

Reverse Earthquake Loading (Negative Moment)

	Forces	Moments	X Center of Rigidity	Y
Story 3	449	1437.3	68.0288	17.6914
Story 2	153	489.1	69.0701	18.2824
Story 1	81	258.0	68.933	18.5144

A 1.0 amplification factor has been applied to these loads

Table 11: EW Reverse earthquake loading (negative moment)

Analysis of Seismic Results

It was found that the regular earthquake loading in the y-direction had the largest shear development in a steel plate shear wall, particularly; SW-13 at column line 12, with a shear of 546.403 kips. Calculations also showed that overturning due to earthquake controlled the design. An overturning moment of 24,276 kip-ft was found in both directions, because of the same story forces used in both directions.

Seismic drift was calculated by ETABS, and compared to the maximum allowable drift by code. Each inter-story drift, for each seismic load direction, passed. A tabulation of these results can be found on page 25.

Seismic Story Drift

Drift induced by seismic loading was tabulated in ETABS, and compared to the maximum allowable drift, per ASCE 7-1998.

Seismic story drift from the computer model was amplified using the Deflection Amplification Factor, C_d , and the importance factor, I_e , using §9.5.3.7.1. This was then compared to the maximum allowable inter-story drift, calculated from Table 9.5.2.8. Each story, for each seismic load case, passed the allowable drift.

East-West (EQ_X)

Level	Drift (in)	Story Height (ft)	Maximum Drift Allowed (in)	Delta*Cd/I	Pass
Story3	0.451619	14	3.36	1.354857	PASS
Story2	0.351024	14	3.36	1.053072	PASS
Story1	0.175374	14	3.36	0.526122	PASS

East-West (EQ_X_REVERSE)

Level	Drift (in)	Story Height (ft)	Maximum Drift Allowed (in)	Delta*Cd/I	Pass
Story3	0.449367	14	3.36	1.348101	PASS
Story2	0.349253	14	3.36	1.047759	PASS
Story1	0.174545	14	3.36	0.523635	PASS

*Drift calculated using ETABS Model Joint 14, UX Direction

North-South (EQ_Y)

Level	Drift (in)	Story Height (ft)	Maximum Drift Allowed (in)	Delta*Cd/I	Pass
Story3	0.045525	14	3.36	0.136575	PASS
Story2	0.030472	14	3.36	0.091416	PASS
Story1	0.016139	14	3.36	0.048417	PASS

North-South (EQ_Y_REVERSE)

Level	Drift (in)	Story Height (ft)	Maximum Drift Allowed (in)	Delta*Cd/I	Pass
Story3	0.190831	14	3.36	0.572493	PASS
Story2	0.144547	14	3.36	0.433641	PASS
Story1	0.062941	14	3.36	0.188823	PASS

*Drift calculated using ETABS Model Joint 14, UY Direction

Table 12: Existing seismic story drift

The maximum drift allowed was calculated using the following table for ASCE 7-1998, for seismic loading.

TABLE 9.5.2.8. Allowable Story Drift, Δ_x^a

Structure	Seismic Use Group		
	I	II	III
Structures, other than masonry shear wall or masonry wall frame structures, 4 stories or less with interior walls, partitions, ceilings and exterior wall systems that have been designed to accommodate the story drifts	0.025 h_{sx} ^b	0.020 h_{sx}	0.015 h_{sx}
Masonry cantilever shear wall structures ^c	0.010 h_{sx}	0.010 h_{sx}	0.010 h_{sx}
Other masonry shear wall structures	0.007 h_{sx}	0.007 h_{sx}	0.007 h_{sx}
Masonry wall frame structures	0.013 h_{sx}	0.013 h_{sx}	0.010 h_{sx}
All other structures	0.020 h_{sx}	0.015 h_{sx}	0.010 h_{sx}

^a h_{sx} is the story height below Level x.

^bThere shall be no drift limit for single-story structures with interior walls, partitions, ceilings, and exterior wall systems that have been designed to accommodate the story drifts. The structure separation requirement of Section 9.5.2.8 is not waived.

^cStructures in which the basic structural system consists of masonry shear walls designed as vertical elements cantilevered from their base or foundation support which are so constructed that moment transfer between shear walls (coupling) is negligible.

Table 13: ASCE 7-1998 Table 9.8.2.8 for maximum story drift

Wind Loading

Wind loading on Heifer International Center was calculated using ASCE 7-1998, and simplified to a large rectangle that was 64'-0" x 491'-0". The four story building, with stair tower, results in several distributed loads along the height of the building. These loads can be resolved into point loads at each level. Once again, the Stair Tower, Roof and Fourth story are added to the lateral force on the top of the third story lateral system. ASCE 7-1998 requires tests of the four main wind cases, which are shown below.

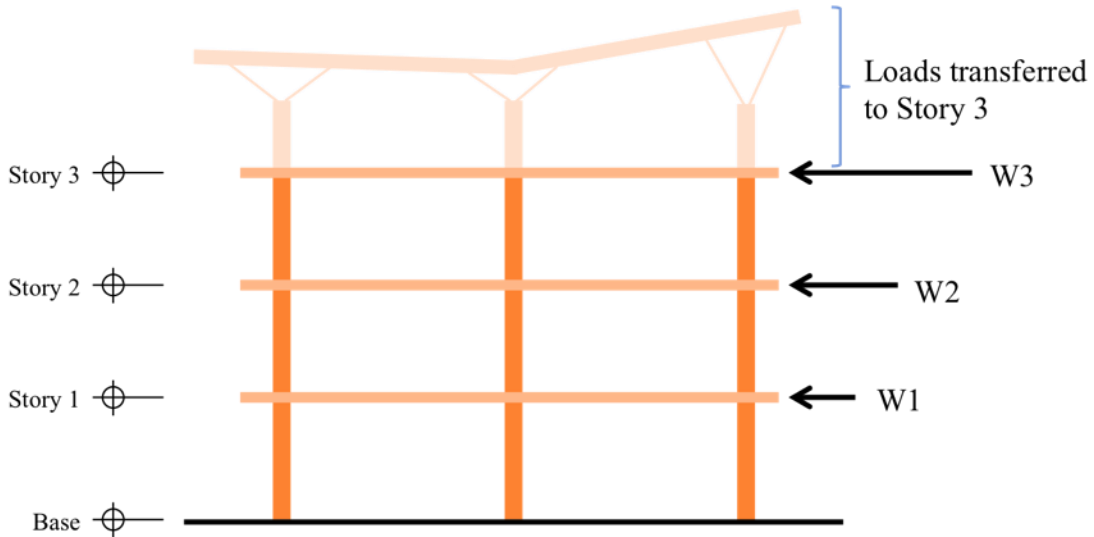


Figure 23: Wind loading distribution

Case 1

A distributed load on each face is applied in the windward and leeward directions. These distributed loads were resolved into a single force in ETABS, for both directions.

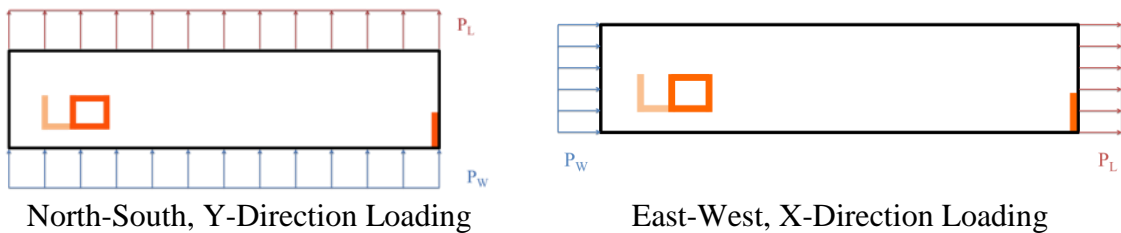


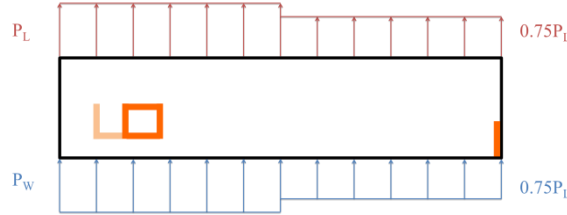
Figure 24: Wind analysis, Case 1, NS and EW

	North-South, Y-Direction			East-West, X-Direction		
	Forces	X	Y	Forces	X	Y
Story3	71.46	112.519	32	130.80	112.519	32
Story2	20.03	112.519	32	38.13	112.519	32
Story1	18.65	112.519	32	34.99	112.519	32

Table 14: Wind analysis, Case 1

Case 2

An unbalanced distributed load on each face was separated into two separate forces, acting in the X and Y directions. Only the worst case torsional effect on the building was tested. These distributions are shown below.



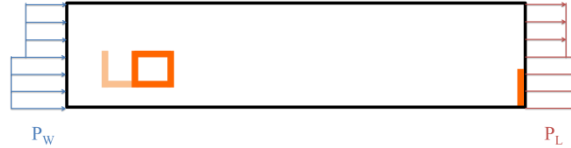
North-South, Y-Direction Loading

Figure 25: Wind analysis, Case 2, NS

North-South, Y-Direction

	1.0P _W and 1.0P _L			0.75P _W and 0.75P _L		
	Forces	X	Y	Forces	X	Y
Story3	192.22	56.25	32	144.17	168.8	32
Story2	52.40	56.25	32	39.30	168.8	32
Story1	47.52	56.25	32	35.64	168.8	32

Table 15: Wind analysis, Case 2, NS



East-West, X-Direction Loading

Figure 26: Wind analysis, Case 2, EW

East-West, X-Direction

	1.0P _W and 1.0P _L			0.75P _W and 0.75P _L		
	Forces	X	Y	Forces	X	Y
Story3	71.46	112.5	16	53.60	112.5	48
Story2	20.03	112.5	16	15.02	112.5	48
Story1	18.65	112.5	16	13.99	112.5	48

Table 16: Wind analysis, Case 2, EW

Case 3

Similar to Case 1, a distributed load on each face is applied in the windward and leeward directions. These distributed loads were resolved into a single force in ETABS, for both directions.

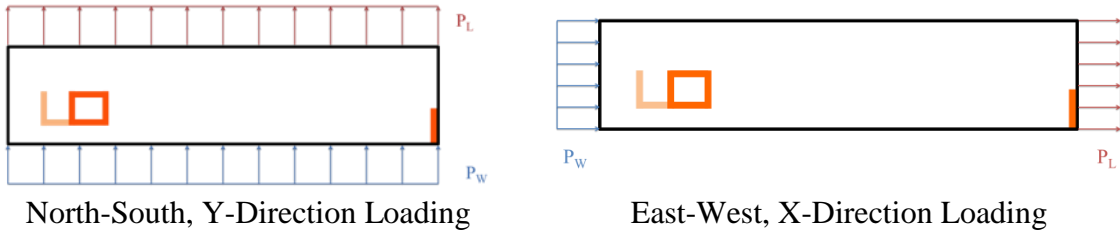


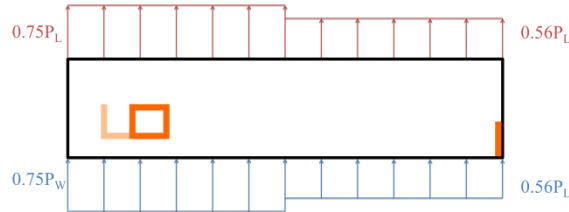
Figure 27: Wind analysis, Case 3, NS and EW

	North-South, Y-Direction			East-West, X-Direction		
	Forces	X	Y	Forces	X	Y
Story3	144.17	112.5	32.0	53.60	112.5	32.0
Story2	15.02	112.5	32.0	15.02	112.5	32.0
Story1	13.99	112.5	32.0	13.99	112.5	32.0

Table 17: Wind analysis, Case 3, NS and EW

Case 4

Case 4 is similar to Case 2. An unbalanced distributed load on each face was separated into two separate forces, acting in the X and Y directions. Only the worst case torsional effect on the building was tested. These distributions are shown below.



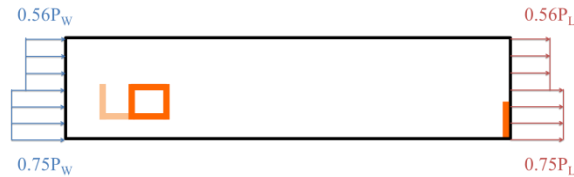
North-South, Y-Direction Loading

Figure 28: Wind analysis, Case 4, NS

North-South, Y-Direction

	0.75P _W and 0.75P _L			0.56P _W and 0.56P _L		
	Forces	X	Y	Forces	X	Y
Story3	53.60	112.5	32.0	144.17	112.5	32.0
Story2	15.02	112.5	32.0	39.30	112.5	32.0
Story1	13.99	112.5	32.0	35.64	112.5	32.0

Table 18: Wind analysis, Case 4, NS



East-West, Y-Direction Loading

Figure 29: Wind analysis, Case 4, EW

East-West, X-Direction

	0.75P _W and 0.75P _L			0.56P _W and 0.56P _L		
	Forces	X	Y	Forces	X	Y
Story3	64.26	112.5	16	40.02	112.5	48
Story2	17.84	112.5	16	11.22	112.5	48
Story1	16.46	112.5	16	10.45	112.5	48

Table 19: Wind analysis, Case 4, EW

Analysis of Wind Results

Analysis of the four cases determined that case 2, in the y-direction would control the design of the lateral system. SW-13 at column line 12 experienced the largest shear, at 208.07 kips. ETABS calculated the drift of the highest level, for each wind case. These drift values were compared to the maximum drift allowed, of $l/400$. Each wind case passed the maximum drift. These results are tabulated below.

While overturning moment was not controlled by wind, it was found the largest moment experienced by the building's base would be 17,860.22 kip-ft due to wind case 2, in the y-direction.

Wind Building Drift

Load Case	Drift (in)	Maximum Drift	
		Allowed (in)	Pass
WIND_C1_X	0.258939	1.95	PASS
WIND_C1_Y	0.444476	1.95	PASS
WIND_C2_X	0.452212	1.95	PASS
WIND_C2_Y	1.027321	1.95	PASS
WIND_C3_X	0.194217	1.95	PASS
WIND_C3_Y	0.484402	1.95	PASS
WIND_C4_X	0.376172	1.95	PASS
WIND_C4_Y	0.767836	1.95	PASS

Table 20: Existing wind building drifts

Torsional Irregularities

Table 9.5.2.3.2 states that if the maximum story drift is more than 1.2 times the average drift of a particular story, irregularity in the building will exist. It was found the torsional irregularities existed in the Seismic Design Category C structure; however, due to the simplified modeling of the building, this may in fact not be true. Torsional irregularity will be studied more in depth in the future.

TABLE 9.5.2.3.2. Plan Structural Irregularities

Irregularity Type and Description	Reference Section	Seismic Design Category Application
1a. Torsional Irregularity	9.5.2.6.4.3	D, E, and F
Torsional irregularity is defined to exist where the maximum story drift, computed including accidental torsion, at one end of the structure transverse to an axis is more than 1.2 times the average of the story drifts at the two ends of the structure along the axis being considered. Torsional irregularity requirements in the reference sections apply only to structures in which the diaphragms are rigid or semi-rigid.	9.5.3.5.2	C, D, E, and F
1b. Extreme Torsional Irregularity	9.5.2.6.4.3	D
Extreme torsional irregularity is defined to exist where the maximum story drift, computed including accidental torsion, at one end of the structure transverse to an axis is more than 1.4 times the average of the story drifts at the two ends of the structure along the axis being considered. Extreme torsional irregularity requirements in the reference sections apply only to structures in which the diaphragms are rigid or semi-rigid.	9.5.3.5.2 9.5.2.6.5.1	C and D E and F
2. Re-entrant Corners	9.5.2.6.4.3	D, E, and F
Plan configurations of a structure and its lateral force-resisting system contain re-entrant corners, where both projections of the structure beyond a re-entrant corner are greater than 15% of the plan dimension of the structure in the given direction.		
3. Diaphragm Discontinuity	9.5.2.6.4.3	D, E, and F
Diaphragms with abrupt discontinuities or variations in stiffness, including those having cutout or open areas greater than 50% of the gross enclosed diaphragm area, or changes in effective diaphragm stiffness of more than 50% from one story to the next.		
4. Out-of-Plane Offsets	9.5.2.6.4.3	D, E, and F
Discontinuities in a lateral force resistance path, such as out-of-plane offsets of the vertical elements.	9.5.2.6.2.11	B, C, D, E, or F
5. Nonparallel Systems	9.5.2.6.3.1	C, D, E, and F
The vertical lateral force-resisting elements are not parallel to or symmetric about the major orthogonal axes of the lateral force-resisting system.		

Table 21: ASCE 7-1998 Table 9.5.2.3.2 Plan Structural Irregularities

Overturning Moment

The overturning moment of the building was calculated by ETABS for each of the seismic and wind cases tested. The resisting moment that is created by the weight of the building was conservatively calculated using the following assumptions:

1. The weight of the building, 15,549 kips, acted at the Center of Mass of the building, not at the geometric center of the building
2. The shortest moment arm of 13'-2" was used in the resisting moment calculation
3. Worst case moment, seismic loading of 24,279 kip-ft acts in either direction and must be resisted by the weight of the building

With these assumptions, a minimum resisting moment of approximately 136,000 kip-ft was calculated. Comparing this to the worst case overturning moment that the building may experience, a factor of safety of 5.6 exist between the worst case overturning moment and the lowest possible resisting moment. The calculation of the overturning moment and resisting moment can be found on the following page.

Foundation Impact

The overturning moment check confirmed that the foundation was adequate for both wind and seismic loading. Uplift was not considered in these calculations and will have to be explored in more detail in the future.

Overturning Moment Calculations

Overturning Moment and Base Shear

Wind Base Shear and Overturning Moment			
Load Case	Base Shear Vx (kip) Vy (kip)	Overturning Moment Mx (kip-ft) My (kip-ft)	
EQ_X	-683 0	0 -24276	
EQ_X_REVERSE	-683 0	0 -24276	
EQ_Y	0 -683	24276 0	
EQ_Y_REVERSE	0 -683	24276 0	

Wind Base Shear and Overturning Moment

Load Case	Base Shear Vx (kip) Vy (kip)	Overturning Moment Mx (kip-ft) My (kip-ft)	
WIND_C1_X	-110.14 0	0 -3823.26	
WIND_C1_Y	-203.92 -22944.875	7051.1 0	
WIND_C2_X	-192.75 0	0 -6690.88	
WIND_C2_Y	0 -511.25	17860.22 0	
WIND_C3_X	-82.61 0	0 -2867.62	
WIND_C3_Y	0 -219.11	7654.5 0	
WIND_C4_X	-160.25 0	0 -5570.18	
WIND_C4_Y	0 -382.71	13369.72 0	

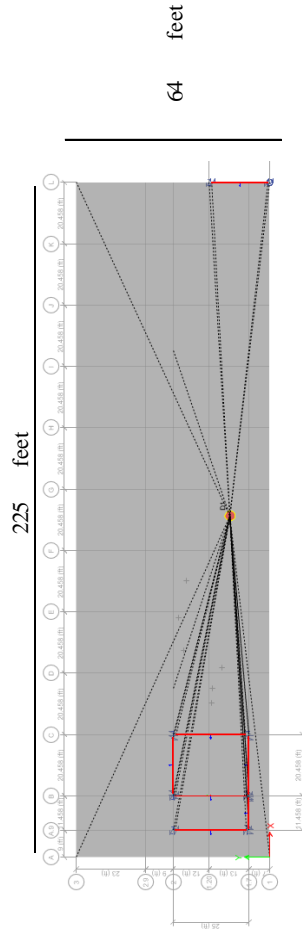
Maximum Moment = 24,276.00 kip-ft experienced by building (assume worst case moment in either direction)
 Resisting Moment = 136,346.93 kip-ft from the weight of the building (assuming smallest moment arm and factor of safety of 1.5)

PASS

Factor of Safety = 5.62

Center of Mass
 X = 113.8292 feet
 Y = 13.1533 feet

Building Effective Weight
 w = 15549 kip



Energy/Virtual Work Diagram

The ETABS computer model was able to calculate the utilization of each member, for each load case. Figure 30 and Figure 31 illustrate how the steel plate shear wall is employed more in resisting lateral loads closer to the base of the building. It should be noted that in Figure 30 the SPSW utilization drops on the first floor, because of the additional shear wall offset on this floor, next to Shear Wall 3.

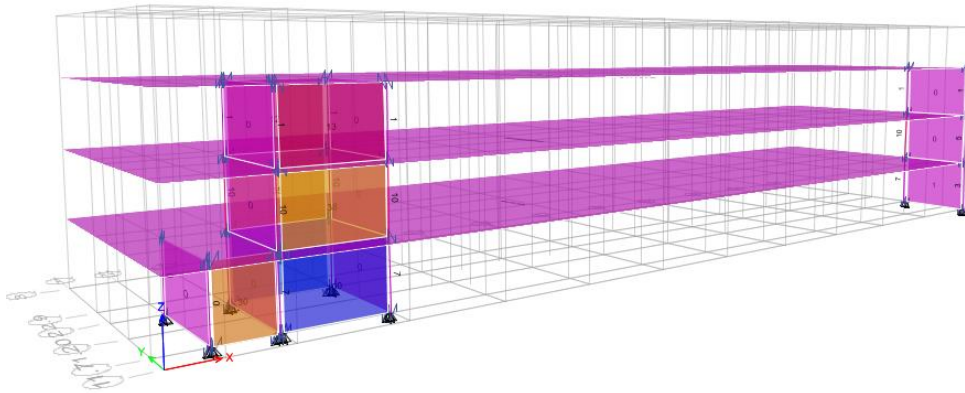


Figure 30: 3D view of member utilization, x-direction loading

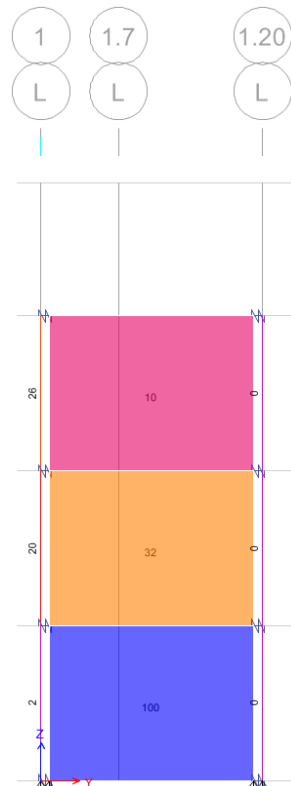


Figure 31: Member utilization of Shear Wall 13 at 12, y-direction loading

Lateral System Spot Checks

The shear in each steel plate shear wall was calculated and compared, for each seismic and wind load case. The largest shear value was tabulated, and this shear wall was analyzed for shear capacity and deflection. This shear wall, SW-13 at column line 12 was controlled by seismic loads.

The ASCE 7-1998 was referenced for the load combinations, which are shown below in Figure 32.

2.3.2 Basic Combinations

Structures, components, and foundations shall be designed so that their design strength equals or exceeds the effects of the factored loads in the following combinations:

1. $1.4(D + F)$
2. $1.2(D + F + T) + 1.6(L + H) + 0.5(L_r \text{ or } S \text{ or } R)$
3. $1.2D + 1.6(L_r \text{ or } S \text{ or } R) + (0.5L \text{ or } 0.8W)$
4. $1.2D + 1.6W + 0.5L + 0.5(L_r \text{ or } S \text{ or } R)$
5. $1.2D + 1.0E + 0.5L + 0.2S$
6. $0.9D + 1.6W + 1.6H$
7. $0.9D + 1.0E + 1.6H$

Figure 32: Basic Combinations for ASCE 7-1998

The worst case load combination controlling was load case 5. Load case 7 was eliminated due to the lack of soil loads on Heifer International Center's lateral system. Load case 5 was calculated and applied to the shear walls. These detailed calculations are found on the following pages.

SPSW Load Combinations

PORTER-GILL		SHEAR WALL CHECK
<p>CONTROLLING SHEAR WALL → SW-13 @ 12</p> <p>CONTROLLED BY SEISMIC</p> <p>$V_{MAX} = 546.403^k$</p> <p>TRIB AREA = 110 SF</p> <p>LOAD CASES</p> <p>(5) $1.2D + 1.0E + 0.5L + 0.2S$</p> <p>(7) $0.9D + 1.0E + 1.6H$ → REDUCES DL, ↑'S OT (NO SOIL LOADS)</p> <p>(5) AXIAL LOADS</p> $P_0 = 1.2D + 0.5L + 0.2S + 1.0E_{VERTICAL}$ $= 1.2[95 \text{ PSF} \times 110 \text{ SF}] \times 3 + 0.5[80 \text{ PSF} \times 110 \text{ SF}] \times 3$ $+ 0.2[10 \text{ PSF} \times 0.5 \text{ SF}] \times 3 + 1.0[0.2(0.3704)(31.35^k)] \times 10000$ <p style="margin-left: 150px;">DISCONT. ↑ FROM ACDF</p> <div style="border: 1px solid black; padding: 5px; width: fit-content; margin-left: 450px;">= 53.14^k AXIAL</div> <div style="border: 1px solid black; padding: 5px; margin-top: 10px;"> <p>$E_{VERTICAL} = 0.2S_{ps} D$ § 9.5.2.17 Eq. 1</p> <p>$S_{ps} = 0.3704 > 0.125$ → YES INCLUDE VERTICAL COMPONENT</p> <p>$p = 10 \text{ W/C SDC C}$ § 9.5.2.4.1</p> <p>$D = 95 \text{ PSF} \times 110 \text{ SF} \times 3 \text{ FLOORS} = 31.35^k$</p> </div>		

PORTER-GILL

SHEAR WALL CHECK

(5) LATERAL

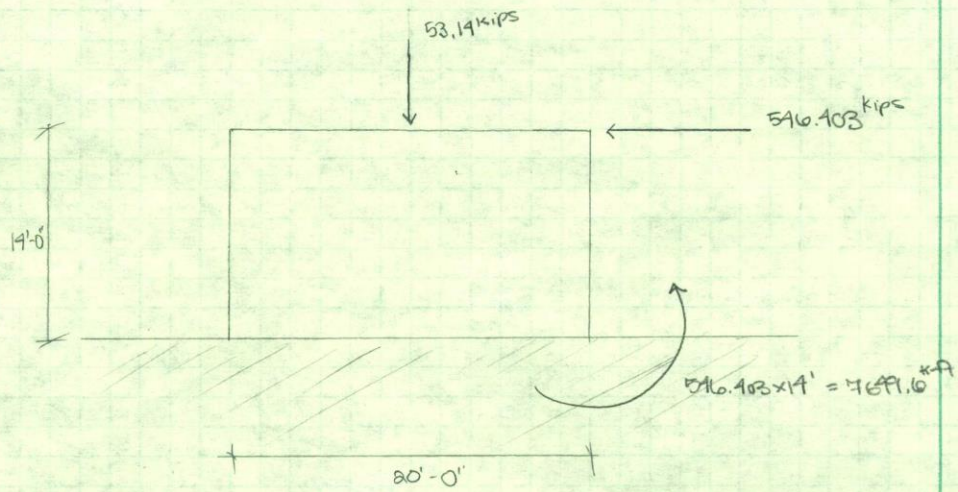
$$L = 1.0 E_{HORIZONTAL} = p Q_E$$

$$p = 1.0 \text{ b/c SDC C } \approx 9.629.1$$

$$Q_E = 546.403^k$$

$$L_o = 1.0(546.403^k) = 546.403^k$$

WE CAN CONCLUDE:



SPSW Shear Capacity

PORTER-GILL	TECH REPORT 4	SHEAR WALL CHECK
-------------	---------------	------------------

CHECK SHEAR CAPACITY OF SPSW:

$V_u = V_{max} = 546.103^k$ w/ QUAKE-Y

SPSW DETAILS:

$t_w = 3/8"$
 $F_y = 36 \text{ ksi STEEL, A36}$
 $\phi = 0.9 \text{ FOR SPSW}$

$$\phi V_n = \phi \cdot 0.12 \cdot F_y \cdot t_w \cdot l_{cp} \cdot \sin(2\alpha)$$

$$l_{cp} = 20' - \left(\frac{12.3''}{2} + \frac{24''}{2} \right) / 12'' = 18.4875'$$

$\therefore \phi V_n = 0.9(0.12) \cdot 36 \cdot (3/8'') \cdot (18.4875') \cdot \sin(2 \cdot 30^\circ)$

CONSERVATIVELY ASSUME \rightarrow

$= 980.48^k$

[if $\alpha = 45^\circ$, $\phi V_n = 1119.9^k$]

$\phi V_n = 980^k \geq 547^k = V_u \quad \checkmark$ GOOD

EACH SPSW IS $3/8"$ THICK \rightarrow ALL LOADS LOWER

SHEAR CAPACITY GOOD FOR ALL SPSW'S \checkmark

SPSW Deflection Check

Deflection of the steel plate shear walls were checked at two joints, on each seismic and wind load case. These two joint locations passed the maximum allowed drift for seismic and wind loads. These results are tabulated below, with drift shown with respect to the direction of loading. Please refer to Figure 33 for the location of the two joints measured.

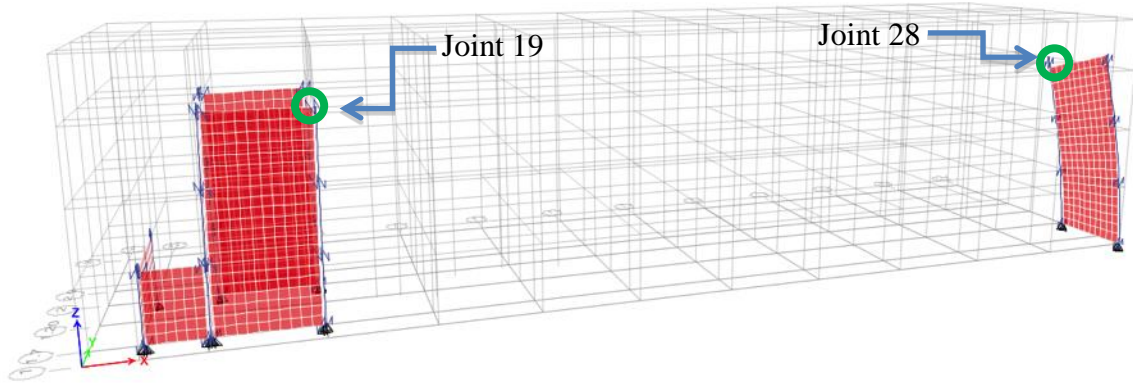


Figure 33: Diagram showing location of joints referenced

Seismic Loading

Joint 19 at Shear Wall 3

Level	Drift (in)*	Story Height (ft)	Maximum Drift	
			Allowed (in)	Pass
East-West (EQ_X)	1.64307	14	3.36	PASS
East-West (EQ_X_REVERSE)	1.6392	14	3.36	PASS
North-South (EQ_Y)	0.40581	14	3.36	PASS
North-South (EQ_Y_REVERSE)	0.710209	14	3.36	PASS

Joint 28 at Shear Wall 13@12

Level	Drift (in)*	Story Height (ft)	Maximum Drift	
			Allowed (in)	Pass
East-West (EQ_X)	1.6305	14	3.36	PASS
East-West (EQ_X_REVERSE)	1.63101	14	3.36	PASS
North-South (EQ_Y)	2.8103	14	3.36	PASS
North-South (EQ_Y_REVERSE)	1.10398	14	3.36	PASS

*Drift with respect to direction of loading

Table 22: Steel plate shear wall deflection check (seismic)

Wind Loading

Joint 19 at Shear Wall 3

Level	Drift (in)*	Story Height (ft)	Maximum Drift	
			Allowed (in)	Pass
WIND_C1_X	0.235866	14	1.95	PASS
WIND_C1_Y	0.182638	14	1.95	PASS
WIND_C2_X	0.3346	14	1.95	PASS
WIND_C2_Y	0.483166	14	1.95	PASS
WIND_C3_X	0.189796	14	1.95	PASS
WIND_C3_Y	0.199211	14	1.95	PASS
WIND_C4_X	0.369934	14	1.95	PASS
WIND_C4_Y	0.361898	14	1.95	PASS

Joint 28 at Shear Wall 13@12

Level	Drift (in)*	Story Height (ft)	Maximum Drift	
			Allowed (in)	Pass
WIND_C1_X	0.255909	14	1.95	PASS
WIND_C1_Y	0.444476	14	1.95	PASS
WIND_C2_X	0.447805	14	1.95	PASS
WIND_C2_Y	1.027321	14	1.95	PASS
WIND_C3_X	0.191944	14	1.95	PASS
WIND_C3_Y	0.484402	14	1.95	PASS
WIND_C4_X	0.372965	14	1.95	PASS
WIND_C4_Y	0.767836	14	1.95	PASS

*Drift with respect to direction of loading

Table 23: Steel plate shear wall deflection check (wind)

Lateral System Conclusion – Simplified Model

Computer modeling of the lateral system of Heifer International Center was performed for the building. Though the ETABS model of the curved office complex did not properly execute, a simplified version of the building was used in the analysis of the lateral system. Half of the building was modeled in ETABS due to the seismic joint that splits the building at approximately its midpoint. Spot checks on lateral elements were performed, and the existing lateral system was found to be adequate for the loads anticipated on the structure.

Seismic loading in the North-South direction controlled the design, with a maximum base shear of 550 kips. The controlling case for wind loading was the y-direction, using Case 2, at a base shear of 210 kips. The 550 kip lateral force was used in the verification of the shear capacity of the steel plate shear wall. This maximum lateral force on the ground level, that the steel plate shear wall must endure, passed with over 400 kips of reserve shear capacity. Each shear wall in the model is the same thickness, thus all shear walls in the building are adequate. Deflection of the shear wall was also tested, and found to pass for both seismic and wind loading. The existing lateral system was found to be sufficient for lateral loads for the Heifer International Center.

Inter-story drift and building drift were found to be within the ASCE 7-1998 maximum allowable drift. Furthermore, the overturning moment was found to have no impact on the foundation system.

A more all-inclusive and definitive computer model was developed later in the report, which can be found in section 2.2 Lateral System Redesign, which more accurately modeled the building and its reaction to various lateral loadings.

1.7 PROBLEM STATEMENT

The Heifer International Center is currently framed in steel with a composite deck; however, the architect wishes to consider a hybrid system of glulam and steel. Their intention is to see if the architectural features of the Education and Visitor Center, a smaller building next door, may also be applied to the Heifer International Center. In addition, a floor system will need to be researched, compared and selected.

The previous Technical Reports II and IV analyzed the existing building's gravity and lateral systems, under ASCE 7-1998. Technical Report III analyzed alternative floor systems using ASCE 7-2010. Each phase of the redesign will reference ASCE 7-2010.

The redesign will affect mechanical and architectural characteristics of the Heifer International Center. Their affects will need to be considered in a systems investigation through the use of two breadths. Due to the use of combustible material, the glulam, as the structural framing, the new classification of the building is Type IV Construction per the International Building Code 2009 §602.4 (existing structure is classified as Type IIIB). This classification negates the use of the current Underfloor Air Distribution System and a new overhead VAV system will be used. Exposed structural members will be changed and these new features will need to be considered in the revised glulam design.

The gravity system of Heifer International Center will be redesigned in glulam and the current layout of the lateral system will be kept. However, in order to better understand a wider variety of lateral force resisting systems, a concrete shear wall will be studied. It is important to understand why a steel plate shear wall was selected in the original design and examine whether it was crucial for the design.

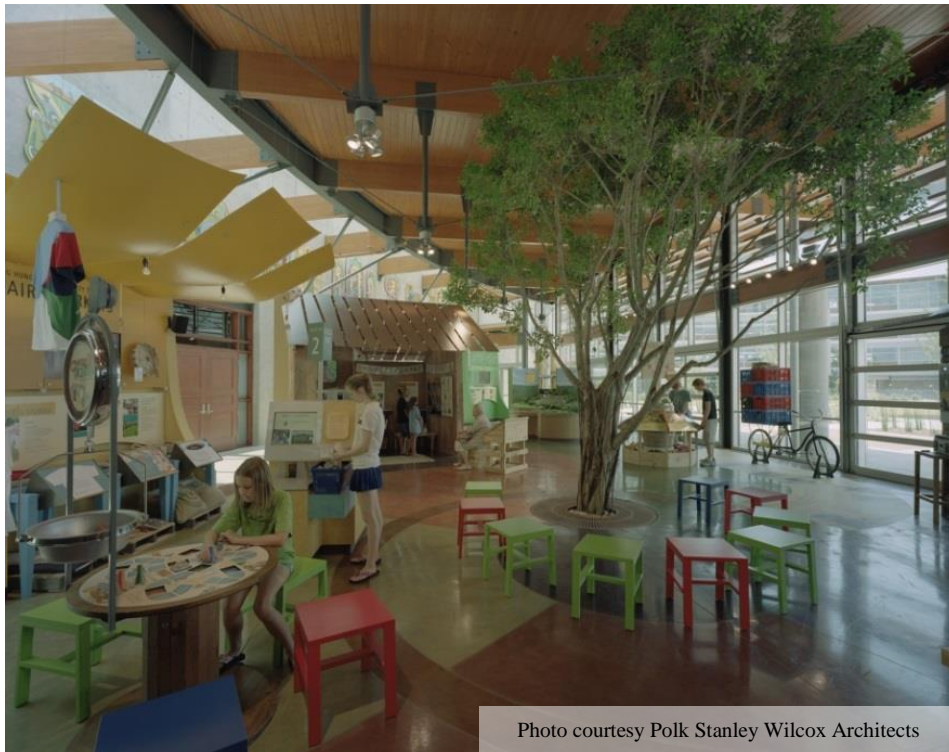


Photo courtesy Polk Stanley Wilcox Architects

Figure 34: Heifer International Education and Visitor Center

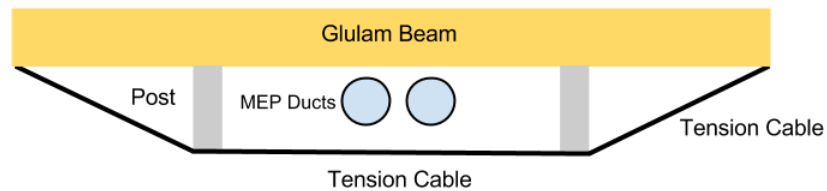
1.8 PROPOSED SOLUTION

The selection of the glulam redesign for the gravity system leaves five potential floor systems that must be considered.

1. Tongue and groove wood plank
2. Concrete floor system
3. Composite concrete and wood system
4. Steel decking and concrete system
5. Post tensioned slab system

These five floor systems will be researched and the most practical floor system for the Heifer International Center's glulam beam gravity redesign will be chosen. The glulam beams will be reinforced with tension cables; in a queen post truss design. This advanced modification to a glulam beam may prove beneficial in integration between the structural, mechanical and architectural disciplines. Due to aesthetics and the ease of connection of the glulam beams, the current HSS columns will be kept in the redesign.

Option 1 - Queen Post with Tension Cable



Option 2 - Queen Post with Curved Tension Cable

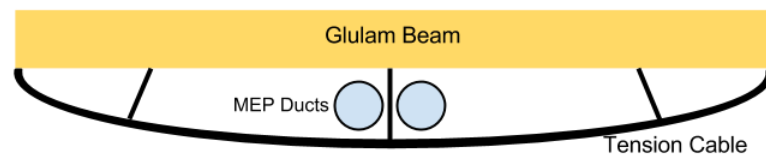


Figure 35: Potential queen post options

Figure 35 shows two potential designs of the queen post truss. Each design relies on posts which hold the tension cable out and away from the primary beam. This queen post truss increases the strength of the system and can be designed to add a slight camber into the primary beam. The queen post truss will be analyzed using SAP2000 with a combination of hand calculations.

The lateral system will be redesigned to incorporate concrete shear walls. This new design will be compared to a steel plate shear wall to determine the utility of the steel plate shear wall used in the current building. Due to difficulties previously experienced in Technical Report IV, a RAM Structural System model will be developed for the computer modeling aspect of the project.

Due to the use of combustible framing material, the building must be reclassified as Type IV Construction. This new classification will negate the use of the current Underfloor Air Distribution System because the use of concealed spaces is excluded from Type IV Construction of the International Building Code 2009 §602.4. Exposed structural members will be changed, and these new features will need to be considered in the revised glulam design.

Furthermore, the use of an architectural guideline will aid in the proper development of structural and mechanical systems, in order to respect and expand upon the architectural characteristics of the Visitor and Education Center.

Breadth Topics

Mechanical and Envelope

A glulam beam system will be used in the redesign of Heifer International Center. Due to the updated construction type, the Underfloor Air Distribution System will be negated. The mechanical system will have to be changed to a new overhead ductwork system. This new system will need to be hung from the ceiling—and it is important that it is incorporated into the revised structural system so it will visually respect other engineering options. The mechanical system will be able to integrate into the queen post, option 1 or 2, previously discussed in this report.

The mechanical breadth will involve generally sizing the building's supply and return ducts and ensuring that the ducts are able to fit through the designed queen post. Due to the open office plan of Heifer International Center, careful consideration will need to be taken in the placement of ductwork and its architectural influence. A study will be performed to understand the new structural system's impact on the thermal envelope, and what may be done to reduce the number of thermal bridges in the current design.

Architectural

Due to the drastic change in structural building materials an architectural study will be performed to understand how the glulam redesign changes the Heifer International Center. The lateral system redesign should not have an effect on architectural considerations. The Education and Visitor Center next door to the Heifer International Center will be used as a design guide to develop architectural characteristics that should be considered during the duration of the structural redesign. This design guide will influence both structural and mechanical disciplines. Revit and AutoCAD will be used to produce renderings of the new architectural features, and the final effect they have on the design.

MAE Coursework Requirement

Coursework of the Graduate School of the Pennsylvania State University will be incorporated into the redesign of the Heifer International Center. AE 530 – Advanced Computer Modeling of Building Structures will be referenced to develop an advanced Bentley RAM Structural System model of the office building. Additionally, a CSi SAP2000 model may be used to analyze, in detail, the potential queen post that will be used in the redesign. In addition, AE 538 – Earthquake Resistant Design of Buildings will be integrated into the design of the lateral force resisting system.

Schreyer Honors College Requirement

This thesis work will be submitted in order to fulfill requirements set by the Schreyer Honors College and the Department of Architectural Engineering. An in depth literature review will be performed of a composite concrete and wood floor system. The intent of this research review will be to gain professional experience as a future Engineering of Record having to specify a floor system not referenced in the International Building Code. The Engineer of Record would have to perform an examination of the proposed system, a composite concrete and wood system, to ensure that it will be safe in the building. This will provide a challenging, in depth examination, of a complex system and reference the work of Dr. Walter G.M. Schneider.

1.9 CONCLUSION TO PROPOSED SOLUTION

A scenario has been created, in which the architect is requesting an alternative material for the structure of the Heifer International Center. The architect wishes to explore a different structural material, for aesthetic purposes, due to the fact that the existing system is exposed. A new hybrid system of glulam and steel will be chosen and will provide a unique opportunity to investigate a queen truss. This will lead to integration between the mechanical and structural disciplines. The building will be reclassified as Type IV, per the International Building Code 2009 §602.4, and will prevent the use of the current Underfloor Air Distribution System. This obstacle will lead to a new overhead system, general sizing of ductwork and the careful placement of this ductwork to respect their aesthetic appearance. A study will be performed to understand the new structural system's impact on the thermal envelope, and how this will in turn affect the mechanical system. Mechanical and electrical equipment can be incorporated into and hung from the queen post truss.

The lateral system of the Heifer International Center will be redesigned using concrete shear walls. This new design will be compared to a steel plate shear wall at the end of the spring semester, to determine the utility of the steel plate shear wall used in the current building.

Furthermore, an architectural study will be performed on the new exposed structural system, comparing the designed system to the architectural intent of the Visitor and Education Center, next door to the Heifer International Center.

This project will present a challenging and in depth investigation of a complex structural gravity and floor system, while also expanding the mechanical and architectural breadths. These two breadths will be directly influenced by the designed structural system, and will pose a unique integration between the three disciplines. For this to be evaluated, an architectural model will be created to compare the existing and redesigned office building.

Graduate level course work will be referenced from AE 530 – Advanced Computer Modeling of Building Structures to develop an advanced CSi ETABS model or a Bentley RAM model of the office building. Knowledge gain in AE 538 – Earthquake Resistant Design of Buildings will be integrated into the design of the lateral force resisting system.

CHAPTER 2

STRUCTURAL DEPTH

2.1 GRAVITY SYSTEM REDESIGN

This section summarizes the gravity system redesign of the Heifer International Center, in which the primary structural material changed from steel to glulam. Glulam beams were used in conjunction with an engineered queen post girder, specifically designed for the Heifer International Center. The gravity system redesign encompassed a combination of 2D hand calculations and computer analysis, with the additional aide of Microsoft Excel. One of the primary goals of the gravity redesign was to minimize changes to the layout of the Heifer International Center, while still adding a new architectural feature to the interior space. Each skewed bay of the curved building, Figure 37, was idealized as 25'-0" x 29'-0" rectangular bays, shown in Figure 36. With the selection of glulam as the primary gravity structural material, five potential floor systems were investigated.

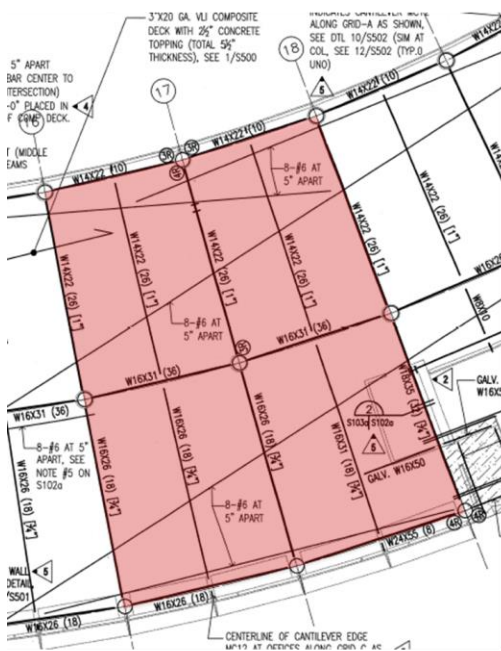


Figure 36: Typical floor plan

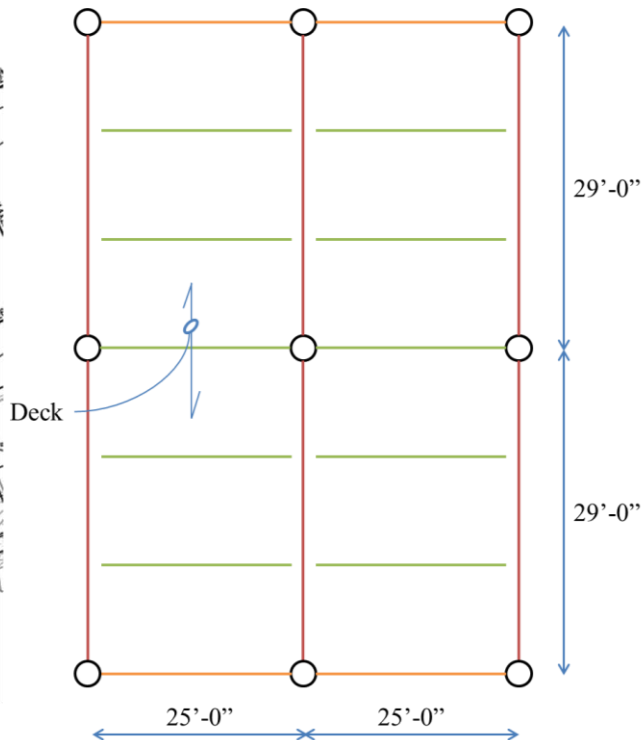


Figure 37: Simplified floor plan

Figure 37 shows the layout of regular glulam beams in green, the designed queen post girder in red and the exterior perimeter beams in orange. The existing HSS24x0.5 columns remained in the redesign and are indicated in black. The conservatively sized 25'-0" x 29'-0" bay was used for the calculation of loads and in the design of member sizes.

Considerations of the Typical Bay Layout

The redesign concentrated on the typical bays of the office and roof, with the objective of integrating the mechanical, electrical and architectural elements of the building. Due to the complexity of the building, a typical office bay was chosen, which extends from the second to the fourth levels, as well as a typical roof bay. Five potential floors systems were investigated and are summarized in Table 24,

<i>Potential Floor System</i>	<i>Advantages and Disadvantages</i>
Tongue and groove wood plank	- Spacing will be an issue
Concrete floor system	- Additional weight may be of concern - Would not match architectural style of building
Composite concrete and wood system	- Intricate calculations required
Steel decking and concrete system	+ In use in existing building + Would match redesign of building
Post tensioned slab	- Not an economical solution - Would have to span in the short distance thus decreasing the utility of the post tensioning

Table 24: Floor system comparison

After thorough examinations of these floor systems, the steel decking and concrete system was chosen, due to its ability to match up closely with the intended architectural style. This system also offered the possibility of reduced cost by using an industry standard composite decking material.

The preliminary design of a typical office bay only included beams running between columns, with a clear span of 25'-0" between beams. It was found that floor decking would not be able to span this distance, even with the aide of shoring. Intermediary beams had be added to adequately support the decking, causing the beam running between the columns to be converted to a girder. This girder became the queen post that would later be designed to have mechanical and electrical equipment pass through it.

Composite Decking Selection

A 3VLI 20 gauge composite deck with 2 ½" of normal weight concrete topping, making a total thickness of 5 ½", was chosen as the decking to span in the 29'-0" direction. The decking will not compositely act with the framing members, due to the lack of shear studs and wide flanges. For this reason the decking is unable to take advantage of concrete in compression and steel in tension (Nucor Corporate, 2013).

Beam Design of Typical Floor and Roof

The beams spanning between the queen post girders must support a tributary area of approximately 10'-0" of dead and live load, highlighted in yellow on Figure 38. The beam members being designed are in green. This significant load must be carried by the newly designed glulam beam. The final design of the beams called for the two items below,

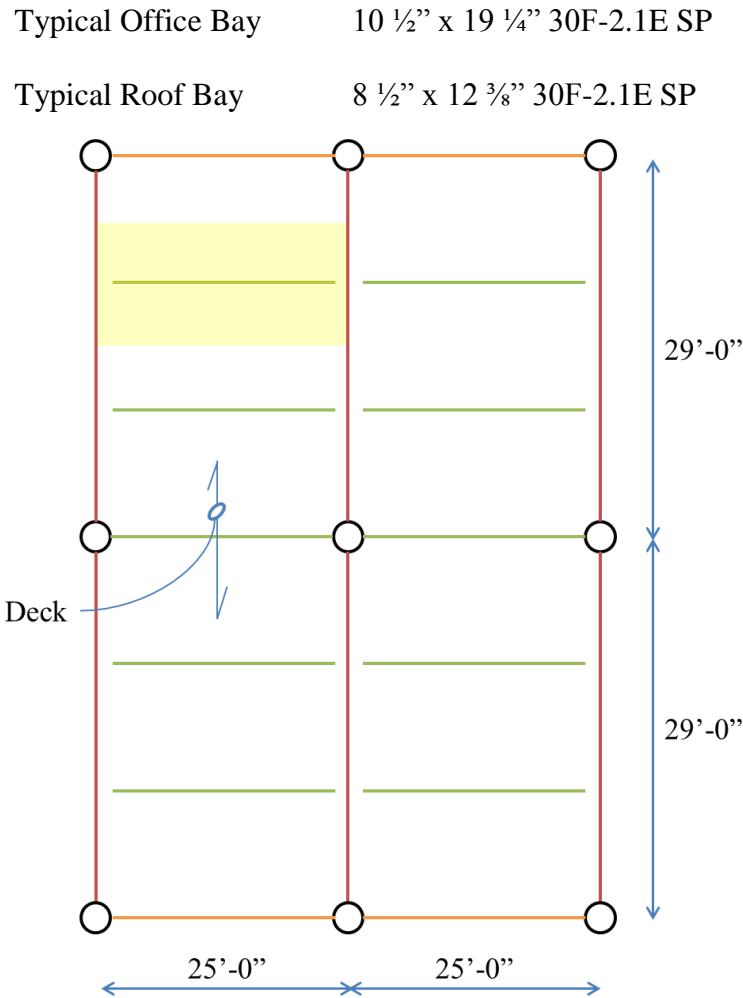


Figure 38: Beams, girders and perimeter beams of typical office

Calculations for sizing the beam can be found in Appendix B.1 - Typical Office Beam Design. These members were designed primarily for bending, per Table 5A of the National Design Standard Supplement. Each of these member sizes will have to be produced by a qualified manufacturer and the final member will be subjected to an additional approval by an accredited inspection agency³. While the depth of the typical floor bay beam is rather large, it should be noted that the floor to floor height is 14'-0", leaving approximately 9'-6" clear distance when considering the 28" deep clearance space for mechanical and electrical equipment and a 5 ½" deep decking. The beams

³ Note 8 page 61 National Design Standard Supplement (American Wood Council, 2013)

supporting the roof are sized in Appendix B.4 - Roof Beam Design and are shown in Figure 39. The same roof decking used in the original design was used in the redesign.

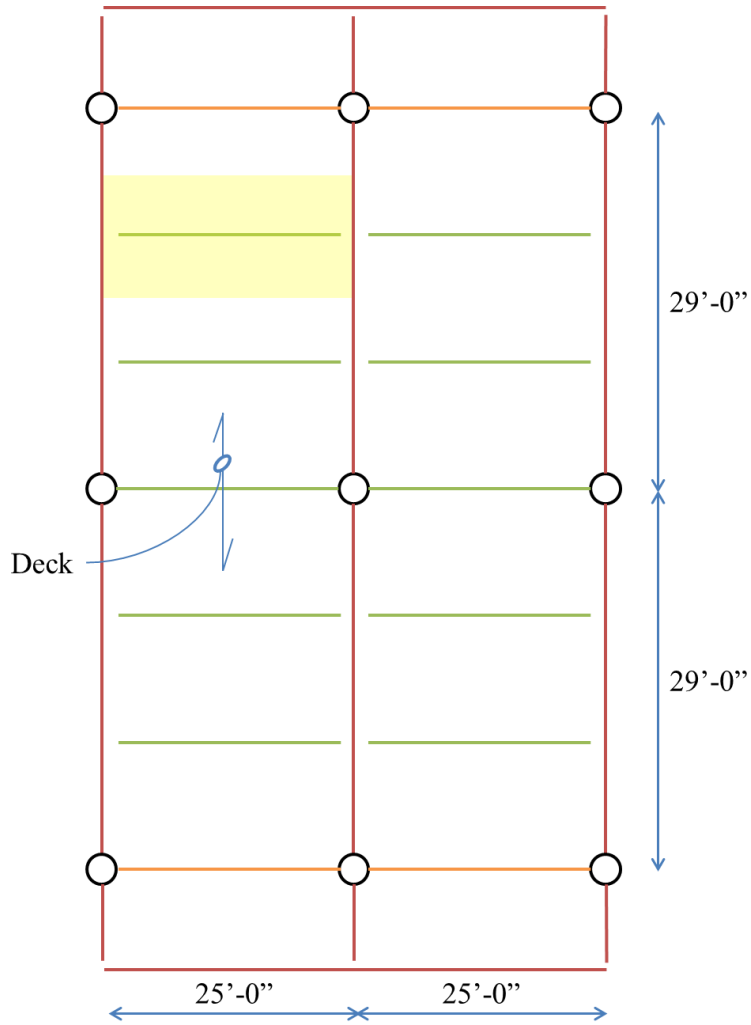


Figure 39: Beams, girders and perimeter beams of roof

The perimeter beams of the typical office bay were designed in both glulam and steel. It was found that the depth of the steel section designed was almost 0'-6" less than the glulam beam sized. These calculations can be found in Appendix B.7 - Typical Office Perimeter Beam, and are shown in orange in Figure 38 and Figure 39 above. The two potential beam size depths vary, allowing more natural light to penetrate the building if the steel wide flange typical office perimeter W14x22 beam is used.

Typical Office Perimeter Beam

Glulam	10 ½" x 17 ⅞" 30F-2.1E SP
Steel	W14x22

The cantilevered section extending past the exterior of the building, on the North and South sides of the typical roof bay were not designed in this exercise. It should be noted that the selection of steel as the perimeter beam material will change the classification of the construction type of the building from Type IV Heavy Timber (HT) to Type IIIB construction, per §602 (International Code Council, 2009).

A reclassification of the building's construction type occurred during the redesign phase and is summarized in Table 25.

	Existing Structure	Redesign (with glulam perimeter)	Redesign (with steel perimeter)
IBC Code	2000	2009	2009
Occupancy Type	Business – Group B	Business – Group B	Business – Group B
Construction Type	IIB	IV	IIIB
Max. Height	75'-0"	65'-0"	75'-0"
Max. Stories	5	5	4
Max. Allowable Area Per Floor	53,438 SF	36,000 SF	60,648 SF
Fire Rating	0 hours	Min. HT ⁴	0 hours

Table 25: IBC 2009 Construction type classification summary

⁴ The minimum width and depth per IBC 2009 was referenced in the design of the HT members.

Queen Post Girder Design

Several iterations were considered for the queen post girder design. The basic principle of an inverted queen post is to reduce the amount of flexure on the member, thus reducing the required size of the member. This is accomplished by transferring a significant portion of the shear, blue on Figure 40, through a post or posts located along the length of the member. This shear is converted into axial compression in the post, shown in red, which in turn is transferred as tension through the cable, shown in green. This tension force in the cable is transferred up into the top chord of the queen post as an axial force, yellow. This causes the top chord member to act primarily in axial compression, but reduces the moment by approximately one-tenth.

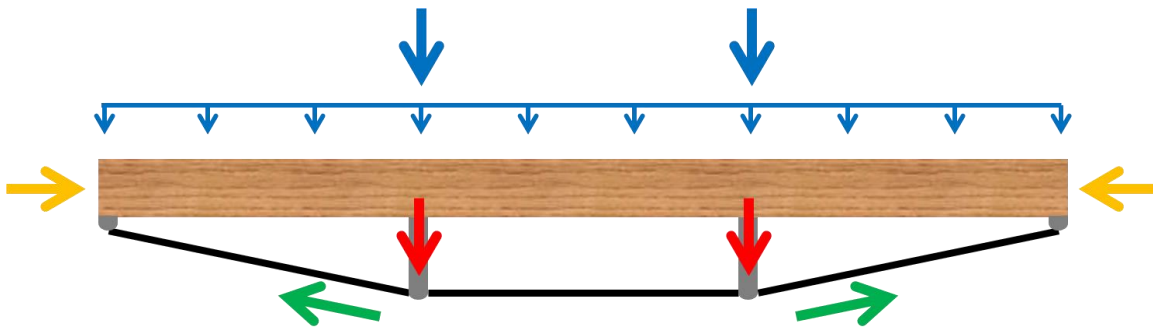


Figure 40: Load path of queen post

A queen post is an indeterminate structure, and was conservatively assumed to be hinged at the post locations. For the design of the queen post, the top chord was composed of glulam, the middle posts were made of square hollow structural steel members, and the bottom chord consisted of several sections of tension cables.



Figure 41: Simplified hinge queen post girder

The assumption of the hinge, shown in Figure 41, allowed for the calculation of the axial load on the posts, the tension in the cables, and the axial load applied to the top chord member. Due to the setup of the typical office and roof bays, each queen post had two point loads acting along its length. To reduce flexure induced by loading, the posts were placed where the incoming beams would frame into the queen post girder. This significantly reduces the moment on the beam and transfers a majority of the loading into the HSS posts.

The sizes chosen for the queen post girders are shown below.

Typical Office Bay	8 ½” x 19 ¼” Stress Class 50 Visual SP 3 ½” x 3 ½” x ⅜” Square HSS Post (2) M56 Macalloy 460 Bars
Typical Roof Bay	8 ½” x 12 ⅜” Stress Class 50 Visual SP 3 ½” x 3 ½” x ⅜” Square HSS Post (2) M16 Macalloy 460 Bars

Appendix B.2 - Queen Post Design Hand Calculation and Appendix B.3 - Typical Office Queen Post Design shows calculations for the design of the queen post. In addition, Appendix B.2 - Queen Post Design Hand Calculation walks through a hand calculation of the first iteration of the queen post design of the typical office floor. At the end of this iteration it was found that the queen post design failed due to the interaction between axial and bending on the member. A combination of 2D computer analysis and Microsoft Excel were used to compute the HSS post axial loads, the tension in the cable and the axial load applied to the top chord glulam member. These values were then adapted into a Microsoft Excel spreadsheet that was developed to quickly and accurately arrive at an economical member size of the top chord. Hand calculations were used to size the HSS post and the tension cable (Macalloy Bar & Cable Systems, 2014).

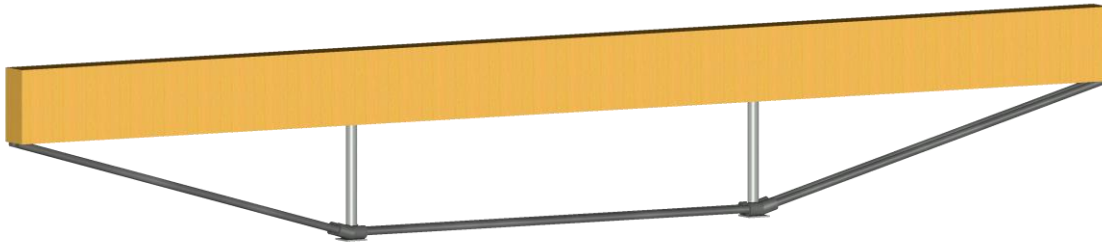


Figure 42: Computer model of queen post girder

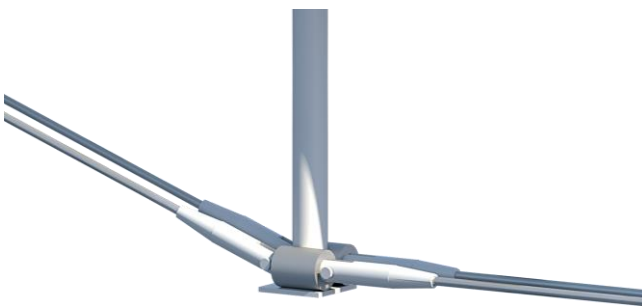


Figure 43: Connection detail for cable of queen post girder

A similar iteration was completed for the Typical Roof Bay, shown in Appendix B.5 - Roof Queen Post Design. A SAP2000 model was also developed to confirm the post and cable forces. This data is found in Appendix B.8 - SAP2000 Queen Post Model and shows that an acceptable amount of error was incurred in the assumption of the hinged queen post (Schneider III, 2014).

Due to an eccentricity which would exist in the design if the cable met the extreme bottom fiber of the top chord glulam member, several conceptual designs were considered for the connection of the cable and glulam, shown in Figure 44, Figure 45 and Figure 46.

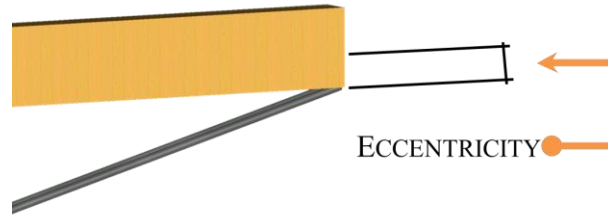


Figure 44: Glulam top chord is eccentrically loaded due to the cable

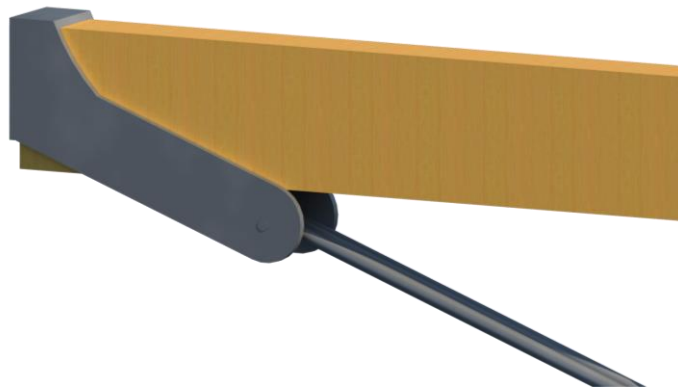


Figure 45: Conceptual design with holster plate and held with a clevis

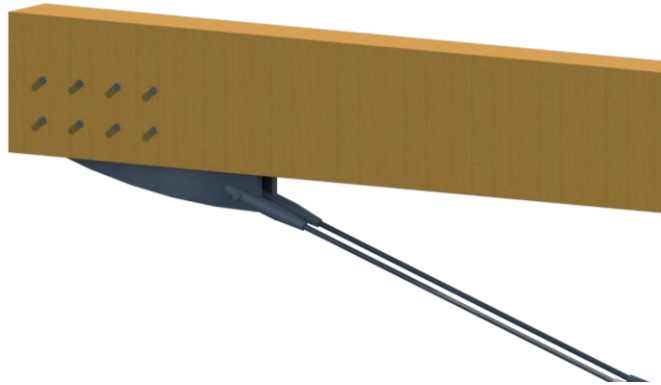


Figure 46: Conceptual design with plate penetration wood glulam beam and held with a clevis

General Framing Plan

A general framing plan was developed for the east side of the building using Revit. This is shown below in Figure 47 and Figure 48.

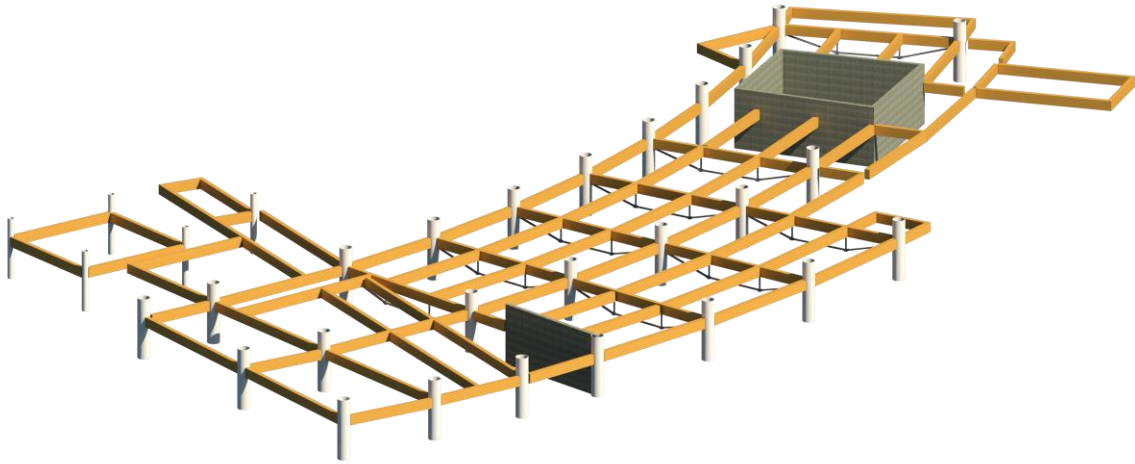


Figure 47: Isometric view of general framing plan

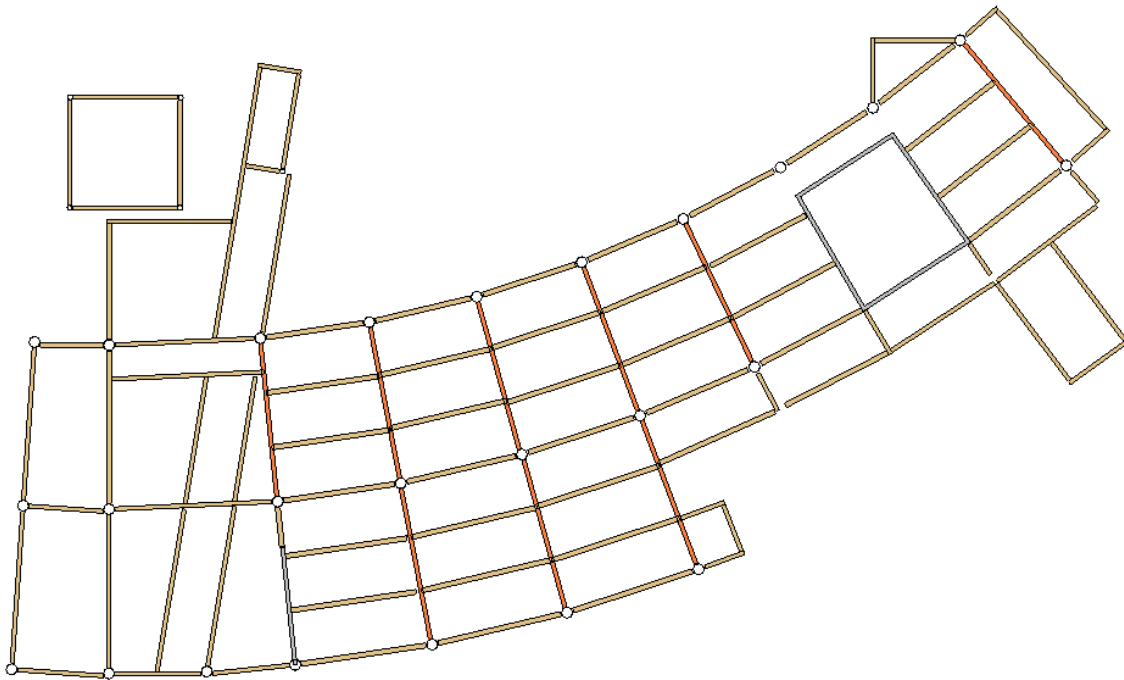


Figure 48: Plan view of general framing plan (East side)

Fire Rating

Although a fire rating for the building was not required, it was important to understand how long the structure would remain structurally sound during a fire. In order to calculate the fire resistance time, the assumption was made that the queen post girder would act purely in axial compression, such as a column. The fire was assumed to occur on 4 sides of the column, and a fire resistance of approximately 1 hour and 15 minutes was calculated (APA - The Engineered Wood Association, 2009).

$$t = 2.54 \cdot Z \cdot B \left[3 - \frac{B}{D} \right]$$

Equation 2: Fire rating for a column with a 4 side fire

Column Design

Due to aesthetics and the ease of connection of the glulam beams, the current HSS columns will be kept in the redesign. The HSS column sizes are confirmed in Appendix B.9 – Column Sizing

Foundation Consideration

With the completion of the design of the building, it was found that the axial loads through the columns were reduced, due to the use of glulam. While the design of a new foundation system was not a part of the proposed solution for this thesis project, the foundation system should be considered. Due to the reduced loading, the existing foundation is sufficient to support the building and prevent overturning. This is further investigated in 2.2 Lateral System Redesign and supporting calculations can be found in Appendix C.4 – Building Overturning Check.

Comparison of Gravity Systems

The change of the structural material to glulam from steel gave the ability to add an aesthetic characteristic to the building, while still adequately supporting the weight of the floors and roof. Below in Table 26 is a comparison of the existing structural system with the redesigned structural system.

		Existing	Redesign
		Steel Wide Flanges	Glulam and Queen Post
System Weight		56 psf	60 psf
Slab Depth		5.5"	5.5"
Height			
Floor to Floor		14'-0"	14'-0"
Option 1		12'-0"	12'-5" ⁵
Option 2		8'-6" ⁶	10'-0" ⁷
Constructability		Easy	Medium
Fire Protection		None	None
Fire Rating		-	1.25 hours
MEP Coordination	Underfloor Air Distribution (UFAD) System @ 18" depth	MEP runs through the structural queen post girders	

Table 26: Comparison of existing and redesigned gravity systems

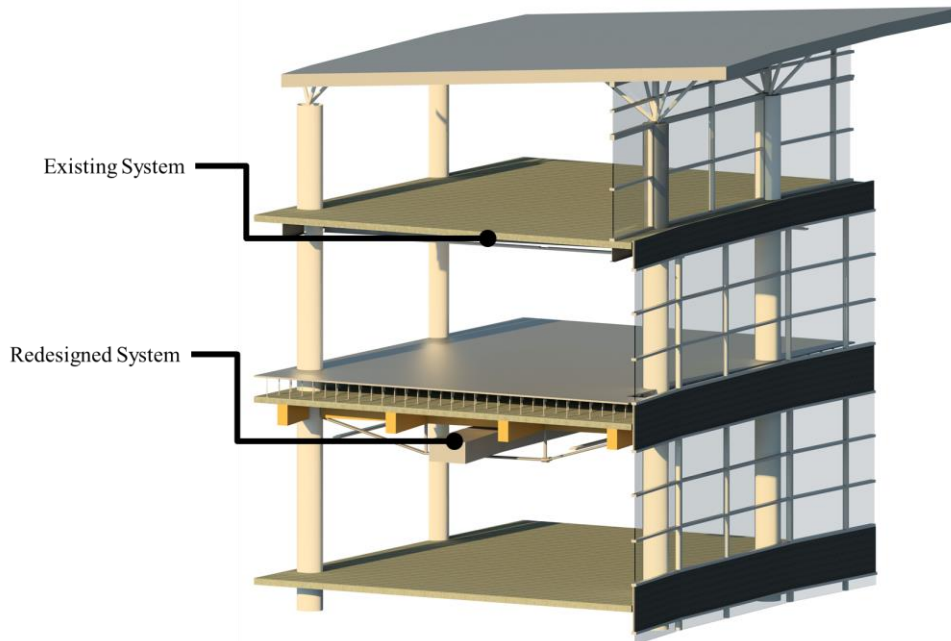


Figure 49: Comparison of existing and redesigned gravity systems

⁵ This height is measured from the floor level to the bottom of the structural beams.

⁶ This height is measured from the floor level to the bottom of the existing luminaire fixtures.

⁷ This height is measured from the floor level to the bottom of the queen post girder's cable.

Existing System Rendering

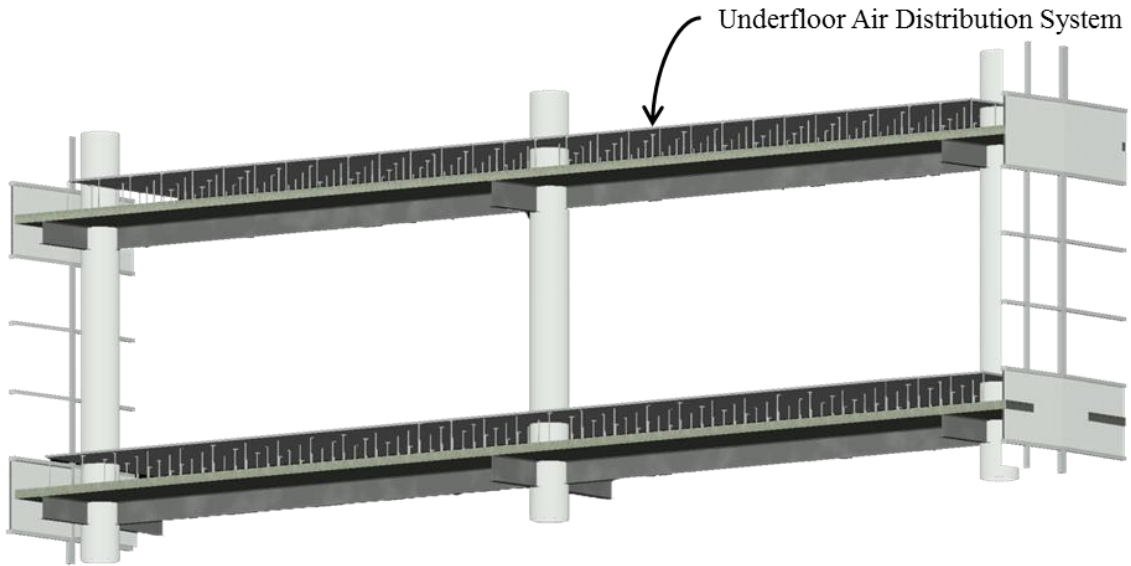


Figure 50: Existing structural system isometric in view

Redesigned System Rendering

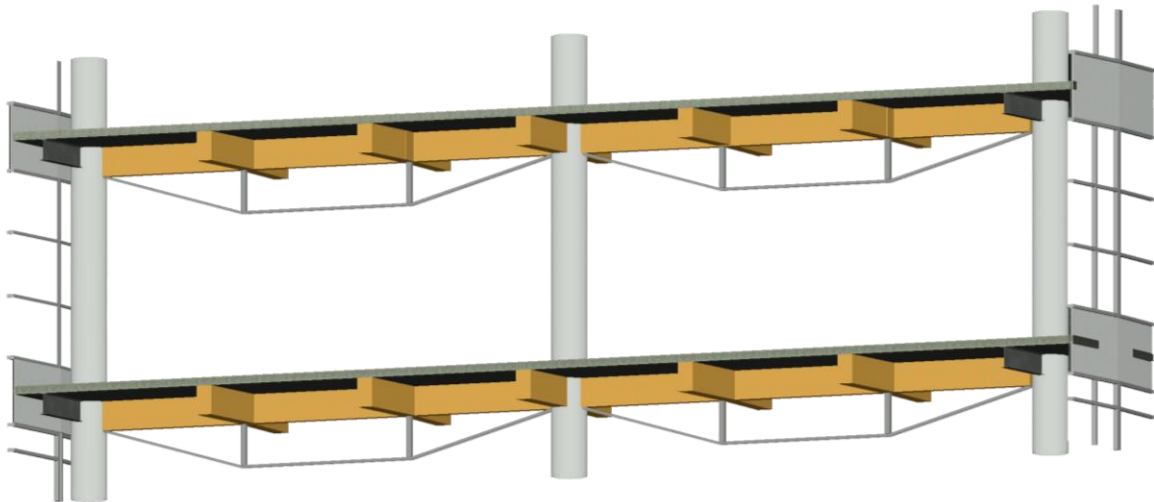


Figure 51: Redesigned structural system isometric in view

Existing System Dimensions

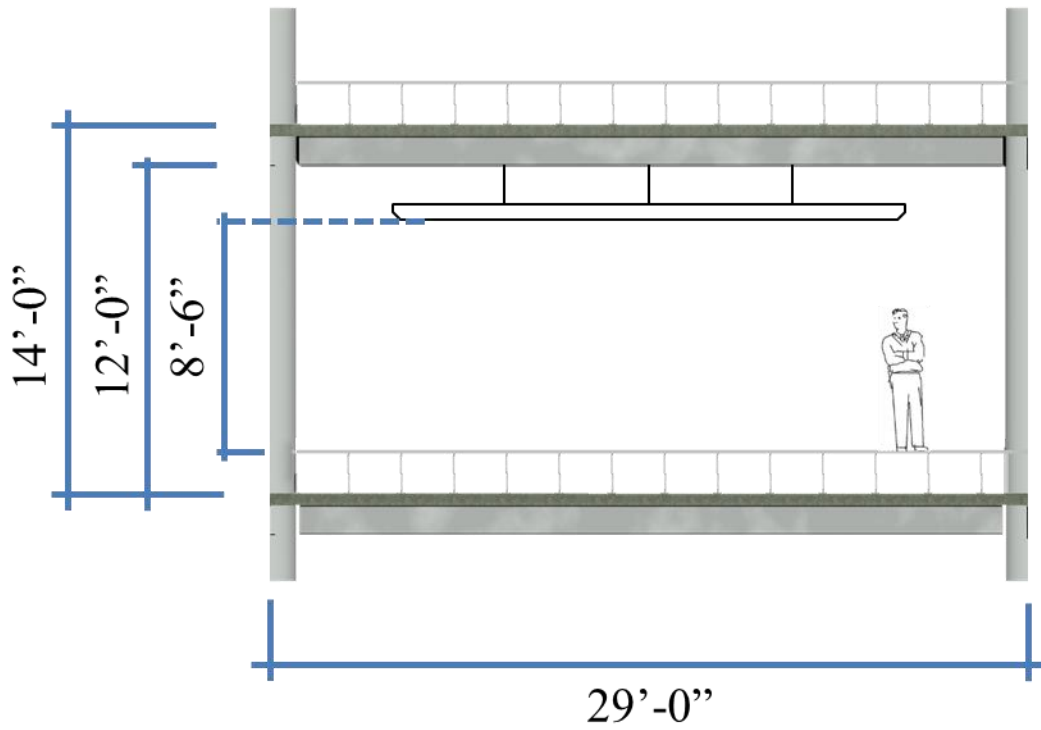


Figure 52: Existing system typical bay (with dimensions)

Redesigned System Dimensions

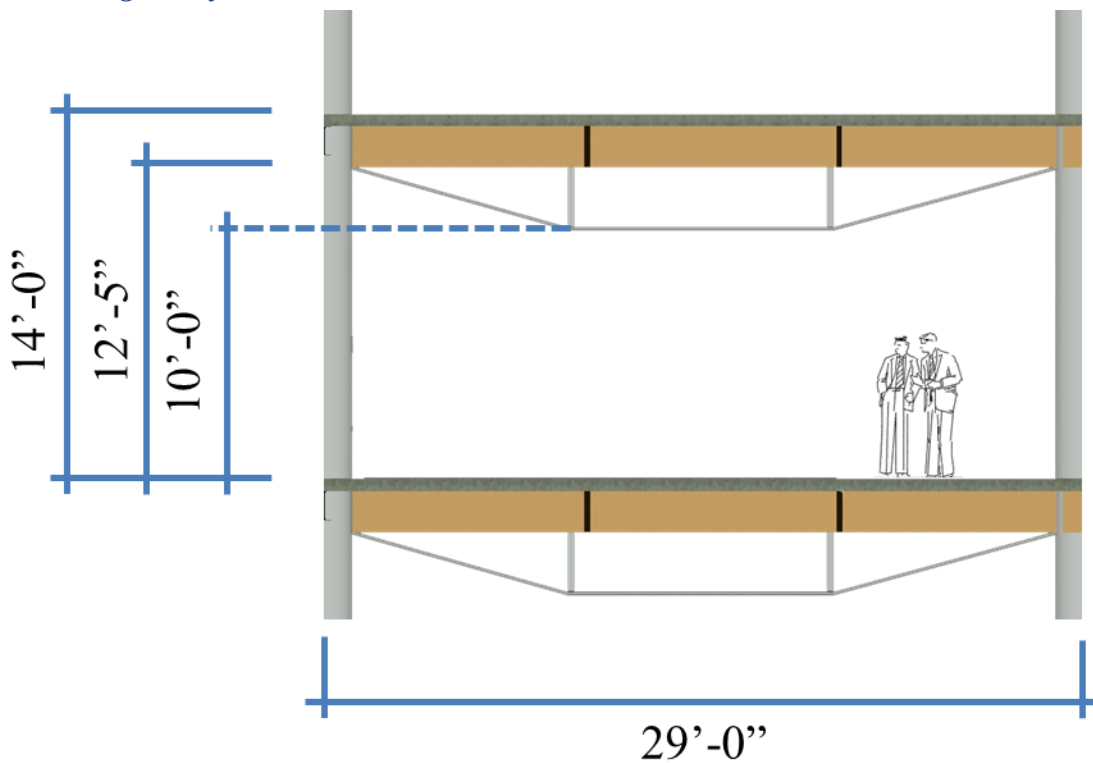


Figure 53: Redesigned system typical bay (with dimensions)

A close up of a potential mechanical and electrical layout is shown in Figure 54.

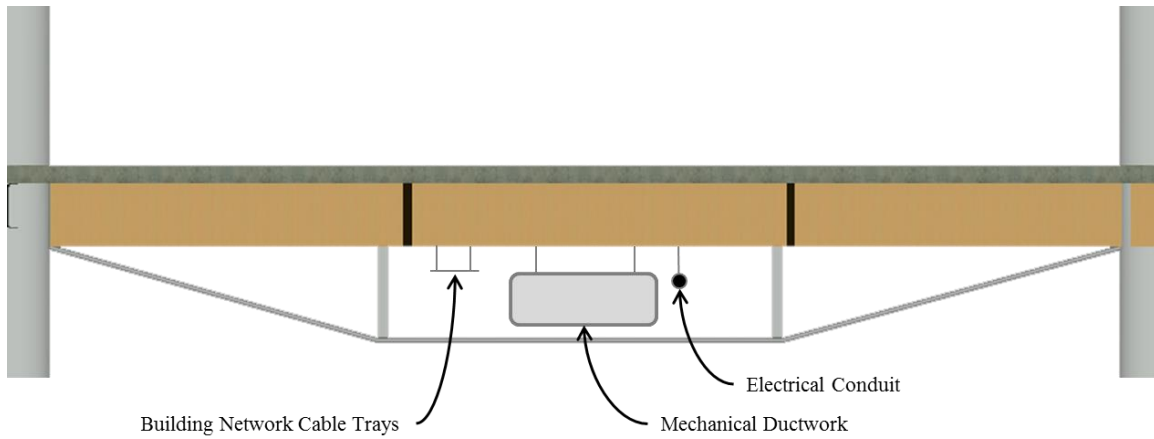


Figure 54: Redesigned structural system and potential mechanical and electrical

2.2 LATERAL SYSTEM REDESIGN

The redesign of the gravity system in glulam lessens the likelihood of the use of a steel plate shear wall system. Instead, a cast-in-place concrete shear wall system was designed as the lateral force resisting system of the Heifer International Center. The shear walls kept the same layout as the existing building and were initially designed using the minimum thickness of walls designed by the empirical design method, per §14.5.3.1 (American Concrete Institute, ACI-318, 2011). The building layout was modeled in RAM Structural System (RAM SS) and the shear walls were designed based on the computer generated seismic and wind loadings.

Computer Modeling Input

The Heifer International Center has a seismic joint at approximately the midpoint of the building, requiring that both sections be modeled separately. The two sections of the building are shown in Figure 55, Figure 56, Figure 57 and Figure 58. Figure 56 and Figure 58 show an isometric of each side of the building from RAM SS. Moreover, the lateral force resisting system does not extend to the fourth level of the building, but instead relies on the fourth level columns and roof diaphragm to transfer lateral load. All mass of the fourth level and roof were applied at the fourth level due to this arrangement.



Figure 55: LFRS of east end of building

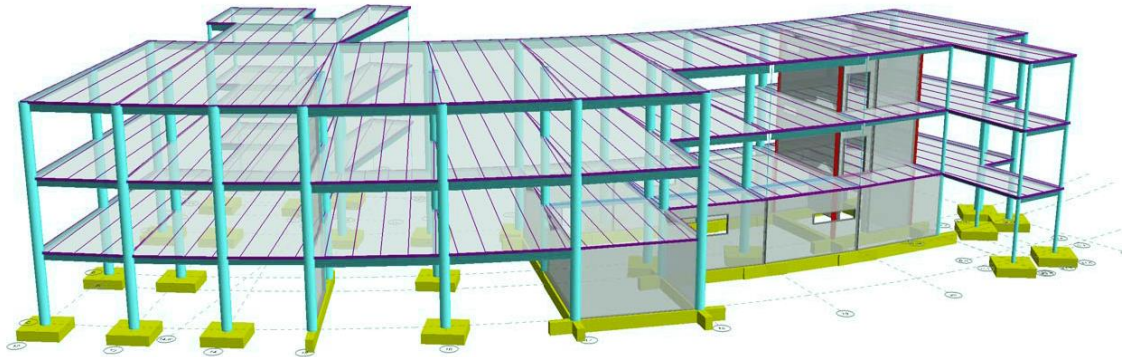


Figure 56: LFRS of east end of building from RAM SS



Figure 57: LFRS of west end of building



Figure 58: LFRS of west end of building from RAM SS

The concrete shear walls were designed as non-bearing shear walls and each level was programmed with the office building's dead and live loads previously calculated in 2.1 Gravity System Redesign. The dead load mass was used in the calculation of computer generated seismic loads. A preliminary size of 8" was chosen using the conservative assumption of a bearing wall which shall have a thickness not "less than 1/25 the supported height or length, whichever is shorter, nor less than 4 in." Each shear wall spans a height of 14'-0" so would have to be a minimum of 6.72", or 8" if a traditional shear wall depth is used (American Concrete Institute, ACI-318, 2011).

The openings in the shear wall were programmed based on the original steel plate shear wall configuration; however, adjustments were made due to the change in the mechanical system. Concrete columns were added at the edges of the shear wall core for stability purposes. In addition, concrete beams were added at the base of the shear walls on level 2, due to a discontinuity of the lateral force resisting system on the ground level.

The following assumptions were made during the modeling process:

- The concrete core wall was modeled as a C-shape (three walls) and a discontinued wall as the fourth wall due to program limitations that do not allow the connection of all four walls.
 - This is a conservative assumption that will make the system less stiff in the computer program, than when compared to the actual monolithic construction pour on the actual site.
- Rigid diaphragm was assumed due to use of composite decking.
- Cracked sections were assumed for the shear walls, per §10.10.4.1, and were assigned moment of inertia property modified of $0.35I_g$ (American Concrete Institute, ACI-318, 2011).

These general steps were used to model the lateral system in RAM Structural System:

- Grid was imported into RAM SS from Autodesk Revit.
- The perimeter of the building was lined with steel beam elements in order for the program to extrapolate an edge of slab.
 - It should be noted that beam self-weight was disabled and did not affect lateral calculations.
- Steel HSS columns were modeled using the HSS24x0.5 of the existing building. This was accomplished by overriding the Master Steel Table of RAM SS and programming in a new HSS size and corresponding properties, seen in Appendix C.1 – HSS24x0.5 Column.
- Shear walls were modeled using the existing building layout.
- RAM Frame was used to program site-specific seismic and wind loads, seen in Appendix C.2 – Seismic and Wind Loading and the two separate sections of the building were then analyzed.
- RAM Concrete was used in the design of the concrete shear walls.

Torsional Irregularities

Vertical and Horizontal Structural Irregularities had to be considered for the design of the Heifer International Center, per Table 12.3-1 and 12.3-2 of §12.3.2 (ASCE-7 10, Minimum Design Loads for Buildings and Other Structures)

It was possible that a Torsional Irregularity (Type 1a) or Extreme Torsional Irregularity (Type 1b) existed in the structure. After the initial programming and verification of the RAM Structural System model, the torsional amplification factor was calculated and irregularity in each direction was tested. This was achieved by calculating the average and maximum drifts of each floor, at transverse locations of the building, shown in the simplified diagram of Figure 59. Appendix C.6 – Trace Locations visually show the two locations used to test irregularity on each section of the building.

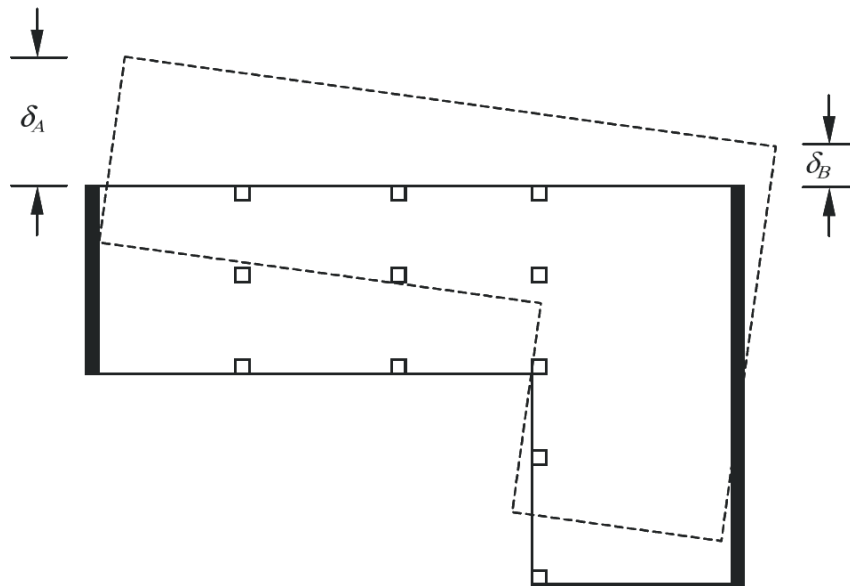


Figure 59: ASCE-7 10 Figure 12.8-1 Torsional Amplification Factor

Due to the seismic joint, the two sections of the building were analyzed separately. Both the x-direction and y-directions were tested for the two sections of the building, east and west sides. The east side of the building was found to have a Type 1b torsional irregularity for all three levels for the x-direction and y-direction. On the other hand, the west side of the building did not have any torsional irregularities in the y-direction; however, had Type 1b irregularity on all levels in the x-direction. This was calculated using Equation 3 below and making a comparison of $1.2\delta_{avg}$ and $1.4\delta_{avg}$. These results are shown in Appendix C.3 – Torsional Irregularity and Seismic Amplification Factor.

$$\delta_{avg} = \frac{\delta_A + \delta_B}{2}$$

Equation 3: Average drift of story

Type 1b is an Extreme Torsional Irregularity and the design of such a building must follow code requirements outlined in Table 12.3-1. These stipulations are summarized below, which are applicable to a Seismic Design Category C building (ASCE-7 10, Minimum Design Loads for Buildings and Other Structures).

- Structural Modeling §12.7.3
 - A 3D computer model incorporating a minimum of three dynamic degrees of freedom was produced for this project.
- Amplification of Accidental Torsional Moment §12.8.4.3
 - The amplification factor, where required, was applied to the accidental torsional moment. Calculations are shown in Appendix C.3 – Torsional Irregularity and Seismic Amplification Factor and references Equation 4.

$$A_x = \left[\frac{\delta_{max}}{1.2\delta_{avg}} \right]^2$$

Equation 4: Amplification Factor

- Story Drift Limit §12.12.1
 - The design story drift of the building was maintained below the allowable story drift, Δ_a , provided in Equation 5. Supporting calculations are shown in the Seismic Story Drift section of Appendix C.2 – Seismic and Wind Loading.

$$\Delta_a = 0.020h_x$$

Equation 5: Allowable story drift

- Table 12.6-1
 - The Seismic Design Category C building was analyzed using the Equivalent Lateral Force Analysis procedure.
- Modeling §16.2.2
 - Similar stipulations as §12.7.3 above.

In addition to torsional horizontal irregularities, Nonparallel System Irregularity Type 5 existed due to the lateral force resisting system not aligning with the orthogonal application for seismic forces, for both the east and west sides. Type 5 requires the following conditions to be met for Seismic Design Category C and is shown in Figure 60 (ASCE-7 10, Minimum Design Loads for Buildings and Other Structures).

- §12.5.3
 - The orthogonal combination procedure was used in the analysis of the building, requiring 100% of the force in one direction to be combined with 30% of the forces in the orthogonal direction.
- Structural Modeling §12.7.3
 - A 3D computer model incorporating a minimum of three dynamic degrees of freedom was produced for this project.
- Table 12.6-1
 - The Seismic Design Category C building was analyzed using the Equivalent Lateral Force Analysis procedure.
- Structural Modeling §12.7.3 and §16.2.2
 - Please see Type 1b Extreme Torsional Irregularity.

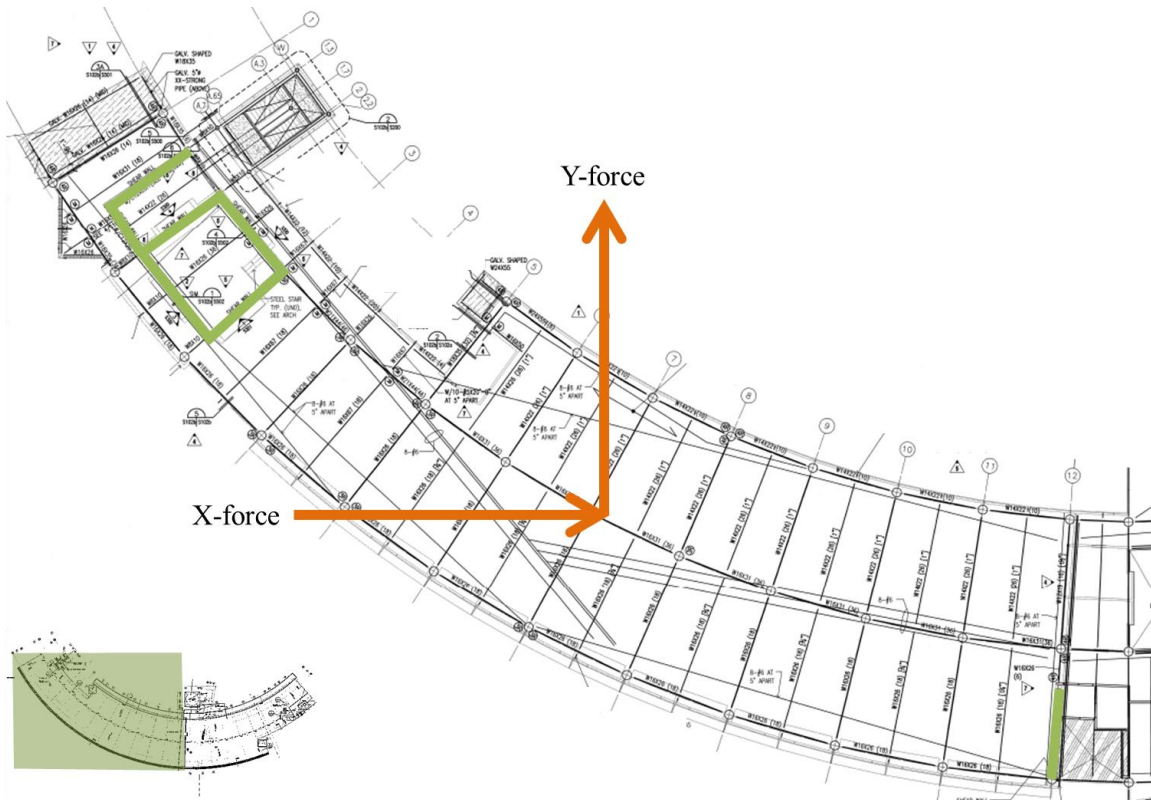


Figure 60: Type 5 Nonparallel System Irregularity

Seismic Design Category C has the potential to qualify for two types of vertical irregularity, per Table 12.3-2: In-Plane Discontinuity in Vertical Lateral Force-Resisting Element Irregularity Type 4, and Type 5b Discontinuity in Lateral Strength-Extreme Weak Story Irregularity. Type 4 irregularity was eliminated because there was no shear wall that was discontinuous from the below levels. Type 5b also did not apply to the Heifer International Center, which does not have any levels that have 65% less lateral strength than the levels above.

Loads Applied to Model

The original analysis of the building used ASCE 7-98; however, the redesign of the building used ASCE 7-10. Due to the drastic change in code requirements only the seismic and wind loadings generated by the computer were used, based on ASCE 7-10. The most up to date wind and seismic data was programmed into the computer and used to generate the loading on each half of the building. The input data can be found in Appendix C.2 – Seismic and Wind Loading. It was previously found in 1.6 Lateral System and Loads of the simplified analysis of the structure, seismic controlled. This was verified for both sections of the building, which were each controlled by a load combination involving seismic loads.

Seismic Loads

Seismic loads were applied to the building and displacements were extracted from the program. These displacements were then used to test if torsional irregularities existed in the building. If Type 1a or Type 1b Horizontal Irregularity existed, the building was checked against and compared to the requirements set forth in Table 12.3-1. In addition, the seismic loads were amplified per the calculated amplification factor. This is shown in Appendix C.3 – Torsional Irregularity and Seismic Amplification Factor and is discussed in greater detail in the Torsional Irregularities section. The torsional moment was first calculated using the original story shear and amplification factor, and then was then resolved into a shear with an eccentricity. This was completed because RAM Frame did not have a function to accept torsional moments, only shear forces.

Seismic drifts were calculated and found to be below the maximum drift allowances for inter-story drift, per §12.12.1 (ASCE-7 10, Minimum Design Loads for Buildings and Other Structures). Seismic forces are summarized below in Table 27 and Table 28.

Seismic Shear Summary - West End

	V_x	V_y
Level	(kips)	(kips)
Level 3	191.97	185.64
Level 2	290.03	282.97
Level 1	341.03	331.21

Table 27: Summary of west end seismic forces

Seismic Shear Summary - East End

	V_x	V_y
Level	(kips)	(kips)
Level 3	221.73	180.16
Level 2	329.23	274.77
Level 1	347.62	325.55

Table 28: Summary of east end seismic forces

Wind Loads

The basic wind speed increased from 90 mph to 115 mph, by changing from ASCE 7-98 to ASCE 7-10. Although this increased wind loads, loads still remained below seismic forces. Building drift was calculated and was compared to the industry accepted drift limit of $l/400$. These findings are summarized in the Wind Building Drift section of Appendix C.2 – Seismic and Wind Loading. Wind forces are summarized below in Table 29 and Table 30.

Wind Shear Summary - West End

Level	V_x (kips)	V_y (kips)
Level 3	35.04	53.91
Level 2	67.36	103.94
Level 1	63.31	98.15

Table 29: Summary of west end wind forces

Wind Shear Summary - East End

Level	V_x (kips)	V_y (kips)
Level 3	35.04	47.25
Level 2	67.36	91.1
Level 1	63.31	86.02

Table 30: Summary of east end wind forces

Building Overturning Moment

The overturning moment of the building was calculated using output from RAM Frame and Microsoft Excel, for wind and seismic cases. This was performed separately for the two sides of the building.

The weight of each side of the building was approximately 4000 kips. The shortest moment arm was calculated to the edge of the building, from each respective side of the building's center of mass, and used in the calculation of the resisting moment. The use of the shortest distance would yield the lowest resisting moment that would prevent the building from overturning. A factor of safety of 1.5 was applied to the calculation of the resisting moment. The worst case moment was calculated for wind and seismic, for both sections of the building and compared to the resisting moment. An overall factor of safety was then calculated for the design, and found to be 5.5 and 3.7, for the west and east ends, respectively. These calculations are shown in Appendix C.4 – Building Overturning Check. Both sides of the building passed for overturning.

Understanding Load Paths

Due to the Heifer International Center’s irregular shape it is important to understand how lateral loads travel through the building’s rigid diaphragm and react with the lateral system and are subsequently transferred to the foundation. The west side of the building was visually analyzed for the application of a wind load (this could also apply to seismic loads, too). Fortunately, the layout of the levels and lateral force resisting system are similar for each level, reducing the likelihood of load transfer through the diaphragm creating issues. This is shown below in Figure 61.

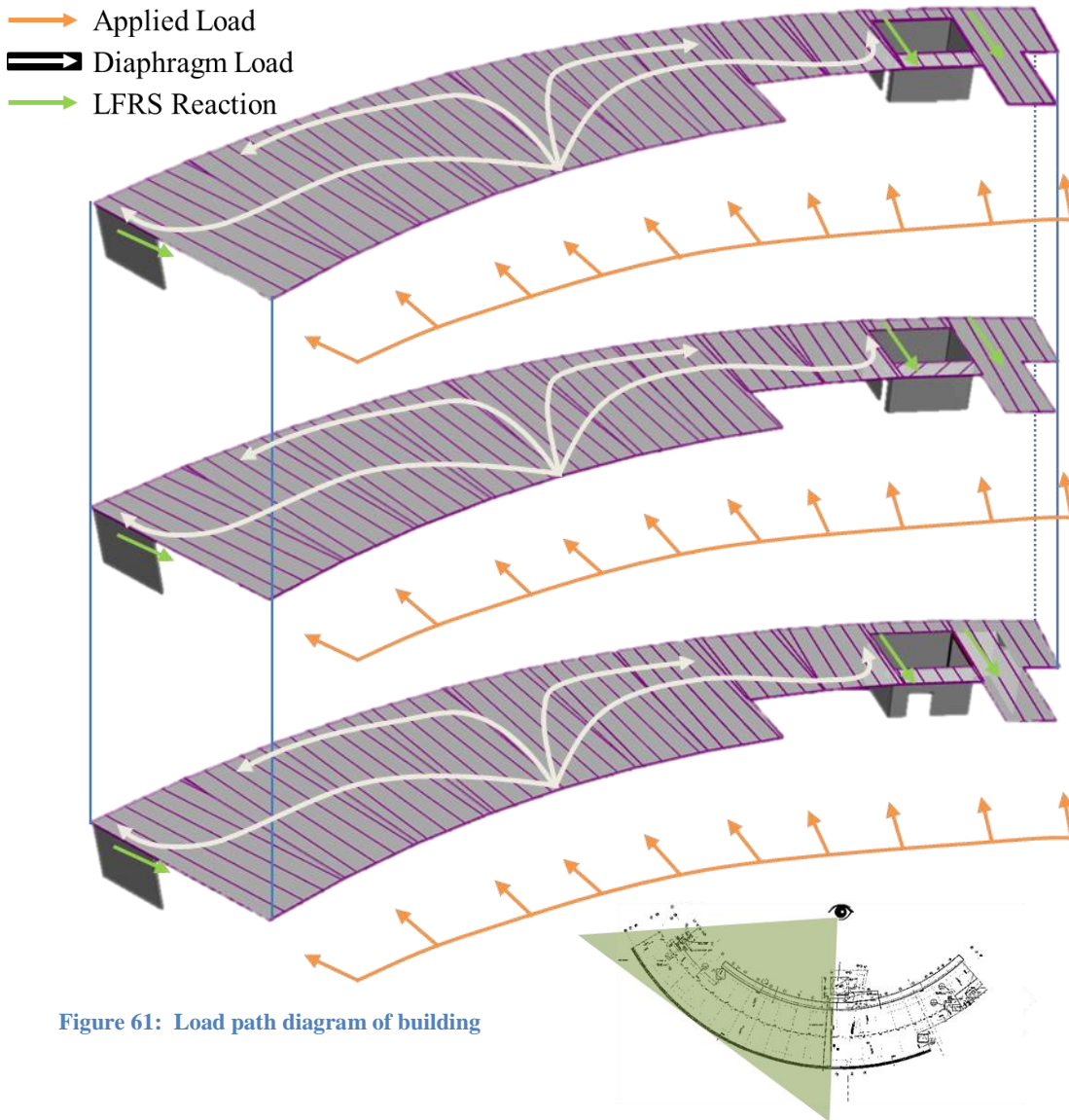


Figure 61: Load path diagram of building

Shear Wall Design

RAM Concrete was used in the design of the concrete shear walls. The shear wall originally checked, SW-13 @ column line 12, in the Lateral System Spot Checks section of 1.6 Lateral System and Loads, was checked against concrete shear wall requirements. The final design from RAM Concrete for SW-13 @ column line 12 is summarized in Table 31 and shown in Figure 62.

#4 @ 18" O.C. Horizontal

#5 @ 15" O.C. Vertical

Table 31: SW-13 at column line 12 rebar design summary

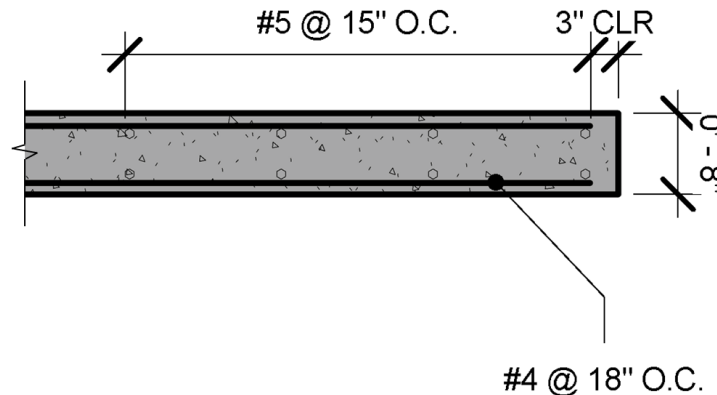


Figure 62: SW-13 at column line 12 section

This shear wall design was manually hand checked using the stipulations outlined for concrete shear walls and reinforcement requirements. These hand checks are shown in Appendix C.5 – Lateral System Hand Checks (American Concrete Institute, ACI-318, 2011), and the RAM Structural System design was found to pass.

The lateral force resisting system concrete shear walls are shown in Figure 63 and Figure 64, which were designed in RAM Structural System. These are shown on the next page. All shear walls in the building were designed to be 8" thick.

Seismic Joint

Analysis of the maximum deflections from each section of the building verified that the existing 4" seismic joint was adequate for the building deflections. Additional information can be found on the seismic joint in the Seismic Joint section of 1.2 Existing Structural Information.

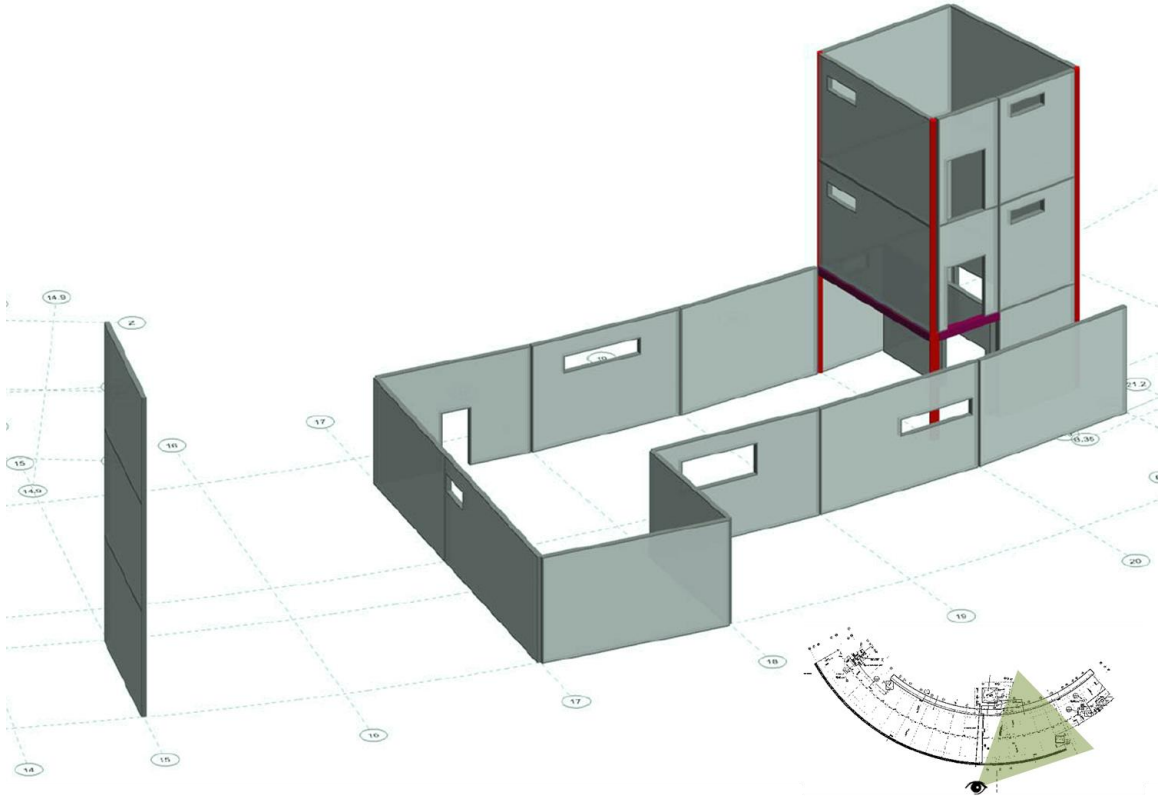


Figure 63: East end of the Heifer International Center

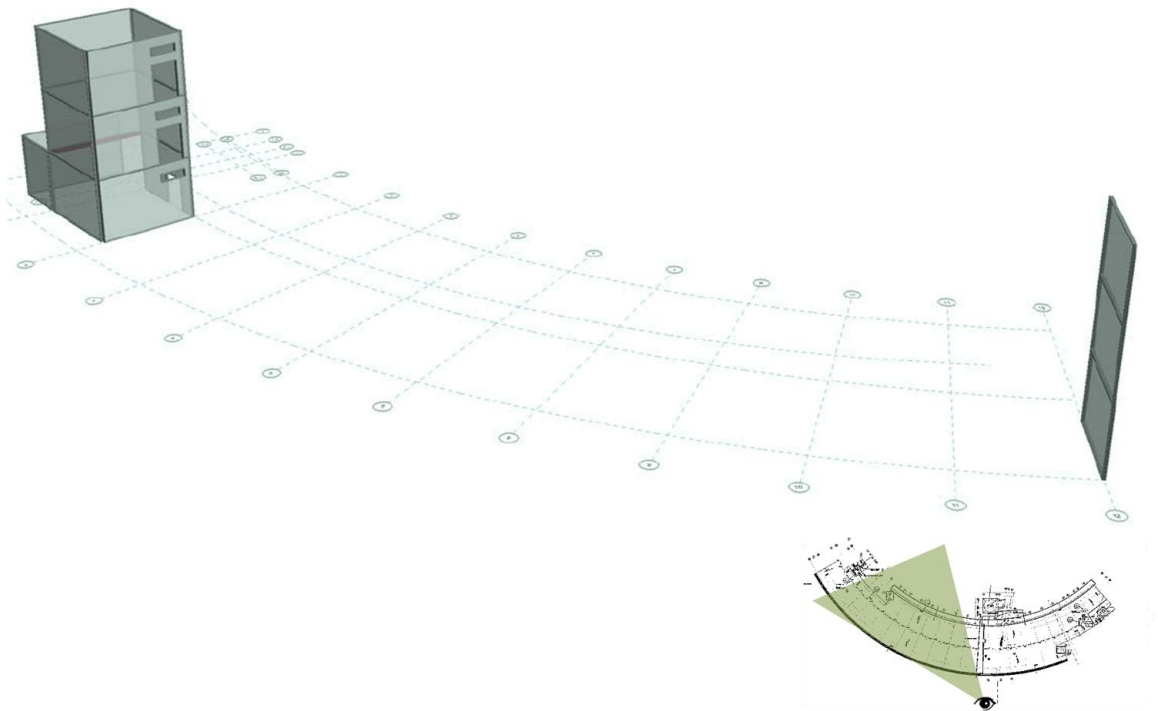


Figure 64: West end of the Heifer International Center

2.3 COMPARISON OF EXISTING AND REDESIGNED SYSTEMS

A comparison can be drawn between the existing and redesigned gravity and lateral systems. Each system has advantages over the other system; however, each also has disadvantages. The redesigned gravity system kept the floor-to-floor height the same and also was able to provide over a foot of additional space, immediately over the offices. Space over the girder location, which the typical office level beams frame into, was reduced because of the increased depth of the queen post girder. It should be noted that most of the depth of the queen post girder is for the space between the bottom of the glulam beam and the steel cable. The space is used for mechanical equipment, integrating the structural and mechanical systems in the redesigned queen post.

The main drawback of the redesigned gravity system is cost. The expense of the special order glulam beams and custom made queen post girder will be high—due to materials and labor. However, if the owner and architect wish to achieve the aesthetic look of the glulam and integration of the mechanical and electrical systems into the structural system—then the redesigned gravity is a decent choice. Moreover, the ability to prefabricate the queen post members and ship them to the site, also adds several environmental, cost and labor advantages to the redesigned system. If prefabricated off site, the members can be shipped onto the site and quickly moved into its respective place in the building. There is a disadvantage because the wood is not located as close as the steel manufacturer.

Next the lateral system redesign will be considered. Due to the use of glulam for the gravity redesign, it was found that a concrete shear wall system would be best for the lateral force resisting system in the Heifer International Center. The concrete shear walls were thought to be the best material to connect the glulam beams that would frame into a portion of the shear walls. In addition, the concrete shear wall system would be constructible, due to its ubiquitous use throughout the building industry. After the redesign of the gravity and lateral systems, a connection system between the two was researched. A Simpson Strong-Tie system of High Capacity Girder Hangers for Concrete and Glulam was studied and found to be a potential system to use in the Heifer International Center. This hanger is shown in Figure 65. It was found that the existing industry standard hangers would not be sufficient to support the beams framing into the concrete shear wall assembly; however, if a small portion of the gravity system was redesigned in the future, it would be conceivable to use the Simpson Strong-Tie hangers. Referencing the Due to an eccentricity which would exist in the design if the

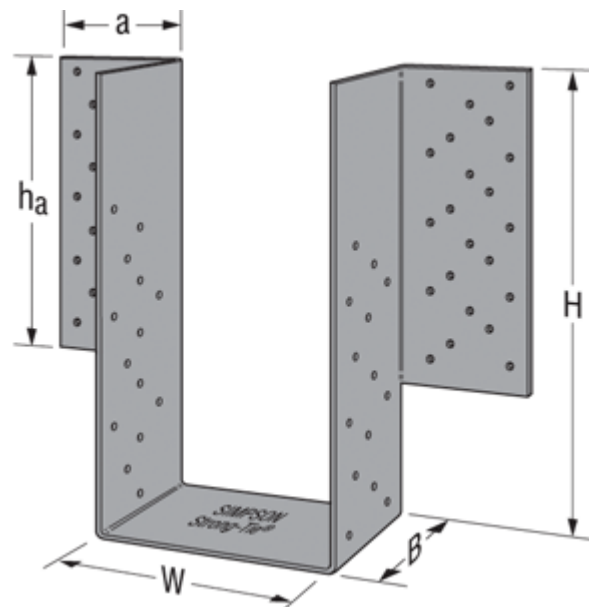


Figure 65: High capacity girder hangers for glulam

cable met the extreme bottom fiber of the top chord glulam member, several conceptual designs were considered for the connection of the cable and glulam, shown in Figure 44, Figure 45 and Figure 46.

General Framing Plan of 2.1 Gravity System Redesign and the supporting calculations of Appendix B.1 - Typical Office Beam Design, it is possible to increase the number of beams over the typical bay near shear walls, from three to four or five. If this was completed, then the bearing at the end of the beam would decrease; allowing the use of the High Capacity Girder Hangers for Concrete and Glulam. The hangers are currently capped at approximately 20 kips of downward load; while the system designed calculated a bearing of 21.5 kips. This slight change in the floor plan, highlighted in Figure 66 below, would allow for the use of the Simpson Strong-Tie hanger system (Simpson Strong-Tie, 2014). It is important to prevent contact between the glulam and concrete and provide lateral and uplift resistance to the glulam member. In addition, a slotted connection between the hanger and glulam should be considered to allow longitudinal movement (Showalter, 2012).

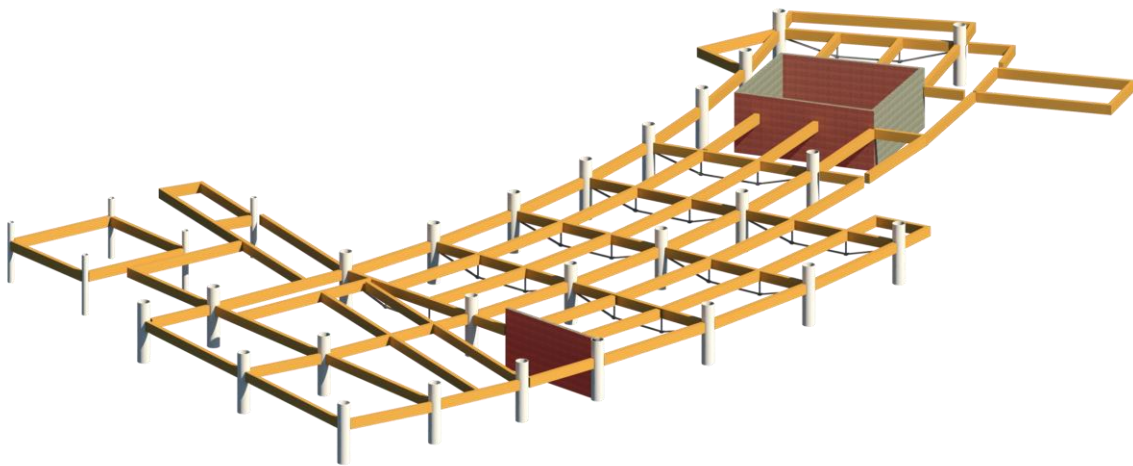


Figure 66: 3D isometric of floor plan highlighting walls to be redesigned

One major question which arose during the project was why the original project used steel plate shear walls. While concrete shear walls are common place in construction, the materials were readily available during the design and construction phases due to a steel manufacturer physically close to the building, making it more economical to use a steel plate shear wall system in the building. In addition, it is possible that the inherent lateral stability of the gravity framing did not require a lateral force resisting system during construction. If this is so, evident by photographs from the time of the construction shown in Figure 67, then it would have been easier to install a



Figure 67: Construction photo with no evident LFRS

steel plate shear wall into the erected structure (Robinson & Ames, 2000).

Another reason why steel plate shear walls may have been chosen is for their utility. It may not have made sense due to the geometrical shape and layout of the building to use concrete shear walls—in other words, an overdesigned system. It was revealed in ETABS SPSW to Concrete Conversion of Appendix A.1 - Existing Lateral System Modeling that the existing steel plate shear walls were equal to approximately 3” of concrete. By code the minimum concrete shear wall thickness would have been 6.72”—a large jump from the equivalent 3” concrete shear wall used for the $\frac{3}{8}$ ” steel plate shear wall.

The lateral force resisting system of the Heifer International Center was redesigned in concrete and found to sufficiently pass code and industry standards. This was achieved without hindering the current layout of the building and also producing an achievable design that can be unified with the redesigned gravity system.

2.4 MAE REQUIREMENTS

The Graduate School curriculum of the Pennsylvania State University was incorporated into the redesign of the Heifer International Center. Course work of graduate level courses was referenced from AE 530 – Advanced Computer Modeling of Building Structures to develop an advanced Bentley RAM Structural System model of the office building. The powerful design and analysis tools which RAM Structural System offers were used for the lateral design of the building. The gravity system of the Heifer International Center was mostly designed by hand, but was verified using a computer model of the primary structural member, the queen post girder. A CSi SAP2000 model was used to analyze, in detail, the queen post girders. In addition, AE 538 – Earthquake Resistant Design of Buildings was integrated into the design of the lateral force resisting system and the advanced torsional checks required by ASCE 7-10.

CHAPTER 3

MECHANICAL AND ENVELOPE

3.1 MECHANICAL AND ENVELOPE BREADTH

The redesign of the Heifer International Center in glulam led to the removal of the existing underfloor air distribution system. Instead, an overhead ductwork system was introduced and incorporated into the queen post girder designed in section 2.1 Gravity System Redesign. In addition, a thermal bridge was eliminated on each external column of the fourth floor of the office building, by redesigning the fourth floor column.

Preliminary Duct Sizing

Using provided mechanical drawings, the air handling units for the Heifer International Center were analyzed for an alternative ductwork system. A TRANE Ductulator[®] was used to preliminary size the ductwork for the new system, using the existing air handling unit's maximum air supply to the various sections of the building. This work is summarized in Table 32 and Table 33. The most important aspect of this research was the determination of the depth of the ductwork. The maximum practical ductwork depth was 25", so the queen post girder was designed at a depth of 28" to easily accommodate the rectangular ductwork.

Mark	Location	Services	Type	Max Supply (CMU)	Min Outside Air (CMU)	Return Air (CMU)
AHU-1E	1st	East	HOR2	6544	2452	4092
AHU-1W	1st	West	HOR2	8920	1715	7205
AHU-2E	2nd	East	HOR2	11122	1655	9467
AHU-2W	2nd	West	HOR2	14403	2839	11564
AHU-3E	3rd	East	HOR2	11400	1655	9745
AHU-3W	3rd	West	HOR2	14842	2839	12003
AHU-4E	4th	East	HOR2	10355	2620	7736
AHU-4W	4th	West	HOR2	12503	2811	9692
OSA-1E	-	East	HOR2	8400	8400	-
OSA-1W	-	West	HOR2	10200	10200	-

Table 32: Air handling unit summary

Mark	Ductulator [®]	Alternative Ductulator [®]
	Size (in)	Size (in)
AHU-1E	25x30	20x38
AHU-1W	25x36	20x48
AHU-2E	25x42	20x55
AHU-2W	25x50	20x70
AHU-3E	25x42	20x55
AHU-3W	25x55	20x75
AHU-4E	25x40	20x50
AHU-4W	25x50	20x65
OSA-1E	25x32	20x42
OSA-1W	25x40	20x50

Table 33: TRANE Ductulator sizing

Thermal Bridge Elimination

The fourth floor of the office building has several columns that are exposed on the exterior and interior of the building, shown in Figure 68 and Figure 69. This is a direct link between the outside and inside of the building that may cause thermal discomfort in the interior space. In order to eliminate the thermal bridge through the structure, the HSS column, which is continuous from the first to fourth floors, was terminated at the third floor. A wide flange was designed for the fourth floor, which is supported by the concrete-filled HSS below.

The final design of the wide flange to support roof and girder loads was a W12x40. It should be noted that a smaller wide flange could have been used; however, smaller wide flanges more easily buckle due to their square shape. These shapes were not considered for the final design. The wide flange would then be covered with an architectural façade, for example aluminum sheathing, on the exterior to give the aesthetic look of the HSS. The cavity would then be filled with insulation and covered on the interior of the building. Calculations for sizing the wide flange can be found in Appendix D.1 – Thermal Bridge Study.

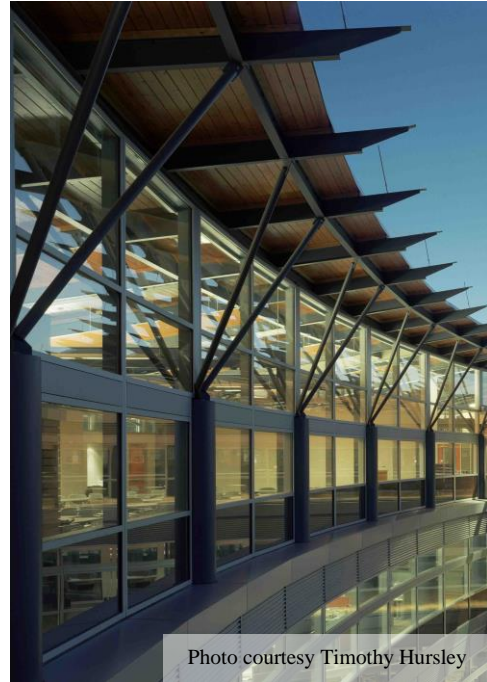


Photo courtesy Timothy Hursley

Figure 68: Exterior shot of columns

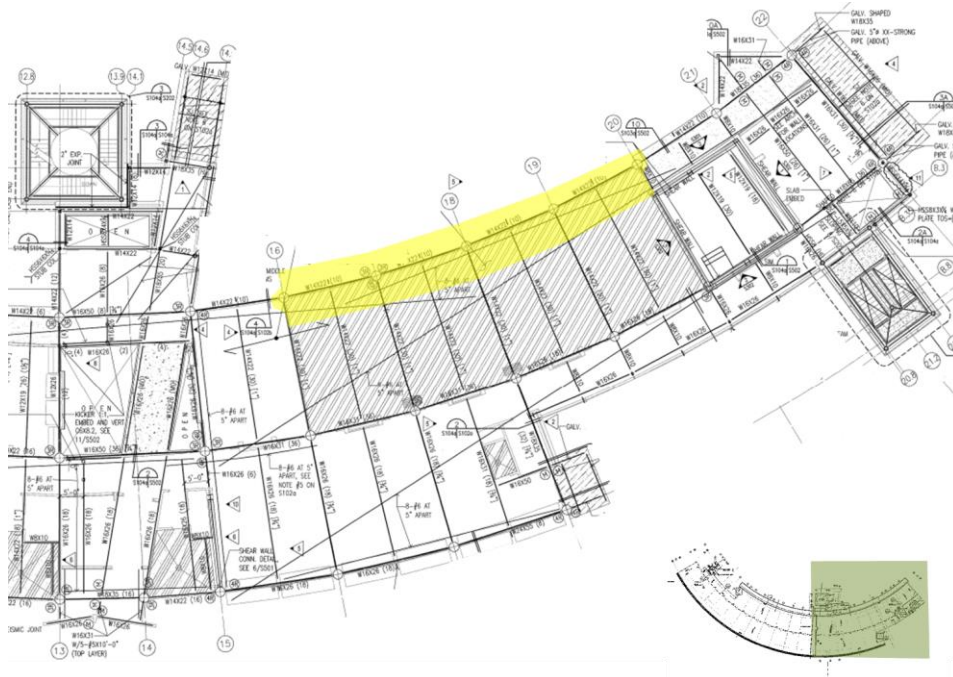


Figure 69: Columns exposed on exterior and interior

Thermal Productivity

A comparison of coefficient of thermal conductivity was drawn between the redesigned system, Table 34 and existing systems, Table 35. The glass façade is summarized in Table 36 and was used for the existing and redesigned systems. The low total U-value of the new system is an improvement over the existing, providing more resistance to temperature change across the system. The worst-case heat travel was considered and is shown in Figure 70.

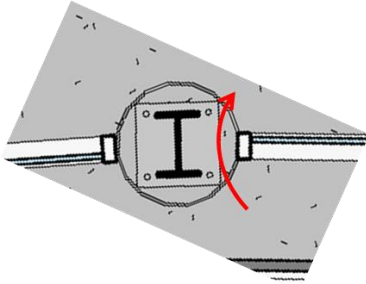


Figure 70: Worst case heat travel

Material	Depth (in)	R (BTU-in/h-ft ² -°F)	U (1/R)
Outside Air Film	-	0.17	5.88
Aluminum Composite	0.5	0.06	15.86
Batt Insulation ⁸	3	11.45	0.09
Aluminum Composite ⁹	0.5	0.06	15.86
Inside Air Film	-	0.68	1.47
Sum		12.43	0.08

Table 34: Redesigned HSS envelope

Material	Depth (in)	R (BTU-in/h-ft ² -°F)	U (1/R)
Outside Air Film	-	0.17	5.88
HSS Steel	0.5	2.24	0.45
Air	23	0.00125	802.57
HSS Steel	0.5	2.24	0.45
Inside Air Film	-	0.68	1.47
Sum		5.33	0.19

Table 35: Existing HSS envelope

Material	Depth (in)	R (BTU-in/h-ft ² -°F)	U (1/R)
Glass	-	3.45	0.29
Sum		3.45	0.29

Table 36: Glass façade envelope

An approximate 140% increase can be observed between the redesigned and existing systems; showing the added benefit of the redesigned column with batt insulation.

⁸ Thermal Batt FIBERGLAS® Insulation (Owens Corning Insulating Systems, LLC, 2007)

⁹ Almaxco ACP Mechanical Properties (Almaxco, 2012)

A thermal gradient was developed for the new column-wall system and is shown below in Figure 71, worst case, and Figure 72, middle condition. These calculations are summarized in Worst Case Thermal Gradient and Middle Case Thermal Gradient of Appendix D.1 – Thermal Bridge Study.

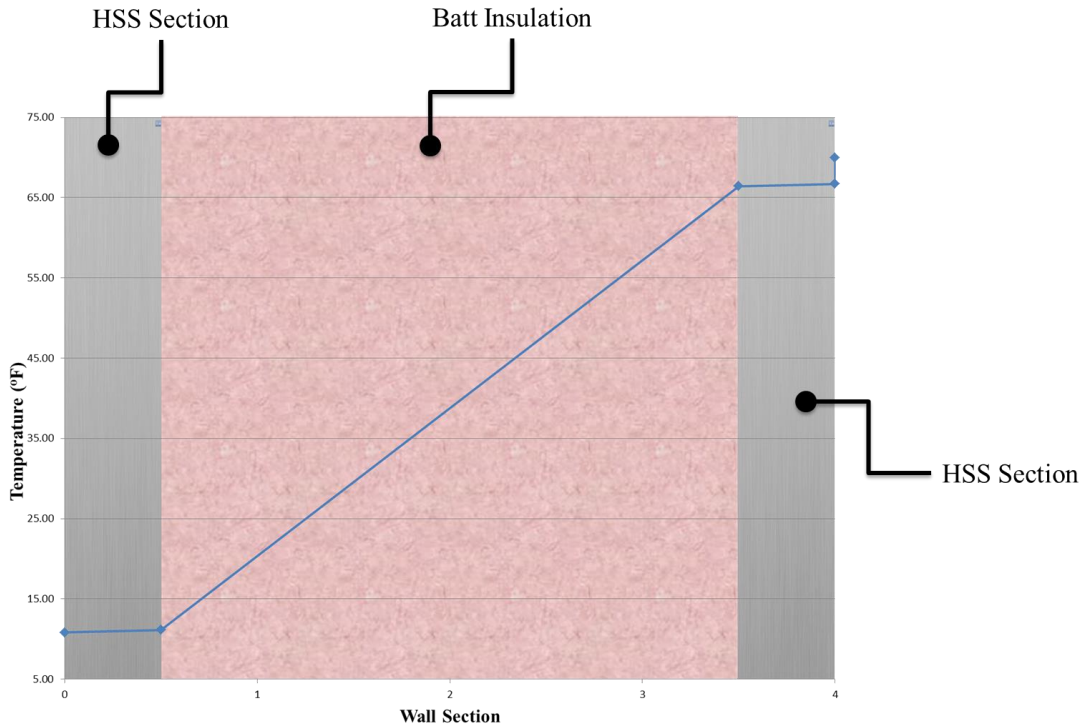


Figure 71: Worst case thermal gradient

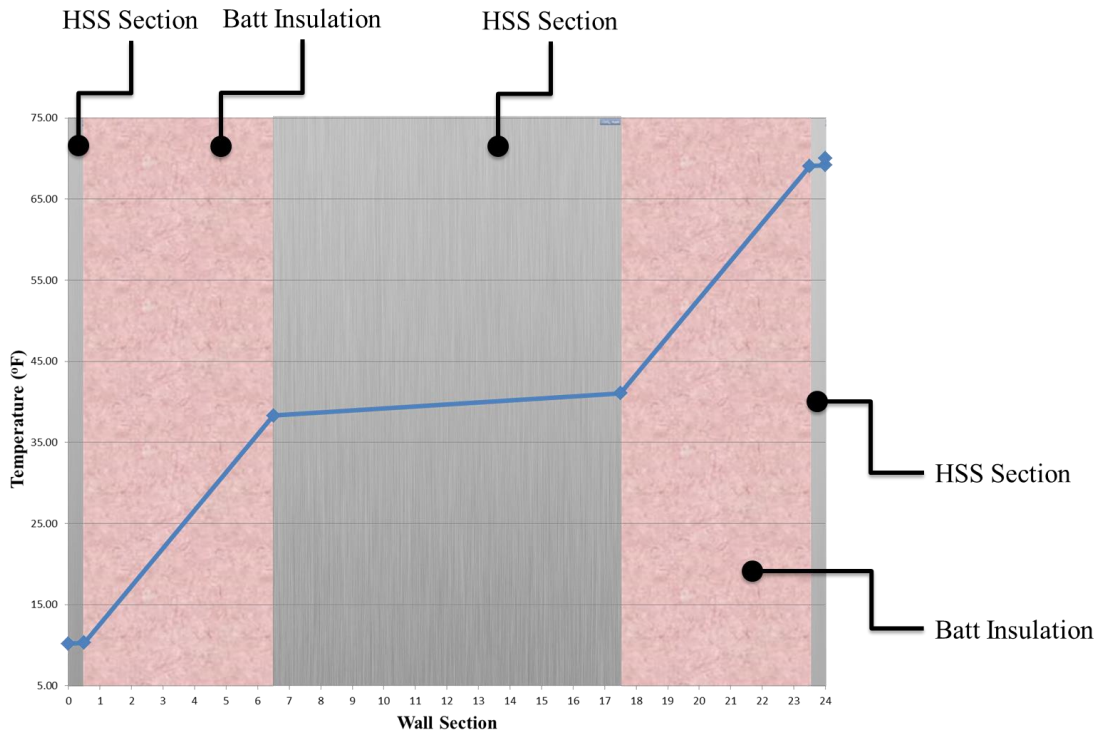


Figure 72: Middle condition thermal gradient

Construction Sequence

A construction sequence for the new design was thoroughly considered and is explained below between Figure 73 and Figure 79.

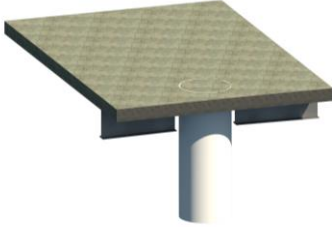


Figure 73: Phase 1 - Column Construction

Construction will begin with the finishing of the fourth floor slab.

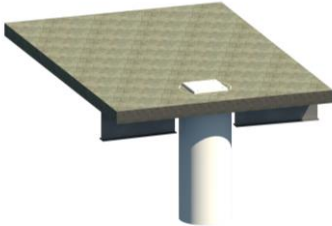


Figure 74: Phase 2 - Column Construction

A base plate will be installed over the third floor concrete filled HSS column.

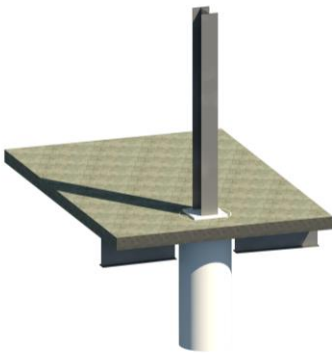
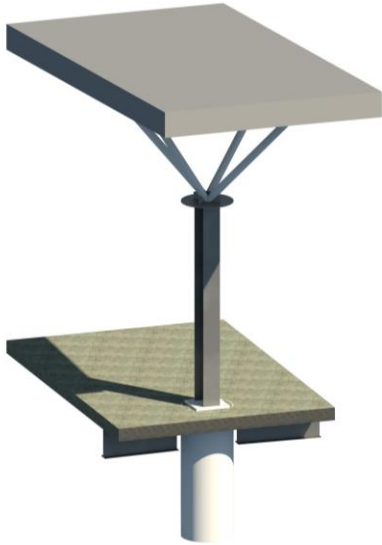


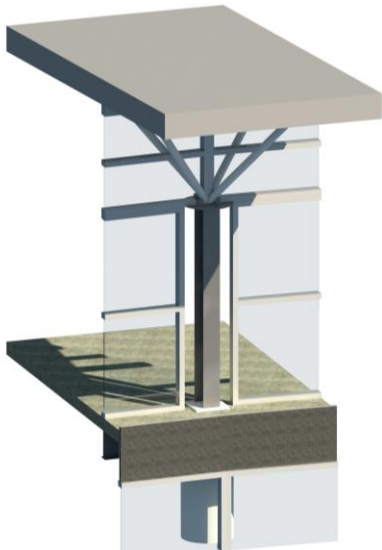
Figure 75: Phase 3 - Column Construction

The W12x40 will be installed to the base plate.



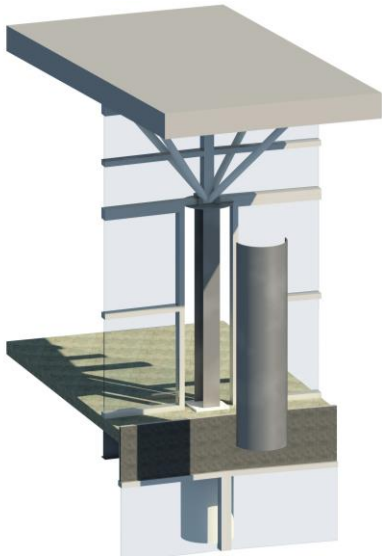
Installation of inverted roof and tree column connection. The same tree column connection was used as the existing building – a $\frac{3}{8}$ " base plate and (2) $\frac{5}{16}$ " flange plates.

Figure 76: Phase 4 - Column Construction



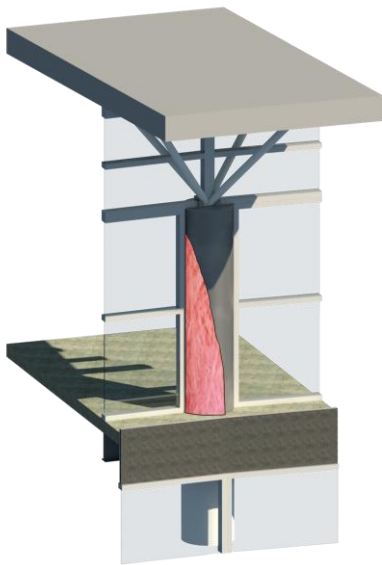
Glass façade installation.

Figure 77: Phase 5 - Column Construction



The aluminum façade sheathing will be placed next, integrating with the glass façade manufacturer's mullion design for easy installation.

Figure 78: Phase 6 - Column Construction



The void between the aluminum sheathing and wide flange is filled with batt insulation, to properly break the thermal bridge of the original design.

Figure 79: Phase 7 - Column Construction

The final design of the new column to prevent the thermal bridge is seen Figure 80.

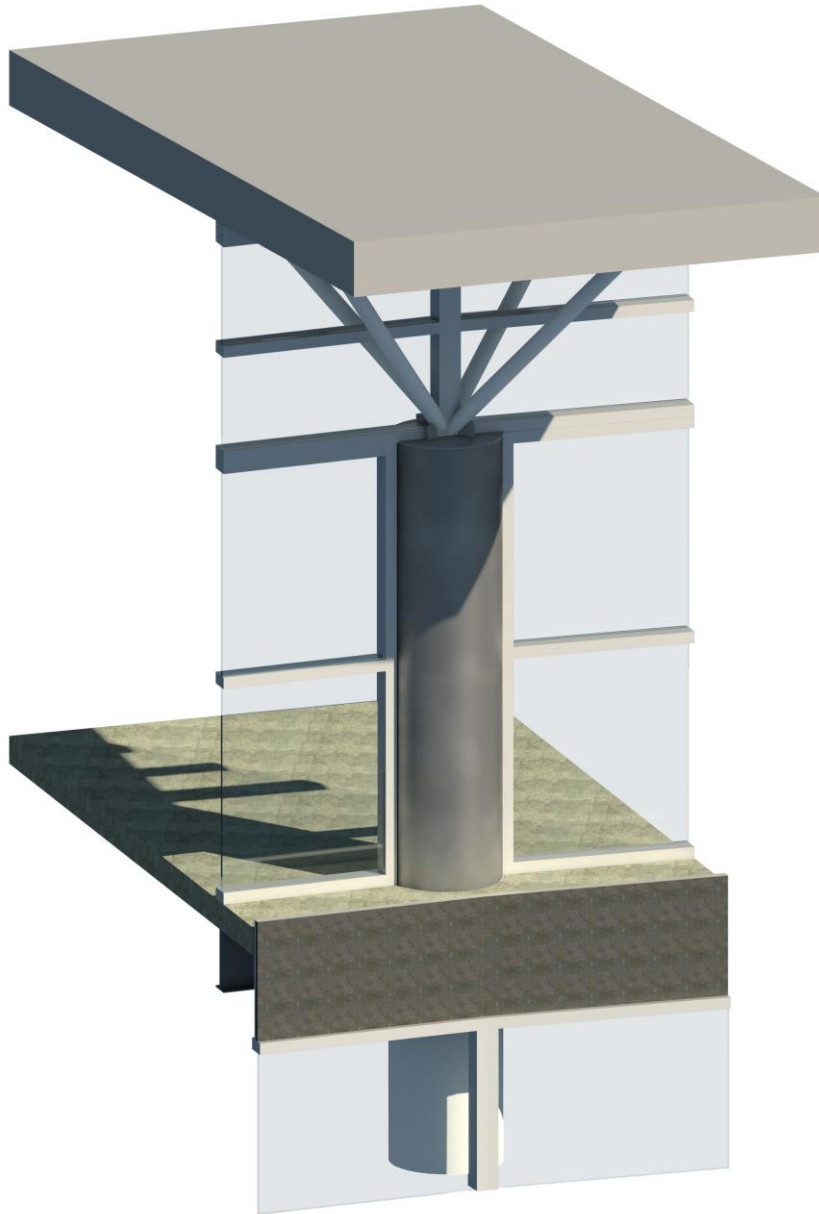


Figure 80: Final column design to prevent thermal bridge

A final rendering of a section of the building is seen below in Figure 81 (level 2 to 4) and also shows a comparison between the existing and redesigned gravity systems. The aluminum façade is shown floating in front of the building to show the new wide flange design.

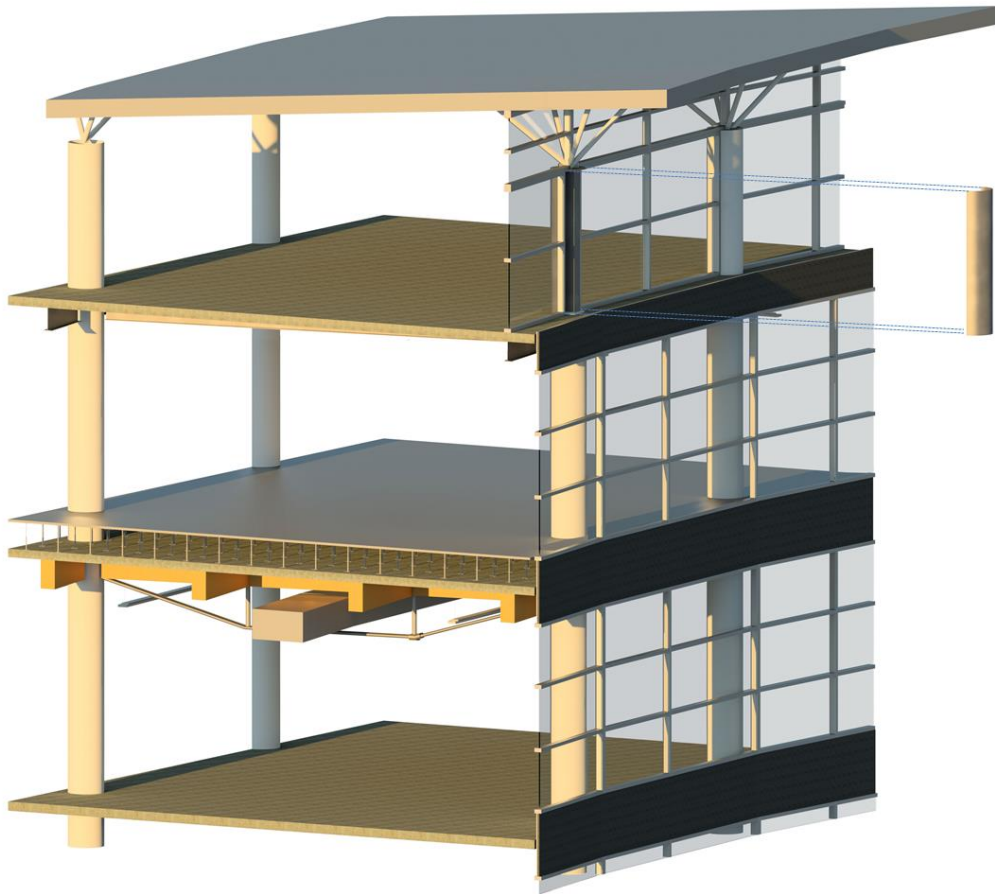


Figure 81: Building section of redesigned column

CHAPTER 4

ARCHITECTURE

4.1 ARCHITECTURE BREADTH

The drastic change in building materials led to a completely new aesthetic to the interior of the building. Besides the slight change in insulating properties of the fourth level, no other façade changes were made to the envelope. The interior changes can be viewed below in Figure 82, while the existing interior can be seen in Figure 83.



Figure 82: Interior aesthetic changes due to gravity redesign



Figure 83: Interior aesthetic from existing gravity system

Impacts from Structural Redesign

A primary goal while examining and redesigning the structural depth of the Heifer International Center was to leave the existing layout of the building the same. This was accomplished through an exhaustive design process for the new hybrid glulam and steel gravity systems, and the new cast-in-place concrete lateral force resisting system. The interior aesthetic of the building was successfully changed and fully integrated with the mechanical and structural disciplines of the building. The new structural queen post girders provide the opportunity for occupants to better connect with the building and visually see the elements that are supporting the floors and the engineering systems which interconnect with building, as well as provide comfort to the occupants.

Architectural Design Guidelines

The following design guideline was established at the inception of the structural depth to aide with the design of, not just the architectural components of the building, but to also positively lead the design of the engineering systems of the building. The desire to enhance the architecture by changing the structural material influenced mechanical, electrical systems and the interior appeal of the building.

These guidelines will aid in the basis for future development of the Heifer International Campus and surrounding area. The standards set forth do not seek to constrain architectural and engineering creativity, but rather to encourage a variety of designs within certain attributes that will ensure to harmonize the campus and encourage public interaction.

The goals of developing these guidelines are:

1. Promote design solutions that lend themselves to educational and visual interactions
2. Express the abstract meanings of charity through the physical form of the building and Heifer International Campus
3. Develop architectural characteristics that should be followed during the duration of the design
4. Lay the foundation for the expansion of the campus in the future and define architectural attributes that should be promoted and which should be discouraged

History of Heifer International

Dan West founded Heifer International almost 70 years ago and the charity has worked tirelessly in the effort to end hunger and poverty throughout the world. By giving power to families to provide for themselves, the organization empowers communities to sustainably support themselves both agriculturally and commercially. This form of dependable food and income is the fundamental ideal of Heifer International, known as *Passing on the Gift* (Heifer International, 2014).

Character of the Campus

Site Circulation

Pedestrian paths, bicycle paths and personal and commercial vehicular movement will be promoted through the site. East 3rd Street acts as a main street to guide pedestrian and vehicular movement, while World Avenue and Shall Avenue will act as secondary streets. The site is conveniently located near a city light rail station and city bus stop. In addition, an exit off Interstate 30 is located approximately one-third of a mile away from the site. This is shown in Figure 84 below.

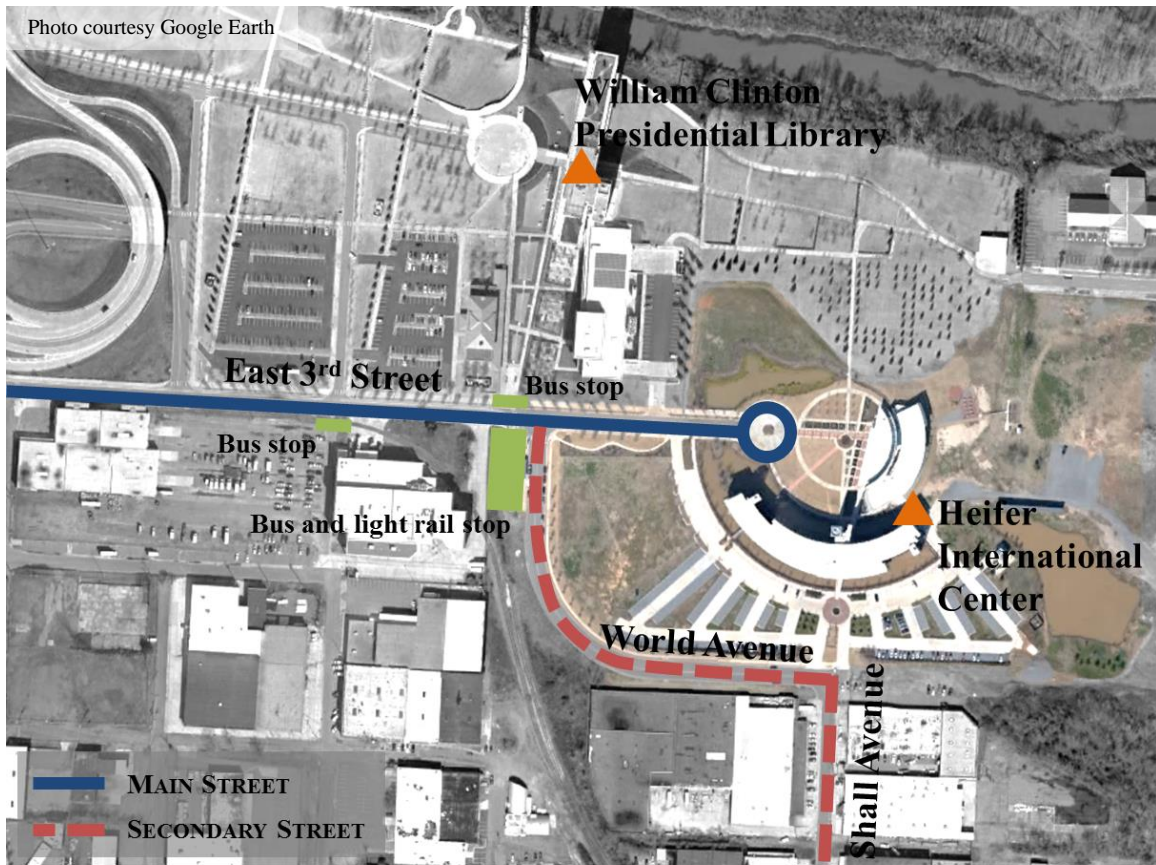


Figure 84: Site circulation of the Heifer International campus

Primary movement through the site will act along East 3rd Avenue, and will be the focal point for pedestrian, bicycle and vehicular entrance into the site. From here pedestrians will be able to move through the accessible campus, seen below in Figure 85.

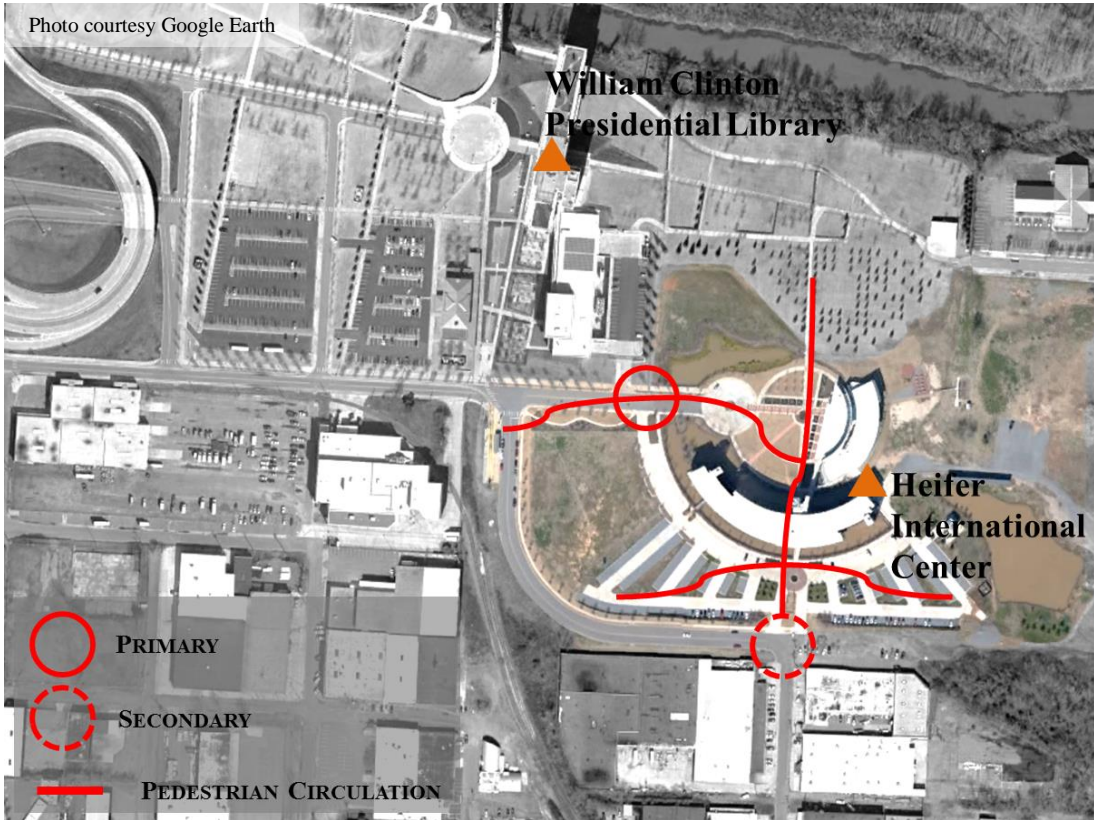


Figure 85: Primary and secondary circulation through Heifer International campus

Movement on the Site

Buildings should create a defined outdoor space and encourage existing views of the landscape. There should be accessibility between existing and proposed buildings and a uniformity imposed on the campus. The following should be used to accomplish this:

- Roads and Parking Areas
 - Local aggregate to match color and texture of existing drive, Figure 86
 - Porous pavement system shall be used in parking areas, and bioswales shall be used to promote local plant and animal life, Figure 87
 - Parking areas shall accommodate pedestrians and vehicular circulation, Figure 88



Figure 86: Local aggregate to match color and texture



Figure 87: Porous pavement used in parking areas



Figure 88: Pedestrian and vehicular activity accommodated in parking lot

- Integrate site drainage into walkways, Figure 89
- Design of site and campus plantings responsibility of landscape architect
- Specify plants indigenous to central Arkansas to promote plant growth and habitat rehabilitation, Figure 90
- Pedestrian Paths, Figure 91
 - Central Walkway: 13'-6" wide
 - Secondary Walkways: 10' wide
 - Wetland Walkways: 8'-0" wide, concrete and heavy timber



Figure 89: Integration of walkways and incorporation of drainage system



Figure 90: Indigenous plantings used on the campus



Figure 91: Central and secondary walkways

Character of Buildings

- Typology
 - Building profile should incorporate vision of Dan West

In all my travels around the world, the important decisions were made where people sat in a circle, facing each other as equals. – Dan West



Figure 92: Circular form of campus



Figure 93: Circular form of building

- Roofs
 - Inverted roof system with a slope ranging from 1/12 to 1/6 shall be used, shown in Figure 94
 - Water collection system shall be designed to capture rainfall for use to offset potable water usage, Figure 95
 - Overhangs shall be at the discretion of the architecture, Figure 96
- Entrances and Bridges
 - Weather protected entry way, Figure 96



Figure 94: Inverted sloped roof



Figure 95: Water collection system tower (far left) and local wetland (front right)

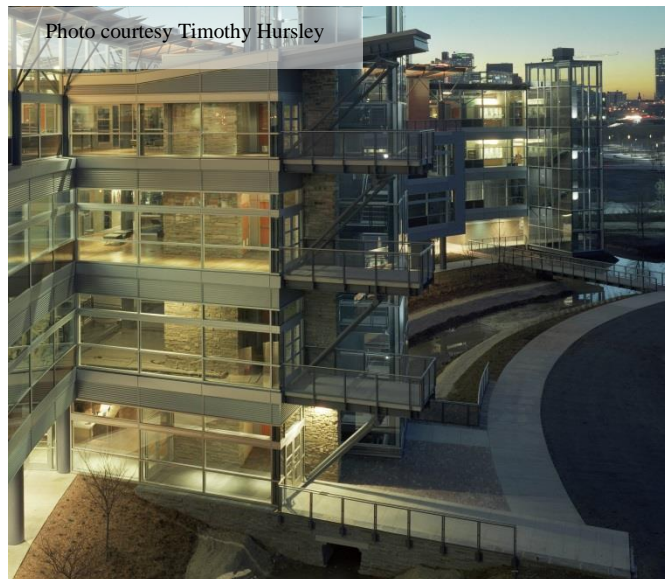


Figure 96: Covered entrance to building

- Walls and Windows
 - Glazing system shall promote connection with outdoors and maximize natural day lighting on all floors of the building, Figure 97 and Figure 98



Figure 97: Natural daylighting in interior of building



Figure 98: Exterior shot of natural daylighting penetrating building façade

Character of the Interior Space

- Fenestration
 - Glazing system shall promote connection with outdoors and maximize natural day lighting, Figure 99 and Figure 100



Figure 99: Interior natural lighting



Figure 100: Exterior view of interior artificial light

- Spacious interior
 - Large flexible environment for a variety of public and private events, Figure 101



Figure 101: Interior spacious environment

- Structural elements
 - Materials
 - Structural materials should focus on glulam, steel and concrete, with the objective of creating a comfortable and homey environment
 - Structural bays
 - A radius should be established and a degree of separation between major structural bays should remain fairly constant
 - A reference point should be located on plans for each circular center, Figure 102

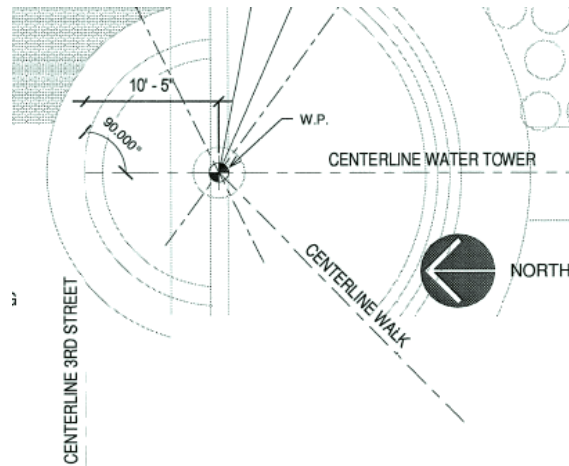


Figure 102: Reference point on plan to mark circular center

- Beams
 - 3 to 4 beam proportions (or sizes) should be used on the project in order to keep a consistent pattern on the gravity system
 - Glulam and steel should be used in the gravity system
 - Steel should be painted with a nature-green color

○ Columns

- An airy atmosphere should be created by the floor to floor heights
- Steel “tree” column
 - Representation of trees in wetlands surrounding the building and a shelter for each of the charity’s employees, Figure 103 and Figure 104
 - Supports inverted roof for rainwater collection
- 2’-0” wide round columns (steel or concrete material), Figure 105 and Figure 106

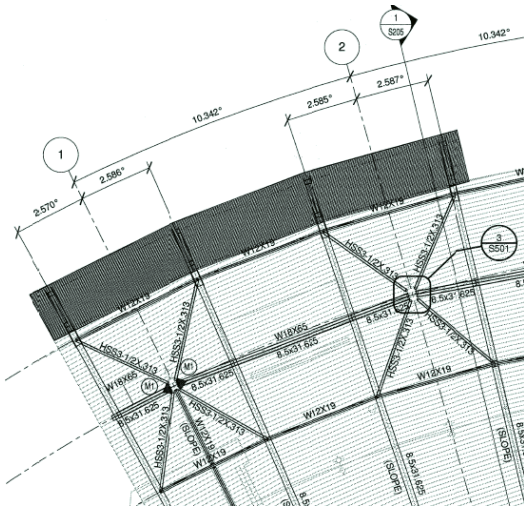


Figure 103: Plan of tree columns

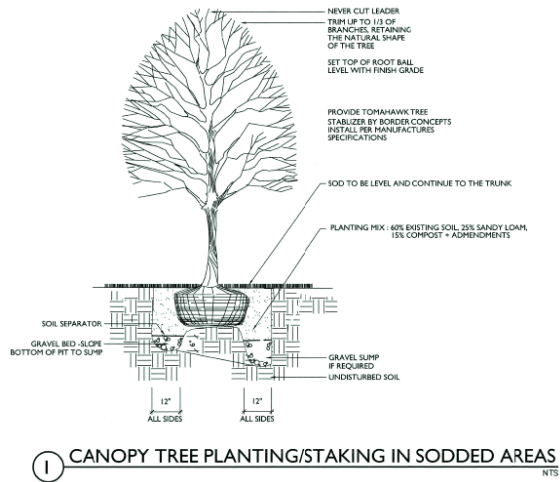
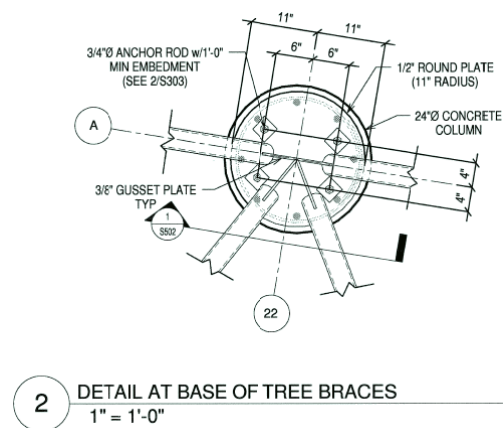
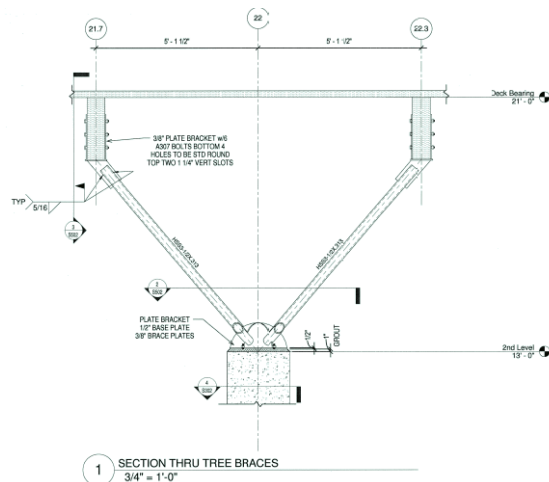


Figure 104: Inspiration for tree column canopy



2 DETAIL AT BASE OF TREE BRACES
1" = 1'-0"

Figure 105: Plan detail of tree column connection



1 SECTION THRU TREE BRACES
3/4" = 1'-0"

Figure 106: Section detail of tree column connection

CHAPTER 5

AN INVESTIGATION OF WOOD-CONCRETE COMPOSITE FLOORING SYSTEMS

A thesis submitted in
partial fulfillment of the requirements for a bachelor degree in Architectural Engineering
with honors in Architectural Engineering

Schreyer Honors College

5.1 COMPOSITE WOOD-CONCRETE FLOOR SYSTEM

A composite wood-concrete system is well matched for the redesigned glulam gravity system of the Heifer International Center. A composite wood-concrete system, also known as a timber-concrete composite (TCC) structure, can be well adapted to the glulam beam and queen post girder system designed for the Heifer International Center. TCC is very useful for restoration work (Gelfii, Giuriani, & Marini, 2002), bridge construction (Yeoh, Fragiacom, Franceschi, & Boon, 2011) and for new building design and construction. The main advantages of TCC are cost savings and the ability of “replacing nonrenewable resource based concrete and steel with a manageable renewable resource, and reduced energy of material production and construction carbon dioxide emissions.” In addition there are technical advantages of using wood and concrete, such as increased fire and acoustical ratings (Gutkowski, Balogh, & To, 2010; Clouston & Schreyer, 2008).

The fundamental design criterion for a TCC system is to keep the neutral axis of the composite cross section close to the boundary of the timber-concrete interface—ensuring that the concrete acts purely in compression and that the timber is mostly subjected to tensile stresses. In addition, a strong and stiff connection system must be in place in order to transfer the shear forces properly and provide an effective cross area for composite action. Lastly, the design criterion calls for a strong timber section, in order to resist bending tensile stresses induced by gravity loads (Yeoh, Fragiacom, Franceschi, & Boon, 2011).

Due to a shortage of steel in Europe after World War I and World War II, TCC systems began to develop and become popular alternatives in restoration projects of older



Photo courtesy Antti Bilund

Figure 107: The Vihantasalmi Bridge of Finland

historical buildings. The existing floor systems of historical buildings were inadequate for sound insulation and fire resistance, and were updated using TCC. This mostly European system expanded throughout the last half century for use in highway bridges and new building construction. As an example, the Vihantasalmi Bridge of Finland was built in 1999 and spans 168 meters. The bridge spans 14 meters wide, 11 meters for the road and 3 meters for a sidewalk. The Vihantasalmi Bridge is shown in Figure 107¹⁰.

¹⁰ Used with permission through the GNU Free Documentation License

Design Standards of TCC

TCC bridges were considered as far back as 1944 with the specification of the American Association of State Highway Official. TCC is not addressed in most standards throughout the world, except the Eurocode 5, Part 2 for timber bridges. Because the interlayer shear connection is not fully rigid, the assumption of plane sections remaining plane does not apply to this type of composite section. The slip between the bottom fiber of concrete and the upper fiber of timber does not allow for the method of transformed sections.

A designer must be aware that partial composite action is possible due to the flexibility of the shear connection and that there are time-dependent properties of the composite materials. A semi-prefabricated TCC floor system is shown in Figure 108¹¹, and had to consider these design phenomena (Yeoh, Fragiacom, Franceschi, & Boon, 2011; European Committee for Standardization, 2004).

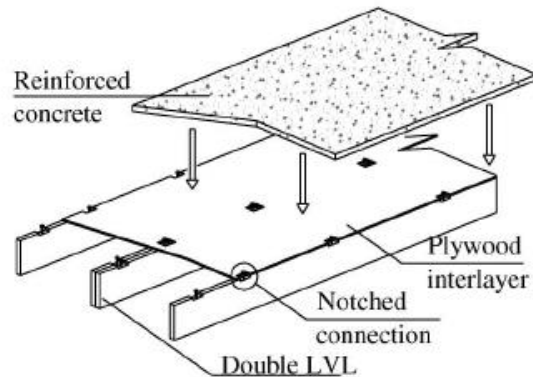


Figure 108: Semi-prefabricated TCC floor system in New Zealand (Yeoh et al.)

A thorough literature review was conducted, limited to the years of 2000 to 2014, to better understand a TCC system and how it may apply to the Heifer International Center. Research of TCC systems have led to the summary of five main systems:

1. Shear connector and wire mesh
2. Shear key connection
3. Hilti and shear key connection
4. Glued composite members
5. Custom lag bolt system

¹¹ Used with permission from Dr. David Yeoh, Universiti Tun Hussein Onn Malaysia (david@uthm.edu.my)

Types of TCC Systems

Shear connector and wire mesh

A continuous steel mesh is used in conjunction with a shear connector to join wood and concrete components. One half of a shear connector is embedded in a wood beam, while the other is embedded in concrete (Clouston, Bathon, & Schreyer, 2005), and is shown in Figure 109¹². This causes composite action between the two materials. This system has been tested in static push-out tests and full scale bending tests, with a span of approximately 33'-0". The wire mesh aids with the composite action, and has performed satisfactorily in adding ductility to the shear connector, but still keeping a stiff connection between the two materials. No design guidelines exist in the United States for TCC systems; however, Eurocode 5 provides formulas which aide in the estimation of design parameters for composite systems with shear connectors (European Committee for Standardization, 2004). Clouston et al. was able to predict failures of the two load test performed on the shear connector and wire mesh composite system using the design parameters of Eurocode 5. Through several iterative tests, it was found that composite action was nearly achieved—“97% effective stiffness and 99% strength of that of a beam with full composite action.”

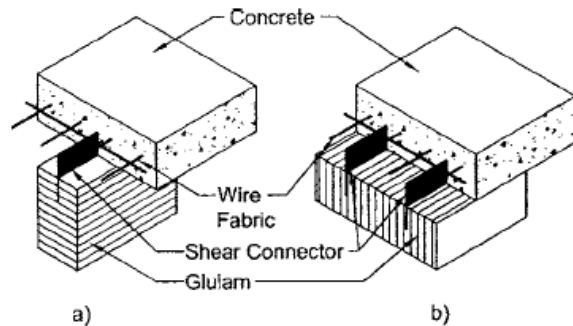


Figure 109: Shear connector and wire mesh (Clouston et al.)

Shear key connection

A second TCC system comprises a construction technique which uses a keyed wood member, shown in the cross section of Figure 110¹³. The beam specimens were monitored during the construction process, and for an overall period of 133 days after the application of the service load. Using a finite element model developed by Department of Civil Engineering of the University of Canterbury, a research team was able to theoretically extend the composite structure through a service life.

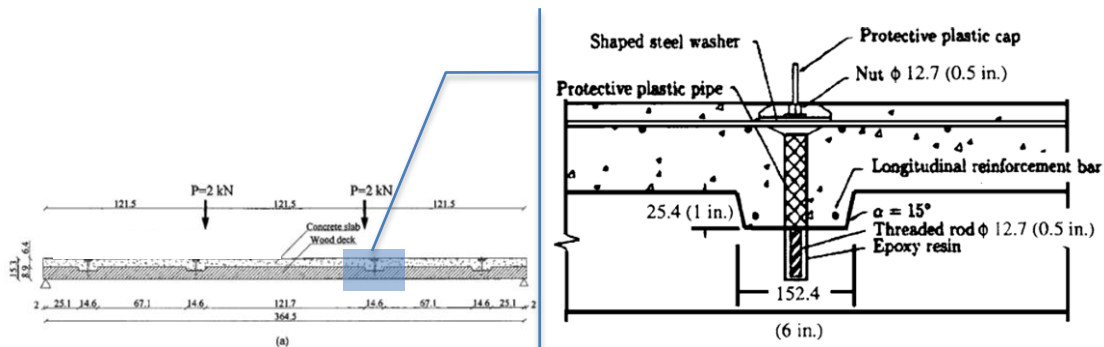


Figure 110: Shear key connection, longitudinal view (Fragiacomo et al.)

¹² Used with permission from Dr. Peggi Clouston, University of Massachusetts (clouston@umass.edu)

¹³ Used with permission from Dr. Massimo Fragiaco, University of Sassari (fragiaco@uniss.it)

It was found that an increase in moisture from bleeding of the concrete into the timber was “not an issue for the durability of the wood deck” and that the type of construction (shored or unshored) does not affect the structural performance of the system (Fragiacomo, Gutkowski, Balogh, & Fast, 2007). Figure 111¹³ shows a cross section of the shear key connection.

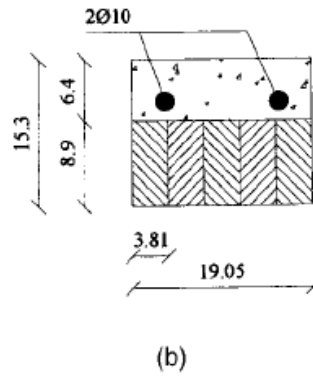


Figure 111: Shear key connection, cross section, (Fragiacomo et al.)

Hilti and shear key connection

The Hilti and shear connection system is very similar to the shear key connection system just discussed; however, the system uses the proprietary system of Hilti, Inc., and is shown in Figure 112¹⁴. The construction of offices, hotels and apartments does not typically use light frame wood floor construction. Instead the industry tends towards cast-in-place reinforced concrete slabs or steel composite decking, as previously discussed. Research of this system has been conducted so that the formwork for the traditional concrete slab can be left in place. This allows for the development of composite action (Gutkowski, Balogh, & To, 2010).

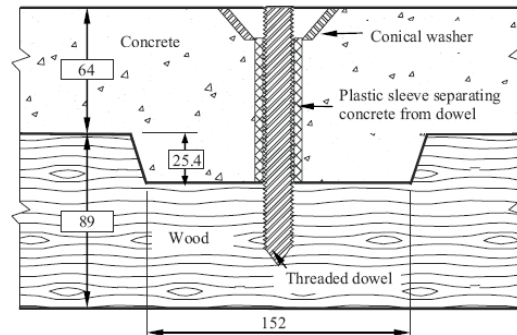


Figure 112: Hilti dowel cross section (Gutkowski et al.)

Research has shown that medium to high composite action is possible for shear key connection solid wood-concrete beam systems. This involves several tests:

- Withdrawal tests of the anchor connector
- Interlayer load-slip tests of the interlayer connection specimens
- Preliminary flexural tests of layered solid wood-concrete beam
- Tests of full scale wood-concrete floors

These tests involved nominal dimension lumber (Brown, Gutkowki, Natterer, & Shigidi, 2008).

¹⁴ Figure from Gutkowski et al. 2010

Glued composite members

The interface of the concrete and wood can be glued. Henrique et al. studied both cast-on-site and prefabricated composite timber-concrete beams, which were produced to simulate the possibility of a partial or full prefabrication composite construction. The

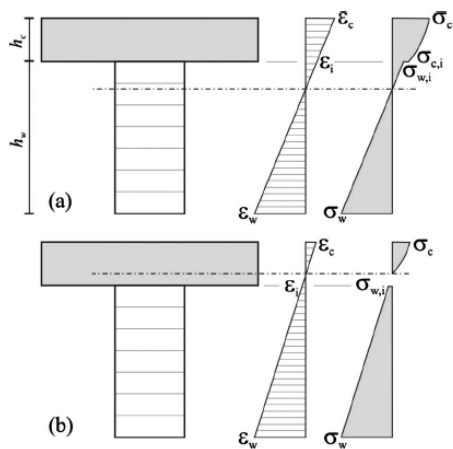


Figure 113: Glued composite, stress and strain distribution (Henrique et al.)

glued interface composite members were compared to shear connector timber-concrete beams. A glued interface beam is shown in Figure 113¹⁵.

Results show that strength is similar between the three groups tested and that a greater stiffness was achieved in the glued composite timber-concrete beams. Due to greater stiffness, less deflection developed in the beam. Under stabilized and dry conditions, the prevailing mode of failure is tension in timber and, when shear failure occurs, it is mostly conditioned by the shear strength of the concrete or timber, not by the adhesive glue. A bending test is shown in Figure 114¹⁵.

Gluing the two sections of the composite wood and concrete beam appear to be a good alternative to a shear connector. The mean and characteristic values of strength are similar for both cases, the glued elements show a stiffer behavior, albeit a small difference under service load. The system was found to have similar results, glued and not glued, for on-site and prefabricated concrete.

Prefabricated beams were governed by flexural tension and in the fresh cast on-site concrete the interface shear prevailed as the failure mode, but the observation of the beams has shown that the collapse was dictated by the concrete, not by the adhesive material or timber (according to the author this is odd behavior for the material). Improvement of stiffness and strength is more than 100% compared to a plain solid timber beam. This leads to the conclusion that the system is reliable; however, long-term behavior and the effect of cyclic loads require a further study (Henrique Jorge de Oliveira Negrão, Miguel Maia de Oliveira, Alexandra Leitão de Oliveira, & Barreto Cachim, 2010).



Figure 114: Bending test of glued composite member (Henrique et al.)

¹⁵ Used with permission from Prof. João Negrão, University of Coimbra (jhnegrão@dec.uc.pt)

Custom lag bolt system

The last system which will be discussed is a custom lag bolt system. This project for the Federal Center South Seattle District Headquarters of the United States Army Corps of Engineers involved reclaiming a substantial amount of wood beams. When paired with reclaimed decking a composite system of timber and concrete could be produced; however, required the use of a lag bolt to sufficiently link the two materials. The lag bolt had to be custom made for the project, increasing costs. The custom lag bolt system is shown in Figure 115¹⁶. Test assemblies were developed to test load durations and load capacity of the system.

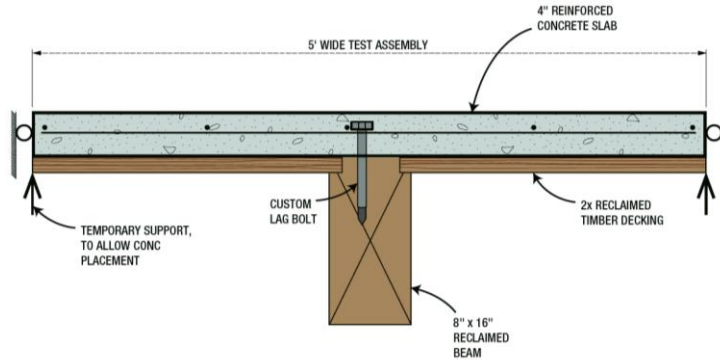


Figure 115: Custom lag bolt system (Swenson et al.)

In order for the design to pass inspection, it had to hold twice the design live load for 24 hours. At the end of the 24 hour period, the deflection of the system would be measured, and then was unloaded. It was required to recover 75% of the measured deflection within the next 24 hour time period. Each test system passed the test. The experiment continued to test failure. It was also found that the system could hold well over 400% of the design dead load and around 550% of the design dead load, with no visible sign of distress to the system. It was not until around 650% of the design live load did cracks appear and “cracking sounds were heard.” After approximately 10 minutes of holding the load at 650% above design live load, the beam failed in flexure, and is shown in Figure 116¹⁶ (Swenson & Black, 2013).



Figure 116: Tested beam before failure (Swenson et al.)

¹⁶ Used with permission from Mr. Jim Swenson, KPFF Consulting Engineers (jim.swenson@kpff.com)

Cyclic Loading Effects to TCC

Repeated and sustained loading have been briefly researched for wood-concrete composite systems. Balogh et al. performed cyclic loading to imitate live loading over a 30 year period for composite beams used for buildings and bridges. After the cyclic imitation loading, the beams were ramp loaded to failure. According to their findings live load cyclic loading led to an “irrecoverable increase in deflection at the end of the 21,600 load cycles on average equal to 18% of the initial elastic deflection.” A steady state deflection was almost reached that was comparable to the number of cycles experienced by a major highway bridge. It was found that two types of failures mechanisms formed on the composite beams:

- Shear in the wood between the exterior notch and beam end, Figure 117¹⁷
- Flexure at midspan of wood member, Figure 118¹⁷



Figure 117: Shear failure of wood notch (Balogh et al.)



Figure 118: Midspan flexural failure (Balogh et al.)

Shear was characterized by a split from the notch to the end of the beam. This was always followed by bending failure at the midspan. The cyclic loading of the beam increased deflection by 18% and decreased beam stiffness by 9% (on average). Balogh et al. stated that the decrease in stiffness is due to the “progressive damage occurring in the connection detail” (Balogh, Fragiaco, Gutkowski, & Fast, 2008; Clouston, Bathon, & Schreyer, 2005).

¹⁷ Used with permission from Dr. Jenő Balogh, Metropolitan State University of Denver (jbalogh@msudenver.edu)

Conclusion to TCC

A timber-concrete composite system offered a unique floor system to study with the new gravity glulam system of the Heifer International Center. While calculations into the design of the floor system were not explored due to time constraints and the challenging design process of TCC systems, a better understanding of the various TCC systems that exist in research and industry was obtained. If the Heifer International Center was in the design phase and a large amount of reclaimed timber was locally available, it should be truly considered as floor system for the building.

Additional References

The following references were also used in the development of this section of the report.

- Loulou, L., Caré, S., Le Roy, R., & Bornert, M. (2010). Damage of Wood-Concrete Composite subjected to variable hygrometric conditions. *EDP Sciences*, 6(28002).
- Nawari, N. (2012, June). BIM Standardization and Wood Structures. *Computing in Civil Engineering*, 293-300.
- Schneider III, W. G. (2005). *Shear Stud Connection Development for Steel Stringer Highway Bridges with Hardwood Glulam Timber Deck*. The Graduate School, Special Individualized Interdisciplinary Doctoral Majors. The Pennsylvania State University.

CHAPTER 6

CONCLUSION

6.1 CONCLUSION

Both the gravity and the lateral systems of the Heifer International Center were chosen for redesign. Glulam was used instead of the original steel structure and a cast-in-place concrete shear wall system instead of the steel plate shear wall system. Conceivable systems were devised that could fulfill the request of the architect to explore different structural materials for aesthetic purposes and achieve an integration among the engineering systems. While the potential cost of the system may be greater than the originally designed steel structure, the incorporation of the breadth studies aided with the understanding of how the architectural components of the building could directly tie to the structural, mechanical and electrical systems of the building.

The glulam queen post girder proved to be extremely beneficial to the design, allowing integration between the structural, mechanical, electrical and architectural disciplines. The queen post girder was able to enhance the architectural characteristic of the building by providing a direct visual link between the occupant and the designed engineering systems. Moreover, the floor-to-floor height was unchanged between the existing and redesigned system, which is important to allow for the sense of the open office atmosphere.

The redesigned lateral system, the cast-in-place concrete shear walls, does not impose any variations to the building layout. A potential connection between the glulam gravity beams and the cast-in-place concrete shear walls was studied. Seismic and wind analyses were completed and found to properly pass. Torsional irregularity was studied in depth in this project and was found to not be a significant issue based on the concrete lateral redesign.

It was important to the structural engineer to not impose any changes to the façade system, while still improving the insulating properties of the wall assembly. This was accomplished through a restructuring of the fourth floor columns, which were exposed to the exterior and interior. The U-value of the façade was greatly improved over the existing system, and yet aesthetically appears the same as the existing system.

Overall, the architect was pleased with the results to the redesign as the goals of Mr. Dan West were incorporated and respected. The redesign added a new sense of openness and strength to the building and will allow for the continuation of the charity's *Passing on the Gift*.

REFERENCES AND WORK CITED

- Almaxco. (2012). *Aluminum Composite Panels*. Singapore: Maxgrow Pte Ltd.
- American Concrete Institute, ACI-318. (2011). *Building Code Requirements for Structural Concrete and Commentary*. Farmington Hills, MI.
- American Institute of Steel Construction. (2011). *Steel Construction Manual* (Fourteenth ed.). American Institute of Steel Construction.
- American Society of Civil Engineers. (2010). *ASCE-7 10, Minimum Design Loads for Buildings and Other Structures*. Reston, VA.
- American Wood Council. (2013). *National Design Specification (NDS) for Wood Construction with Commentary 2012 Edition*. Leeburg, VA.
- APA - The Engineered Wood Association. (2009). *Calculating Fire Resistance of Glulam Beams and Columns*. Tacoma.
- Balogh, J., Fragiacomio, M., Gutkowski, R. M., & Fast, R. S. (2008, March). Influence of Repeated and Sustained Loading on the Performance of Layered Wood–Concrete Composite Beams. *Journal of Structural Engineering*, 134(3), 430-439.
- Brown, K., Gutkowski, R., Natterer, J., & Shigidi, A. (2008, June). Laboratory tests of composite wood-concrete beams. *Construction and Building Materials*, 22(6), 1059-1066.
- Clouston, P., & Schreyer, A. (2008, November). Design and Use of Wood–Concrete Composites. *Practice Periodical on Structural Design and Construction*, 13(4), 167-174.
- Clouston, P., Bathon, L. A., & Schreyer, A. (2005, September). Shear and Bending Performance of a Novel Wood–Concrete Composite System. *Journal of Structural Engineers*, 131(9), 1404-1412.
- European Committee for Standardization. (2004). *EN 1995: Design of timber structures*. European Committee for Standardization.
- Frangiaco, M., Gutkowski, R. M., Balogh, J., & Fast, R. S. (2007, September). Long-Term Behavior of Wood-Concrete Composite Floor/Deck Systems with Shear Key Connection Detail. *Journal of Structural Engineering*, 133(9), 1307-1315.

- Gelfii, P., Giuriani, E., & Marini, A. (2002, December). Stud Shear Connection Design for Composite Concrete Slab and Wood Beams. *Journal of Structural Engineering*, 128(12), 1544-1550.
- Gutkowski, R. M., Balogh, J., & To, L. G. (2010, June). Finite-Element Modeling of Short-Term Field Response of Composite Wood-Concrete Floors/Decks. *Journal of Structural Engineering*, 136(6), 707-714.
- Heifer International. (2014). *Heifer International | Charity Ending Hunger and Poverty*. Retrieved from Heifer International: <http://www.heifer.org/>
- Henrique Jorge de Oliveira Negrão, J., Miguel Maia de Oliveira, F., Alexandra Leitão de Oliveira, C., & Barreto Cachim, P. (2010, October). Glued Composite Timber-Concrete Beams. II: Analysis and Tests of Beam Specimens. *Journal of Structural Engineering*, 136(10), 1246-1254.
- International Code Council. (2009). *International Building Code*. International Code Council.
- Macalloy Bar & Cable Systems. (2014, February 6). Macalloy Tensile Structure Systems. Sheffield, South Yorkshire S25, United Kingdom.
- Nucor Corporate. (2013). *Vulcraft Deck Catalog*. Retrieved from Vulcraft: <http://www.vulcraft.com/>
- Owens Corning Insulating Systems, LLC. (2007). *Thermal Batt FIBERGLAS Insulation*. Toledo: Owens Corning.
- Robinson, K., & Ames, D. (2000, January). Steel Plate Shear Walls: Library Seismic Upgrade. *Modern Steel Construction*.
- Schneider III, W. G. (2014). BE 462 - Design of Wood Structures. The Pennsylvania State University.
- Showalter, J. (2012). Connection Solutions for Wood-frame Structures. *The American Institute of Architects Continuing Education Systems*. American Wood Council.
- Simpson Strong-Tie. (2014). *LGU/MGU/HGU/HHGU High Capacity Girder Hangers for Glulam*. Retrieved from Simpson Strong-Tie: <http://www.strongtie.com/>
- Swenson, J. O., & Black, J. (2013, April). A Worthy Wager. *STRUCTURE magazine*, pp. 26-29.

U.S. Geological Survey. (2013, July). *U.S. Seismic Design Maps*. Retrieved from U.S. Geological Survey: <http://www.usgs.gov/>

Yeoh, D., Fragiaco, M., Franceschi, M., & Boon, K. (2011, October). State of the Art on Timber-Concrete Composite Structures: Literature Review. *Journal of Structural Engineering*, 137(10), 1085-1095.

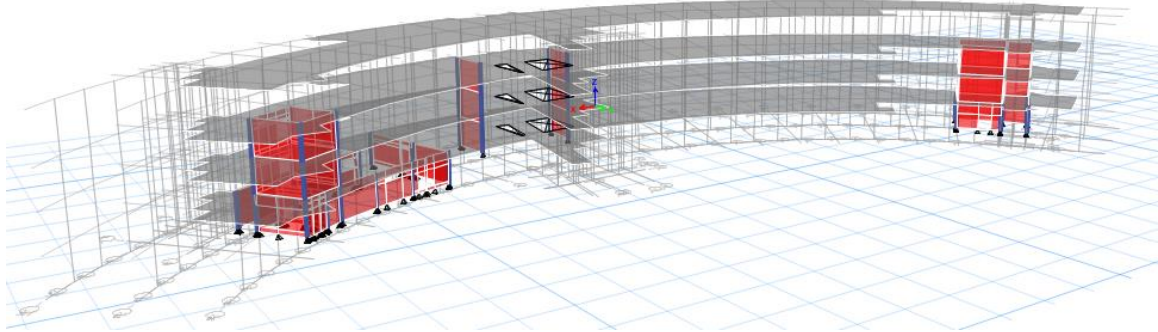
APPENDIX A

EXISTING STRUCTURAL ANALYSIS

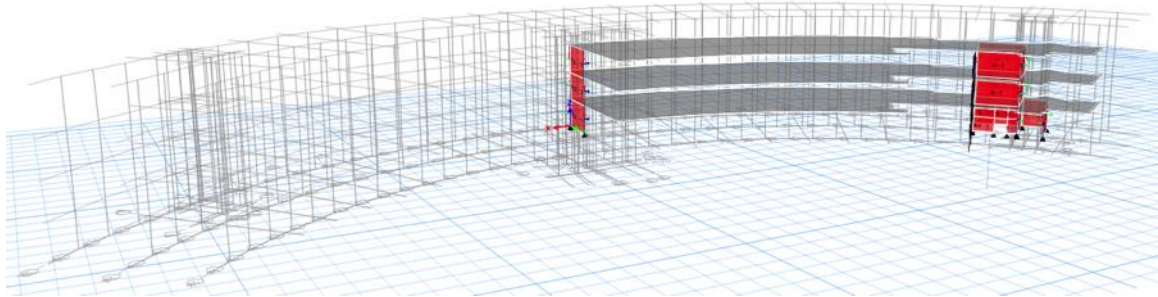
APPENDIX A.1 - EXISTING LATERAL SYSTEM MODELING

Evolution of the ETABS Model

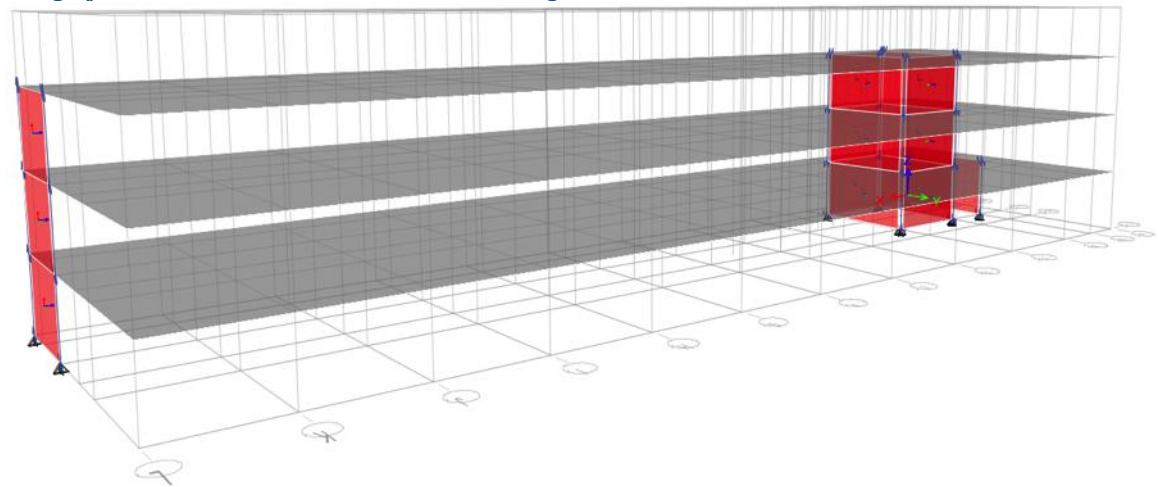
Model of entire building



Model of half of the building, east side



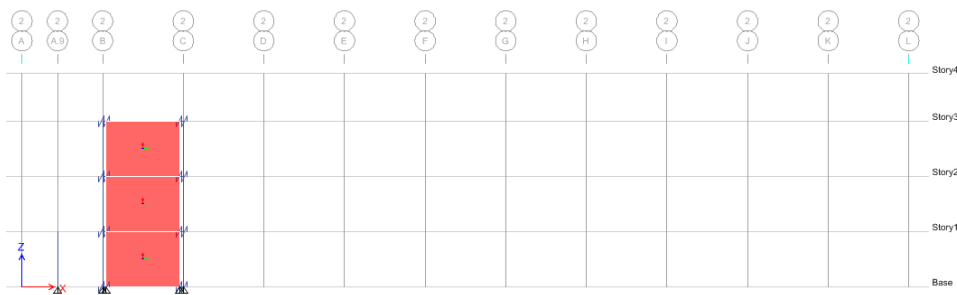
Simplified model used in this technical report



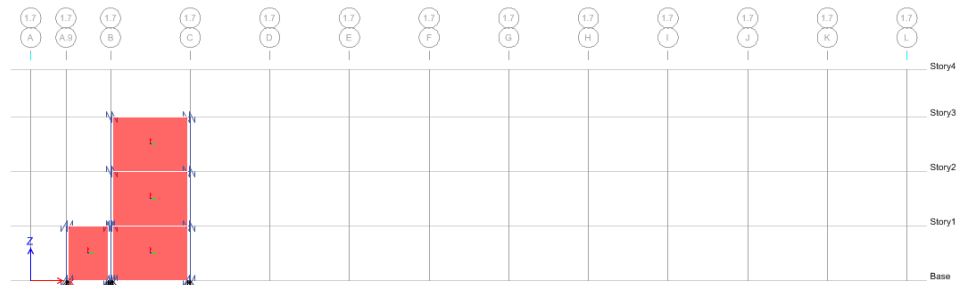
Elevations of Shear Walls



Shear Wall 1



Shear Wall 2, 4, 5, and 13@12



Shear Wall 3 and 3 (offset)

ETABS SPSW to Concrete Conversion

The steel plate shear wall lateral system was converted into an equivalent concrete shear wall system, using an effective stiffness method. This equates the stiffness of the steel plate shear wall to the stiffness of a concrete shear wall. This allows for an equivalent depth, of the concrete shear wall, to be solved for. It was found an equivalent depth of 2.98” would be used in the model.

Please find the calculations for the conversion of steel to effective concrete on the next page.

The steel plate shear wall lateral system was converted into an equivalent concrete shear wall system, using an effective stiffness method. This equates the stiffness of the steel plate shear wall to the stiffness of a concrete shear wall. This allows for the an equivalent depth, of the concrete shear wall, to be solved for.

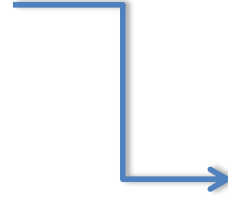
A36 STEEL

E = 29000 ksi
 G = 11603 ksi
 t = 0.375 in

CONCRETE

f'c = 4000
 wc = 145
 E = 3644
 G = 1458

WALL DIMENSIONS				SPSW WALL PROPERTIES		SPSW STIFFNESS		UPDATED WALL PROPERTIES		EQUIVALENT CONCRETE SHEAR WALL	
h (ft)	h (in)	b (ft)	b (in)	Area (in ²)	Inertia (in ⁴)	k _{fixed} (k/in)	Area (in ²)	Inertia (in ⁴)	t _{effective} (in)		
14	168	20	240	90	432000	4452	240	1152000	2.984901		
14	168	25	300	112.5	843750	5862	300	2250000	2.984936		
14	168	11.46	137.50	51.56	81230.87	1981	137.50	216615.65	2.984752		
14	168	20.46	245.50	92.06	462363.75	4583	245.50	1232970.01	2.984905		



EQUIVALENT DEPTH = 2.98 inches

Hand Calculation of SPSW to Concrete Conversion

PORTER-GILL	TECH REPORT 4	EFFECTIVE SPSW
<p>CONVERT SPSW TO EFFECTIVE THICKNESS OF CONCRETE:</p>		
$K = \frac{1}{\frac{h^3}{12EI} + \frac{1.2hw}{AG}}$ $I = \frac{tb^3}{12}$ $A = bt$		
SPSW	<p>SPSW: $b = 20'$ $h = 14'$</p> <p>$E = 29000 \text{ ksi}$ $G = 11603 \text{ ksi}$</p>	<p>$t = 0.376''$</p>
$K_{SPSW} = \frac{1}{\frac{(14 \times 12)^3}{12(29000) \cdot \left(\frac{0.376(20 \times 12)^3}{12}\right)} + \frac{1.2(14 \times 12)}{(0.376(20 \times 12))(11603)}}$ <p style="text-align: center;">$= 4152.18 \sim 4158 \text{ k/in FOR SPSW}$</p>		
CONC.	<p>CONC: $b = 20'$ $h = 14'$</p> <p>$E = 3644$ $G = 1458$</p>	<p>$t = (\text{SOLVE})$</p>
$4152.18 = \frac{1}{\frac{(14 \times 12)^3}{12 \cdot 3644 \cdot \left(\frac{t \cdot (20 \times 12)^3}{12}\right)} + \frac{1.2(14 \times 12)}{(t \cdot (20 \times 12))(1458)}}$		
<p>$t = 2.98''$ THICK CONCRETE WALL FOR COMPARABLE 3/8" THICK SPSW</p>		

Controlling Case Data Output

The controlling case for the building was found to be the earthquake loading in the y-direction.

PORTER-GILL

TECH REPORT 4

SHEAR FORCES AND LOAD COMBINATIONS

Story 1 Shear Forces

Pier	Load Case/Combo	V2	Absolute Value
SW-1	QUAKE_X	-13.836	13.836
SW-1	QUAKE_X_REV	-3.049	3.049
SW-1	QUAKE_Y	-5.438	5.438
SW-1	QUAKE_Y_REVERSE	159.8	159.795
SW-1	C1_X	3.92	3.92
SW-1	C1_Y	34.435	34.435
SW-1	C2_X	5.784	5.784
SW-1	C2_Y	96.926	96.926
SW-1	C1_X	2.94	2.94
SW-1	C1_Y	37.213	37.213
SW-1	C4_X_COMBINED	4.262	4.262
SW-1	C4_Y_COMBINED	72.673	72.673
Pier	Load Case/Combo	V2	Absolute Value
SW-13 (12)	QUAKE_X	25.141	25.141
SW-13 (12)	QUAKE_X_REV	3.689	3.689
SW-13 (12)	QUAKE_Y	546.4	546.403
SW-13 (12)	QUAKE_Y_REVERSE	217.8	217.797
SW-13 (12)	C1_X	-8.222	8.222
SW-13 (12)	C1_Y	90.98	90.98
SW-13 (12)	C2_X	-12.229	12.229
SW-13 (12)	C2_Y	208.07	208.07
SW-13 (12)	C1_X	-6.167	6.167
SW-13 (12)	C1_Y	97.827	97.827
SW-13 (12)	C4_X_COMBINED	-9.072	9.072
SW-13 (12)	C4_Y_COMBINED	155.52	155.524
Pier	Load Case/Combo	V2	Absolute Value
SW-2	QUAKE_X	280.65	280.654
SW-2	QUAKE_X_REV	282.62	282.619
SW-2	QUAKE_Y	-40.502	40.502
SW-2	QUAKE_Y_REVERSE	-10.397	10.397
SW-2	C1_X	46.339	46.339
SW-2	C1_Y	-5.434	5.434
SW-2	C2_X	80.897	80.897
SW-2	C2_Y	-11.833	11.833
SW-2	C1_X	34.756	34.756
SW-2	C1_Y	-5.865	5.865
SW-2	C4_X_COMBINED	67.152	67.152
SW-2	C4_Y_COMBINED	-8.837	8.837
Pier	Load Case/Combo	V2	Absolute Value
SW-3	QUAKE_X	299.17	299.17
SW-3	QUAKE_X_REV	297.85	297.85
SW-3	QUAKE_Y	27.798	27.798
SW-3	QUAKE_Y_REVERSE	7.573	7.573
SW-3	C1_X	47.395	47.395
SW-3	C1_Y	3.847	3.847
SW-3	C2_X	83.077	83.077
SW-3	C2_Y	8.428	8.428
SW-3	C1_X	35.548	35.548
SW-3	C1_Y	4.147	4.147
SW-3	C4_X_COMBINED	69.135	69.135
SW-3	C4_Y_COMBINED	6.295	6.295

Max Shear = 159.795 for SW-1
Controlling Load Case = QUAKE_Y_REVERSE
Tributary Area = 125 SF

Max Shear = 546.403 for SW-13 (12)
Controlling Load Case = QUAKE_Y
Tributary Area = 215 SF

Max Shear = 282.619 for SW-2
Controlling Load Case = QUAKE_X_REV
Tributary Area = 175 SF

Max Shear = 299.17 for SW-3
Controlling Load Case = QUAKE_X
Tributary Area = 200 SF

PORTER-GILL

TECH REPORT 4

SHEAR FORCES AND LOAD COMBINATIONS

Pier	Load Case/Combo	V2	Absolute Value
SW-3 (OFFSET)	QUAKE_X	155.27	155.267
SW-3 (OFFSET)	QUAKE_X_REV	154.53	154.534
SW-3 (OFFSET)	QUAKE_Y	14.225	14.225
SW-3 (OFFSET)	QUAKE_Y_REVERSE	2.997	2.997
SW-3 (OFFSET)	C1_X	24.213	24.213
SW-3 (OFFSET)	C1_Y	1.731	1.731
SW-3 (OFFSET)	C2_X	42.447	42.447
SW-3 (OFFSET)	C2_Y	3.692	3.692
SW-3 (OFFSET)	C1_X	18.161	18.161
SW-3 (OFFSET)	C1_Y	1.875	1.875
SW-3 (OFFSET)	C4_X_COMBINED	35.364	35.364
SW-3 (OFFSET)	C4_Y_COMBINED	2.756	2.756
Pier	Load Case/Combo	V2	Absolute Value
SW-4	QUAKE_X	-7.941	7.941
SW-4	QUAKE_X_REV	-0.615	0.615
SW-4	QUAKE_Y	39.025	39.025
SW-4	QUAKE_Y_REVERSE	151.24	151.243
SW-4	C1_X	2.925	2.925
SW-4	C1_Y	36.319	36.319
SW-4	C2_X	4.375	4.375
SW-4	C2_Y	97.667	97.667
SW-4	C1_X	2.194	2.194
SW-4	C1_Y	38.888	38.888
SW-4	C4_X_COMBINED	3.261	3.261
SW-4	C4_Y_COMBINED	73.191	73.191
Pier	Load Case/Combo	V2	Absolute Value
SW-5	QUAKE_X	-2.309	2.309
SW-5	QUAKE_X_REV	0.402	0.402
SW-5	QUAKE_Y	119.54	119.536
SW-5	QUAKE_Y_REVERSE	161.07	161.068
SW-5	C1_X	1.2	1.2
SW-5	C1_Y	44.728	44.728
SW-5	C2_X	1.819	1.819
SW-5	C2_Y	114.53	114.53
SW-5	C1_X	0.9	0.9
SW-5	C1_Y	47.967	47.967
SW-5	C4_X_COMBINED	1.37	1.37
SW-5	C4_Y_COMBINED	85.765	85.765

Max Shear = 155.267 for SW-3 (OFFSET)

 Controlling Load Case = QUAKE_X
 Tributary Area = 90 SF

Max Shear = 151.243 for SW-4

 Controlling Load Case = QUAKE_Y_REVERSE
 Tributary Area = 140 SF

Max Shear = 161.068 for SW-5

 Controlling Load Case = QUAKE_Y_REVERSE
 Tributary Area = 200 SF

OVERALL MAXIMUM SHEAR CONTROLLING = 546.4 kip

APPENDIX A.2 - EXISTING SEISMIC AND WIND ANALYSIS

Seismic Loading Calculations

add large page of calculations

Seismic Amplification Factor

The seismic amplification factor, A_x , was calculated for each story, for each earthquake loading. The worst case of a particular floor, for each case, was applied to calculate the total torsional moment and accidental torsional moment. 9.5.3.5.2 covers the amplification factor that must be applied to these moments.

$$A_x = \left(\frac{\delta_{\max}}{1.2\delta_{\text{avg}}} \right)^2 \quad (\text{Eq. 9.5.3.5.2})$$

QUAKE_X_REGULAR

Level	Maximum Displacement	Average Displacement	Amplification Factor	Updated Amplification Factor
Story3	1.650297	1.633777	0.708559251	1.0
Story2	0.888202	0.879394	0.708425206	1.0
Story1	0.295822	0.293091	0.707446301	1.0

QUAKE_X_REVERSE

Level	Maximum Displacement	Average Displacement	Amplification Factor	Updated Amplification Factor
Story3	1.637171	1.632025	0.698830707	1.0
Story2	0.881133	0.878502	0.698610216	1.0
Story1	0.293522	0.29287	0.697539891	1.0

QUAKE_Y_REGULAR

Level	Maximum Displacement	Average Displacement	Amplification Factor	Updated Amplification Factor
Story3	2.21301	1.271017	2.105239655	2.1
Story2	1.212938	0.691314	2.137784916	2.1
Story1	0.42688	0.229725	2.397908479	2.4

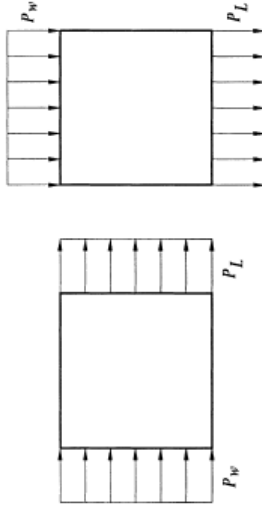
QUAKE_Y_REVERSE

Level	Maximum Displacement	Average Displacement	Amplification Factor	Updated Amplification Factor
Story3	1.358426	0.974261	1.350077945	1.4
Story2	0.744244	0.525585	1.392458523	1.4
Story1	0.262932	0.173467	1.59547742	1.6

Indicates controlling amplification factor

Wind Loading Calculations

Case 1



CASE 1

Case 1, Y-Direction
North-South
 L = 225 feet

Level	P_w	P_L
1	11.00	-3.95
2	11.14	-3.95
3	12.69	-3.95
4	13.72	-3.95
Roof	14.89	-3.95
Stair Tower	15.79	-3.95

	P_w	P_L
Stair Tower	15.79	-3.95
Roof	14.89	-3.95
4	13.72	-3.95
3	12.69	-3.95
2	11.14	-3.95

	Force (k)	Force (k)
Stair Tower	0.1422	-0.036
Roof	0.1340	-0.077
4	0.1235	-0.069
3	0.1142	-0.055
2	0.1002	-0.055

Loads Applied to Diaphragm

	P_w	P_L
Modified Roof	0.2762	-0.1125
4	0.1235	-0.0691
3	0.114185095	-0.05528166
2	0.1002	-0.0553

Case 1, X-Direction
East-West
 L = 64 feet

Level	P_w	P_L
1	10.91	-9.78
2	11.04	-9.78
3	12.57	-9.78
4	13.60	-9.78
Roof	14.76	-9.78
Stair Tower	15.65	-9.78

	P_w	P_L
Stair Tower	15.65	-9.78
Roof	14.76	-9.78
4	13.60	-9.78
3	12.57	-9.78
2	11.04	-9.78

	Force (k)	Force (k)
Stair Tower	0.1409	-0.088
Roof	0.2878	-0.191
4	0.2380	-0.171
3	0.1760	-0.137
2	0.1545	-0.137

Loads Applied to Diaphragm

	P_w	P_L
Modified Roof	0.4286	-0.2788
4	0.2380	-0.1712
3	0.17601584	-0.136955
2	0.1545	-0.1370

North-South, Y

Point Load	Location X	Y
87.46		
130.80	112.5	32
38.13	112.5	32
34.99	112.5	32

East-West, X

Point Load	Location X	Y
45.28		
71.46	112.5	32
20.03	112.5	32
18.65	112.5	32

Case 2

Case 2 - ASCE-7 1998

Case 2, X-Direction
East-West

L = 64 feet

Level	P_w	$0.75P_w$	P_L	$0.75P_L$
1	10.91	8.18	-9.78	-7.34
2	11.04	8.28	-9.78	-7.34
3	12.57	9.43	-9.78	-7.34
4	13.60	10.20	-9.78	-7.34
Roof	14.76	11.07	-9.78	-7.34
Stair Tower	15.65	11.74	-9.78	-7.34

Level	P_w	$0.75P_w$	P_L	$0.75P_L$
Stair Tower	15.65	11.74	-9.78	-7.34
Roof	14.76	11.07	-9.78	-7.34
4	13.60	10.20	-9.78	-7.34
3	12.57	9.43	-9.78	-7.34
2	11.04	8.28	-9.78	-7.34

Level	Force (k)	Force (k)	Force (k)	Force (k)
Stair Tower	0.1409	0.106	-0.0880	-0.066
Roof	0.2878	0.216	-0.1908	-0.143
4	0.2380	0.178	-0.1712	-0.128
3	0.1760	0.132	-0.1370	-0.103
2	0.1545	0.116	-0.1370	-0.103

Loads Applied to Diaphragm

Level	P_w	$0.75P_w$	P_L	$0.75P_L$
Modified Roof	0.4286	0.3215	-0.2788	-0.2091
4	0.2380	0.1785	-0.1712	-0.1284
3	0.1760	0.132	-0.1370	-0.103
2	0.1545	0.1159	-0.1370	-0.1027

Case 2, Y-Direction
North-South

L = 225 feet

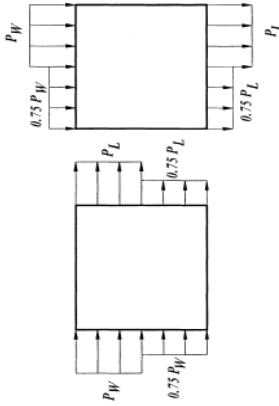
Level	P_w	$0.75P_w$	P_L	$0.75P_L$
1	11.00	8.25	-3.95	-2.96
2	11.14	8.35	-3.95	-2.96
3	12.69	9.52	-3.95	-2.96
4	13.72	10.29	-3.95	-2.96
Roof	14.89	11.17	-3.95	-2.96
Stair Tower	15.79	11.85	-3.95	-2.96

Level	P_w	$0.75P_w$	P_L	$0.75P_L$
Stair Tower	15.79	11.85	-3.95	-2.96
Roof	14.89	11.17	-3.95	-2.96
4	13.72	10.29	-3.95	-2.96
3	12.69	9.52	-3.95	-2.96
2	11.14	8.35	-3.95	-2.96

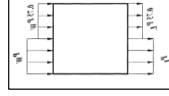
Level	Force (k)	Force (k)	Force (k)	Force (k)
Stair Tower	0.1422	0.107	-0.0555	-0.027
Roof	0.2904	0.218	-0.0770	-0.058
4	0.2402	0.180	-0.0691	-0.052
3	0.1776	0.133	-0.0553	-0.041
2	0.1559	0.117	-0.0553	-0.041

Loads Applied to Diaphragm

Level	P_w	$0.75P_w$	P_L	$0.75P_L$
Modified Roof	0.4325	0.3244	-0.1125	-0.0844
4	0.2402	0.1801	-0.0691	-0.0518
3	0.1776	0.133	-0.0553	-0.041
2	0.1559	0.1169	-0.0553	-0.0415

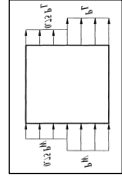


CASE 2



North-South for 1.0P

Point Load	Location X	Location Y
122.64		
192.22	56.25	32
52.40	56.25	32
47.52	56.25	32



East-West for 1.0P

Point Load	Location X	Location Y
45.28		
71.46	112.5	16
20.03	112.5	16
18.65	112.5	16

East-West for 0.75P

Point Load	Location X	Location Y
33.96		
53.60	112.5	48
15.02	112.5	48
13.99	112.5	48

North-South for 0.75P

Point Load	Location X	Location Y
91.98		
144.17	168.75	32
39.30	168.75	32
35.64	168.75	32

Case 3
Case 3 - ASCE-7 1998
Case 3, X-Direction
 East-West

Level	0.75P _w	0.75P _L
1	8.18	-7.34
2	8.28	-7.34
3	9.43	-7.34
4	10.20	-7.34
Roof	11.07	-7.34
Stair Tower	11.74	-7.34

0.75P _w	0.75P _L
11.74	-7.34
11.07	-7.34
10.20	-7.34
9.43	-7.34
8.28	-7.34

Force (k)	Force (k)
0.1057	-0.066
0.2158	-0.143
0.1785	-0.128
0.1320	-0.103
0.1159	-0.103

Loads Applied to Diaphragm

Modified Roof	0.75P _w	0.75P _L
4	0.3215	-0.2091
3	0.1785	-0.1284
2	0.1320	-0.1027

Case 3, Y-Direction
 North-South

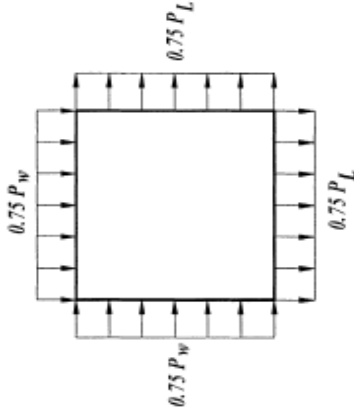
Level	0.75P _w	0.75P _L
1	8.25	-2.96
2	8.35	-2.96
3	9.52	-2.96
4	10.29	-2.96
Roof	11.17	-2.96
Stair Tower	11.85	-2.96

0.75P _w	0.75P _L
11.85	-2.96
11.17	-2.96
10.29	-2.96
9.52	-2.96
8.35	-2.96

Force (k)	Force (k)
0.1066	-0.027
0.2178	-0.058
0.1801	-0.052
0.1332	-0.041
0.1169	-0.041

Loads Applied to Diaphragm

Modified Roof	0.75P _w	0.75P _L
4	0.3244	-0.0844
3	0.1801	-0.0518
2	0.1332	-0.0415


CASE 3

East-West

Point Load	Location
X	Y
33.96	
53.60	112.5
15.02	112.5
13.99	112.5

North-South

Point Load	Location
X	Y
91.98	
144.17	112.5
39.30	112.5
35.64	112.5

Case 4
Case 4 - ASCE-7 1998
**Case 4, X-Direction
East-West**

Level	L = 64 feet			
	0.75P _w	0.56P _w	0.75P _L	0.56P _L
1	8.18	6.11	-7.34	-5.48
2	11.04	6.18	-7.34	-5.48
3	12.57	7.04	-7.34	-5.48
4	13.60	7.62	-7.34	-5.48
Roof	14.76	8.26	-7.34	-5.48
Stair Tower	15.65	8.77	-7.34	-5.48
0.75P_w 0.56P_w 0.75P_L 0.56P_L				
Stair Tower	15.65	8.77	-7.34	-5.48
Roof	14.76	8.26	-7.34	-5.48
4	13.60	7.62	-7.34	-5.48
3	12.57	7.04	-7.34	-5.48
2	11.04	6.18	-7.34	-5.48

Force (k)	Force (k)	Force (k)	Force (k)	
Stair Tower	0.1409	0.079	-0.0660	-0.049
Roof	0.2878	0.161	-0.1431	-0.107
4	0.2380	0.133	-0.1284	-0.096
3	0.1760	0.099	-0.1027	-0.077
2	0.1545	0.087	-0.1027	-0.077

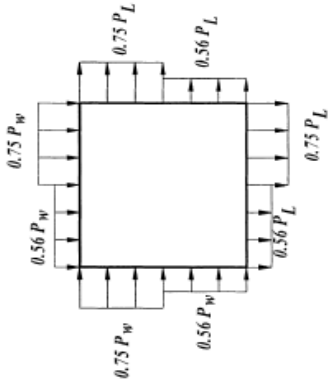
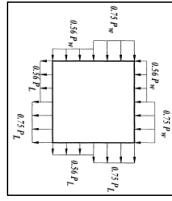
Loads Applied to Diaphragm				
	0.75P _w	0.56P _w	0.75P _L	0.56P _L
Modified Roof	0.4286	0.2400	-0.2091	-0.1561
4	0.2380	0.1333	-0.1284	-0.0959
3	0.1760	0.099	-0.1027	-0.077
2	0.1545	0.0865	-0.1027	-0.0767

**Case 4, Y-Direction
North-South**

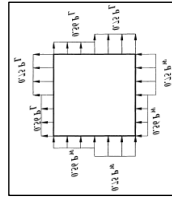
Level	L = 225 feet			
	0.75P _w	0.56P _w	0.75P _L	0.56P _L
1	8.25	6.16	-2.96	-2.21
2	8.35	6.24	-2.96	-2.21
3	9.52	7.10	-2.96	-2.21
4	10.29	7.68	-2.96	-2.21
Roof	11.17	8.34	-2.96	-2.21
Stair Tower	11.85	8.85	-2.96	-2.21
0.75P_w 0.56P_w 0.75P_L 0.56P_L				
Stair Tower	11.85	8.85	-2.96	-2.21
Roof	11.17	8.34	-2.96	-2.21
4	10.29	7.68	-2.96	-2.21
3	9.52	7.10	-2.96	-2.21
2	8.35	6.24	-2.96	-2.21

Force (k)	Force (k)	Force (k)	Force (k)	
Stair Tower	0.1066	0.080	-0.0267	-0.020
Roof	0.2178	0.163	-0.0577	-0.043
4	0.1801	0.134	-0.0518	-0.039
3	0.1332	0.099	-0.0415	-0.031
2	0.1169	0.087	-0.0415	-0.031

Loads Applied to Diaphragm				
	0.75P _w	0.56P _w	0.75P _L	0.56P _L
Modified Roof	0.3244	0.2422	-0.0844	-0.0630
4	0.1801	0.1345	-0.0518	-0.0387
3	0.1332	0.099	-0.0415	-0.031
2	0.1169	0.0873	-0.0415	-0.0310


CASE 4


North-South for 0.75P		
Point Load	Location	Location
	X	Y
91.98		
144.17	56.25	32
39.30	56.25	32
35.64	56.25	32



East-West for 0.75P		
Point Load	Location	Location
	X	Y
40.81		
64.26	112.5	16
17.84	112.5	16
16.46	112.5	16

North-South for 0.56P		
Point Load	Location	Location
	X	Y
68.68		
107.64	168.75	32
29.35	168.75	32
26.61	168.75	32

East-West for 0.56P		
Point Load	Location	Location
	X	Y
25.35		
40.02	112.5	48
11.22	112.5	48
10.45	112.5	48

APPENDIX B

REDESIGN OF GRAVITY SYSTEM

APPENDIX B.1 - TYPICAL OFFICE BEAM DESIGN

BEAM DESIGN (FRAMING INTO QUEEN POST)

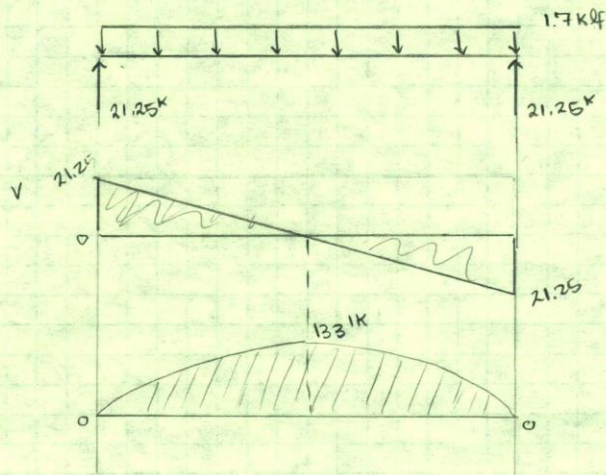
$w = 164.5 \text{ PSF}$

TRIB. WIDTH: $9'-8" \approx 9.67' \rightarrow$ ROUND TO $10'$

$164.5 \text{ PSF} \times 10' = 1645 \text{ PLF}$ or 1.7 KLF
ON BEAMS

$M = \frac{1.7(25')^2}{8} = 133 \text{ K}$

$R = \frac{1.7(25)}{2} = 21.25 \text{ K}$



$M_{max} = 133 \text{ K}$

GLULAM, PRIMARILY IN BENDING \rightarrow TABLE 5A

PLEASE SEE EXCEL SHEET FOR INTERPOLATED
GLULAM SIZE...

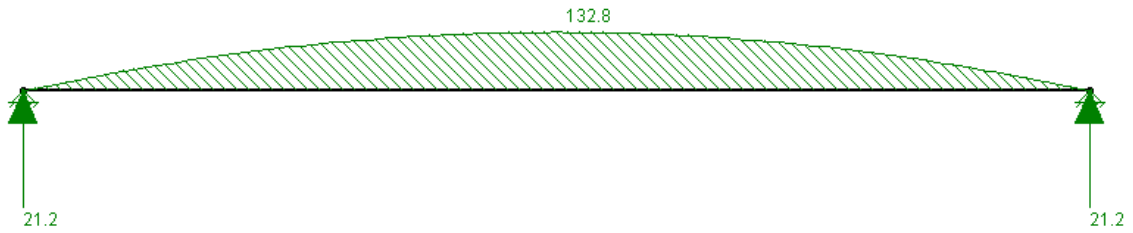
Loading

Computer analysis loading



Flexure and Reactions

Computer analysis results, showing the maximum moment is 132.8 kip-ft or 133 kip-ft



Computer Analysis Data

Designer : SIKANDAR PORTER-GILL

BEAM ANALYSIS

 February 11, 2014
 12:09 PM
 Checked By:

Member Data

Member Label	I Joint	J Joint	Area in ²	Moment of Inertia in ⁴	Elastic Modulus ksi	End Releases I-End	J-End	Length ft
M1	N1	N2	10	100	29000			25

Member Distributed Loads

Member Label	Direction	Start Magnitude (k/ft, F)	End Magnitude (k/ft, F)	Start Location (ft or %)	End Location (ft or %)
M1	Y	-1.7	-1.7	0	0

Reactions

Joint Label	X Force (k)	Y Force (k)	Moment (k-ft)
N1	0	21.25	0
N2	0	21.25	0
Totals:	0	42.5	

Member Section Forces

Member Label	Section	Axial (k)	Shear (k)	Moment (k-ft)
M1	1	0	21.25	0
	2	0	10.625	99.609
	3	0	0	132.812
	4	0	-10.625	99.609
	5	0	-21.25	0

Member Sizing

Flexure in Beam

 Moment **133** kip-ft

$$F'_b = F_b \times C_D \times C_M \times C_t \times C_L \times C_V \times C_{fu} \times C_c \times C_i$$

Pick a size,	10-1/2" x 19-1/4"
	10.5 x 19.25
where the $A_{provided} =$	202.1 in ²
$S_{sect\ modulus} =$	648.5 in ³

$C_D =$	1.00	because live load controls	§2.3.2
$C_M =$	1.00	because interior beam in conditioned space	§5.3.3
$C_t =$	1.00	because interior beam in conditioned space	§5.3.4
$C_L =$	0.987	calculated below	§5.3.5
$C_V =$	0.934	calculated below	§5.3.6
$C_{fu} =$	1.00	because not loaded parallel to wide faces of lamin.	§5.3.7
$C_c =$	1.00	because no curvature to beam	§5.3.8
$C_i =$	1.00	because no tapering of beam	§5.3.9

Pick a Visually Graded Southern Pine Stress Group

Table 5A

 Group = **30F-2.1E SP**
 $F_b =$ **3000** psi

 $E_{min} =$ **1110000** psi

Calculate C_t Adjustment Factor

 $l_u =$ **25.00** ft, the unbraced length of the girder

 $d =$ **19.25** in, chosen to be consistent with girder depth

$$l_u / d = 15.58$$

so now we can calculate l_e ,

$$l_e =$$
 552 in, or 46.00 ft

reliant on inequality on page 16, Supplement

$$R_B = 9.82$$

$$F_{bE} = \frac{1.20E'_{min}}{(R_B)^2} = 13820.2$$

$$F_b^* = F_b \times C_D \times C_M \times C_t \times C_c \times C_i = 3000 \text{ psi}$$

$$F_{bE} / F_b^* = 4.61$$

$$C_L = \frac{1 + F_{bE} / F_b^*}{1.9} - \sqrt{\left(\frac{1 + F_{bE} / F_b^*}{1.9}\right)^2 - \frac{F_{bE} / F_b^*}{0.95}} = 0.987$$

Calculate C_V Adjustment Factor

$$C_V = \left(\frac{21}{L}\right)^{1/x} \left(\frac{12}{d}\right)^{1/x} \left(\frac{5.125}{b}\right)^{1/x} \leq 1.0$$

$L = 25$ ft $x = 20$ for Southern Pine
 $d = 19.25$ in
 $b = 10.5$ in

$$C_V = 0.934 < 1.0$$

Calculate F_b' Using the Minimum of C_V or C_L

$$\min \begin{cases} C_L = 0.987 \\ C_V = 0.934 \end{cases}$$

$$F_b' = 2802 \text{ psi}$$

$$f_b = \frac{M}{S} = 2461.1 \text{ psi} < F_b'$$

Calculate f_b and Determine if Selected Beam Passes

$$f_b = 2461 \text{ psi} < F_b' = 2802$$

Bending Passes

Use a 10-1/2" x 19-1/4" for the beam

APPENDIX B.2 - QUEEN POST DESIGN HAND CALCULATION

QUEEN POST DESIGN

LOADS:

- SUPERIMPOSED DL
 - 1.5 CARPET
 - 12 COMPUTER
 - 10 SDW (MECH + LTG + SPRINKLER)
 - 10 FRAMING

 33.5 PSF DL
- LIVE LOADS
 - 80 OFFICE + PARTITIONS
- DEAD LOAD
 - 51 3/4" x 20" VULCRAFT DECKING

ASD → $80 \text{ LL} + \text{DL} = 33.5 + 51 + 80 = 164.5 \text{ PSF}$

BEAMS (INTERIOR)

TRIB. WIDTH = 9'-8" ~ 10'

$164.5 \text{ PSF} \times 10' = 1645 \text{ PLF}$ OR 1.7 KLF ON BEAMS

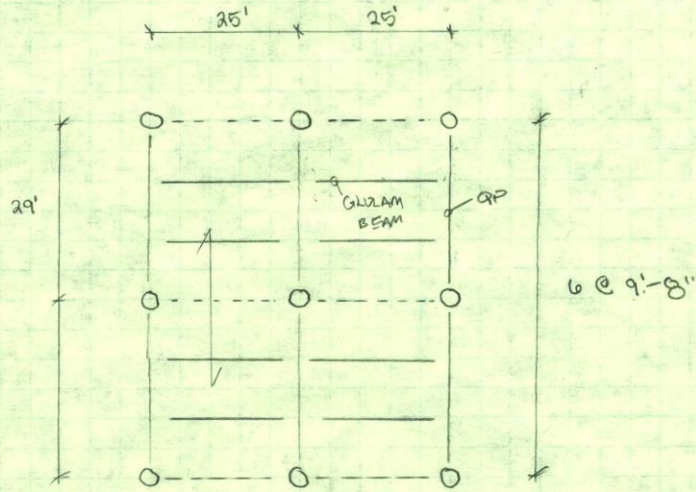
$M = \frac{wL^2}{8} = \frac{1.7 (25')^2}{8} = 133 \text{ K'} \text{ MAX ON BEAMS (INTERIOR)}$

$R = \frac{wL}{2} = \frac{1.7 (25')}{2} = 21.25 \text{ REACTION AT ENDS}$

X2 BIG 2 BEAMS
FALL ON EA. GIRDER
SECTION

= 42.5K

GENERAL FRAMING LAYOUT



DUE TO ASSUMPTION OF HINGE, ALL 42.5^k WOULD BE TRANSFERRED
INTO POST

TABULATED IN EXCEL PRINTOUTS

LET'S CHOOSE 9'-8" FROM BEAM END TO POST W/ 2.25" HIGH POST

$$f_c = 181.37^k \text{ AXIAL LOAD (PARALLEL TO BEAM GRAIN)}$$

$$f_{c\perp} = 42.5^k \text{ SHEAR LOAD (PERPENDICULAR TO BEAM GRAIN)}$$

$$f_b = \frac{M}{S} \quad (\text{BENDING})$$

SOUTHERN PINE WILL BE USED

COMPRESSION PARALLEL TO BEAM GRAIN

$$F_c' = F_c \times C_M \times C_t \times C_p$$

TABLE 53.1

ADJUSTMENT FACTORS

$$C_D = 1.0$$

$$C_M = 1.0$$

$$C_t = 1.0$$

$$C_p = 0.65 \text{ assumed}$$

$F_c = 1900 \text{ psi}$ FOR 47 VISUALLY GRADED SOUTHERN PINE
FOR 4 OR MORE LAMINATIONS

$$\Delta_0 \quad F_c' = (2300) \times 1 \times 1 \times 1 \times 0.65$$

$$= 1235 \text{ psi}$$

we know $f_c = 181.37 \text{ kips} \sim 182 \text{ kips} / \text{AREA}$

$$f_c \leq F_c'$$

$$\frac{182 \text{ kips} \times 1000 \text{ lb/k}}{\text{AREA}} \leq 1235 \text{ psi}$$

$$\text{AREA} = 147.36 \text{ in}^2$$

$$\text{a } 10\text{-}\frac{1}{2}\text{"} \times 15\text{-}\frac{1}{8}\text{"} \rightarrow \text{A} = 158.8 \text{ in}^2$$

CHECK $C_p = 0.65$ ASSUMPTION

$$C_p = \frac{1 + F_{CE}/F_c^*}{2C} - \sqrt{\left(\frac{1 + F_{CE}/F_c^*}{2C}\right)^2 - \frac{F_{CE}/F_c^*}{C}}$$

$$F_c^* = F_c \times C_D \times C_M \times C_t$$

$$= 1900 \times 1 \times 1 \times 1 = 1900 \text{ psi}$$

$$\frac{h_e}{d} = \frac{9.67' \times 12''}{10.5} = 11.05 < 50 \checkmark \rightarrow \text{Controls}$$

$$= \frac{9.67' \times 12''}{15.125} = 7.67 < 50 \checkmark$$

$$E'_{min} = E_{min} \times C_m \times C_t$$

$$= (0.77 \times 10^6) \times 1.0 \times 1.0$$

$$= 0.77 \times 10^6$$

$$F_{CE} = \frac{0.822 E'_{min}}{(h_e/d)^2} = \frac{0.822 (0.77 \times 10^6)}{(11.05^2)}$$

$$= 4982$$

$$F_{CE}/F_c^* = 4982/1900 = 2.62 \text{ ratio}$$

$$C_p = \frac{1 + 2.62}{2 \times 0.9} - \sqrt{\left(\frac{1 + 2.62}{2 \times 0.9}\right)^2 - \frac{2.62}{0.9}}$$

$$C_p = 0.916 > 0.65 = C_{p \text{ assumed}}$$

So, member can be smaller...

lets assume $C_p = 0.9$ instead

$$F'_c = 1900 \times 1 \times 1 \times 1 \times 0.9 = 1710 \text{ psi}$$

$$A_{req} = \frac{182^k \times 1000}{1710} = 106.43 \text{ in}^2 \rightarrow 8\text{-}1/2" \times 13\text{-}3/4"$$

$$A_{prov} = 116.9 \text{ in}^2$$

Now check, $C_p = 0.9$

$$F_c^* = 1900 \text{ psi (no change)}$$

$$l/d = \frac{9.67' \times 12''/1}{8.5} = 13.65 < 50 \checkmark \rightarrow \text{CONTROLS}$$

$$= \frac{9.67' \times 12''/1}{13.75} = 8.13 < 50 \checkmark$$

$$E_{min} = 0.74 \times 10^6 \text{ psi (no change)}$$

$$F_{CE} = \frac{0.822(0.74 \times 10^6)}{13.65^2} = 3264.6 \text{ psi}$$

$$F_{CE}/F_c^* = 3265/1900 = 1.71$$

$$C_p = \frac{1 + 1.71}{2 \cdot 0.9} - \sqrt{\left(\frac{1 + 1.71}{2 \cdot 0.9}\right)^2 - \frac{1.71}{0.9}}$$

$$C_p = 0.9067 \checkmark \text{ GOOD ASSUMPTION}$$

$$A_0, F'_c = 1710 \times 116.9 \text{ in}^2 / 1000 = 199.89^k \text{ allowed}$$

$$f_c = \frac{182^k \times 1000}{116.9} = 1556 \text{ psi}$$

$$f_c = 1556 < F'_c = 1710 \checkmark \text{ GOOD}$$

8 1/2 x 13-3/4

SELF WEIGHT OF SELECTED MEMBER

$$D = 62.4 \left(\frac{G}{1 + G(0.009)(M.C.)} \right) \left(1 + \frac{M.C.}{100} \right)$$

$G = 0.55$ FOR 4" SOUTHERN PINE GLULAM

M.C. = 5% WIG INSIDE
OR 10%

$$D = 62.4 \left(\frac{0.55}{1 + 0.55(0.009)(5)} \right) \left(1 + \frac{5}{100} \right)$$

= 35.17 or 35.97 PCF

we have $8^{-1/2} \times 13^{-3/4}$, $A = 116.9 \text{ in}^2$

$$A = 116.9 \text{ in}^2 \times \frac{1 \text{ ft}^2}{12^2 \text{ in}^2} = 0.8118 \text{ ft}^2$$

$$35.97 \frac{\text{lb}}{\text{ft}} \times 0.8118 \text{ ft}^2 = 29.2 \text{ plf}$$

SELF WEIGHT AND POINT LOADS CAUSE MOMENT (MAX) OF 3.819k ~ 8.9k COMPUTER ANALYSIS

BENDING ANALYSIS

$$F_b = F_b \times C_D \times C_M \times C_t \times C_L \times C_V \times C_{Fu} \times C_c \times C_I$$

$$F_b = 1400 \text{ psi (about x-x)}$$

ADJUSTMENT FACTORS

$$C_D = 1.0$$

$$C_M = 1.0$$

$$C_t = 1.0$$

$$C_L \neq 1.0$$

$$\left. \begin{array}{l} l_u = 9.67' \\ d = 13.75'' \end{array} \right\} \rightarrow l_u/d = \frac{9.67' \times 12''}{13.75''} = 8.44$$

$$7 \leq l_u/d \leq 14.3$$

$$l_c = 1.63l_u + 3d$$

$$= 1.63(9.67' \times 12) + 3(13.75'')$$

$$= 230.39'' \text{ or } 19.19'$$

$$R_B = \sqrt{\frac{l_c d}{b^2}} = \sqrt{\frac{(19.19 \times 12)(13.75)}{(8.5)^2}} = 6.62$$

$$F_{bE} = \frac{1.20 E'_{min}}{R_B^2} = \frac{1.2(0.574 \times 10^6)}{(6.62)^2} = 20263$$

$$F_b^* = F_b \times C_D \times C_M \times C_t \times C_L \times C_I$$

$$= 1400 \times 1 \times 1 \times 1 \times 1 \times 1 = 1400 \text{ psi}$$

$$F_{bE}/F_b^* = 20263/1400 = 14.47$$

$$C_L = \frac{1 + F_{DE}/F_{D^*}}{1.9} - \sqrt{\left(\frac{1 + F_{DE}/F_{D^*}}{1.9}\right)^2 - \frac{F_{DE}/F_{D^*}}{0.95}}$$

$$C_L = 0.9963$$

$$C_V = \left(\frac{21}{29}\right)^{1/20} \cdot \left(\frac{12}{13.75}\right)^{1/20} \cdot \left(\frac{0.125}{8.5}\right)^{1/20} = 0.953$$

$$\min \begin{cases} C_L = 0.9963 \\ C_V = 0.953 \end{cases} \rightarrow 0.953 \text{ CONTROLS}$$

$C_{F_b} = 1.0$ bc NOT loaded parallel to wide faces of laminations

$$C_c = 1.0$$

$$C_T = 1.0$$

$$\text{Now, } F_b' = 1100 \times 1 \times 1 \times 1 \times 0.953 \times 1 \times 1 \times 1 \\ = 1334.2 \text{ psi}$$

$$f_b = \frac{M}{S} = \frac{8.9'' \times 12}{267.8} = 0.3988 \text{ ksi} < 1334 \text{ psi allowed}$$



$$f_b = 398.8 \text{ psi} < 1334 \text{ psi} = F_b'$$

✓ Gross
8-1/2" x 13-3/4"

COMBINED AXIAL AND LOADING

$$\left(\frac{f_c}{F_c}\right)^2 + \frac{f_{b1}}{F_{b1}(1 - f_c/F_{CE})} \leq 1.0$$

$$\left(\frac{15560}{1710}\right)^2 + \frac{398.8}{1334(1 - 15560/8540)} = 1.191 \neq 1.0$$

X FAILS INTERACTION

where,

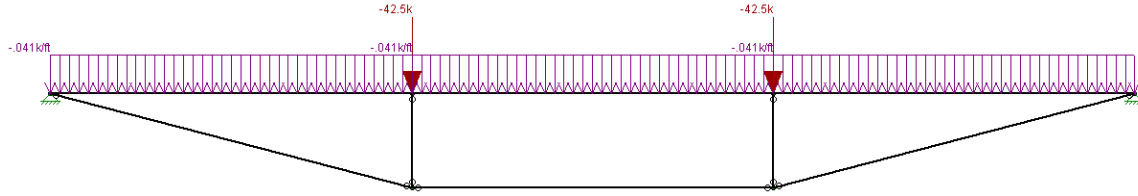
$$F_{CE} = \frac{0.822 E_{min}}{(l_e/d_1)^2} = \frac{0.822(6.74 \times 10^6)}{\left(\frac{9.67' \times 12}{13.75}\right)^2} = 8540$$

AN EXCEL SHEET WILL BE USED TO INTERPOLATE THE SIZE OF THE GLULAM BEAM REQUIRED...

APPENDIX B.3 - TYPICAL OFFICE QUEEN POST DESIGN

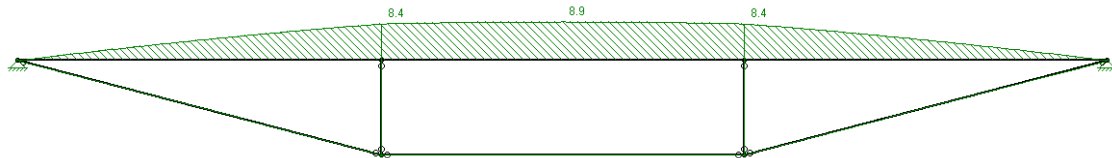
Loading

Computer analysis loading



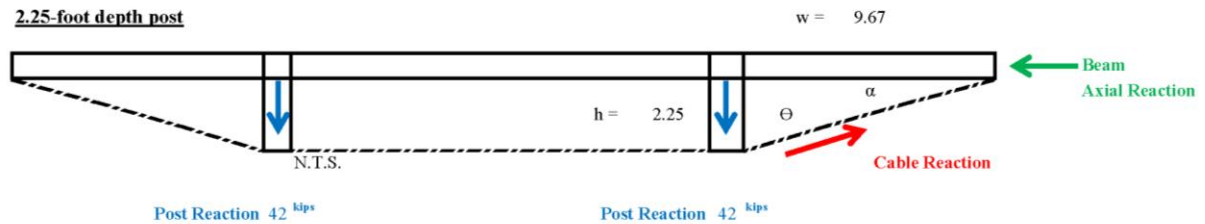
Flexure and Reactions

Computer analysis results, showing the maximum moment is 8.9 kip-ft



Axial Cable and Girder Forces

The assumption of the hinged queen post was used to determine the post reactions, cable tension and girder axial forces.



PRELIMINARY CALCULATIONS

$$\Theta = \tan^{-1}(w/h) = 1.34 \text{ radians}$$

$$\alpha = 88.66 \text{ radians}$$

CALCULATE RESULTANT FORCES IN CABLE AND BEAM

Cable Reaction 186.21 kips

Beam Axial Reaction 181.37 kips

Computer Analysis Data

Designer : SIKANDAR PORTER-GILL

GIRDER ANALYSIS

February 11, 2014

12:03 PM

Checked By:

Member Data

Member Label	I Joint	J Joint	Area in ²	Moment of Inertia in ⁴	Elastic Modulus ksi	End Releases I-End	J-End	Length ft
M1	N1	N2	10	100	29000			9.67
M2	N2	N3	10	100	29000			9.66
M3	N3	N4	10	100	29000			9.67
M4	N1	N5	10	100	29000	PIN	PIN	9.988
M5	N5	N6	10	100	29000	PIN	PIN	9.66
M6	N6	N4	10	100	29000	PIN	PIN	9.988
M7	N2	N5	10	100	29000	PIN	PIN	2.5
M8	N3	N6	10	100	29000	PIN	PIN	2.5

Joint Loads/Enforced Displacements

Joint Label	[L]oad or [D]isplacement	Direction	Magnitude (k, k-ft, in, rad)
N2	L	Y	-42.5
N3	L	Y	-42.5

Member Distributed Loads

Member Label	Direction	Start Magnitude (k/ft, F)	End Magnitude (k/ft, F)	Start Location (ft or %)	End Location (ft or %)
M1	Y	-.041	-.041	0	0
M2	Y	-.041	-.041	0	0
M3	Y	-.041	-.041	0	0

Reactions

Joint Label	X Force (k)	Y Force (k)	Moment (k-ft)
N1	-162.565	43.095	0
N4	162.565	43.094	0
Totals:	0	86.189	

Member Section Forces

Member Label	Section	Axial (k)	Shear (k)	Moment (k-ft)
M1	1	0	1.066	0
	2	0	.967	2.458
	3	0	.868	4.676
	4	0	.769	6.655
	5	0	.67	8.394
M2	1	0	.198	8.394
	2	0	.099	8.752
	3	0	0	8.872
	4	0	-.099	8.752
	5	0	-.198	8.394
M3	1	0	-.67	8.394
	2	0	-.769	6.655
	3	0	-.868	4.676
	4	0	-.967	2.458
	5	0	-1.066	0
M4	1	-167.91	0	0
	2	-167.91	0	0
	3	-167.91	0	0

Designer : SIKANDAR PORTER-GILL

February 11, 2014
12:03 PM
Checked By: _____

GIRDER ANALYSIS

Member Section Forces

Member Label	Section	Axial (k)	Shear (k)	Moment (k-ft)
	4	-167.91	0	0
	5	-167.91	0	0
M5	1	-162.565	0	0
	2	-162.565	0	0
	3	-162.565	0	0
	4	-162.565	0	0
	5	-162.565	0	0
M6	1	-167.91	0	0
	2	-167.91	0	0
	3	-167.91	0	0
	4	-167.91	0	0
	5	-167.91	0	0
M7	1	42.028	0	0
	2	42.028	0	0
	3	42.028	0	0
	4	42.028	0	0
	5	42.028	0	0
M8	1	42.028	0	0
	2	42.028	0	0
	3	42.028	0	0
	4	42.028	0	0
	5	42.028	0	0

Top Chord Member Sizing

Compression Parallel to Beam Grain

Axial Compression **181.37** kips

$$F'_c = F_c \times C_D \times C_M \times C_t \times C_p$$

Adjustment Factors

$C_D =$	1.00	because live load controls	§2.3.2
$C_M =$	1.00	because interior beam in conditioned space	§5.3.3
$C_t =$	1.00	because interior beam in conditioned space	§5.3.4
$C_p =$	0.92	assumed value	§3.7.1

Pick a Visually Graded Southern Pine Stress Group

Table 5B

Group =	50
$F_c =$	2300 psi
$E_{min} =$	1000000 psi

so,

$$F'_c = 2116 \text{ psi} \quad \text{allowable compression stress}$$

now the required area would be,

$$A = 86 \text{ in}^2 \quad \text{required area of glulam}$$

Pick a,	8-1/2" x 19-1/4"
	8.5 x 19.25
where the $A_{provided} =$	163.6 in ²
Is the area greater than required area?	Yes

Check the Assumption of the C_p Adjustment Factor

$$C_p = \frac{1 + F_{CE}/F_c^*}{2c} - \sqrt{\left(\frac{1 + F_{CE}/F_c^*}{2c}\right)^2 - \frac{F_{CE}/F_c^*}{c}}$$

$$F_c^* = F_c \times C_D \times C_M \times C_t = 2300 \text{ psi}$$

$$l_e/d = 13.65 \quad \text{and} \quad 6.03 \quad \text{where} \quad 13.65 \quad \text{controls}$$

< 50

 < 50

$$E_{min}' = E_{min} \times C_M \times C_t = 1000000 \text{ psi}$$

$$F_{CE} = \frac{0.822E_{min}'}{(l_e/d)^2} = 4414 \text{ psi}$$

$$F_{CE}/F_c^* = 1.92 \quad c = 0.9$$

now the C_p adjustment factor can be calculated

$$C_p = 0.92 < C_{p,assumed}$$

Calculate f_c and Determine if Selected Beam Passes

$$f_c = 1108 \text{ psi} < F_c' = 2116$$

Compression Parallel to Grain Passes

Moment Induced by Self-Weight of Member

$$G = 0.55 \quad \text{Table 5B}$$

$$\text{M.C.} = 5\% \text{ or } 10\% \\ \text{because interior beam in conditioned space}$$

$$D = 62.4 \left(\frac{G}{1+G(0.009)(\text{M.C.})} \right) \left(1 + \frac{\text{M.C.}}{100} \right) = 35.17 \text{ pcf, or } 35.97 \text{ pcf}$$

we will take the maximum,

$$D = 35.97 \text{ pcf}$$

we have a 8-1/2" x 19-1/4" glulam beam with,

$$A = 163.6 \text{ in}^2$$

convert to square feet,

$$A = 1.1363 \text{ ft}^2$$

now calculate the linear load created by its self weight, over a 29' span

$$w = 40.87 \text{ plf}$$

Flexure in Queen Post Girder

 Moment **8.9** kip-ft

$$F'_b = F_b \times C_D \times C_M \times C_t \times C_L \times C_V \times C_{fu} \times C_c \times C_i$$

Adjustment Factors

$C_D =$	1.00	because live load controls	§2.3.2
$C_M =$	1.00	because interior beam in conditioned space	§5.3.3
$C_t =$	1.00	because interior beam in conditioned space	§5.3.4
$C_L =$	0.994	calculated below	§5.3.5
$C_V =$	0.937	calculated below	§5.3.6
$C_{fu} =$	1.00	because not loaded parallel to wide faces of lamin.	§5.3.7
$C_c =$	1.00	because no curvature to beam	§5.3.8
$C_i =$	1.00	because no tapering of beam	§5.3.9

Pick a Visually Graded Southern Pine Stress Group

Table 5B

Group =	50
$F_b =$	2100 psi
$E_{min} =$	1000000 psi

Calculate C_L Adjustment Factor

$$l_u = 9.67 \text{ ft, the unbraced length of the girder}$$

$$d = \mathbf{19.25} \text{ in, depth chosen in compression parallel to grain calculation}$$

$$l_u / d = 6.03$$

so now we can calculate l_e ,

$$l_e = 246.83 \text{ in, or } 20.57 \text{ ft}$$

$$R_B = 8.11$$

$$F_{bE} = \frac{1.20E'_{min}}{(R_B)^2} = 18247$$

$$F_b^* = F_b \times C_D \times C_M \times C_t \times C_c \times C_i = 2100 \text{ psi}$$

$$F_{bE} / F_b^* = 8.69$$

$$C_L = \frac{1 + F_{bE}/F_b^*}{1.9} - \sqrt{\left(\frac{1 + F_{bE}/F_b^*}{1.9}\right)^2 - \frac{F_{bE}/F_b^*}{0.95}} = 0.994$$

Calculate C_V Adjustment Factor

$$C_V = \left(\frac{21}{L}\right)^{1/x} \left(\frac{12}{d}\right)^{1/x} \left(\frac{5.125}{b}\right)^{1/x} \leq 1.0$$

$L = 29$ ft $x = 20$ for Southern Pine
 $d = 19.25$ in
 $b = 8.5$ in

$C_V = 0.937 < 1.0$

Calculate F'_b Using the Minimum of C_V or C_L

min		$C_L = 0.994$	Section Modulus (x) =	525 in ³
		$C_V = 0.937$		

$F'_b = 1968$ psi

$f_b = \frac{M}{S} = 203.4$ psi < F'_b

Calculate f_b and Determine if Selected Beam Passes

$f_b = 203$ psi < $F'_b = 1968$

Bending Passes

Combined Axial and Bending Loading Interaction

$$\left(\frac{f_c}{F_c'}\right)^2 + \frac{f_{b1}}{F_{b1}'\left(1 + f_c/F_{CE1}\right)} \leq 1.0 \quad \text{§3.9.2}$$

$f_c = 1108$ psi $E_{min}' = 1000000$ psi
 $F_c' = 2116$ psi
 $f_{b1} = 203$ psi
 $F_{b1}' = 1968$ psi

$F_{CE1} = \frac{0.822E_{min}'}{(l_{e1}/d_1)^2} = 22621.3$ psi where,
 $l_{e1} = 9.67$ ft
 $d_1 = 19.25$ in
 $f_c < F_{CE1}$ True

0.274 + 0.099 = 0.373 < 1.0

Combined Axial and Bending Pass	
Use a,	8-1/2" x 19-1/4"
	for the glulam queen post
With a,	Southern Pine Group of 50

Tension Cable Sizing

QUEEN POST - TENSION CABLE

186.21 kips → 190 kips

MACALLOY 400 BAR SYSTEM		
	MIN YIELD	MIN BREAK
M56	205 ^k	271.8 ^k
M64	270.7 ^k	358.8 ^k

M56 205^k > 190^k TOTAL ✓ GOOD

DESIGN CALLS FOR TWO CABLES
✓ FOR STABILITY
✓ ADDED SAFETY

(2) M56 MACALLOY 400 BARS
FOR TENSION WILL BE USED



Macalloy 460 Bar System

Table 1 - Tendon Capacities for Carbon Macalloy 460

Thread	mm inch	M10 3/8	M12 1/2	M16 5/8	M20 3/4	M24 1	M30 1 1/4	M36 1 3/8	M42 1 5/8	M48 2	M56 2 1/4	M64 2 1/2	M76 3	M85 3 3/8	M90 3 1/2	M100 4
Nominal Bar Dia.	mm inch	10 0.39	11 0.43	15 0.59	19 0.75	22 0.87	28 1.1	34 1.34	39 1.54	45 1.77	52 2.05	60 2.36	72 2.83	82 3.23	87 3.43	97 3.82
Min. Yield Load	kN kip	25 5.6	36 8.1	69 15.5	108 24.3	156 35.1	249 56	364 81.8	501 112.6	660 148.4	912 205	1204 270.7	1756 394.7	2239 503.3	2533 569.4	3172 713.1
Min. Break Load	kN kip	33 7.4	48 10.8	91 20.5	143 32.1	207 46.5	330 74.2	483 108.6	665 149.5	875 196.7	1209 271.8	1596 358.8	2329 523.6	2969 667.4	3358 754.9	4206 945.5
Design Resistance to EC3	kN kip	24 5.4	35 7.87	66 14.84	103 25.16	149 33.5	238 53.5	348 78.23	479 107.7	630 141.63	870 195.58	1149 258.31	1677 377	2138 480.64	2418 543.59	3029 680.95
Nominal Bar Weight	(kg/m) (lb/ft)	0.5 0.34	0.75 0.5	1.4 0.94	2.2 1.48	3 2.02	4.8 3.23	7.1 4.77	9.4 6.32	12.5 8.4	16.7 11.22	22.2 14.92	32 21.5	41.5 27.89	46.7 31.38	58 38.97



Macalloy 460 in Application

Engineers all over the world have used Macalloy systems in the most diverse of applications. Among these are bridges, government buildings, stadia, airports, and hotels, to name just a few. The longevity and design again reflect the level of innovation and quality, which have become firm components of Macalloy products.

Macalloy 460 Carbon Bars

Macalloy 460 is a manufactured carbon steel, with excellent mechanical properties. The thread is rolled, rather than cut. This gives rise to the use of smaller diameter bars for a given metric thread, resulting in material cost saving. The carbon Macalloy 460 is also a weldable steel with a maximum carbon equivalent of 0.55%. Arc welding may be carried out using standard techniques and low hydrogen rods.

The Macalloy 460 bar has the following mechanical properties:

Minimum Yield Stress	460 N/mm ²
Minimum Breaking Stress	610 N/mm ²
Minimum Elongation	19%
Minimum Charpy Impact Value	27J @ -20°C
Young's Modulus	205 kN/mm ²
Minimum Yield Stress	66,700 psi
Minimum Breaking Stress	88,400 psi
Minimum Elongation	19%
Minimum Charpy Impact Value	20 ft-lb @ 4°F
Young's Modulus	29,700 ksi

The standard diameter range for this system is from M10 (3/8") to M100 (4"). In addition, other diameters can be supplied but are subject to longer lead times. Tendons up to and including M16 (5/8") diameters can be supplied in lengths of 6m (19'8"). For larger diameters, lengths of up to 11.95m (39'2") are available. Greater lengths are possible using couplers and turnbuckles. These fittings are designed to take the full load of the bar.

Adjustment

Adjustments within each fork or spade are:
 M10 to M56: +/- 1/2 thread diameter
 M64 to M100: +/-25mm / 1"

Turnbuckles give additional adjustments of:
 M10 to M24: +/-25mm / 1"
 M30 to M100: +/-50mm / 2"

Special turnbuckles, with a greater adjustment, are available on request.

Fatigue

Threads are rolled on to the bar and are therefore more resistant to fatigue. Testing a range of diameters has been carried out over 2 million cycles, the results of which are available from the Macalloy technical department.

Corrosion Protection

Macalloy tendons can be supplied in plain carbon steel, primed, or hot dip galvanized

finish. If requested at the time of order, hot dip galvanizing can be applied to tendons after the threading process. The threads are then brushed to remove any excess zinc.

Length permitting, galvanized bars are delivered pre-assembled. This procedure ensures that threads are 100% operational. Connected bars, greater than 11.95m (39'2"), are delivered part assembled. Please note that hot dip galvanizing is not comparable with a paint finish. The visual appearance of forks and spades may differ in appearance from that of the bar, by virtue of the different material compositions.

Paint

For architectural purposes, it is recommended a painted finish is applied to the galvanizing. The corrosion resistance of the bar can then be enhanced.

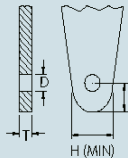
Macalloy offers any kind of paint finish (primer, paint or fire protection) for hot dip galvanized, or self color tendons. These finishes will be sourced from certified suppliers.

European Approval

The Macalloy 460 system has European CE approval under the ETA number 07/0215 for all standard diameters from M10 (3/8") and M100 (4"). When specifying, always ask for CE approved systems.

Table 2 - Macalloy 460 Gusset Plate Dimensions

Thread	mm inch	M10 3/8	M12 1/2	M16 5/8	M20 3/4	M24 1	M30 1 1/4	M36 1 3/8	M42 1 5/8	M48 2	M56 2 1/4	M64 2 1/2	M76 3	M85 3 3/8	M90 3 1/2	M100 4
T (Thickness)	mm inch	10 0.39	10 0.39	12 0.47	15 0.59	20 0.79	22 0.87	30 1.18	35 1.38	40 1.57	45 1.77	55 2.17	70 2.76	70 2.76	80 3.15	85 3.35
D	mm inch	11.5 0.45	13 0.51	17 0.67	21.5 0.85	25.5 1	31.5 1.24	37.5 1.48	43.5 1.71	49.5 1.95	57.5 2.26	65.5 2.58	78.5 3.09	91.5 3.6	96.5 3.8	111.5 4.39
E	mm inch	18 0.71	22 0.87	30 1.18	37 1.46	43 1.69	56 2.2	64 2.52	74 2.91	84 3.31	101 3.98	112 4.41	132 5.2	160 6.3	166 6.54	196 7.72
H (min)	mm inch	28 1.1	34 1.34	48 1.89	60 2.36	68 2.68	90 3.54	103 4.06	118 4.65	135 5.31	163 6.42	180 7.09	211 8.31	259 10.2	266 10.47	317 12.48



EXPERIENCE

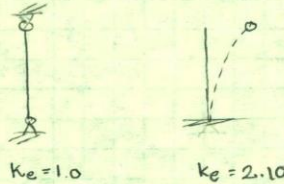
INNOVATION

QUALITY

Steel Square HSS Sizing

QUEEN POST - STEEL POST DESIGN

assuming $l_e = 28'' \times 1$ or $\times 2.10 = 28''$ or $58.8''$



Let's use the more conservative value, assuming the cable offers a "free" constraint.

$l_e = 58.8''$ or $1.9'$

CHOOSE $3\text{-}1/2'' \times 3\text{-}1/2'' \times 3/8''$ SQUARE HSS

l_e	A5D P (KIPS)
4	102
4.9	97.2
5	96.7

→ INTERPOLATED VALUE (Pg. 4-61 OF STL. MANUAL)

$97.2K > 42.5K$ MAX. AXIAL FORCE

✓ (GOOD)

∴ USE $3\text{-}1/2 \times 3\text{-}1/2'' \times 3/8''$
SQUARE HSS
FOR EACH POST

Deflection Check

DEFLECTION CHECK - TYP. OFFICE BAY

TYP. OFFICE - BEAM

$$\frac{5wL^4}{384EI} = \frac{5(1.9)(25^4)}{384(2.156)(6292)} \times 12^3 = 0.0011 < \frac{L}{600} = \frac{25 \times 12}{600} = 0.5''$$

\uparrow 30F-2.156F \uparrow 10-1/2" x 19-1/4" \checkmark GOOD

TYP. OFFICE - QP

$$\frac{5wL^4}{384EI} = \frac{5(6.0987)(29^4)}{384(1.956)(5053)} \times 12^3 = 0.000067' \text{ due to self weight}$$

\uparrow TYPE 505P \uparrow 8-1/2" x 19-1/4"

$$\frac{PL^3}{28EI} = \frac{11.5(29^3)}{28(1.956)(5053)} \times 12^3 = 0.193'' \text{ due to point loads}$$

\uparrow
 two point loads

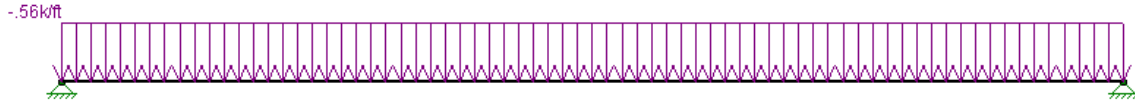
$$0.193067'' < \frac{L}{600} = \frac{29 \times 12}{600} = 0.58''$$

\checkmark GOOD

APPENDIX B.4 - ROOF BEAM DESIGN

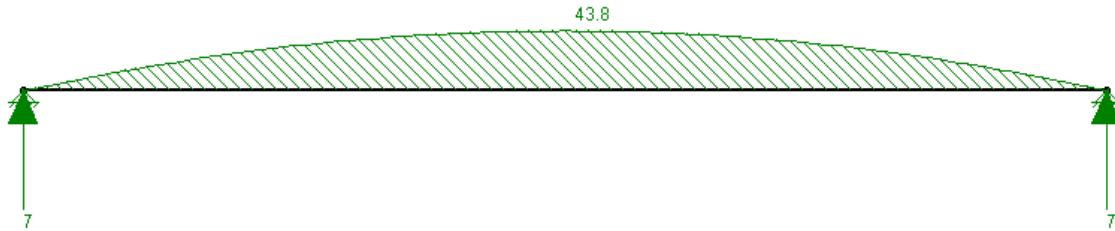
Loading

Computer analysis loading



Flexure and Reactions

Computer analysis results, showing the maximum moment is 43.8 kip-ft, or 44 kip-ft



Computer Analysis Data

Designer : SIKANDAR PORTER-GILL

BEAM ANALYSIS

February 11, 2014

12:18 PM

Checked By:

Member Data

Member Label	I Joint	J Joint	Area in ²	Moment of Inertia in ⁴	Elastic Modulus ksi	End Releases		Length ft
						I-End	J-End	
M1	N1	N2	10	100	29000			25

Member Distributed Loads

Member Label	Direction	Start Magnitude (k/ft, F)	End Magnitude (k/ft, F)	Start Location (ft or %)	End Location (ft or %)
M1	Y	-56	-56	0	0

Reactions

Joint Label	X Force (k)	Y Force (k)	Moment (k-ft)
N1	0	7	0
N2	0	7	0
Totals:	0	14	

Member Section Forces

Member Label	Section	Axial (k)	Shear (k)	Moment (k-ft)
M1	1	0	7	0
	2	0	3.5	32.812
	3	0	0	43.75
	4	0	-3.5	32.813
	5	0	-7	0

Member Sizing

ROOF BEAM DESIGN

LOADS

° SUPERIMPOSED DL

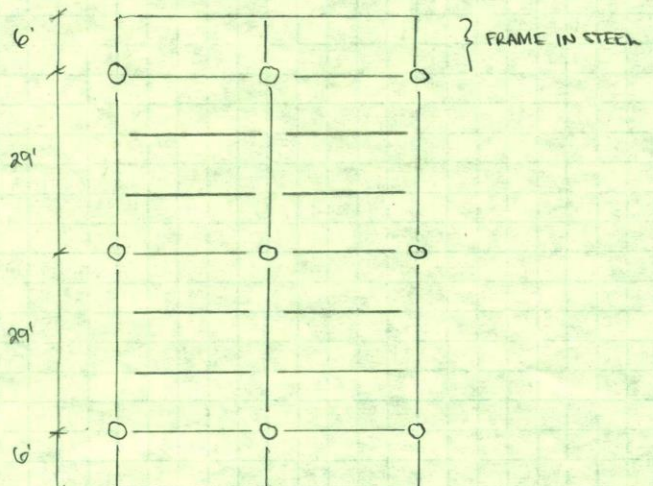
0.29	ROOF MEMBRANE
6	4" RIGID INSULATION
7.3	T&G WOOD DECK
9	3" WOOD NAILER
4	MECH.
4	LTG.
3	SPRINKLER
1	MECSDL

34.59 PSF ~ 36 PSF DL

LIVE LOADS

20 PSF ROOF (PER DRAWINGS) > 10 PSF ASCE-10 SNOW FOR ARKANSAS

ASD → LL + DL = 30 + 20 = 50 PSF



} FRAME IN STEEL

$$560 \text{ PSF} \times (10') = 5600 \text{ PLF}$$

↑
APPROX. TRUSS
WIDTH

$$M = \frac{0.560(25')^2}{8} = 43.75 \text{ KIP FT}$$

USING ESTABLISHED EXCEL DESIGN TABLE,
USE 8-1/2" x 12-3/8" BEAM
GROUP 30F-2.1E 5P

$$R = \frac{0.560(25')}{2} = 7 \text{ KIPS} \times 2 \rightarrow 14 \text{ KIPS}$$

APPLIED TO
QP GIRDER

Flexure in Beam - Roof

 Moment **44** kip-ft

$$F'_b = F_b \times C_D \times C_M \times C_t \times C_L \times C_V \times C_{fu} \times C_c \times C_i$$

Pick a size,		
8-1/2" x 12-3/8"		
8.5	x	12.375
where the A_{provided} =	105.2	in^2
$S_{\text{sect modulus}}$ =	216.9	in^3

$C_D =$	1.00	because live load controls	§2.3.2
$C_M =$	1.00	because interior beam in conditioned space	§5.3.3
$C_t =$	1.00	because interior beam in conditioned space	§5.3.4
$C_L =$	0.987	calculated below	§5.3.5
$C_V =$	0.965	calculated below	§5.3.6
$C_{fu} =$	1.00	because not loaded parallel to wide faces of lamin.	§5.3.7
$C_c =$	1.00	because no curvature to beam	§5.3.8
$C_i =$	1.00	because no tapering of beam	§5.3.9

Pick a Visually Graded Southern Pine Stress Group

Table 5A

 Group = **30F-2.1E SP**
 $F_b =$ **3000** psi

 $E_{min} =$ **1110000** psi

Calculate C_L Adjustment Factor

 $l_u =$ **25.00** ft, the unbraced length of the girder

 $d =$ **12.375** in, chosen to be consistent with girder depth

$$l_u / d = 24.24$$

so now we can calculate l_e ,

$$l_e = \mathbf{552} \text{ in, or } 46.00 \text{ ft}$$

reliant on inequality on page 16, Supplem

$$R_B = 9.72$$

$$F_{bE} = \frac{1.20 E'_{min}}{(R_B)^2} = 14088.3$$

$$F_b^* = F_b \times C_D \times C_M \times C_t \times C_c \times C_i = 3000 \text{ psi}$$

$$F_{bE} / F_b^* = 4.70$$

$$C_L = \frac{1 + F_{bE} / F_b^*}{1.9} - \sqrt{\left(\frac{1 + F_{bE} / F_b^*}{1.9}\right)^2 - \frac{F_{bE} / F_b^*}{0.95}} = 0.987$$

Calculate C_V Adjustment Factor

$$C_V = \left(\frac{21}{L}\right)^{1/x} \left(\frac{12}{d}\right)^{1/x} \left(\frac{5.125}{b}\right)^{1/x} \leq 1.0$$

$$L = 25 \text{ ft} \quad x = 20 \text{ for Southern Pine}$$

$$d = 12.375 \text{ in}$$

$$b = 8.5 \text{ in}$$

$$C_V = 0.965 < 1.0$$

Calculate F_b' Using the Minimum of C_V or C_L

$$\min \begin{cases} C_L = 0.987 \\ C_V = 0.965 \end{cases}$$

$$F'_b = 2895 \text{ psi}$$

$$f_b = \frac{M}{S} = 2434.3 \text{ psi} < F'_b$$

Calculate f_b and Determine if Selected Beam Passes

$$f_b = 2434 \text{ psi} < F'_b = 2895$$

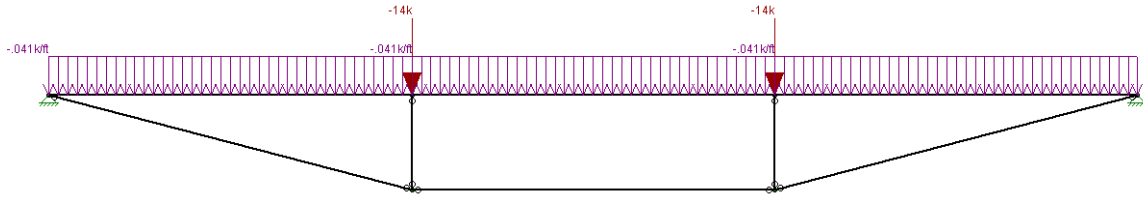
Bending Passes

Use a 8-1/2" x 12-3/8" for the beam

APPENDIX B.5 - ROOF QUEEN POST DESIGN

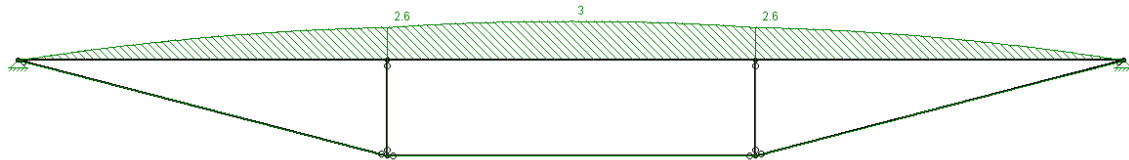
Loading

Computer analysis loading



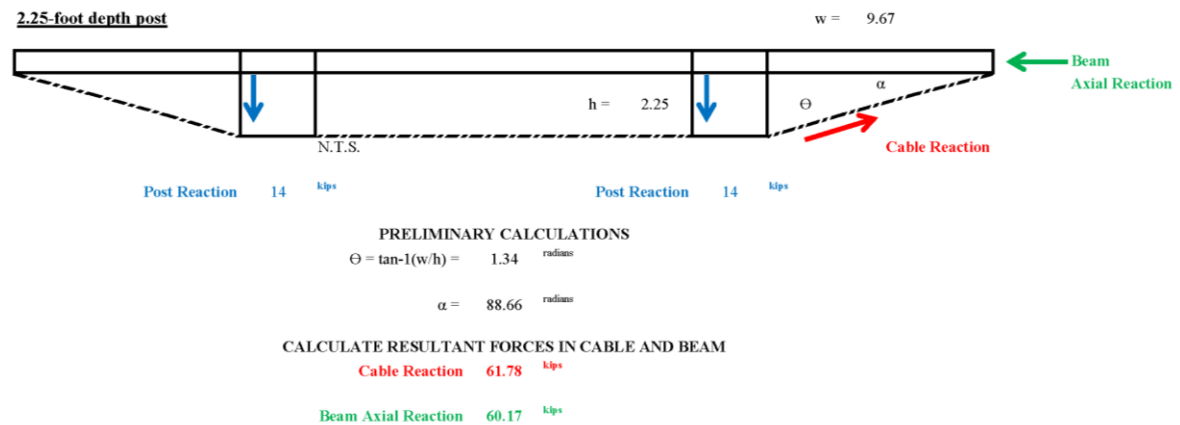
Flexure and Reactions

Computer analysis results, showing the maximum moment is 3 kip-ft, or 3.1 kip-ft



Axial Cable and Girder Forces

The assumption of the hinged queen post was used to determine the post reactions, cable tension and girder axial forces.



Computer Analysis Data

Designer : SIKANDAR PORTER-GILL

GIRDER ANALYSIS

February 11, 2014

12:04 PM

Checked By: _____

Member Data

Member Label	I Joint	J Joint	Area in ²	Moment of Inertia in ⁴	Elastic Modulus ksi	End Releases		Length ft
						I-End	J-End	
M1	N1	N2	10	100	29000			9.67
M2	N2	N3	10	100	29000			9.66
M3	N3	N4	10	100	29000			9.67
M4	N1	N5	10	100	29000	PIN	PIN	9.988
M5	N5	N6	10	100	29000	PIN	PIN	9.66
M6	N6	N4	10	100	29000	PIN	PIN	9.988
M7	N2	N5	10	100	29000	PIN	PIN	2.5
M8	N3	N6	10	100	29000	PIN	PIN	2.5

Joint Loads/Enforced Displacements

Joint Label	[L]oad or [D]isplacement	Direction	Magnitude (k, k-ft, in, rad)
N2	L	Y	-14
N3	L	Y	-14

Member Distributed Loads

Member Label	Direction	Start Magnitude (k/ft, F)	End Magnitude (k/ft, F)	Start Location (ft or %)	End Location (ft or %)
M1	Y	-.041	-.041	0	0
M2	Y	-.041	-.041	0	0
M3	Y	-.041	-.041	0	0

Reactions

Joint Label	X Force (k)	Y Force (k)	Moment (k-ft)
N1	-54.658	14.595	0
N4	54.658	14.594	0
Totals:	0	29.189	

Member Section Forces

Member Label	Section	Axial (k)	Shear (k)	Moment (k-ft)
M1	1	0	.464	0
	2	0	.365	1.001
	3	0	.266	1.763
	4	0	.166	2.285
	5	0	.067	2.568
M2	1	0	.198	2.568
	2	0	.099	2.927
	3	0	0	3.046
	4	0	-.099	2.927
	5	0	-.198	2.568
M3	1	0	-.067	2.568
	2	0	-.166	2.285
	3	0	-.266	1.763
	4	0	-.365	1.001
	5	0	-.464	0
M4	1	-56.455	0	0
	2	-56.455	0	0
	3	-56.455	0	0

Designer : SIKANDAR PORTER-GILL

February 11, 2014
12:04 PM
Checked By: _____

GIRDER ANALYSIS

Member Section Forces

Member Label	Section	Axial (k)	Shear (k)	Moment (k-ft)
	4	-56.455	0	0
	5	-56.455	0	0
M5	1	-54.658	0	0
	2	-54.658	0	0
	3	-54.658	0	0
	4	-54.658	0	0
	5	-54.658	0	0
M6	1	-56.455	0	0
	2	-56.455	0	0
	3	-56.455	0	0
	4	-56.455	0	0
	5	-56.455	0	0
M7	1	14.131	0	0
	2	14.131	0	0
	3	14.131	0	0
	4	14.131	0	0
	5	14.131	0	0
M8	1	14.131	0	0
	2	14.131	0	0
	3	14.131	0	0
	4	14.131	0	0
	5	14.131	0	0

Top Chord Member Sizing

Compression Parallel to Beam Grain Axial Compression **60.17** kips

$$F'_c = F_c \times C_D \times C_M \times C_t \times C_p$$

Adjustment Factors

$C_D = 1.00$ because live load controls §2.3.2

$C_M = 1.00$ because interior beam in conditioned space §5.3.3

$C_t = 1.00$ because interior beam in conditioned space §5.3.4

$C_p = 0.92$ assumed value §3.7.1

Pick a Visually Graded Southern Pine Stress Group Table 5B

Group = 50

$F_c = 2300$ psi

$E_{min} = 1000000$ psi

so,

$F'_c = 2116$ psi allowable compression stress

now the required area would be,

$A = 28$ in² required area of glulam

Pick a,	8-1/2" x 12-3/8"
	8.5 x 12.375
where the $A_{provided} =$	105.2 in ²
Is the area greater than required area?	Yes

Check the Assumption of the C_p Adjustment Factor

$$C_p = \frac{1 + F_{CE}/F_c^*}{2c} - \sqrt{\left(\frac{1 + F_{CE}/F_c^*}{2c}\right)^2 - \frac{F_{CE}/F_c^*}{c}}$$

$$F_c^* = F_c \times C_D \times C_M \times C_t = 2300 \text{ psi}$$

$$l_e/d = 13.65 \quad \text{and} \quad 9.37 \quad \text{where } 13.65 \text{ controls}$$

< 50

 < 50

$$E_{min}' = E_{min} \times C_M \times C_t = 1000000 \text{ psi}$$

$$F_{CE} = \frac{0.822 E_{min}'}{(l_e/d)^2} = 4414 \text{ psi}$$

$$F_{CE} / F_c^* = 1.92 \qquad c = 0.9$$

now the C_p adjustment factor can be calculated

$$C_p = 0.92 < C_{p,assumed}$$

Calculate f_c and Determine if Selected Beam Passes

$$f_c = 572 \text{ psi} < F_c' = 2116$$

Compression Parallel to Grain Passes

Moment Induced by Self-Weight of Member

$$G = 0.55 \quad \text{Table 5B}$$

$$\text{M.C.} = 5\% \text{ or } 10\% \\ \text{because interior beam in conditioned space}$$

$$D = 62.4 \left(\frac{G}{1+G(0.009)(\text{M.C.})} \right) \left(1 + \frac{\text{M.C.}}{100} \right) = 35.17 \text{ pcf, or } 35.97 \text{ pcf}$$

we will take the maximum,

$$D = 35.97 \text{ pcf}$$

we have a 8-1/2" x 12-3/8" glulam beam with,

$$A = 105.2 \text{ in}^2$$

convert to square feet,

$$A = 0.7305 \text{ ft}^2$$

now calculate the linear load created by its self weight, over a 29' span

$$w = 26.28 \text{ plf} > 0.041 \text{ klf assumed in maximum moment calculation}$$

Flexure in Queen Post Girder - Roof

 Moment **3.1** kip-ft

$$F'_b = F_b \times C_D \times C_M \times C_t \times C_L \times C_V \times C_{fu} \times C_c \times C_i$$

Adjustment Factors

$C_D =$	1.00	because live load controls	§2.3.2
$C_M =$	1.00	because interior beam in conditioned space	§5.3.3
$C_t =$	1.00	because interior beam in conditioned space	§5.3.4
$C_L =$	0.996	calculated below	§5.3.5
$C_V =$	0.958	calculated below	§5.3.6
$C_{fu} =$	1.00	because not loaded parallel to wide faces of lamin.	§5.3.7
$C_c =$	1.00	because no curvature to beam	§5.3.8
$C_i =$	1.00	because no tapering of beam	§5.3.9

Pick a Visually Graded Southern Pine Stress Group

Table 5B

Group =	50
$F_b =$	2100 psi
$E_{min} =$	1000000 psi

Calculate C_L Adjustment Factor

$$l_u = 9.67 \text{ ft, the unbraced length of the girder}$$

$$d = 12.375 \text{ in, depth chosen in compression parallel to grain calculation}$$

$$l_u / d = 9.37$$

so now we can calculate l_e ,

$$l_e = 226.205 \text{ in, or } 18.85 \text{ ft}$$

$$R_B = 6.22$$

$$F_{bE} = \frac{1.20 E'_{min}}{(R_B)^2} = 30972.2$$

$$F_b^* = F_b \times C_D \times C_M \times C_t \times C_c \times C_i = 2100 \text{ psi}$$

$$F_{bE} / F_b^* = 14.75$$

$$C_L = \frac{1 + F_{bE} / F_b^*}{1.9} - \sqrt{\left(\frac{1 + F_{bE} / F_b^*}{1.9} \right)^2 - \frac{F_{bE} / F_b^*}{0.95}} = 0.996$$

Calculate C_V Adjustment Factor

$$C_V = \left(\frac{21}{L}\right)^{1/x} \left(\frac{12}{d}\right)^{1/x} \left(\frac{5.125}{b}\right)^{1/x} \leq 1.0$$

$L = 29$ ft $x = 20$ for Southern Pine
 $d = 12.375$ in
 $b = 8.5$ in

$C_V = 0.958 < 1.0$

Calculate F'_b Using the Minimum of C_V or C_L

min		$C_L = 0.996$	Section Modulus (x) =	267.8 in^3
		$C_V = 0.958$		

$F'_b = 2012$ psi

$f_b = \frac{M}{S} = 138.9$ psi < F'_b

Calculate f_b and Determine if Selected Beam Passes

$f_b = 139$ psi < $F'_b = 2012$

Bending Passes

Combined Axial and Bending Loading Interaction

$$\left(\frac{f_c}{F_c'}\right)^2 + \frac{f_{b1}}{F_{b1}'\left(1 + f_c/F_{CE1}\right)} \leq 1.0 \quad \text{\$3.9.2}$$

$f_c = 572$ psi $E_{min}' = 1000000$ psi
 $F_c' = 2116$ psi
 $f_{b1} = 139$ psi
 $F_{b1}' = 2012$ psi

$F_{CE1} = \frac{0.822 E_{min}'}{(l_{e1}/d_1)^2} = 9348.6$ psi where,
 $l_{e1} = 9.67$ ft
 $d_1 = 12.375$ in
 $f_c < F_{CE1}$ True

0.073 + 0.065 = 0.138 < 1.0

Combined Axial and Bending Pass

Use a,
8-1/2" x 12-3/8"
 for the glulam queen post

With a,
 Southern Pine Group of **50**

Member Summary, Tension Cable and Steel Square HSS Sizing

ROOF QUEEN POST DESIGN

CONSERVATIVELY ASSUME 0.041 K/FT SELF WEIGHT
 ↳ REFERENCING TYP. FLOOR QP

FROM COMPUTER ANALYSIS: $M_{max} = 1.615 \text{ Kft} \rightarrow 1.7 \text{ Kft}$
 QP
 girder

AN EXCEL TABLE WILL BE USED TO CALCULATE
 THE SUFFICIENT QP GIRDER SIZE...
 ↳ REFER DESIGN SUMMARY

8-112" X 12-2/8"
 GLULAM QP, GROUP 50 SP

TENSION CABLE

61.72^k → 62^{kips}

	Min. Yield	Min. Break
M16	69	91
M20	108	143

M16 69^k > 62^k TOTAL ✓ GOOD

DESIGN CALLS FOR TWO CABLES
 ✓ FOR STABILITY
 ✓ ADDED SAFETY

(2) M16 MACALLOY 160 BARS
 FOR TENSION WILL BE USED

QP POST (following previously sized post)

$l_e = 58.8''$ or $4.9'$ with $14k$ axial

USE SAME POST, $3\text{-}1/2'' \times 3\text{-}1/2'' \times 3/8''$ SQUARE HSS

$94.2k > 14k$ MAX. AXIAL FORCE

✓ GOOD

∴ USE $3\text{-}1/2'' \times 3\text{-}1/2'' \times 3/8''$

FOR EACH POST

ROOF QUEEN POST DESIGN SUMMARY

$3\text{-}1/2'' \times 12\text{-}3/8''$, GALVALUM QP
GROUP 50 SP

WITH (2) A60 MACALLOY BARS

WITH $3\text{-}1/2'' \times 3\text{-}1/2'' \times 3/8''$ POST/S

Deflection Check

DEFLECTION CHECK - ROOF BAY

BEAM

$$\frac{5(0.56)(25^4)}{384(2.106)(1342)} \times 12^3 = 0.0017 < \frac{l}{600} = \frac{25' \times 12}{600} = 0.5''$$

\uparrow 30F-2.1E8P \uparrow 3 1/2" x 12 3/8"

✓ Good

QUEEN POST

$$\frac{5(0.04087)(29^4)}{384(1.966)(1342)} \times 12^3 = 0.00049$$

\uparrow type 80 \uparrow 3 1/2" x 12 3/8"

$$\frac{14(29^4)}{23(1.966)(1342)} \times 12^3 = 0.23$$

$$= 0.2304'' < \frac{l}{600} = 0.58''$$

✓ Good

APPENDIX B.6 - SUMMARY OF BEAM SIZES

- The typical office beam will be specified as a 10 ½" x 19 ¼" 30F-2.1E Southern Pine.
- The typical office queen post will be specified as an 8 ½" x 19 ¼" Stress Class 50 Visual Southern Pine, with 3 ½" x 3 ½" x ¾" Square HSS Post and (2) M56 Macalloy 460 Bars
- The typical roof beam will be specified as a 8 ½" x 12 ¾" 30F-2.1E Southern Pine.
- The typical roof queen post will be specified as a 8 ½" x 12 ¾" Stress Class 50 Visual Southern Pine, with 3 ½" x 3 ½" x ¾" Square HSS Post and (2) M16 Macalloy 460 Bars

APPENDIX B.7 - TYPICAL OFFICE PERIMETER BEAM

TYPICAL OFFICE - PERIMETER BEAM

FROM PREV. TECH REPORT 11: 280 PLF ON EDGE

$$\text{TRIB.} = \frac{9.67'}{2} + 2' = 6.84' \sim 7'-0" \times 164.5 \text{ PSF OFFICE}$$

↑
edge

$$= 1151.5 \text{ PLF} \sim 1.2 \text{ KLF}$$

$$+ 0.28 \text{ KLF}$$

$$1.48 \text{ KLF} \sim 1.5 \text{ KLF}$$

$$M = \frac{1.5(25^2)}{8} = 117.18 \text{ KFT} \sim 117.2 \text{ K}$$

$$R = \frac{1.5(25)}{2} = 18.75 \text{ K}$$

GLULAM:

SIZE 10-1/2" x 17-7/8", 30F-2.1E SP

d = 19.25"

STEEL

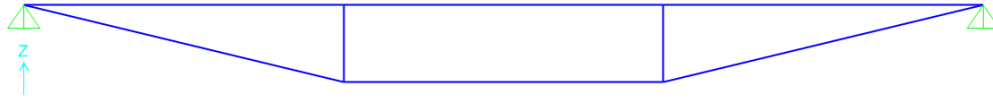
SIZE W14x22, SAME AS ACTUAL DESIGN
(ETL MANUAL, PG. 3-26)

d = 13.7"

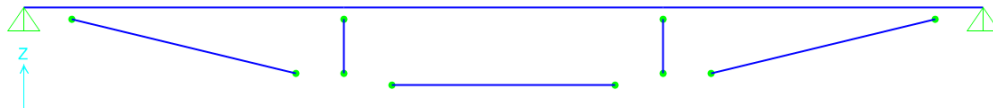
* IT SHOULD BE NOTED THAT THE USE OF
STEEL PERIMETER BEAMS WILL CHANGE
IBC 2009 CONSTRUCTION TYPE.

APPENDIX B.8 - SAP2000 QUEEN POST MODEL

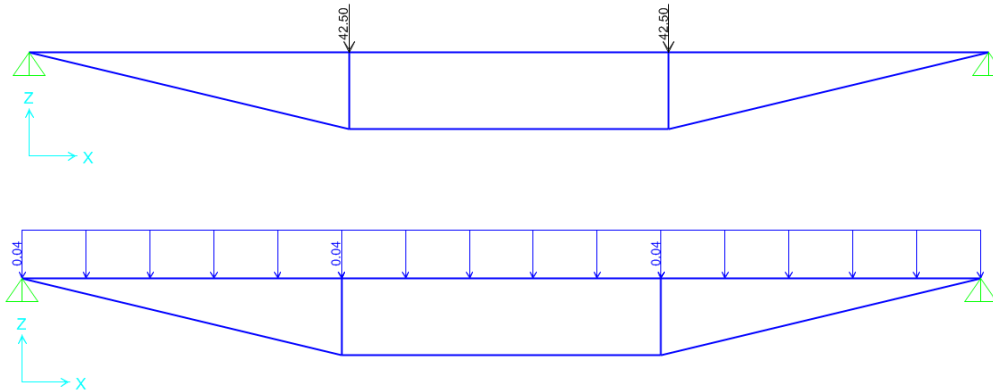
Original Model



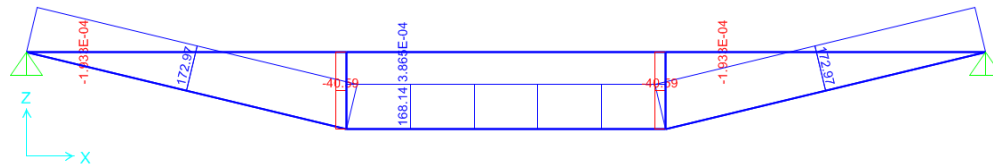
Member Releases



Loading



Axial Loading



Member	Force	Percent Error (from actual)
Cable	172.97	7.1%
Cable	168.141	9.7%
Cable	172.97	7.1%
Post	-40.586	3.4%
Post	-40.586	3.4%

APPENDIX B.9 – COLUMN SIZING

COLUMN CONFIRMATION

FOR EDGE OF CONNECTION AND AESTHETICS, THE SAME COLUMNS WILL BE USED FROM EXISTING BUILDING DESIGN

→ 24" DIAMETER, MIN THICKNESS = 0.438" @ 19'-0" effective

PERIMETER BEAM 18.75k X 2 / FLOOR

QUEEN POST (OFF) 43k

QUEEN POST (ROOF) 14.5k

CONSERVATIVE
VALUE
↓
ASSUMED

$$P_0 = 3 \times (18.75(2) + 43) + 1 \times (14.5 + 18.75(2))$$

$$= 293.5k > ASD_{axial} = 691k$$

for HSS 20x20x0.5
(STL. MANUAL 4-68)

HSS 24x24x0.5 > HSS 20x20x0.5 \checkmark (Good)

APPENDIX C

REDESIGN OF LATERAL SYSTEM

APPENDIX C.1 – HSS24x0.5 COLUMN

The Master Steel Table for RAM SS was modified to account for the larger HSS24x0.5 used in the Heifer International Center (American Institute of Steel Construction, 2011).

RAMAISC.TAB - Notepad													
File	Edit	Format	View	Help									
HSS4X2X3/16	R	4	0.174	2	0.174	1.89	3.66	1.83	2.34	1.22	1.22	1.43	3.08
HSS4X2X1/8	R	4	0.116	2	0.116	1.30	2.65	1.32	1.66	0.898	0.898	1.02	2.20
HSS3.5X3.5X3/8	R	3.5	0.349	3.5	0.349	4.09	6.49	3.71	4.69	6.49	3.71	4.69	11.2
HSS3.5X3.5X5/16	R	3.5	0.291	3.5	0.291	3.52	5.84	3.34	4.14	5.84	3.34	4.14	9.89
HSS3.5X3.5X1/4	R	3.5	0.233	3.5	0.233	2.91	5.04	2.88	3.50	5.04	2.88	3.50	8.35
HSS3.5X3.5X3/16	R	3.5	0.174	3.5	0.174	2.24	4.05	2.31	2.76	4.05	2.31	2.76	6.56
HSS3.5X3.5X1/8	R	3.5	0.116	3.5	0.116	1.54	2.90	1.66	1.93	2.90	1.66	1.93	4.58
HSS3.5X2X1/4	R	3.5	0.233	2	0.233	2.21	3.17	1.81	2.36	1.30	1.30	1.58	3.16
HSS3.5X2X3/16	R	3.5	0.174	2	0.174	1.71	2.61	1.49	1.89	1.08	1.08	1.27	2.55
HSS3.5X2X1/8	R	3.5	0.116	2	0.116	1.19	1.90	1.09	1.34	0.795	0.795	0.912	1.83
HSS3.5X1.5X1/4	R	3.5	0.233	1.5	0.233	1.97	2.55	1.46	1.98	0.638	0.851	1.06	1.79
HSS3.5X1.5X3/16	R	3.5	0.174	1.5	0.174	1.54	2.12	1.21	1.60	0.544	0.725	0.867	1.49
HSS3.5X1.5X1/8	R	3.5	0.116	1.5	0.116	1.07	1.57	0.896	1.15	0.411	0.548	0.630	1.09
HSS3X3X3/8	R	3	0.349	3	0.349	3.39	3.78	2.52	3.25	3.78	2.52	3.25	6.64
HSS3X3X5/16	R	3	0.291	3	0.291	2.94	3.45	2.30	2.90	3.45	2.30	2.90	5.94
HSS3X3X1/4	R	3	0.233	3	0.233	2.44	3.02	2.01	2.48	3.02	2.01	2.48	5.08
HSS3X3X3/16	R	3	0.174	3	0.174	1.89	2.46	1.64	1.97	2.46	1.64	1.97	4.03
HSS3X3X1/8	R	3	0.116	3	0.116	1.30	1.78	1.19	1.40	1.78	1.19	1.40	2.84
HSS3X2.5X5/16	R	3	0.291	2.5	0.291	2.64	2.92	1.94	2.51	2.18	1.74	2.20	4.34
HSS3X2.5X1/4	R	3	0.233	2.5	0.233	2.21	2.57	1.72	2.16	1.93	1.54	1.90	3.74
HSS3X2.5X3/16	R	3	0.174	2.5	0.174	1.71	2.11	1.41	1.73	1.59	1.27	1.52	3.00
HSS3X2.5X1/8	R	3	0.116	2.5	0.116	1.19	1.54	1.03	1.23	1.16	0.931	1.09	2.13
HSS3X2X5/16	R	3	0.291	2	0.291	2.35	2.38	1.59	2.11	1.24	1.24	1.58	2.87
HSS3X2X1/4	R	3	0.233	2	0.233	1.97	2.13	1.42	1.83	1.11	1.11	1.38	2.52
HSS3X2X3/16	R	3	0.174	2	0.174	1.54	1.77	1.18	1.48	0.932	0.932	1.12	2.05
HSS3X2X1/8	R	3	0.116	2	0.116	1.07	1.30	0.867	1.06	0.692	0.692	0.803	1.47
HSS2.5X2.5X5/16	R	2.5	0.291	2.5	0.291	2.35	1.82	1.46	1.88	1.82	1.46	1.88	3.20
HSS2.5X2.5X1/4	R	2.5	0.233	2.5	0.233	1.97	1.63	1.30	1.63	1.63	1.30	1.63	2.79
HSS2.5X2.5X3/16	R	2.5	0.174	2.5	0.174	1.54	1.35	1.08	1.32	1.35	1.08	1.32	2.25
HSS2.5X2.5X1/8	R	2.5	0.116	2.5	0.116	1.07	0.998	0.799	0.947	0.998	0.799	0.947	1.61
HSS2.5X2X1/4	R	2.5	0.233	2	0.233	1.74	1.33	1.06	1.37	0.930	0.930	1.17	1.90
HSS2.5X2X3/16	R	2.5	0.174	2	0.174	1.37	1.12	0.894	1.12	0.786	0.786	0.956	1.55
HSS2.5X2X1/8	R	2.5	0.116	2	0.116	0.956	0.833	0.667	0.809	0.589	0.589	0.694	1.12
HSS2.5X1.5X1/4	R	2.5	0.233	1.5	0.233	1.51	1.03	0.822	1.11	0.449	0.599	0.764	1.10
HSS2.5X1.5X3/16	R	2.5	0.174	1.5	0.174	1.19	0.882	0.705	0.915	0.390	0.520	0.636	0.929
HSS2.5X1.5X1/8	R	2.5	0.116	1.5	0.116	0.840	0.668	0.535	0.671	0.300	0.399	0.469	0.687
HSS2.5X1X3/16	R	2.5	0.174	1	0.174	1.02	0.646	0.517	0.713	0.143	0.285	0.360	0.412
HSS2.5X1X1/8	R	2.5	0.116	1	0.116	0.724	0.503	0.403	0.532	0.115	0.230	0.274	0.322
HSS2X2X1/4	R	2	0.233	2	0.233	1.51	0.747	0.747	0.964	0.747	0.747	0.964	1.31
HSS2X2X3/16	R	2	0.174	2	0.174	1.19	0.641	0.641	0.797	0.641	0.641	0.797	1.09
HSS2X2X1/8	R	2	0.116	2	0.116	0.840	0.486	0.486	0.584	0.486	0.486	0.584	0.796
PIPE													
HSS24.000X0.500	R	24.000	0.465	34.400	2381.400	198.400	257.600						
HSS20.000X0.500	R	20.000	0.465	28.500	1360.000	136.000	177.000						
HSS20.000X0.375	R	20.000	0.349	21.500	1040.000	104.000	135.000						
HSS18.000X0.500	R	18.000	0.465	25.600	985.000	109.000	143.000						
HSS18.000X0.375	R	18.000	0.349	19.400	754.000	83.800	109.000						
HSS16.000X0.625	R	16.000	0.581	28.100	838.000	105.000	138.000						
HSS16.000X0.500	R	16.000	0.465	22.700	685.000	85.700	112.000						
HSS16.000X0.438	R	16.000	0.407	19.900	606.000	75.800	99.000						
HSS16.000X0.375	R	16.000	0.349	17.200	526.000	65.700	85.500						
HSS16.000X0.312	R	16.000	0.291	14.400	443.000	55.400	71.800						
HSS16.000X0.250	R	16.000	0.233	11.500	359.000	44.800	57.900						
HSS14.000X0.625	R	14.000	0.581	24.500	552.000	78.900	105.000						
HSS14.000X0.500	R	14.000	0.465	19.800	453.000	64.800	85.200						
HSS14.000X0.375	R	14.000	0.349	15.000	349.000	49.800	65.100						
HSS14.000X0.312	R	14.000	0.291	12.500	295.000	42.100	54.700						
HSS14.000X0.250	R	14.000	0.233	10.100	239.000	34.100	44.200						
HSS12.750X0.500	R	12.750	0.465	17.900	339.000	53.200	70.200						
HSS12.750X0.375	R	12.750	0.349	13.600	262.000	41.000	53.700						
HSS12.750X0.250	R	12.750	0.233	9.160	180.000	28.200	36.500						
HSS10.750X0.500	R	10.750	0.465	15.000	199.000	37.000	49.200						
HSS10.750X0.375	R	10.750	0.349	11.400	154.000	28.700	37.800						
HSS10.750X0.250	R	10.750	0.233	7.700	106.000	19.800	25.800						
HSS10.000X0.625	R	10.000	0.581	17.200	191.000	38.300	51.600						
HSS10.000X0.500	R	10.000	0.465	13.900	159.000	31.700	42.300						
HSS10.000X0.375	R	10.000	0.349	10.600	123.000	24.700	32.500						
HSS10.000X0.312	R	10.000	0.291	8.880	105.000	20.900	27.400						
HSS10.000X0.250	R	10.000	0.233	7.150	85.300	17.100	22.200						
HSS10.000X0.188	R	10.000	0.174	5.370	64.800	13.000	16.800						
HSS9.625X0.500	R	9.625	0.465	13.400	141.000	29.200	39.000						
HSS9.625X0.375	R	9.625	0.349	10.200	110.000	22.800	30.000						

APPENDIX C.2 – SEISMIC AND WIND LOADING

Seismic ASCE 7-10

General Programming Input

Risk Category II

For ordinary reinforced concrete shear walls, Classification 1.2 of §12.2-1

$$C_d = 4.0$$

$$R = 4.0$$

Please review the Summary and Detailed Report on the next page for the following values (U.S. Geological Survey, 2013):

$$S_S = 0.410g$$

$$S_1 = 0.165g$$

$$TL = 12 \text{ sec}$$

Site Class C

The Structure Period, T_a :

Value calculated by RAM SS using the Standard Equation

$C_t = 0.020$ was used for “all other structural systems” per Table 12.8-2

Orthogonal Effects Considered at 100%/30%

(American Society of Civil Engineers, ASCE-7 10, Minimum Design Loads for Buildings and Other Structures, 2010)

U.S. Geological Survey Report

2/20/14

Design Maps Summary Report

Design Maps Summary Report

User-Specified Input

Report Title Heifer International Center –2010
Thu February 20, 2014 17:15:04 UTC

Building Code Reference Document ASCE 7-10 Standard
(which utilizes USGS hazard data available in 2008)

Site Coordinates 34.74492°N, 92.25781°W

Site Soil Classification Site Class C – “Very Dense Soil and Soft Rock”

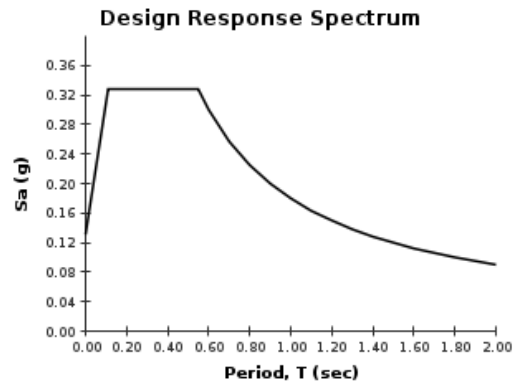
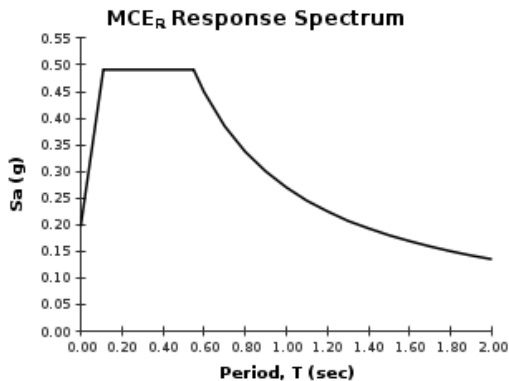
Risk Category I/II/III



USGS-Provided Output

$S_S = 0.410 \text{ g}$	$S_{MS} = 0.491 \text{ g}$	$S_{DS} = 0.328 \text{ g}$
$S_1 = 0.165 \text{ g}$	$S_{M1} = 0.270 \text{ g}$	$S_{D1} = 0.180 \text{ g}$

For information on how the S_S and S_1 values above have been calculated from probabilistic (risk-targeted) and deterministic ground motions in the direction of maximum horizontal response, please return to the application and select the “2009 NEHRP” building code reference document.



For PGA_{Mf} , T_U , C_{RSf} , and C_{R1} values, please [view the detailed report](#).

geohazards.usgs.gov/designmaps/us/summary.php?template=minimal&latitude=34.7449152&longitude=-92.2578128&siteclass=2&riskcategory=0&edition=asc... 1/2

2/20/14

Design Maps Detailed Report


Design Maps Detailed Report

ASCE 7-10 Standard (34.74492°N, 92.25781°W)

Site Class C – “Very Dense Soil and Soft Rock”, Risk Category I/II/III

Section 11.4.1 — Mapped Acceleration Parameters

Note: Ground motion values provided below are for the direction of maximum horizontal spectral response acceleration. They have been converted from corresponding geometric mean ground motions computed by the USGS by applying factors of 1.1 (to obtain S_s) and 1.3 (to obtain S_1). Maps in the 2010 ASCE-7 Standard are provided for Site Class B. Adjustments for other Site Classes are made, as needed, in Section 11.4.3.

 From [Figure 22-1](#) ^[1]
 $S_s = 0.410 \text{ g}$

 From [Figure 22-2](#) ^[2]
 $S_1 = 0.165 \text{ g}$
Section 11.4.2 — Site Class

The authority having jurisdiction (not the USGS), site-specific geotechnical data, and/or the default has classified the site as Site Class C, based on the site soil properties in accordance with Chapter 20.

Table 20.3-1 Site Classification

Site Class	\bar{v}_s	\bar{N} or \bar{N}_{ch}	\bar{s}_u
A. Hard Rock	>5,000 ft/s	N/A	N/A
B. Rock	2,500 to 5,000 ft/s	N/A	N/A
C. Very dense soil and soft rock	1,200 to 2,500 ft/s	>50	>2,000 psf
D. Stiff Soil	600 to 1,200 ft/s	15 to 50	1,000 to 2,000 psf
E. Soft clay soil	<600 ft/s	<15	<1,000 psf
Any profile with more than 10 ft of soil having the characteristics:			
<ul style="list-style-type: none"> ■ Plasticity index $PI > 20$, ■ Moisture content $w \geq 40\%$, and ■ Undrained shear strength $\bar{s}_u < 500 \text{ psf}$ 			
F. Soils requiring site response analysis in accordance with Section 21.1	See Section 20.3.1		

 For SI: 1ft/s = 0.3048 m/s 1lb/ft² = 0.0479 kN/m²

2/20/14

Design Maps Detailed Report

Section 11.4.3 — Site Coefficients and Risk-Targeted Maximum Considered Earthquake (MCE_R) Spectral Response Acceleration Parameters

 Table 11.4-1: Site Coefficient F_a

Site Class	Mapped MCE_R Spectral Response Acceleration Parameter at Short Period				
	$S_s \leq 0.25$	$S_s = 0.50$	$S_s = 0.75$	$S_s = 1.00$	$S_s \geq 1.25$
A	0.8	0.8	0.8	0.8	0.8
B	1.0	1.0	1.0	1.0	1.0
C	1.2	1.2	1.1	1.0	1.0
D	1.6	1.4	1.2	1.1	1.0
E	2.5	1.7	1.2	0.9	0.9
F	See Section 11.4.7 of ASCE 7				

 Note: Use straight-line interpolation for intermediate values of S_s
For Site Class = C and $S_s = 0.410$ g, $F_a = 1.200$

 Table 11.4-2: Site Coefficient F_v

Site Class	Mapped MCE_R Spectral Response Acceleration Parameter at 1-s Period				
	$S_1 \leq 0.10$	$S_1 = 0.20$	$S_1 = 0.30$	$S_1 = 0.40$	$S_1 \geq 0.50$
A	0.8	0.8	0.8	0.8	0.8
B	1.0	1.0	1.0	1.0	1.0
C	1.7	1.6	1.5	1.4	1.3
D	2.4	2.0	1.8	1.6	1.5
E	3.5	3.2	2.8	2.4	2.4
F	See Section 11.4.7 of ASCE 7				

 Note: Use straight-line interpolation for intermediate values of S_1
For Site Class = C and $S_1 = 0.165$ g, $F_v = 1.635$

2/2014

Design Maps Detailed Report

Equation (11.4-1): $S_{MS} = F_s S_s = 1.200 \times 0.410 = 0.491 \text{ g}$

Equation (11.4-2): $S_{M1} = F_v S_1 = 1.635 \times 0.165 = 0.270 \text{ g}$

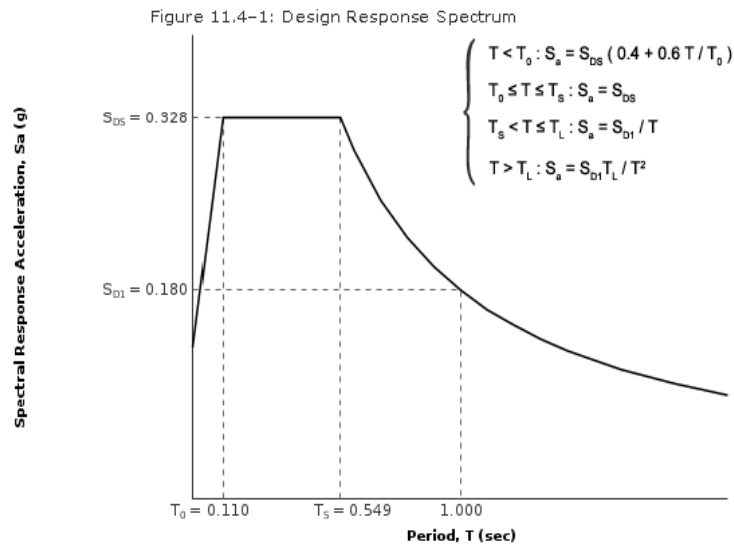
Section 11.4.4 — Design Spectral Acceleration Parameters

Equation (11.4-3): $S_{DS} = \frac{2}{3} S_{MS} = \frac{2}{3} \times 0.491 = 0.328 \text{ g}$

Equation (11.4-4): $S_{D1} = \frac{2}{3} S_{M1} = \frac{2}{3} \times 0.270 = 0.180 \text{ g}$

Section 11.4.5 — Design Response Spectrum

From [Figure 22-12](#)^[3] $T_L = 12 \text{ seconds}$

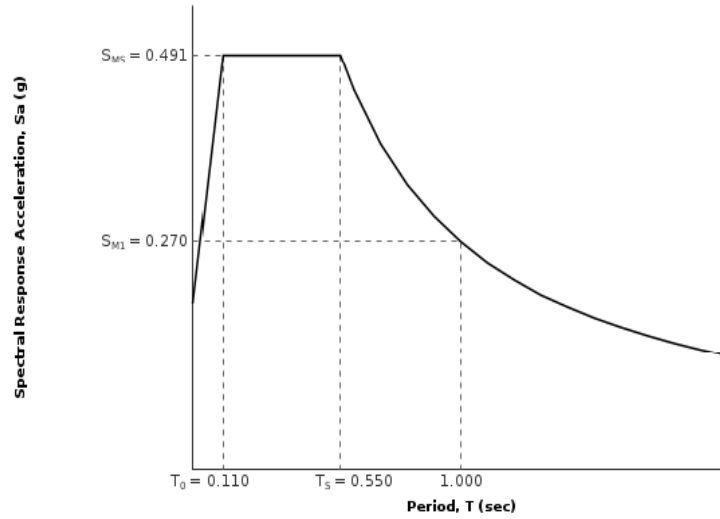


2/2014

Design Maps Detailed Report

Section 11.4.6 — Risk-Targeted Maximum Considered Earthquake (MCE_R) Response Spectrum

The MCE_R Response Spectrum is determined by multiplying the design response spectrum above by 1.5.



geohazards.usgs.gov/designmaps/us/report.php?template=minimal&latitude=34.7449152&longitude=-92.2578128&siteclass=2&riskcategory=0&edition=asce-2... 4/6

2/20/14

Design Maps Detailed Report

Section 11.8.3 — Additional Geotechnical Investigation Report Requirements for Seismic Design Categories D through F

 From [Figure 22-7](#) ^[4]
 $PGA = 0.213$
Equation (11.8-1):

$$PGA_M = F_{PGA}PGA = 1.187 \times 0.213 = 0.253 \text{ g}$$

 Table 11.8-1: Site Coefficient F_{PGA}

Site Class	Mapped MCE Geometric Mean Peak Ground Acceleration, PGA				
	PGA ≤ 0.10	PGA = 0.20	PGA = 0.30	PGA = 0.40	PGA ≥ 0.50
A	0.8	0.8	0.8	0.8	0.8
B	1.0	1.0	1.0	1.0	1.0
C	1.2	1.2	1.1	1.0	1.0
D	1.6	1.4	1.2	1.1	1.0
E	2.5	1.7	1.2	0.9	0.9
F	See Section 11.4.7 of ASCE 7				

Note: Use straight-line interpolation for intermediate values of PGA

For Site Class = C and PGA = 0.213 g, $F_{PGA} = 1.187$
Section 21.2.1.1 — Method 1 (from Chapter 21 – Site-Specific Ground Motion Procedures for Seismic Design)

 From [Figure 22-17](#) ^[5]
 $C_{RS} = 0.829$

 From [Figure 22-18](#) ^[6]
 $C_{R1} = 0.816$

2/20/14

Design Maps Detailed Report

Section 11.6 — Seismic Design Category

Table 11.6-1 Seismic Design Category Based on Short Period Response Acceleration Parameter

VALUE OF S_{DS}	RISK CATEGORY		
	I or II	III	IV
$S_{DS} < 0.167g$	A	A	A
$0.167g \leq S_{DS} < 0.33g$	B	B	C
$0.33g \leq S_{DS} < 0.50g$	C	C	D
$0.50g \leq S_{DS}$	D	D	D

For Risk Category = I and $S_{Ds} = 0.328g$, Seismic Design Category = B

Table 11.6-2 Seismic Design Category Based on 1-S Period Response Acceleration Parameter

VALUE OF S_{D1}	RISK CATEGORY		
	I or II	III	IV
$S_{D1} < 0.067g$	A	A	A
$0.067g \leq S_{D1} < 0.133g$	B	B	C
$0.133g \leq S_{D1} < 0.20g$	C	C	D
$0.20g \leq S_{D1}$	D	D	D

For Risk Category = I and $S_{D1} = 0.180g$, Seismic Design Category = C

Note: When S_1 is greater than or equal to 0.75g, the Seismic Design Category is **E** for buildings in Risk Categories I, II, and III, and **F** for those in Risk Category IV, irrespective of the above.

Seismic Design Category \equiv "the more severe design category in accordance with Table 11.6-1 or 11.6-2" = C

Note: See Section 11.6 for alternative approaches to calculating Seismic Design Category.

References

1. Figure 22-1: http://earthquake.usgs.gov/hazards/designmaps/downloads/pdfs/2010_ASCE-7_Figure_22-1.pdf
2. Figure 22-2: http://earthquake.usgs.gov/hazards/designmaps/downloads/pdfs/2010_ASCE-7_Figure_22-2.pdf
3. Figure 22-12: http://earthquake.usgs.gov/hazards/designmaps/downloads/pdfs/2010_ASCE-7_Figure_22-12.pdf
4. Figure 22-7: http://earthquake.usgs.gov/hazards/designmaps/downloads/pdfs/2010_ASCE-7_Figure_22-7.pdf
5. Figure 22-17: http://earthquake.usgs.gov/hazards/designmaps/downloads/pdfs/2010_ASCE-7_Figure_22-17.pdf
6. Figure 22-18: http://earthquake.usgs.gov/hazards/designmaps/downloads/pdfs/2010_ASCE-7_Figure_22-18.pdf

geohazards.usgs.gov/designmaps/us/report.php?template=minimal&latitude=34.7449152&longitude=-92.2578128&siteclass=2&riskcategory=0&edition=asce-2... 6/6

Seismic Story Drift

Seismic Story Drift - West End

$$C_d = 4$$

$$I = 1$$

X-direction Seismic Loading

Level	δ , Actual Displacement (in)	δ_x , Modified Displacement (in)	Story Height (ft)	Δ , Design Story Drift (in)	Δ_a , Allowable Story Drift (in)	Pass
Story3	0.3799	1.5196	14	0.6464	3.36	PASS
Story2	0.2183	0.8732	14	0.5816	3.36	PASS
Story1	0.0729	0.2916	14	0.2916	3.36	PASS

@ RAM Frame Location EX A @ (-156.198, -393.277), trace Location 1

X-direction Seismic Loading

Level	δ , Actual Displacement (in)	δ_x , Modified Displacement (in)	Story Height (ft)	Δ , Design Story Drift (in)	Δ_a , Allowable Story Drift (in)	Pass
Story3	0.2436	0.9744	14	0.4084	3.36	PASS
Story2	0.1415	0.566	14	0.3784	3.36	PASS
Story1	0.0469	0.1876	14	0.1876	3.36	PASS

@ RAM Frame Location EX B @ (-379.546, -319.250), trace Location 3

West Side

Y-direction Seismic Loading

Level	δ , Actual Displacement (in)	δ_x , Modified Displacement (in)	Story Height (ft)	Δ , Design Story Drift (in)	Δ_a , Allowable Story Drift (in)	Pass
Story3	0.4542	1.8168	14	0.7776	3.36	PASS
Story2	0.2598	1.0392	14	0.674	3.36	PASS
Story1	0.0913	0.3652	14	0.3652	3.36	PASS

@ RAM Frame Location EX A @ (-156.198, -393.277), trace Location 1

Y-direction Seismic Loading

Level	δ , Actual Displacement (in)	δ_x , Modified Displacement (in)	Story Height (ft)	Δ , Design Story Drift (in)	Δ_a , Allowable Story Drift (in)	Pass
Story3	0.1035	0.414	14	0.1736	3.36	PASS
Story2	0.0601	0.2404	14	0.1744	3.36	PASS
Story1	0.0165	0.066	14	0.066	3.36	PASS

@ RAM Frame Location EX B @ (-379.546, -319.250), trace Location 3

Please refer to Appendix C.6 – Trace Locations for a visual location of EX A and EX B

Seismic Story Drift - East End

$$C_d = 4$$

$$I = 1$$

X-direction Seismic Loading

Level	δ , Actual Displacement (in)	δ_x , Modified Displacement (in)	Story Height (ft)	Δ , Design Story Drift (in)	Δ_a , Allowable Story Drift (in)	Pass
Story3	0.2051	0.8204	14	0.3948	3.36	PASS
Story2	0.1064	0.4256	14	0.38	3.36	PASS
Story1	0.0114	0.0456	14	0.0456	3.36	PASS
@ RAM Frame Location		EX C @ (-365.149, -844.326), trace location 4				

X-direction Seismic Loading

Level	δ , Actual Displacement (in)	δ_x , Modified Displacement (in)	Story Height (ft)	Δ , Design Story Drift (in)	Δ_a , Allowable Story Drift (in)	Pass
Story3	0.4083	1.6332	14	0.8188	3.36	PASS
Story2	0.2036	0.8144	14	0.74	3.36	PASS
Story1	0.0186	0.0744	14	0.0744	3.36	PASS
@ RAM Frame Location		EX D @ (-556.445, -926.789), trace location 5				

East Side

Y-direction Seismic Loading

Level	δ , Actual Displacement (in)	δ_x , Modified Displacement (in)	Story Height (ft)	Δ , Design Story Drift (in)	Δ_a , Allowable Story Drift (in)	Pass
Story3	0.2524	1.0096	14	0.5116	3.36	PASS
Story2	0.1245	0.498	14	0.4592	3.36	PASS
Story1	0.0097	0.0388	14	0.0388	3.36	PASS
@ RAM Frame Location		EX C @ (-365.149, -844.326), trace location 4				

Y-direction Seismic Loading

Level	δ , Actual Displacement (in)	δ_x , Modified Displacement (in)	Story Height (ft)	Δ , Design Story Drift (in)	Δ_a , Allowable Story Drift (in)	Pass
Story3	-0.219	-0.876	14	-0.472	3.36	PASS
Story2	-0.101	-0.404	14	-0.376	3.36	PASS
Story1	-0.007	-0.028	14	-0.028	3.36	PASS
@ RAM Frame Location		EX D @ (-556.445, -926.789), trace location 5				

Please refer to Appendix C.6 – Trace Locations for a visual location of EX C and EX D

Wind ASCE 7-10

Exposure C

Mean roof height = 65'-0" (conservatively assumed)

$k_{zt} = 0$ due to no hills near building

Use calculated n for x and y for natural frequency

$V = 115 \text{ mph}$ for basic wind speed

$G = 0.85$ (conservatively assumed)

(American Society of Civil Engineers, ASCE-7 10, Minimum Design Loads for Buildings and Other Structures, 2010)

Wind Building Drift

Wind Building Drift - West End

$h_{\text{building}} = 65$ ft

X-direction, Wind Loading

Load Case	Total Building Displacement (in)	Maximum Building Drift Allowed (in)	Pass
W1	0.211	1.95	PASS
W2	0.067	1.95	PASS
W3	0.139	1.95	PASS
W4	0.178	1.95	PASS
W5	0.093	1.95	PASS
W6	0.007	1.95	PASS
W7	0.208	1.95	PASS
W8	0.108	1.95	PASS
W9	0.109	1.95	PASS
W10	0.203	1.95	PASS
W11	0.034	1.95	PASS
W12	0.128	1.95	PASS

Y-direction, Wind Loading

Load Case	Total Building Displacement (in)	Maximum Building Drift Allowed (in)	Pass
W1	0.109	1.95	PASS
W2	0.346	1.95	PASS
W3	0.032	1.95	PASS
W4	0.131	1.95	PASS
W5	0.369	1.95	PASS
W6	0.149	1.95	PASS
W7	0.340	1.95	PASS
W8	-0.178	1.95	PASS
W9	0.136	1.95	PASS
W10	0.375	1.95	PASS
W11	-0.253	1.95	PASS
W12	-0.014	1.95	PASS

EX A @ (-156.198, -393.277), trace Location 1

Wind Building Drift - West End

$h_{\text{building}} = 65 \text{ ft}$

X-direction, Wind Loading

Load Case	Total Building Displacement (in)	Maximum Building Drift Allowed (in)	Pass
W1	0.159	1.95	PASS
W2	-0.001	1.95	PASS
W3	0.126	1.95	PASS
W4	0.113	1.95	PASS
W5	-0.015	1.95	PASS
W6	0.014	1.95	PASS
W7	0.119	1.95	PASS
W8	0.120	1.95	PASS
W9	0.105	1.95	PASS
W10	0.073	1.95	PASS
W11	0.105	1.95	PASS
W12	0.074	1.95	PASS

Y-direction, Wind Loading

Load Case	Total Building Displacement (in)	Maximum Building Drift Allowed (in)	Pass
W1	-0.048	1.95	PASS
W2	0.142	1.95	PASS
W3	-0.008	1.95	PASS
W4	-0.065	1.95	PASS
W5	0.043	1.95	PASS
W6	0.169	1.95	PASS
W7	0.070	1.95	PASS
W8	-0.142	1.95	PASS
W9	0.121	1.95	PASS
W10	-0.016	1.95	PASS
W11	-0.038	1.95	PASS
W12	-0.175	1.95	PASS

EX B @ (-379.546, -319.250), trace Location 3

Wind Building Drift - East End

$$h_{\text{building}} = 65 \text{ ft}$$

X-direction, Wind Loading

Load Case	Total Building Displacement (in)	Maximum Building Drift Allowed (in)	Pass
W1	0.072	1.95	PASS
W2	0.009	1.95	PASS
W3	0.056	1.95	PASS
W4	0.052	1.95	PASS
W5	0.000	1.95	PASS
W6	0.013	1.95	PASS
W7	0.061	1.95	PASS
W8	0.048	1.95	PASS
W9	0.052	1.95	PASS
W10	0.039	1.95	PASS
W11	0.042	1.95	PASS
W12	0.030	1.95	PASS

Y-direction, Wind Loading

Load Case	Total Building Displacement (in)	Maximum Building Drift Allowed (in)	Pass
W1	0.051	1.95	PASS
W2	0.059	1.95	PASS
W3	0.010	1.95	PASS
W4	0.067	1.95	PASS
W5	0.144	1.95	PASS
W6	-0.056	1.95	PASS
W7	0.083	1.95	PASS
W8	-0.006	1.95	PASS
W9	-0.035	1.95	PASS
W10	0.158	1.95	PASS
W11	-0.101	1.95	PASS
W12	0.092	1.95	PASS

EX C @ (-365.149, -844.326), trace location 4

Wind Building Drift - East End

$$h_{\text{building}} = 65 \text{ ft}$$

X-direction, Wind Loading

Load Case	Total Building Displacement (in)	Maximum Building Drift Allowed (in)	Pass
W1	0.125	1.95	PASS
W2	-0.071	1.95	PASS
W3	0.065	1.95	PASS
W4	0.123	1.95	PASS
W5	0.048	1.95	PASS
W6	-0.155	1.95	PASS
W7	0.041	1.95	PASS
W8	0.147	1.95	PASS
W9	-0.067	1.95	PASS
W10	0.129	1.95	PASS
W11	0.013	1.95	PASS
W12	0.208	1.95	PASS

Y-direction, Wind Loading

Load Case	Total Building Displacement (in)	Maximum Building Drift Allowed (in)	Pass
W1	-0.072	1.95	PASS
W2	0.244	1.95	PASS
W3	-0.011	1.95	PASS
W4	-0.097	1.95	PASS
W5	0.032	1.95	PASS
W6	0.334	1.95	PASS
W7	0.129	1.95	PASS
W8	-0.237	1.95	PASS
W9	0.242	1.95	PASS
W10	-0.049	1.95	PASS
W11	-0.032	1.95	PASS
W12	-0.323	1.95	PASS

EX D @ (-556.445, -926.789), trace location 5

APPENDIX C.3 – TORSIONAL IRREGULARITY AND SEISMIC AMPLIFICATION FACTOR

Amplification Factor - West Side of Heifer International Center

X-direction Seismic Loading

Level	δ EX A + Ext	A (in)	δ EX B + Ext	B (in)	δ Average	δ Maximum	A_x	1.2(δ Average)	1.4(δ Average)	Irregularity Type 1a (Table 12.3-1)	Irregularity Type 1b (Table 12.3-1)
Story3	0.380	0.244	0.244	0.312	0.380	0.380	1.03	0.374	0.436	NA	Type 1b
Story2	0.218	0.142	0.142	0.180	0.218	0.218	1.02	0.216	0.252	NA	Type 1b
Story1	0.073	0.047	0.047	0.060	0.073	0.073	1.03	0.072	0.084	NA	Type 1b
Controlling Case	E5										

EX A @ (-156.198, -393.277), trace Location 1

EX B @ (-379.546, -319.250), trace Location 3

Level	A_x	V_i (kips)	e (ft)	M_z (k-ft)	V_{apply} (kips)
Story3	1.03	186.15	11.26	2162	191.97
Story2	1.02	283.64	11.26	3266	290.03
Story1	1.03	331.55	11.26	3840	341.03

Eccentricity calculated by RAM Frame

Shear only from x-direction of case E5, conservative assumption

Amplification Factor - West Side of Heifer International Center

Y-direction Seismic Loading

Level	δ EY A + Ext	δ EY B + Ext	δ Average	δ Maximum	A_x	1.2(δ Average)	1.4(δ Average)	Irregularity Type 1a (Table 12.3.1)	Irregularity Type 1b (Table 12.3.1)
Story3	0.454	0.104	0.279	0.454	1.84	0.335	0.390	NA	NA
Story2	0.260	0.060	0.160	0.260	1.83	0.192	0.224	NA	NA
Story1	0.091	0.017	0.054	0.091	1.99	0.065	0.075	NA	NA
Controlling Case	E9								

EY A @ (-156.198, -393.277), trace Location 1
 EY B @ (-379.546, -319.250), trace Location 3

Level	A_x	V_i (kips)	e (ft)	M_r (k-ft)	V_{apply} (kips)
Story3	1.00	185.64	7.88	1463	185.64
Story2	1.00	282.97	7.88	2230	282.97
Story1	1.00	331.21	7.88	2610	331.21

Eccentricity calculated by RAM Frame

Shear only from y-direction of case E9, conservative assumption

Amplification Factor - East Side of Heifer International Center

X-direction Seismic Loading

Level	δ EX C + Ext	δ EX D + Ext	δ Average	δ Maximum	A_x	1.2(δ Average)	1.4(δ Average)	Irregularity Type 1a (Table 12.3-1)	Irregularity Type 1b (Table 12.3-1)
Story3	0.205	0.408	0.307	0.408	1.23	0.368	0.429	NA	Type 1b
Story2	0.106	0.204	0.155	0.204	1.20	0.186	0.217	NA	Type 1b
Story1	0.011	0.019	0.015	0.019	1.07	0.018	0.021	NA	Type 1b
Controlling Case	E21								

EX C @ (-365.149, -844.326), trace location 4

EX D @ (-556.445, -926.789), trace location 5

Level	A_x	V_i (kips)	e (ft)	M_z (k-ft)	V_{apply} (kips)
Story3	1.23	180.16	9.87	2188	221.73
Story2	1.20	274.77	9.87	3249	329.23
Story1	1.07	325.55	9.87	3431	347.62

Eccentricity calculated by RAM Frame

Shear only from x-direction of case E21, conservative assumption

Amplification Factor - East Side of Heifer International Center

Y-direction Seismic Loading

Level	δ EY C + Ext	C (in)	δ EY D + Ext	D (in)	δ Average	δ Maximum	A_x	1.2(δ Average)	1.4(δ Average)	Irregularity Type 1a (Table 12.3-1)	Irregularity Type 1b (Table 12.3-1)
Story3	0.252	-0.219	0.236	0.252	0.252	0.252	1.00	1.252	0.744	NA	Type 1b
Story2	0.125	-0.101	0.113	0.125	0.125	0.125	1.00	1.125	0.619	NA	Type 1b
Story1	0.010	-0.007	0.008	0.010	0.010	0.010	1.00	1.010	0.509	NA	Type 1b

Controlling Case E21

EX C @ (-365,149, -844.326), trace location 4

EX D @ (-556,445, -926.789), trace location 5

Level	A_x	V_i (kips)	e (ft)	M_x (k-ft)	V_{apply} (kips)
Story3	1.00	180.16	5.63	1014	180.16
Story2	1.00	274.77	5.63	1547	274.77
Story1	1.00	325.55	5.63	1833	325.55



Eccentricity calculated by RAM Frame

Shear only from y-direction of case E21, conservative assumption

APPENDIX C.4 – BUILDING OVERTURNING CHECK

Overturning Moment and Base Shear - West End

Building Effective Weight = 4022.94 kips

Wind Base Shear and Overturning Moment

Load Case	Level	Elevation (ft)	Base Shear		Overturning Moment	
			Vx (kip)	Vy (kip)	Mx (kip-ft)	My (kip-ft)
Wind X	Level 3	42	35.04	0		
	Level 2	28	67.36	0		
	Level 1	14	63.31	0	4,244.10	-
Wind Y	Level 3	42	0	53.91		
	Level 2	28	0	103.94		
	Level 1	14	0	98.15	-	6,548.64

Seismic Base Shear and Overturning Moment

Load Case	Level	Elevation (ft)	Base Shear		Overturning Moment	
			Vx (kip)	Vy (kip)	Mx (kip-ft)	My (kip-ft)
Seismic X	Level 3	42	184.71	0		
	Level 2	28	96.62	0		
	Level 1	14	48.55	0	11,142.88	-
Seismic Y	Level 3	42	0	184.49		
	Level 2	28	0	96.67		
	Level 1	14	0	48.72	-	11,137.42

Maximum moment = 11,142.88 kip-ft experienced by bulking (assume worst case moment in either direction)
 Resisting Moment = 60,800.03 kip-ft from the weight of the building (assuming smallest moment arm and factor of safety of 1.5)

Factor of Safety = 5.5

Overturning Passes

	Weight (kips)	Mass (k-s ² /ft)	Center of Mass		Building Edge	
			X	Y	X	Y
Story 3	1560.4	48.46	-260.6	-385.83	-155.803	-392.882
Story 2	1226.43	38.088	-264.46	-383.47	-155.803	-392.882
Story 1	1236.11	38.388	-265.33	-382.93	-155.803	-392.882

Distance for Measurement	Distance to Edge	
	COM to N	COM to S
	104.797	
	108.657	23.2
	109.527	23.08
		22.67
		33.56

Overtuning Moment and Base Shear - East End

Building Effective Weight = 3966.09 kips

Wind Base Shear and Overtuning Moment

Load Case	Level	Elevation (ft)	Base Shear		Overtuning Moment	
			Vx (kip)	Vy (kip)	Mx (kip-ft)	My (kip-ft)
Wind X	Level 3	42	35.04	0	4,244.10	-
	Level 2	28	67.36	0		
	Level 1	14	63.31	0		
Wind Y	Level 3	42	0	47.25	-	5,739.58
	Level 2	28	0	91.1		
	Level 1	14	0	86.02		

Seismic Base Shear and Overtuning Moment

Load Case	Level	Elevation (ft)	Base Shear		Overtuning Moment	
			Vx (kip)	Vy (kip)	Mx (kip-ft)	My (kip-ft)
Seismic X	Level 3	42	178.93	0	10,876.46	-
	Level 2	28	93.81	0		
	Level 1	14	52.48	0		
Seismic Y	Level 3	42	0	178.93	-	10,876.46
	Level 2	28	0	93.81		
	Level 1	14	0	52.48		

Maximum moment = 10,876.46 kip-ft experienced by building (assume worst case moment in either direction)
 Resisting Moment = 40,136.83 kip-ft from the weight of the building (assuming smallest moment arm and factor of safety of 1.5)

 Factor of Safety = 3.7

Overtuning Passes

	Weight (kips)	Mass (k-s ² /ft)	Center of Mass		Building Edge	
			X	Y	X	Y
Story 3	1487.45	46.194	-471.97	-875.62	-364.201	-844.61
Story 2	1169.75	36.328	-468.17	-874.49	-364.201	-844.61
Story 1	1308.89	40.649	-465.25	-875.26	-364.201	-844.61

Distance for Measure at	Distance to Edge	
	COM to N	COM to S
107.769	15.18	43.36
103.969	15.25	44.19
101.049	16.93	42.03

APPENDIX C.5 – LATERAL SYSTEM HAND CHECKS
LATERAL SYSTEM HAND CHECK

WHAT IS CONTROLLING LOAD COMBINATION?

$$(5) 1.2D + 1.0E + L + 0.2S$$

$$(7) 0.9D + 1.0E$$

WHERE,

$$D = 113.98^k$$

$$W = 133.77^k \text{ WIND CASE}$$

$$E = QE = 406.05^k$$

$$L = 2.75^k$$

PER § 12.4.2

$$E = E_w \pm E_v$$

$$(+ \rightarrow (5))$$

$$(- \rightarrow (7))$$

$$E_w = \rho QE = (1.0)(406.05^k) = 406.05^k$$

$$\rho = 1.0 \text{ SDC C PER § 12.3.4.1}$$

$$E_v = 0.2 S_{DS} D = 0.2(0.328)(113.98) = 7.477^k$$

$$S_{DS} = 0.328 \text{ FROM U.S.G.S}$$

~~$$\text{So, (5) } P_u = 1.2D + 1.0E_v + L + 0.2S$$~~

~~$$= 1.2(113.98) + 1.0(7.477) + 2.75 + 0.2S$$~~

~~$$= 147.008^k$$~~

$$V_u = 1.0E_w$$

$$= 1.0(406.05)$$

$$= 406.05^k$$

$$(7) P_u = 0.9D + 1.0E_v$$

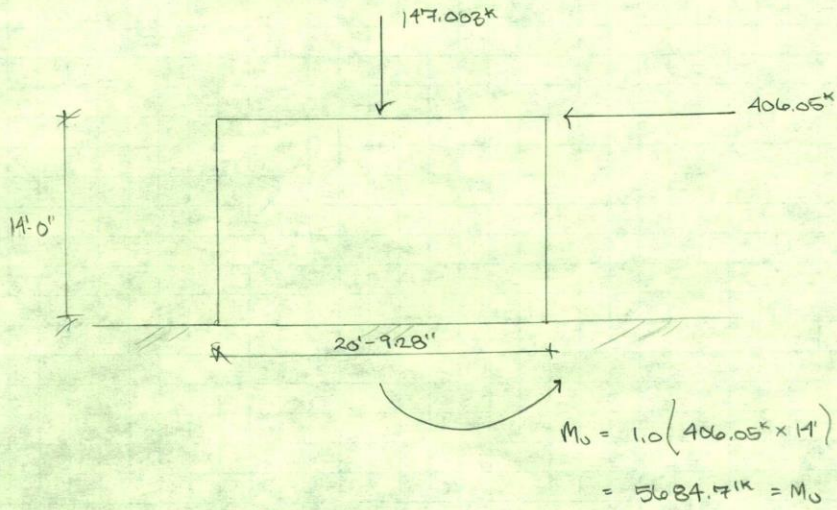
$$= 0.9(113.98) + 1.0(7.477)$$

$$= 110.059^k$$

$$V_u = 1.0E_w = 406.05^k \text{ (FROM ABOVE)}$$

 DISCONT.
 FROM ROOF

thus, CASE B CONTROLS



CHECK CONCRETE SHEAR WALL

ENSURE, $\phi V_n > V_u = 406.05^k$

What is V_c ?

PER ACI 318-11, CHAPTER 11

$$V_c = 3.32 \sqrt{f'_c} \cdot h \cdot d + \frac{N_u \cdot d}{4 l_w} \quad (\text{eq. 11-27})$$

$$\lambda = 1.0$$

$$f'_c = 4000 \text{ psi}$$

$$h = 8''$$

$$d = 0.8 l_w = 0.8 (20 + \frac{9.28}{12}) \times 12 = 199.424''$$

$$N_u = 1.2 (118.98) = 136.776^k$$

$$\text{So, } V_c = 3.3(1) \sqrt{4000} \cdot 8 \cdot 199.424 + \left(\frac{136.776^k \cdot 199.424''}{4(20 \times 12 + 9.28)} \right) / 1000$$

$$= 333.00^k$$

ALSO CHECK,

$$V_c = \left[0.16 \lambda \sqrt{f'_c} + \frac{l_w \left(1.25 \lambda \sqrt{f'_c} + 0.2 \frac{N_u}{l_w h} \right)}{\frac{M_u}{V_u} - \frac{l_w}{2}} \right] \cdot h \cdot d \quad (\text{eq. 11-28})$$

$$= \left[0.16(1) \sqrt{4000} + \frac{199.424 \cdot \left(1.25(1) \sqrt{4000} + 0.2 \cdot \frac{136.776}{(20 \times 12 + 9.28)(8)} \right)}{\frac{5689.7 \times 12^{1/4}}{406.05} - \frac{(20 \times 12 + 9.28)}{2}} \right] \times 8 \times 199.424$$

$$= 785.77^k$$

$$\text{So, } V_c = \frac{333}{\text{min. } 786^k} \rightarrow V_c = 333^k < 406.05^k$$

$$\phi V_n = 0.75(333) = 249.75^k < 406.05^k$$

X INSUFFICIENT

what is V_s ?

$$V_s = \frac{A_v f_y d}{s} \quad \text{HORIZONTAL REINF: \#1 @ 18" O.C.}$$

$$A_v = \left(\frac{14' \times 12''}{18''} + 1 \right) (0.2)(2) = 4.13$$

$$f_y = 60$$

$$d = 199.424''$$

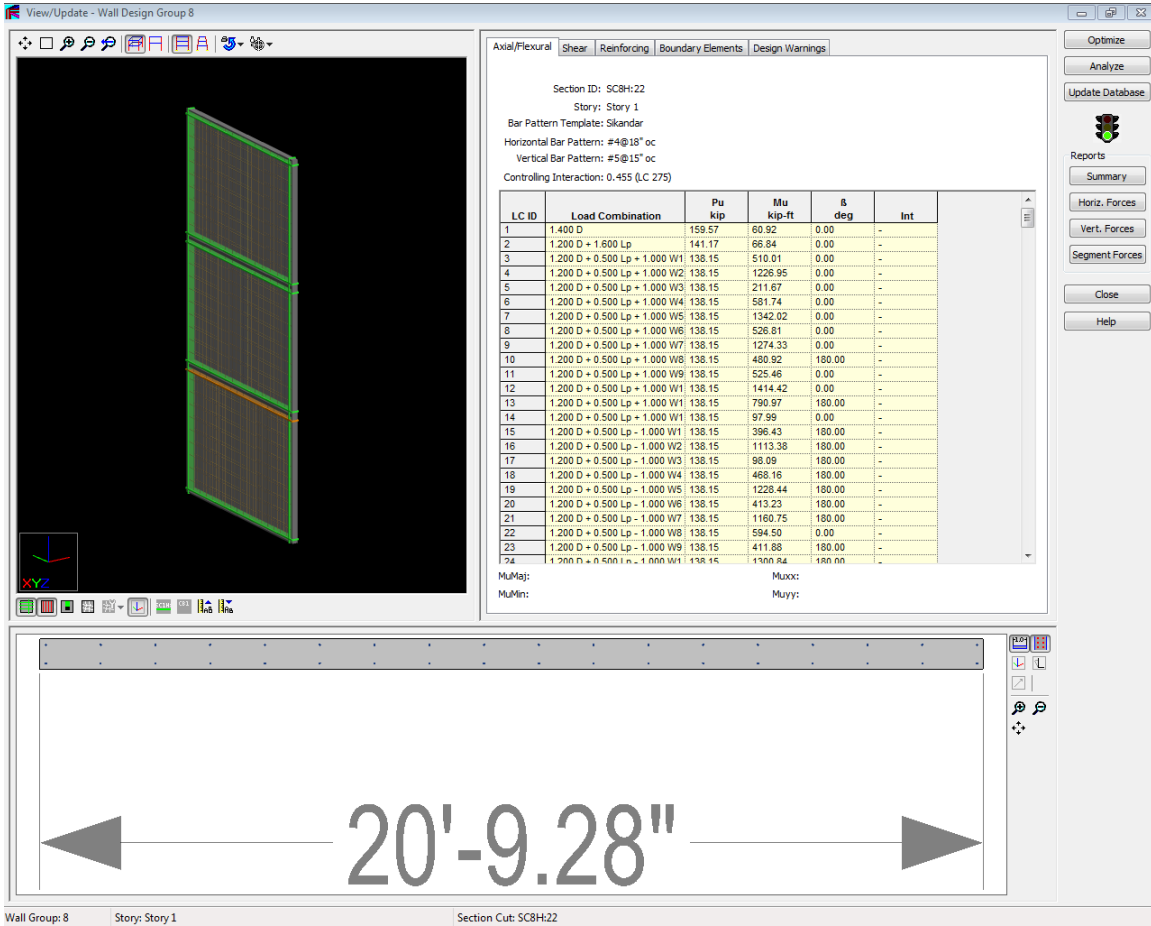
$$\text{So, } V_s = \frac{4.13(60)(199.424)}{18} = 2747.6^k$$

$$\text{now, } \phi V_n = 0.75(333 + 2747.6) = 2310^k > 406.05^k$$

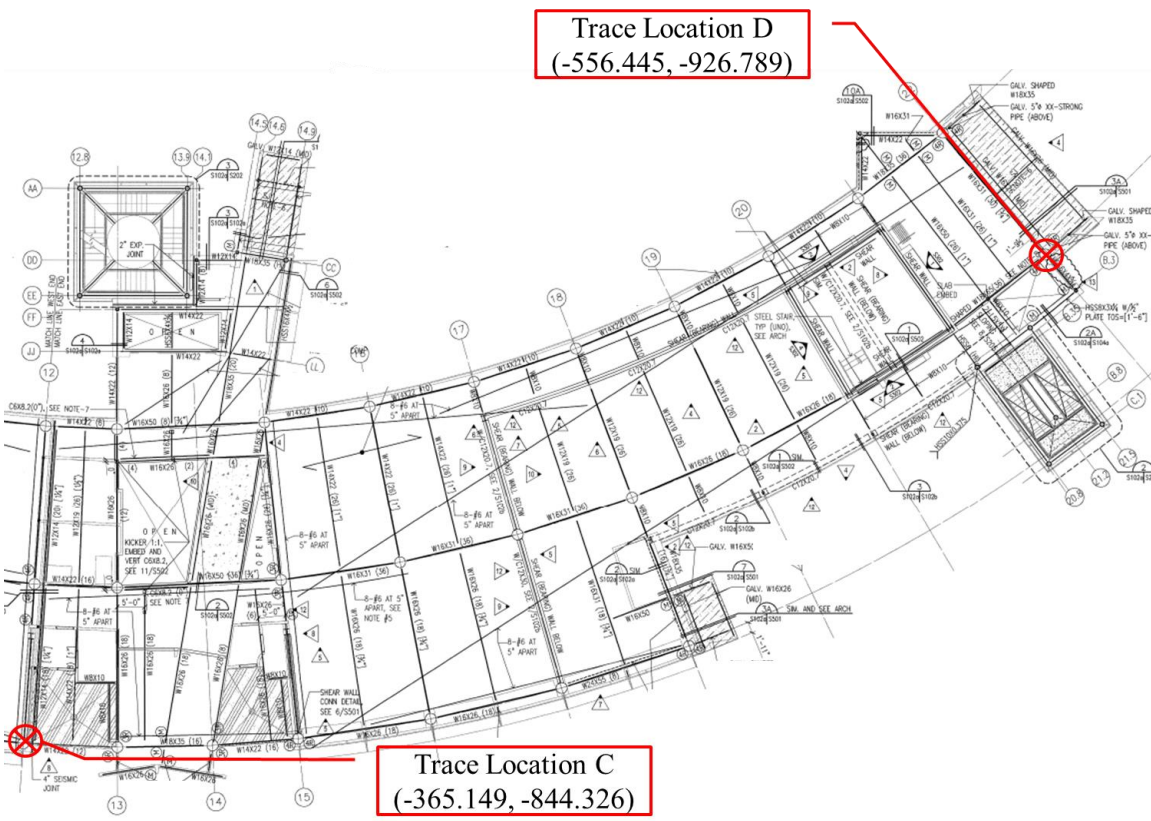
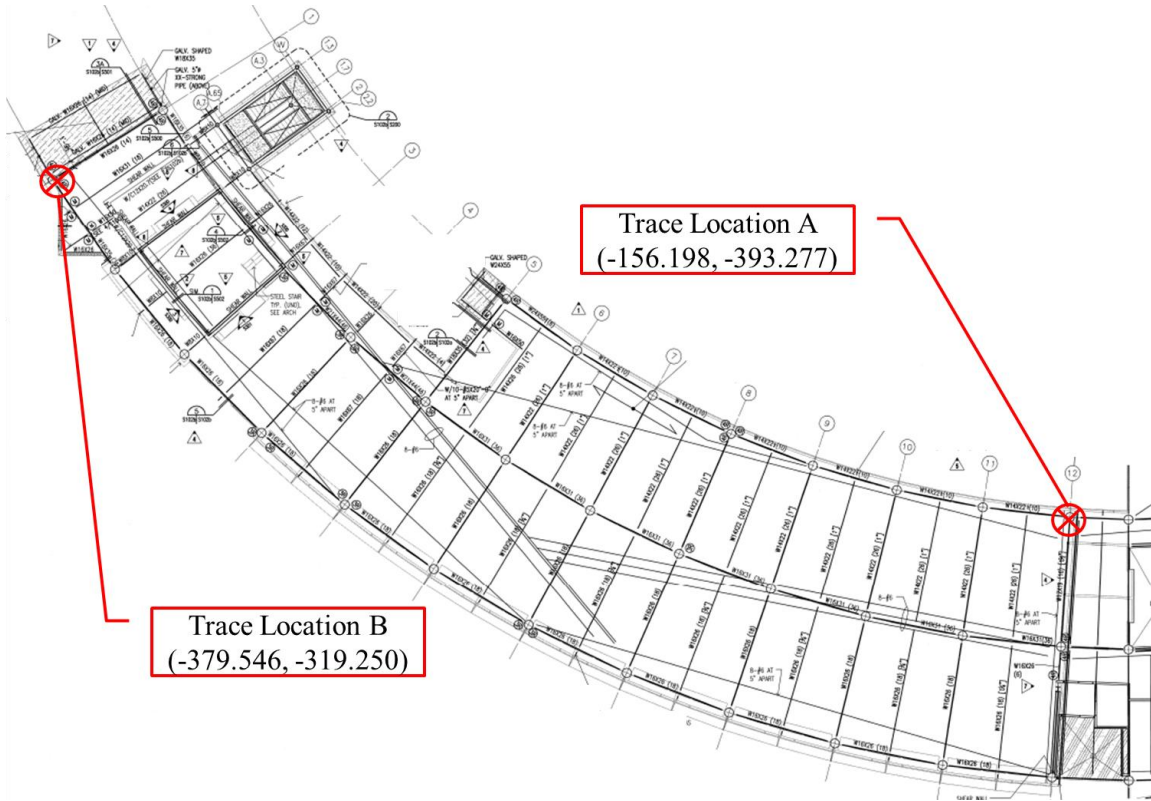
✓ GOOD

DESIGN GENERATED
BY RAM SS ARE
SUFFICIENT...

RAM Concrete was used in the design of the shear walls for the Heifer International Center. SW 13 @ column 12 is shown below.



APPENDIX C.6 – TRACE LOCATIONS

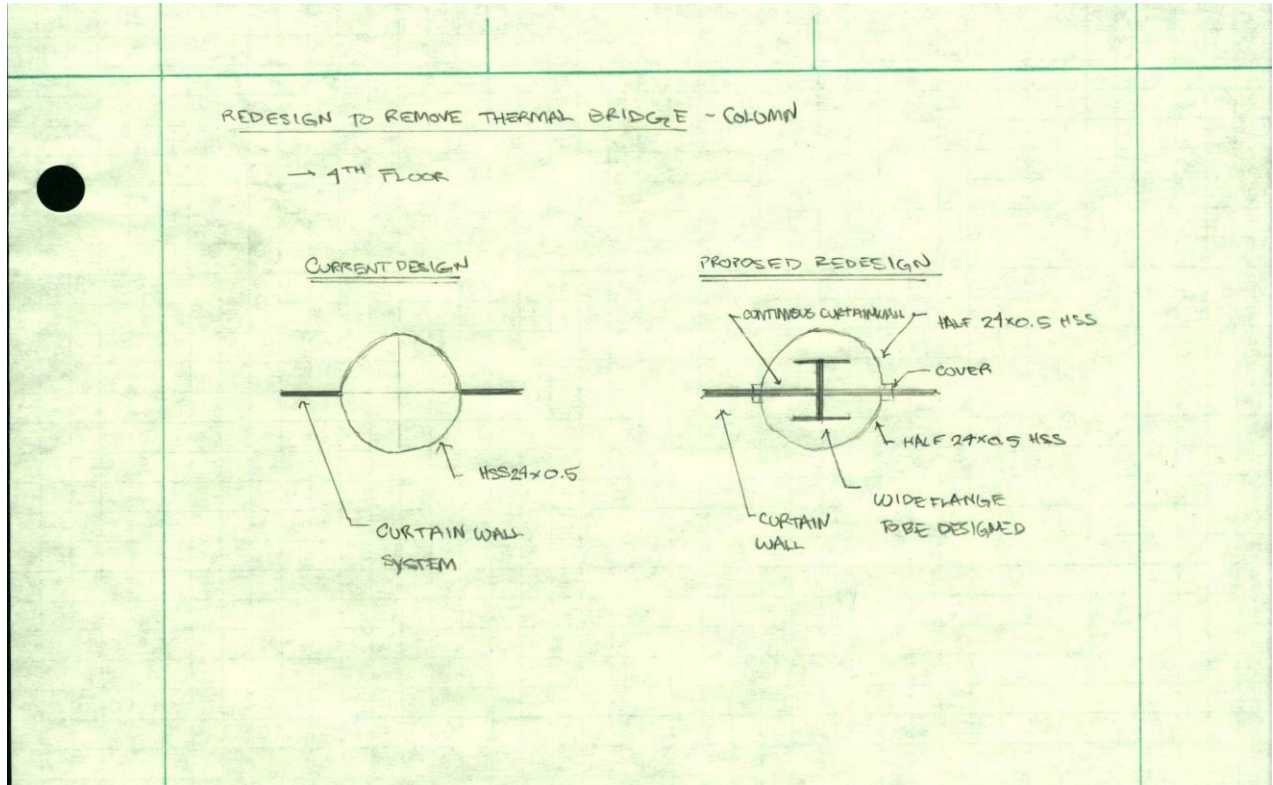


APPENDIX D

MECHANICAL AND ENVELOPE BREADTH

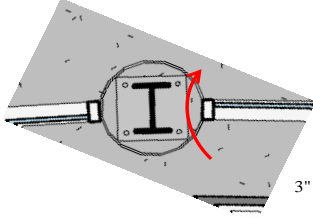
APPENDIX D.1 – THERMAL BRIDGE STUDY

Column Design



Worst Case Thermal Gradient

Worst Case Condition



Let's say:

$$\begin{aligned} T_i &= 70 \\ T_o &= 10 \\ T_i - T_o &= 60 \\ T_{dp} &= 14.69 \end{aligned}$$

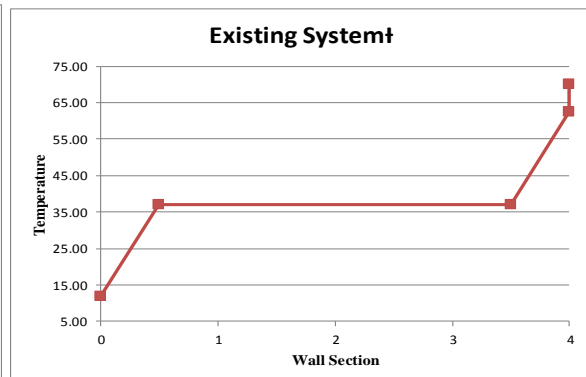
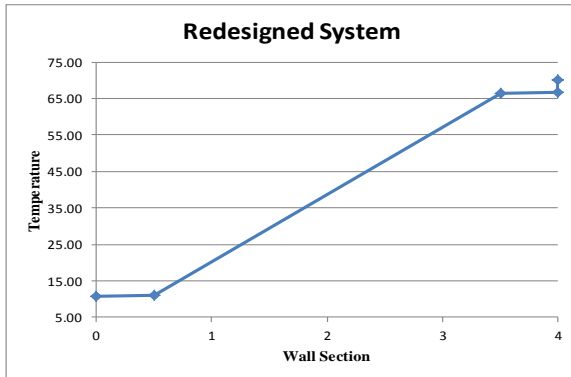
Redesigned System

Material	Depth (in)	R (BTU-in/h-ft ² -°F)	U (1/R)	ΣR _{o-x}	T _x	Reference
0 Outside Air Film	-	0.17	5.88	0.17	10.82	
0.5 Aluminum Composite	0.5	0.06	15.86	0.23	11.12	Almaxco - Aluminum Composite Panels
3.5 Batt Insulation	3	11.45	0.09	11.69	66.41	Owens Corning Insulation Systems, LLC
4 Aluminum Composite	0.5	0.06	15.86	11.75	66.72	Almaxco - Aluminum Composite Panels
4 Inside Air Film	-	0.68	1.47	12.43	70.00	
Sum		12.43	0.08			

Existing System¹

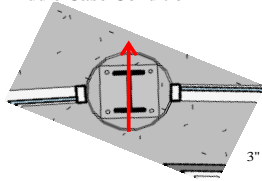
Material	Depth (in)	R (BTU-in/h-ft ² -°F)	U (1/R)	ΣR _{o-x}	T _x	Reference
0 Outside Air Film	-	0.17	5.88	0.17	11.91	
0.5 HSS Steel	0.5	2.24	0.45	2.41	37.12	Wolfram Alpha, LLC
3.5 Air	23	0.00125	802.57	2.41	37.14	Wolfram Alpha, LLC
4 HSS Steel	0.5	2.24	0.45	4.65	62.35	
4 Inside Air Film	-	0.68	1.47	5.33	70.00	Wolfram Alpha, LLC
Sum		5.33	0.19			

¹this is really a thermal bridge



Middle Case Thermal Gradient

Middle Case Condition



3" of insulation assumed

Let's say:

$$\begin{aligned} T_i &= 70 \\ T_o &= 10 \\ T_i - T_o &= 60 \\ T_{sp} &= 14.69 \end{aligned}$$

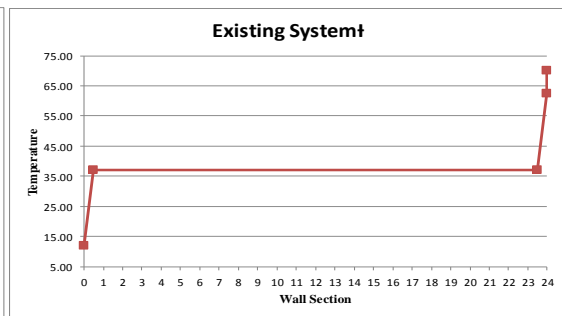
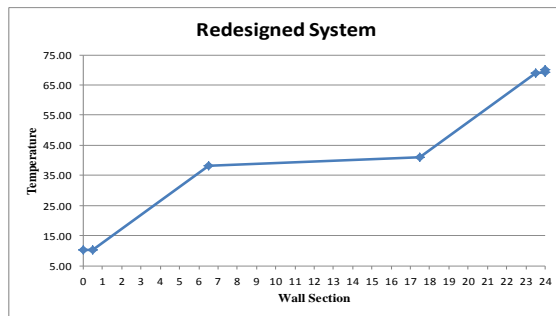
Redesigned System

Material	Depth (in)	R (BTU-in/h-ft ² -°F)	U (1/R)	ΣR _{tot}	T _s	Reference
0 Outside Air Film	-	0.17	5.88	0.17	10.21	
0.5 Aluminum Composite	0.5	0.06	15.86	0.23	10.29	Almaxco - Aluminum Composite Panels
6.5 Batt Insulation	6	22.91	0.04	23.14	38.32	Owens Corning Insulation Systems, LLC
17.5 Wide Flange	11	2.24	0.45	25.38	41.06	
23.5 Batt Insulation	6	22.91	0.04	48.29	69.09	
24 Aluminum Composite	0.5	0.06	15.86	48.35	69.17	Almaxco - Aluminum Composite Panels
24 Inside Air Film	-	0.68	1.47	49.03	70.00	
Sum		49.03	0.02			

Existing System¹

Material	Depth (in)	R (BTU-in/h-ft ² -°F)	U (1/R)	ΣR _{tot}	T _s	Reference
0 Outside Air Film	-	0.17	5.88	0.17	11.91	
0.5 HSS Steel	0.5	2.24	0.45	2.41	37.12	Wolfram Alpha, LLC
23.5 Air	23	0.00125	802.57	2.41	37.14	Wolfram Alpha, LLC
24 HSS Steel	0.5	2.24	0.45	4.65	62.35	
24 Inside Air Film	-	0.68	1.47	5.33	70.00	Wolfram Alpha, LLC
Sum		5.33	0.19			

¹this is really a thermal bridge



ACADEMIC VITA

SIKANDAR PORTER-GILL

sporterhill@gmail.com | 240.505.4956

EDUCATION

The Pennsylvania State University

Integrated Bachelor and Master of Architectural Engineering
Structural Option | Five-year professional degree | ABET accredited
EIT Certified upon graduation | Schreyer Honors College

University Park, PA

Graduation, May 2014

The Tsinghua University

Summer School for International Construction

Beijing, China

Summer 2012

The University of Hong Kong

The Department of Real Estate and Construction

Pokfulam, Hong Kong

Summer 2012

WORK EXPERIENCE

Penn State University | Research and Education Institute

Indeterminate Analysis and Computer Modeling Teaching Assistant

University Park, PA

August 2013 – present

- Provide feedback to students by evaluating homework and exams

Holbert Apple Associates, Inc. | Structural Engineer Consultants

Engineering Intern

Washington D.C. Area

May 2013 – August 2013

- Performed analysis on existing framing and design of new framing, with limited site visits
- Reviewed shop drawings for concrete reinforcing and structural steel
- Prepared construction documents using AutoCAD and Revit
- Worked with RAM SBeam, spSlab, PROFIS, Enercalc and Decon STDesign

Penn State University | Research and Education Institute

Undergraduate Researcher | Laboratory Scholar

University Park, PA

January 2010 – May 2013

- Tested Structural Insulated Panels for intended wide spread use
- Examined formaldehyde reduction in buildings using gypsum dry board
- Engineered working models in RISA, ETABS and SAP 2000
- Managed ordering of project
- Conceptualized fuel cell productivity using printed biofilms on the electrode and examined immobilization of biofilms using latex substance

Sustainable Design Group | Design and Construction Firm

Intern

Gaithersburg, MD

May 2011 – August 2011

- Prepared construction documents for residential and business projects
- Evaluated sustainable design research for developing countries
- Oversaw permitting application for counties in Maryland and Virginia
- Worked with Graphisoft ArchiCAD 13/15, Photoshop CS.5, and Google Sketchup

PUBLICATIONS

Wagner, R., Porter-Gill, S. "Immobilization of anode-attached microbes in a microbial fuel cell." AMB Express. 2012.

Porter-Gill, S. "Overview of the Causes and Remediation of Sinkholes." The American Society of Civil Engineers TCFE. 2013.